

**Syn- and post-depositional sand bodies in lignite –
The interrelationship of tectonics and sedimentation
in the Lower Rhine Embayment**

Dissertation

zur

Erlangung des Doktorgrades (Dr. rer. nat.)

der

Mathematisch-Naturwissenschaftlichen Fakultät

der

Rheinischen Friedrich-Wilhelms-Universität Bonn

vorgelegt von

Linda Prinz

aus

Wipperfürth

Bonn, Dezember 2017

Angefertigt mit Genehmigung der Mathematisch-Naturwissenschaftlichen Fakultät der
Rheinischen Friedrich-Wilhelms-Universität Bonn

1. Gutachter: Prof. Dr. Tom McCann

2. Gutachter: Prof. Dr. Barbara Reichert

Tag der Promotion: 16.04.2018

Erscheinungsjahr: 2018

Versicherung an Eides Statt

gem. § 6 der Promotionsordnung vom 17. Juni 2011

Ich, Linda Prinz, Bevingsweg 20A, 51109 Köln, Matr.-Nr.: 3040550

versichere an Eides statt durch meine Unterschrift, dass ich die vorliegende Dissertation selbständig und ohne fremde Hilfe angefertigt und alle Stellen, die ich wörtlich dem Sinne nach aus Veröffentlichungen entnommen habe, als solche kenntlich gemacht habe, und mich auch keiner anderen als der angegebenen Literatur oder sonstiger Hilfsmittel bedient habe. Die vorgelegte Arbeit oder ähnlich Arbeiten wurden nicht anderweitig als Dissertation eingereicht.

Ich versichere an Eides Statt, dass ich die vorgenannten Angaben nach bestem Wissen und Gewissen gemacht habe und dass die Angaben der Wahrheit entsprechen und ich nichts verschwiegen habe.

Ort, Datum

Unterschrift

Acknowledgement

This study was funded by the RWE Power AG.

First of all, I would like to thank Prof. Dr. Tom McCann, for his valuable scientific and personal support during the past 3 years. Thank you for the hours of discussions, and for helping me to bring out the best of myself.

Thanks to Dr. Andreas Schäfer, for supporting my first steps into the geology of the Lower Rhine Embayment, and for many interesting discussions.

I would also like to thank the members of the Department of Deposit Geology (COC-L, RWE Power AG), for so kindly welcoming me. Special thanks to Peter Lokay for all his support during the past years, and to Sven Asmus, who facilitated this cooperation. I would also like to thank Michaela Schneider and Hans Münch, as well as Ulrich Krüger, Horst Hassel, Sonja Weiler and Dr. Thomas Thielemann for editing datasets. Glückauf!

Thanks to my colleges from the Steinmann Institute for their support, especially Prof. Dr. Gösta Hoffmann, Prof. Dr. Barbara Reichert, Laura Heiß, Eddi Grigowski, Sophia Rütters, Eva-Maria Heumann Lange, Dr. Sven Oliver Franz, Dr. Mario Valdivia-Manchego, Dirk Handwerk, Reiner Schwarz, and Carola Kubus.

One of my manuscripts would not exist without the great support of Prof. Dr. Ralf Littke from the RWTH Aachen.

I would also like to express my thanks to my family and friends, for their patience and their support. Special thanks to Sven, Papa, Mama and Aliça – the past 3 years greatly benefitted from our hikes and our days on the water - life begins at 40 knots.

Most of all, thank you Sven.

Abstract

The Cenozoic-age Lower Rhine Embayment is part of the European Cenozoic Rift System, which initiated in Eocene times as a result of passive, intracontinental rifting. The Lower Rhine Embayment formed in an extensional regime, related to the reactivation of Late Variscan fracture systems located to the NW of the Rhenish Massif. The Lower Rhine Embayment extends along the Rhine River from Bonn in the SE through to Belgium and the North Sea Basin in the NW Netherlands.

Deposition of the Cenozoic-age basin infill of the Lower Rhine Embayment was controlled by the interaction of tectonic activity and sedimentary processes related to sea-level fluctuations and climatic changes. In the subtropical climatic conditions of Miocene times, extensive paralic mires formed across the basin, and as a result of continuous basin subsidence, extremely thick (up to 270 m) peat deposits accumulated in the Lower Rhine Embayment. These lignite seams (up to 100 m thick) have been mined for more than 150 years in the so-called Rhenish Lignite District.

Within the Garzweiler mining area, one of the three active lignite open-cast mines in the Lower Rhine Embayment (which are run by the RWE Power AG), the presence of sand bodies affect the industrial exploitation of the lignite. Due to the variable dimensions and irregular distribution of these sand bodies, the processing of future lignite volumes is difficult and often problematic. Therefore, this study aims to improve the understanding of sand body emplacement within the Miocene-age Frimmersdorf Seam, and to facilitate the early and precise recognition of sand bodies within the future mining area.

The analyses of sand bodies within the Miocene-age Frimmersdorf Seam is mainly based on three years of fieldwork within the constantly refreshed outcrops of the Garzweiler open-cast mine, but also includes older data from the RWE Power AG archive, for example, maps, geophysical measurements and drilling well data. The interpretation of the various fieldwork and analytical approaches revealed that a variety of both syn- and post-depositional mechanisms were responsible for the emplacement of the various sand bodies within the peat/lignites of the Frimmersdorf Seam, providing evidence of the extreme complexity of the depositional and post-depositional systems. Syn-depositional sand bodies were formed in fluvial and estuarine channels in the extensive mires, or by episodic flooding events from the adjacent North Sea. The presence of post-depositional sand injectites within the Frimmersdorf Seam is related to liquefaction and fluidization of unconsolidated, overpressurized sands (i.e. the Frimmersdorf and Neurath sands), and the natural hydraulic fracturing of the sealing host strata, i.e. the Frimmersdorf Seam.

Organic petrological and inorganic geochemical analyses were carried out on lignite and sand samples to investigate the influence of sand body emplacement on the adjacent lignite. The ash contents, as well as thin section analyses revealed that the lignite was not influenced by sand body deposition, not even at the direct contact areas. Additionally, this study provided some useful information on the depositional environment, for example the mineralisation of the water, which was present during peat/lignite formation. The analyses of sulphur and ash contents of the lignite samples indicate that the depositional environment was controlled by freshwaters. On the other hand, the presence of glauconite minerals in one of the sand sample, and low Ca/Mg ratios would suggest that the sand body emplacement was controlled by marine currents. The organic petrological and inorganic geochemical analyses, therefore, provide evidence of the complex interaction of marine processes (tides, waves, storm events) with the river systems in the paralic mires.

Finally, a three-dimensional reconstruction of the Frimmersdorf Seam was modelled. This integrated model was based on pre-existing contour line maps of the lignite boundaries, as well as information on lignite thicknesses (based on the RWE Power AG reservoir model), and measurements of the sand body distributions and orientations. The interpretation of the 3D model revealed a close interrelationship between sand bodies and seam morphology on the one hand, and between sand injectites and the occurrence and orientation of the fault systems on the other. The hydraulic fracturing of the lignite, and, therefore, the orientation of the sand injectites, were largely controlled by tectonic activity within the study area. Fracturing of the peat/lignite occurred under the stress field that prevailed during the time of sand injectite formation.

Zusammenfassung

Die känozoische Niederrheinische Bucht ist Teil des Nordwest-Europäischen Riftsystems, das im Eozän durch die passive, intra-kontinentale Dehnung der Erdkruste gebildet wurde. Die Niederrheinische Bucht entstand durch die Reaktivierung von variszischen Störungssystemen am NW-Rand des Rheinischen Schiefergebirges in einem extensionalen Regime. Sie erstreckt sich von Bonn im SO über Belgien bis zum Nordsee-Becken in den NW Niederlanden.

Die känozoische Beckenfüllung der Niederrheinischen Bucht entstand durch die Wechselwirkung von Tektonik und Sedimentationsprozessen, die hauptsächlich durch Meeresspiegel- und Klimaschwankungen gesteuert wurden. In den subtropischen klimatischen Bedingungen des mittleren Miozäns bildeten sich in weiten Teilen der Niederrheinischen Bucht ausgedehnte Moore, und durch die kontinuierliche Absenkung des Untergrunds wurden extrem mächtige Torfe (bis zu 270 m) abgelagert. Diese heute bis zu 100 m mächtigen Braunkohlen-Flöze werden seit mehr als 150 Jahren im Rheinischen Braunkohlenrevier abgebaut.

In einem der drei aktiven Tagebaue der RWE Power AG in der Niederrheinischen Bucht, wird der Abbau eines Braunkohlenflözes durch das Vorkommen von Sand-Einschaltungen in der Kohle gestört. Ihr unregelmäßiges Auftreten (sowohl in Bezug auf die Größenordnung, als auch ihre Verbreitung) erschwert die genaue Kalkulation von zukünftigen Braunkohlemengen im Tagebau Garzweiler. Daher soll im Rahmen dieser Dissertation untersucht werden, wie die Sand-Einschaltungen entstehen konnten, und ob ein verbessertes Verständnis zu einer genaueren Prognose über das Auftreten von Sanden im weiteren Abbaufeld des Tagebau Garzweilers führt.

Die Analyse der Sand-Einschaltungen im miozänen Flöz Frimmersdorf basiert zum größten Teil auf Gelände-Beobachtungen in den ständig erneuerten Aufschlüssen des Tagebau Garzweilers. Außerdem wird bereits vorhandenes Datenmaterial aus den umfangreichen RWE-Archiven hinzu gezogen, wie z.B. Karten, geophysikalische Messungen oder Daten von Bohrkernen. Durch die Interpretation der verschiedenen Geländebeobachtungen und analytischen Ergebnisse konnte gezeigt werden, dass eine Vielzahl verschiedener syn- und post-genetischer Entstehungsmechanismen für den Eintrag von Sand in die Kohle des Flözes Frimmersdorf verantwortlich waren. Syn-genetische Sand-Einschaltungen wurden in fluviatilen oder estuarinen Rinnen in den ausgedehnten Braunkohlenmooren abgelagert, oder durch episodische Überflutungsereignisse eingetragen, die von der angrenzenden Nordsee ausgingen. Die post-genetische Entstehung von Sand Injektionen (*sand injectites*) wird auf

das Verflüssigen von unverfestigten Sanden unter Überdruck zurückgeführt, gefolgt vom hydraulischen Aufbrechen der versiegelnden Schichten, d.h. der Braunkohle.

Zusätzlich zu den Geländearbeiten wurden kohlenpetrologische und geochemische Analysen durchgeführt, um den Einfluss des Sand-Eintrags auf die angrenzende Braunkohle zu untersuchen. Anhand der Asche-Gehalte der Braunkohlen und an Dünnschliffen konnte gezeigt werden, dass der Eintrag von Sand die Braunkohle nicht mal im direkten Kontaktbereich beeinflusst oder verändert hat. In diesem Abschnitt der Dissertation konnten außerdem wichtige Informationen über die miozänen Ablagerungsbedingungen gewonnen werden. Die Analysen von Schwefel- und Aschegehalten der Kohleproben deuten darauf hin, dass diese Torfe in einem Ablagerungsraum akkumulierten, der durch Süßwasser geprägt war. Glaukonit-Minerale in eine der beprobten Sand-Einschaltungen, und geringe Ca/Mg-Werte weisen dagegen auf einen marinen Eintrag hin. Die kohlenpetrologischen und geochemischen Analysen bestätigen, dass der miozäne Ablagerungsraum der Niederrheinischen Bucht durch das Zusammenwirken von marinen Einflüssen der Nordsee (Tiden, Wellen, Stürme) und den Flusssystemen in den ausgedehnten Braunkohlemooren geformt wurde.

Zuletzt wurde ein drei-dimensionales Modell des Flözes Frimmersdorf (innerhalb der Tagebau-Grenzen) anhand von Höhenlinien-Karten der Flöz-Grenzen erstellt (basierend auf dem Lagerstättenmodell der RWE Power AG), das außerdem Informationen zu Kohlemächtigkeiten und die Messdaten über die Verteilung und Orientierung von Sand-Einschaltungen beinhaltet. Die genaue Analyse dieses 3D Modells zeigte, dass zwischen dem Auftreten der Sand-Einschaltungen und der Flöz-Geometrie, sowie zwischen den *sand injectites* und dem Störungssystem im Tagebau Garzweiler enge Zusammenhänge bestehen. Das hydraulische Aufbrechen des Torfs/der Braunkohle, und damit nachfolgend auch die Orientierung der *sand injectites*, steht in engem Zusammenhang mit der tektonischen Entwicklung der Niederrheinischen Bucht, und erfolgte parallel zu dem Stressfeld, das zum Zeitpunkt des Sand-Eintrags vorherrschte.

Table of contents

Abstract	IX
Zusammenfassung	XI
Table of contents	XIII
List of figures	XVII
List of tables	XXIV
1 Structure of the thesis	1
2 Introduction	4
2.1 Study location.....	5
2.2 Motivation and research approach.....	9
2.3 Methods	11
2.3.1 Fieldwork.....	11
2.3.2 Analytical approaches.....	11
2.3.3 3D model.....	12
3 Geological framework	13
3.1 Tectonic evolution of the Lower Rhine Embayment	15
3.2 Depositional history of the Lower Rhine Basin.....	18
3.2.1 Palaeogene	20
3.2.2 Neogene.....	21
3.2.3 Quaternary	24
4 The geometry, distribution and development of sand bodies in the Miocene-age Frimmersdorf Seam (Garzweiler open-cast mine), Lower Rhine Basin, Germany: Implications for seam exploitation.	26
4.1 Abstract.....	26
4.2 Introduction	27
4.3 Geological Setting	31
4.4 Classification of sand bodies in the Frimmersdorf Seam	34
4.4.1 Position.....	35
4.4.2 Morphology.....	35
4.4.3 Orientation.....	37
4.4.4 Composition	40
4.4.5 Grain size and sorting.....	41
4.4.6 Sedimentary structures.....	42
4.4.7 Sand body complexity.....	43
4.4.8 Frimmersdorf Seam and Frimmersdorf Sand Boundary.....	45
4.5 Discussion.....	45

4.5.1	Syn-depositional features	46
4.5.2	Post-depositional emplacement mechanisms	52
4.5.3	Time frame	57
4.6	Conclusions	58
5	Channel deposits in the Miocene-age Frimmersdorf Seam	61
5.1	Abstract	61
5.2	Introduction.....	61
5.3	Geological framework.....	62
5.4	Methods	62
5.5	Results	63
5.6	Interpretation & Discussion.....	66
5.7	Conclusions.....	70
6	Syn- and post-depositional sand bodies in lignite – the role of coal analysis in their recognition. A study from the Frimmersdorf Seam, Garzweiler open-cast mine, western Germany.....	71
6.1	Abstract.....	71
6.2	Introduction.....	72
6.3	Geological background.....	75
6.3.1	Geological setting	75
6.3.2	Climate and sea level fluctuations.....	77
6.4	Methods	79
6.4.1	Sampling strategy.....	79
6.4.2	Sample preparation	79
6.4.3	Ash yield and elemental analysis	80
6.4.4	Humic substances	80
6.4.5	Coal petrography	81
6.4.6	Inorganic geochemistry and mineralogy.....	81
6.5	Results and discussion.....	83
6.5.1	Syn-depositional sand features.....	83
6.5.2	Post-depositional sand features.....	91
6.5.3	Evaluating the coal petrology and inorganic geochemistry in terms of syn-depositional and post-depositional processes.....	93
6.5.4	Depositional environment	95
6.6	Transport energy	99
6.7	Conclusions.....	99
7	Sand injectites - from source to emplacement: an example from the Miocene-age Frimmersdorf Seam, Garzweiler open-cast mine, Lower Rhine Embayment.	102

7.1	Abstract.....	102
7.2	Introduction	103
7.3	Geological background.....	107
7.3.1	Stratigraphic record	109
7.4	Sand injectites in the Frimmersdorf Seam	110
7.5	Parent sand units	111
7.6	Intrusive complex	114
7.6.1	Sand injectites	114
7.6.2	Host unit	116
7.7	Discussion.....	120
7.7.1	From source... ..	121
7.7.2	...to emplacement.	121
7.8	Conclusions.....	129
8	Conclusions	131
9	References.....	137
	Appendix	150
A	Facies analysis and depositional model of the Serravallian-age Neurath Sand, Lower Rhine Basin (W Germany).....	150
A.1	Abstract.....	150
A.2	Introduction	151
A.3	Geological Framework.....	154
A.3.1	Regional distribution of the Neurath Sand in the Lower Rhine Basin	156
A.4	Methods	158
A.5	Sedimentary Facies and Facies Analysis	158
A.5.1	Muddy sands with chert-pebble lag (Smu)	159
A.5.2	Fine-grained sands (Sf)	161
A.5.3	Fine- to medium-grained sands (Sfm).....	166
A.5.4	Medium-grained sands (Sm).....	167
A.5.5	Coarse- to medium-grained sands (Sc)	168
A.5.6	Lignite (L)	169
A.6	Facies Associations in sediment profiles	169
A.6.1	Facies Association 1	171
A.6.2	Facies Association 2.....	172
A.6.3	Facies Association 3.....	173
A.6.4	Facies Association 4.....	174
A.6.5	Facies Association 5.....	175
A.6.6	Facies Association 6.....	175

A.7	Discussion	176
A.7.1	Depositional model	176
A.7.2	Channel deposits	180
A.7.3	Depositional environment: tidal delta vs. estuary	182
A.8	Conclusions	185
A.9	References	186
B	Supplementary Material	192
B.1	Carbon, ash and sulphur contents of samples (Locations 1 to 6)	192
B.2	Maceral composition of 55 lignite samples (Locations 1 to 6)	194
C	Publications	195

List of figures

Fig. 2-1: Aerial view of the Garzweiler open-cast mine in the Lower Rhine Embayment (source: google earth).

Fig. 2-2: Bucket-wheel excavator in the Garzweiler open-cast mine, removing upper parts of the Neurath Sand.

Fig. 2-3: Mine dump at the E side of the Garzweiler open-cast mine.

Fig. 2-4: Sand bodies in the Frimmersdorf Seam (coin for scale).

Fig. 2-5: High-resolution GPS-measurements of sand bodies (yellow) within an outcrop of the Frimmersdorf Seam (grey). The boundary between the Frimmersdorf Seam and the underlying Frimmersdorf Sand is indicated by the brown, dashed line.

Fig. 3-1: A structural map of the Lower Rhine Embayment (after Schäfer et al., 1996; Houtgast & van Balen, 2000; Klett et al. 2002; Schäfer & Utescher, 2014). EF: Erft Fault, FF: Feldbiss Fault, JH: Jackerath Horst, PF: Peel Fault, RF: Rur Fault, TF: Tegelen fault, VF: Viersen Fault. The former and active open-cast mines (RWE Power AG) are indicated by the yellow areas (G: Garzweiler, H: Hambach, I: Inden open-cast mines). The red lines (A-B, C-D) indicate the position of two cross sections, which are shown in Fig. 3-2).

Fig. 3-2: Cross section A-B (NW-SE) and C-D (W-E; as indicated in Fig. 3-1). MS: Main Seam; M: Morken Seam, F: Frimmersdorf Seam, G: Garzweiler Seam.

Fig. 3-3: Stratigraphic log of the Lower Rhine Basin (modified after Klett et al. 2002; Schäfer et al. 2004, 2005; Schäfer & Utescher 2014; Prinz et al. 2018). The log is based on two well logs (RWE Power AG), and represents the stratigraphy in the centre of the Erft Block (see Fig. 3-1). The lithostratigraphical code was established by Schneider & Thiele (1965). Biostratigraphical ages (Ma, left) after Berggren et al. (1995), cycle ages (Ma, right) after Haq et al. (1987, 1988) & Hardenbol et al. (1998).

Fig. 4-1: A structural map of the NW European Cenozoic Rift System. At its northern end the Upper Rhine Graben bifurcates into the Hessen and Leine grabens to the NE, and the Lower Rhine Basin in the NW (Rhenish Triple Junction in the area of Frankfurt; after Schumacher, 2002; Sissingh, 2003 and Rasser et al., 2008).

Fig. 4-2: Stratigraphic log of the Lower Rhine Basin (after Klett et al., 2002; Schäfer et al., 2004, 2005; Schäfer & Utescher, 2014). The lithostratigraphy is a synthesis based on the SNQ 1 (Erft Block) and Efferen (Köln Block) wells (RWE Power AG), and

taken to represent the stratigraphy at the centre of the Erft Block (lithostratigraphical code established by Schneider & Thiele, 1965). Biostratigraphical ages [Ma] on the left after Berggren et al. (1995), cycle ages [Ma] after Hardenbol et al (1998).

Fig. 4-3: N-S-oriented cross section of the Lower Rhine Basin (N-S line in structural map, Fig. 4-4), cross cutting the Jackerath Horst, the Garzweiler open-cast mine (rectangle) and a series of normal and reverse faults. The Main Seam is present in the SE, subdividing into the Morcken, Frimmersdorf and Garzweiler seams in the NW (Ville Fm indicated by oval; stratigraphy based on RWE data).

Fig. 4-4: Structural maps of the Lower Rhine Basin. a) The NW part of the Lower Rhine Basin comprises the Peel, Venlo and Krefeld blocks in the N and the Rur, Erft and Köln blocks in the S (after Schäfer & Utescher, 2014; RWE Power AG); each of the blocks are separated by major fault systems; section N-S: see Fig. 4-3. b) Distribution of lignite within the Lower Rhine Basin (yellow Morcken Seam; green: Frimmersdorf Seam; blue: Garzweiler Seam; based on RWE data). JH = Jackerath Horst; G = Garzweiler open-cast mine; H = Hambach open-cast mine; I = Inden open-cast mine.

Fig. 4-5: Sand bodies within the Frimmersdorf Seam illustrating the different morphologies present: a) concordant sand beds, with even upper and wavy lower boundaries; b) thick (up to 1.8 m) channel-like sand body, c) irregular shaped sand body, and, d) reticulate sand bodies.

Fig. 4-6: Sand bodies illustrating the orientation; a) combination of sills and dykes, b) vertical dyke between to sills c) sills with vertical offset of 1-2 cm; and, d) sills with vertical offsets of up to 10 cm.

Fig. 4-7: Stereographic projection of lignite surfaces, a) symbol '+' illustrating fault planes, 'x' reflecting bedding surfaces; b) Density diagram; c) Rose plot.

Fig. 4-8: Stereographic projection of sand surfaces, a) symbol '+' illustrating sills and dykes, 'x' reflecting bedding surfaces; b) Density diagram; c) Rose plot.

Fig. 4-9: Composition of the sand bodies; a) lignite lens at the top, lignite clasts at the bottom of a sand body; b) subrounded lignite clasts; c) mud lens, and, d) chert pebbles.

Fig. 4-10: Petrographic view of sand from a sill-like sand body. The sorting of the quartz grains results from a variation of grain sizes and grain packing; the pore space is filled by dark humic substances. Note the presence of elongated organic particles oriented parallel to lamination.

Fig. 4-11: Thick sand body underlain by laminated lignite. The sand body also contains a variety of chert pebbles and lignite clasts.

Fig. 4-12: Classification of sand bodies; 1) concordant layers/beds (tabular); 2) channel-like sand bodies; 3) sill-like sand bodies (tabular), a) isolated or several parallel sills, b) sill-like sand bodies with cross lamination; 4) dyke-like sand bodies, a) isolated dykes on top of the Frimmersdorf seam with connection to the overlying Neurath Sand, b) isolated or parallel dykes within the seam, without connection to the Neurath or Frimmersdorf sands; 5) combination of sills and dykes, a) dykes intruding into the Frimmersdorf Seam from the underlying Frimmersdorf Sand, b) symmetric sills and dykes within the seam; c) dykes connected to tabular sand bodies; 6) sand bodies with irregular morphology; 7) reticulate sand bodies.

Fig. 4-13: Groden bedding (within the green lines), formed as a result of storm-controlled flooding of the swamp area, in the upper metres of the Frimmersdorf Sand. The red line marks the boundary between the Frimmersdorf Sand and the Frimmersdorf Seam above. Note the presence of the root horizon at the sand-groden boundary (yellow arrows).

Fig. 5-1: Laser scanning of one sand body in the upper part of the Frimmersdorf Seam (11.11.2015).

Fig. 5-2: High-resolution image of the laser scanning, based on the different reflectivity of sand and lignite.

Fig. 5-3: Graphical interpretation of the seven consecutive sand body sections; from SE (blue section) to NW (violet section).

Fig. 5-4: a) Sand-lignite alternations at the base of the sand body; b) Chert pebbles at the base of the sand body, and within the underlying lignite (pencil for scale).

Fig. 5-5: Section of the stratigraphical log of the Lower Rhine Basin. The fluvial sand bed, which is indicated by the red bar within the lignite, separates the seam into Frimmersdorf a and Frimmersdorf b. This sand bed, which was exposed in the Hambach open-cast mine, was associated with the Mid-Miocene Unconformity.

Fig. 6-1: A structural map of the Lower Rhine Embayment in the NW of the Rhenish Massif (after Houtgast and van Balen, 2000; Klett et al., 2002; Prinz et al., 2018; Schäfer et al., 1996; Schäfer and Utescher, 2014). Red lines mark the position of the fault systems, which separate the basin into six main tectonic blocks. Key: EF Erft Fault, JH Jackerath Horst, PF Peel Fault, RF Rur Fault, TF Tegelen Fault, VF Viersen Fault. Pink line: Germany-Netherlands-Belgium borders. The Rur Block (Germany)

extends into the Roer Valley Graben in the Netherlands. The figure also includes the position of the three active open-cast mines: G Garzweiler, H Hambach, and I Inden, as well as former open-cast mines and pits (Fortuna, Bergheim, Frechen and Ville).

Fig. 6-2: Stratigraphic log of the Lower Rhine Basin (modified after Klett et al., 2002; Schäfer et al., 2004, 2005; Schäfer and Utescher, 2014; Prinz et al., 2018). The lithostratigraphic log represents the stratigraphy of the Lower Rhine Basin in the centre of the Erft Block (based on two well logs, SNQ 1 on the Erft Block, and Efferen on the Köln Block; RWE Power AG); lithostratigraphical code established by Schneider and Thiele (1965). Biostratigraphical ages (Ma; left) after Berggren et al. (1995), cycle ages (Ma; right) after Haq et al. (1987; 1988) & Hardenbol et al. (1998).

Fig. 6-3: Sand bodies in the Frimmersdorf Seam, Garzweiler open-cast mine. a) A syn-depositional sand body comprising (trough) cross lamination; this sand body was deposited in a fluvial-estuarine environment; b) A variety of post-depositional sand bodies, including sills and dykes.

Fig. 6-4: Sea level fluctuation and climatic variations in the North Sea (after Buchardt, 1978; Haq et al., 1987; Zagwijn and Hager, 1987; Hager & Prüfert, 1988; Hager, 1993), compared to global climatic changes (after Zachos et al., 2001). International chronostratigraphic chart after Cohen et al. (2013; updated).

Fig. 6-5: Plot of the ash yields of the lignite samples from Locations 1-6, which are distributed on a nearly vertical section from the bottom to the top of the Frimmersdorf Seam. The light grey marks indicate lignite samples that were taken from contact areas with sand bodies.

Fig. 6-6: Sulphur contents from lignite samples from Locations 1 to 6. The thin black line represents sulphur contents measured by Stock et al. (2016) in their study on the Frimmersdorf Seam.

Fig. 6-7: Distribution of humic substances. a) Humin, b) Humic acid, c) Fulvic acid, in relation to the position of the sampled lignite within the Frimmersdorf Seam (see text for location details).

Fig. 6-8: Microphotographs of samples from Location 2 in incident- (a, c) and UV-light (b, d) showing examples of structured macerals: (a, b) ulminite (U) and corpohuminite (C) surrounded by suberinit (S); (c, d) funginite (F) in a matrix of attrinite (A) and densinite (D). The yellow scale (lower left corner) is 50µm.

- Fig. 6-9:** Contour map of the sulphur content of the Frimmersdorf Seam in the Garzweiler open-cast mine (RWE Power AG; see Fig. 6-1 for location).
- Fig. 6-10:** GWI/VI-, and GI/TPI ratios of samples from Locations 1 to 6. The GWI/VI ratios (a) were plotted onto the mire palaeoenvironment diagram of Calder et al. (1991). b) Classification of the paleo-mire type after Diessel (1986), in which the TPI are plotted against GI values.
- Fig. 6-11:** FeO/TiO₂ and MnO/TiO₂ ratios are used as indicators for the energy level of sediment transport in tidal flat marshes (Kolditz et al., 2012). a) Plot of FeO/TiO₂ ratios of the analysed lignites in comparison to the ratios of an “Average shale” and ilmenite after Wedepohl (1971). b) Plot of MnO/TiO₂ ratios of the analysed lignites, compared to the ratios of the “Average shale” and “Relocated sand” (after Kolditz et al., 2012).
- Fig. 7-1:** A structural map of the Lower Rhine Embayment (Germany/Belgium/The Netherlands), comprising the Roer Valley Graben and the Lower Rhine Basin. The red lines represent the major fault systems within the Lower Rhine Embayment (EF: Erft Fault, FF: Feldbiss Fault, JH: Jackerath Horst, PF: Peel Fault, RF: Rur Fault, TF: Tegelen fault, VF: Viersen Fault). The yellow areas mark the positions of former and active open-cast mines (G: Garzweiler, H: Hambach, I: Inden open-cast mines). The green stars indicate locations where sand injectites have been observed (1: present study location, 2: see Bajor (1958) and Berger (1958), 3: see Vanneste et al. (1999). The grey area represents the distribution of the Frimmersdorf Seam (RWE Power AG; western border is not specified). After Schäfer et al. (1996); Houtgast & van Balen (2000); Klett et al. (2002); Schäfer & Utescher (2014); Prinz et al. (2018).
- Fig. 7-2:** Stratigraphic log of the Lower Rhine Basin (modified after Klett et al. 2002; Schäfer et al. 2004, 2005; Schäfer & Utescher 2014; Prinz et al. 2018). The log is based on two well logs (RWE Power AG), and represents the stratigraphy in the centre of the Erft Block (see Fig. 1). The lithostratigraphical code was established by Schneider & Thiele (1965). Biostratigraphical ages (Ma, left) after Berggren et al. (1995), cycle ages (Ma, right) after Haq et al. (1987, 1988) & Hardenbol et al. (1998).
- Fig. 7-3:** and injectites within the Frimmersdorf Seam, (a) Sills and dykes within the Frimmersdorf Seam. Though sand injectites may be very thin, when compared to the entire seam thickness, their occurrence in swarms result in a noticeable decrease in economic value of the lignite. (b) Sand injectites within the

Frimmersdorf Seam are highly variable, both in terms of their morphology and orientation (pencil for scale).

Fig. 7-4: Classification of the parent sand unit (1) and intrusive complex (2), comprising the host unit (2a) and the sand injectites (2b).

Fig. 7-5: Syn-depositional channel fill at the base of the Frimmersdorf Seam, comprising trough cross lamination. Individual laminae may contain mm-fine organic remains, as well as cm-large wood fragments.

Fig. 7-6: Boundaries between the Frimmersdorf Sand (parent sand unit) and the Frimmersdorf Seam (host unit). (a) Well-defined root horizons, extending down into the Frimmersdorf Seam; (b) Roots, as well as syn-sedimentary structures are missing, sand, lignite and larger wood remains were probably reworked.

Fig. 7-7: Sand injectites within the Frimmersdorf Seam. (a) Sills (upper part) and high-angle dykes (lower part); (b) Sills (which may divide and reconnect along their length), dykes and irregularly-shaped injectites.

Fig. 7-8: 3D model of the Frimmersdorf Seam within the Garzweiler open-cast mine. (a) Top view with study locations (black points) and faults (red lines). Interestingly, the SW-NE-trending prominent depressions noted on the lower boundary (and which also occur on the upper boundary, see 8b) exactly parallel the orientation of the Variscan-age Aachen Fault, a notable thrust which faulted the Palaeozoic-age basement of the Lower Rhine Embayment (see Ribbert & Wrede 2005). (b) Lower (green) and upper (blue) boundaries of the lignite seam (vertical exaggeration x20), fault planes (red). The E-W trending Jackerath Horst faults show offsets of up to 100 m, while those of the faults to the N of the open-cast mine (NW-SE-trending) have offsets of only c. 1-15 m. The area to the E of the seam has a greater concentration of exploratory wells (being close to the exploration slope), thus providing a much more detailed picture of the geology of this particular zone.

Fig. 7-9: (a-i) Boundary types of the Frimmersdorf Seam (in areas where sand injectites occur) and their expression in the under- and overlying Frimmersdorf and Neurath sands, respectively.

Fig. 7-10: Rose diagrams of (a) the faults within the Garzweiler open-cast mine, (b) lignite surfaces from outcrops in the Frimmersdorf Seam, and (c) injectites that were exposed within the Frimmersdorf Seam.

Fig. 7-11: Map of the Frimmersdorf Seam within the Garzweiler open-cast mine. Modified after a RWE reservoir model (status 2016). The colour trends from green to red

represent the lignite contents (green areas: no sand within the seam, lignite completely exploitable; red areas: less than 10% of the seam usable for electricity generation). The blue lines represent the positions of the faults in the mining area.

Fig. 7-12: Dykes which are fed by the underlying Frimmersdorf Sand. (a) Asymptotic injectites, (b) Injectites with dyke-sill junction of 90°.

List of tables

Table 4-1: List of the criteria used for the classification of the sand bodies, their description and interpretation

Table 4-2: Broad time frame for the development of the various structures observed within the lignite of the Frimmersdorf Seam.

Table 6-1: Carbon, sulphur and ash contents at Locations 1-6; s: sample type, L: Location, n: number of samples.

Table 6-2: distribution of humic substances and Loss of Ignition (LOI); n = 27 samples; L = Location.

Table 6-3: Major element distribution from lignite samples from Locations 1-5, based on XRF analysis of 15 lignite samples; L: Location, n: sample ID.

1 Structure of the thesis

The thesis contains 7 chapters. Chapter 1 provides an overview of the layout of the thesis. The thesis has been written as a cumulative work, where individual chapters were submitted to international peer-reviewed journals. To date, two of these have been published, while a third is currently in review (see below for details).

Chapter 2 provides an introduction to the thesis, including some introductory remarks on the Lower Rhine Embayment and the Rhenish Lignite District. Section 2.1 includes a detailed description of the study location, i.e. the Garzweiler open-cast mine, and some general remarks on lignite mining in open-cast mines. In Section 2.2 the motivation for this thesis (both the scientific, as well as the economic motivated aspects), and the main research aims are specified. Section 2.3 comprises an overview of the methods that were used to improve our understanding of sand body occurrence within the Frimmersdorf Seam, Garzweiler open-cast mine, western Germany.

Chapter 3 is an overview of the geological framework of the Lower Rhine Embayment from Oligocene times through to the present day. Section 3.1 focusses on the tectonic evolution of the Lower Rhine Embayment in terms of the broader plate tectonic situation as well as its effects on local fault patterns. In Section 3.2, the sedimentary history of the Lower Rhine Embayment is described. This is closely associated with the history of basin subsidence providing accommodation space for the accumulating sediments, as well as changes in both climate and sea-level.

Chapter 4 is an overview of the sand bodies which were examined in detail in the Garzweiler open-cast mine from August 2014 to December 2015. The sand bodies within the Frimmersdorf Seam are extremely variable, in terms of – for example – their distribution, orientation, or composition. Therefore, an initial systematic classification was essential in order to provide a preliminary overview of the sand bodies and to contextualise them within the broader depositional and deformational mechanisms operating in the region both at the time of deposition and subsequently. This work also aided a better understanding of their formation. This chapter has been published in 2018 (published online in 2016) as a paper entitled ‘The geometry, distribution and development of sand bodies in the Miocene-age Frimmersdorf Seam (Garzweiler open-cast mine), Lower Rhine Basin, Germany: implications for seam exploitation’ in the Geological Magazine.

Chapter 5 comprises a detailed analysis of one sand body that was exposed in the Garzweiler open-cast mine in November 2015. The chapter comprises the graphical evaluation of the high-resolution laser scanning of this sand body in seven consecutive sections. The interpretation of the various sedimentological features present within the sand body provides detailed information on the depositional environment of the Lower Rhine Embayment in Langhian/Serravallian times.

In Chapter 6, the results of a high-resolution analytical investigation of the interrelationship between sand bodies and the adjacent lignite are presented. Detailed geochemical, coal petrological and micropetrographical analyses were conducted in order to improve our understanding of the emplacement mechanisms of sand in the lignite. A secondary aim was to examine the Miocene-age depositional environment. The study, which developed in a cooperation with the LEK (Lehrstuhl für Geologie, Geochemie und Lagerstätten des Erdöls und der Kohle; RWTH Aachen) was published in the *International Journal of Coal Geology* (179, June 2017), with the title 'Syn- and post-depositional sand bodies in lignite – the role of coal analysis in their recognition. A study from the Frimmersdorf Seam, Garzweiler open-cast mine, western Germany'.

Chapter 7 focusses on the presence of sand injection structures within the Frimmersdorf Seam. In particular, the relationship between the host unit, the sand injectites and the parent sand units were analysed. The collective data on sand bodies within the Garzweiler open-cast mine were integrated with a 3D reconstruction of the Frimmersdorf Seam, in order to understand the interrelationship between sand body occurrence and the seam morphology on the one hand, and the presence and orientation of faults on the other. The resulting manuscript, entitled 'Sand injectites – from source to emplacement: an example from the Miocene-age Frimmersdorf Seam, Garzweiler open-cast mine, Lower Rhine Embayment' has been recently submitted to a Special Volume of the Geological Society of London entitled *Subsurface Sand Remobilization and Injection*. The invitation to submit the manuscript to that Special Publication was based on my participation at the conference 'Subsurface Sand Remobilization and Injection: implications for oil and gas exploration and development' from 22-23 March 2017.

Chapter 8 comprises a summary of the main conclusions of the work, in which the motivations and research aims for this thesis are recapitulated.

The Appendix comprises supplementary material, as well an additional manuscript. This manuscript, entitled 'Facies analysis and depositional model of the Serravallian-age Neurath Sand, Lower Rhine Basin (W Germany)' is not actually part of the PhD project, as it is based on data from the preceding diploma thesis. However, the publication was written during the period of this PhD study, and comprises a completely reviewed interpretation, as well as a new

discussion. Additionally, the facies analysis of the Neurath Sand (forming one of the parent sand units, see above), directly overlying the Frimmersdorf Seam, revealed some important information on the Serravallian-age estuarine depositional environment, especially in terms of sea-level fluctuations and the energy levels of waves and tides.

2 Introduction

The Lower Rhine Embayment is an extended, flat area in NW Germany, Belgium and the Netherlands, which is crossed by the Rhine River from the SE to NW. Rich lignite deposits in the German part of the basin have been exploited since the mid-19th century, when lignite seams were exposed at the surface. Lignite exploration commenced in the southern parts of the Lower Rhine Embayment, and moved progressively to the NW following the submerging lignite seams. Presently, the lignite is exploited in three open-cast mines, which are run by the RWE Power AG.

The Lower Rhine Embayment is an Eocene-age rift basin (e.g. Zagwijn, 1989; Hager, 1993; Ziegler, 1992; Schäfer et al., 1996, 2005). It forms part of the European Cenozoic Rift System, which developed as a result of the Alpine and Pyrenean collision phases (Schumacher, 2002; Sissingh, 2003; Dèzes et al., 2004; Ziegler & Dèzes, 2005, 2007). The Lower Rhine Embayment can be subdivided into two major areas, namely the Lower Rhine Basin in Germany, and the Roer Valley Rift System in The Netherlands and Belgium. Within the German part of the basin, up to 1300 m of siliciclastic sediments were deposited from Oligocene times on (Schäfer et al., 1996; Klett et al., 2002). The peat accumulation in extended mires, in combination with sea-level fluctuations, ongoing subsidence, and optimal climatic conditions (Hager et al., 1981; Hager, 1986, 1993; Schäfer et al., 1996; Utescher et al., 2000, 2009; Zachos et al., 2001) resulted in the formation of the present-day Rhenish Lignite Deposits. Mining of lignite in open-cast mines requires that the groundwater level is constantly lowered. Therefore, numerous wells surrounding the open-cast mines were drilled to dewater deep and extended funnel-shaped areas. Up to 570 Mio km² groundwater per year are removed from the underground, and conducted to adjacent rivers or wetlands.

The long-term lignite exploration in the numerous pits and open-cast mines in the Lower Rhine Basin facilitated an intense geologic research in the area. The stratigraphic record of the Lower Rhine Embayment is based on close analysis of the various outcrops exposed in the numerous open-cast mines (both former and active), as well as the dense network of exploration and dewatering wells across the entire area. These have provided a wealth of not only stratigraphical information (e.g. Zagwijn & Hager, 1987; Hager, 1993; Klett et al., 2002; Schäfer et al., 2004, 2005; Schäfer & Utescher, 2014) but also have facilitated detailed analysis of the sedimentological (e.g. Boersma, 1981; Schäfer et al., 1996, 2005; Schäfer & Utescher, 2014), paleobotanical (e.g. Thomson, 1956; Teichmüller, M., 1958; Van der Burgh, 1973; Mosbrugger et al., 1994; Figueiral et al., 1999) and climatic (e.g. Mosbrugger et al., 2005; Utescher et al., 2000, 2009, 2012) information.

Lignite mining and combustion is certainly controversial in terms of resettlement, fine dust pollution, and CO₂ emissions. However, in terms of its scientific usefulness, working within an active open-cast mine offers great advantages, since it provides accessibility to stratigraphic records and tectonic features that would otherwise only be available in drilling cores or as geophysical well logs.

2.1 Study location

The study location, the Garzweiler open-cast mine, is located in the German part of the Lower Rhine Embayment, i.e. the Lower Rhine Basin. The Lower Rhine Basin is a c. 100 km long and 50 km wide, triangular shaped basin (Klett et al., 2002) that cuts into the NW margin of the Rhenish Massif (Schäfer et al., 1996; Klett et al., 2002).

There are two major river systems crossing the Lower Rhine Embayment, which drain the Rhenish Massif to the S: the Rhine River in the German part with an SE-NW-trending course, and the Maas River crossing the Belgian and Netherlands parts from SW to NE. Both river systems join in the NW part of the Netherlands to form one extended delta system entering the North Sea S of Rotterdam.

The Lower Rhine Basin is one of three active lignite mining locations in Germany. The combustion of lignite from the study area, as well as the Central Germany and the Lusatia districts in the E generates c. 26% of the electricity produced in Germany (Ballisoy & Schiffer, 2001). In the Lower Rhine Basin, a total of 100 Mio tons of lignite are exploited per year. The lignites in the Lower Rhine Basin are of great economic interest, due to the seam thicknesses of up to 100 m (Hager et al., 1981; Hager, 1986; Schäfer et al., 1996) as well as the generally low ash and sulphur contents (Stock et al., 2016; this study).

Within the Lower Rhine Basin there are presently three active open-cast mines: the Inden, Hambach and Garzweiler open-cast mines, which are run by the RWE Power AG. They are located W of the Rhine River, between Köln to the SE, Mönchengladbach to the NE, Aachen to the SW, and Roermond to the NW. Within the Inden open-cast mine, 19 Mio t per year of lignites from the Köln Fm (Chattian-early Burdigalian) are exploited. The overburden-lignite-ratio amounts to 2:1. Here, lignite mining will end in 2030 (www.rwe.com). In the Hambach open-cast mine, the up to 100 m thick lignites of the so called Main Seam (Ville Fm; early Burdigalian-Serravallian) are mined, with up to 40 Mio t of lignite being exploited each year (www.rwe.com). The overburden-lignite-ratio in this mine is 6:1. Lignite mining probably will continue until 2040.



Fig. 2-1: Aerial view of the Garzweiler open-cast mine in the Lower Rhine Embayment (source: google earth).

The study location, i.e. the Garzweiler open-cast mine (Fig. 2-1), is located on the so called Venlo Block and is surrounded by a series of major fault systems such as the Jackerath Horst to the S or the Erft Fault System to the SE. Mining activity in the Garzweiler open-cast mine commenced in 1987 as a result of the amalgamation of the former Frimmersdorf-Süd and Frimmersdorf-Nord mining locations, which developed as part of the NW extension of the former lignite pits (e.g. the Bergheim, Fortuna-Garsdorf and Neurath pits), which are considered to be fully exploited (RWE Power AG).

The Garzweiler open-cast mine comprises two mining areas, the former Garzweiler I and the currently active Garzweiler II open-cast mines. In total, the approved mining area of Garzweiler II contains c. 1.3 billion tons of lignite in an area of 48 km², with c. 35-40 Mio t of lignite per year being exploited from three separate seams (namely the Morcken, Frimmersdorf and Garzweiler seams; RWE Power AG).

The overburden thickness ranges between 40 and 210 m, with an overburden-lignite-ratio of 4:1. At the western exploitation slope, lignite and overburden (i.e. mainly mud, sand and gravel) are extracted by 6 bucket wheel excavators (see Fig. 2-2) and, thus, the mining area is extended by 300 m per year from E to W. The lignite and overburden are transferred to their destination points by a system of conveyor belts with a total length of 92 km. The overburden,

which consists of fine to coarse-grained siliciclastic deposits is transported to the mine dump at the E side of the open-cast mine (see Fig. 2-3), in order to refill the areas of the Garzweiler open-cast mine that have already been fully exploited. The major part of the lignite is transferred to the coal-fired power plants, where it is used for electricity generation.



Fig. 2-2: Bucket-wheel excavator in the Garzweiler open-cast mine, removing upper parts of the Neurath Sand.



Fig. 2-3: Mine dump at the E side of the Garzweiler open-cast mine.

As a result of the mining activities in the Garzweiler area, 13 villages were relocated between 1961 and 2017. Based on the current state of the German energy management policy, mining activity will continue until 2045 (RWE Power AG). Following the cessation of active mining, the resulting recultivated areas will cover an area of 4400 ha, with 75% forestry, 20% agriculture, and 5% other use, e.g. wetlands (www.rwe.com). The recultivation of these areas benefits from the addition of rich loess deposits. These previously covered the mining area, and as part of the recultivation programme are spread on top of the backfill areas.

Due to the loss of volume as a result of the exploitation of the lignite, the mining area can only be partly refilled. The loss in volume will be landscaped to form a lake, which will cover an area of 23 km² and reach depths of up to 190 m. This artificial lake will be filled by groundwater backflow and precipitation, and additional water that will be drained from the Rhine River. The filling of the lake and the stabilization of the natural groundwater level will be completed approximately after c. 50 years.

2.2 Motivation and research approach

The present study was undertaken as a co-operative project between the Steinmann Institute and RWE Power AG (Cologne, Department GOC-L, Geological Deposits), which runs the Garzweiler open-cast mine. In the Garzweiler II open-cast mine, sand bodies (Fig. 2-4) within the Miocene-age Frimmersdorf Seam have been recognized for over 30 years. Due to their irregular distribution, their variable nature and their dark colouring when freshly cut, these sand bodies are extremely difficult to detect, both in the active mining ramp, as well as within the existing reservoir model. However, in order to avoid the uncontrolled input of sand into the coal-fired power plants, it is essential to be able to recognize the precise sand content of the lignite. While the combustion of sand-rich lignites reduces the efficiency of the power plants significantly, lower sand contents of up to 6% in the lignite are useful, since the abrasive effect of the sands in the boilers, and the modulation of the Fe:Si ratio (resulting in higher slagging temperatures) both increase the economic efficiency. However the sand should be fine-grained and absolutely homogeneous. Thus, sand bodies which are generally fine- to medium-grained but which may also contain pebbles are problematic.



Fig. 2-4: Sand bodies in the Frimmersdorf Seam (coin for scale).

Indeed, since 2008, the increasing occurrence of sand bodies in the lignites of the Frimmersdorf Seam has complicated both the mining activities and the processing of the lignite. Lignite that contains $\geq 17\%$ sand is classified as barren, so that in the past, up to 1.5 million tons of lignite had to be discarded. Though the introduction of new coal preparation plants at the conveyor belts reduced the waste significantly, the high-resolution detection of sand bodies within the future mining areas and, therefore, the calculation of future lignite volumes remain difficult and are often imprecise. The precise detection of the entire sand volume within future mining areas is further complicated by both the large distances between

the exploration and drainage wells, and the relatively low resolution of the geophysical well logs (sand bodies can only be detected if they are at least 10 cm thick).

The presence of the sand bodies in the lignites, here, in addition to their economic impact, also play a scientific role in that they help to elucidate the depositional environments and post-depositional processes of this segment of the Lower Rhine Embayment. The main research aims of the study on sand bodies in the Frimmersdorf Seam are as follows:

1. A **classification** of the sand bodies within the Frimmersdorf Seam, based on
 - 1.1 A detailed examination of the morphology and distribution of sand bodies within the outcrops of the Garzweiler open-cast mine, providing
 - 1.2 Six criteria to classify the highly variable sand bodies: (a) position, (b) morphology, (c) orientation, (d) composition, (e) grain size and (d) sedimentary structures.

2. To determine possible **emplacement mechanisms** of sand within the peat/lignite of the present-day Frimmersdorf Seam, including
 - 2.1 The timing of sand body formation
 - 2.2 Geochemical, coal petrological and micropetrographical analyses. In particular, (a) the interrelationship of sand bodies with the adjacent lignite, and, (b) the depositional environment in terms of water availability and its nature (freshwater/marine water) were analysed, in order to improve the understanding of sand body emplacement.

3. To improve the early and precise **prediction** of sand body occurrence in future mining area, based on:
 - 3.1 A three-dimensional reconstruction of the Frimmersdorf Seam (including lignite thicknesses, existing sand body positions, and fault orientations), in order to elucidate the influence of sand body occurrence on the seam morphology, and
 - 3.2 The comparison of measured sand body orientations with the regional fault systems.

2.3 Methods

2.3.1 Fieldwork

The analyses of sand bodies in the Frimmersdorf Seam were mainly based on fieldwork within the Garzweiler open-cast mine in the German part of the Lower Rhine Embayment (i.e. Lower Rhine Basin). Fieldwork analyses were carried out from August 2014 through to November 2017.

Working within an active mining area has the advantage that the outcrops are constantly refreshed. Therefore, an area covering the mining progress of three years could be analysed, and this also provides access to a three-dimensional outcrop. However, direct access to the sand bodies was only possible on ramps that connected two adjacent working floors. Therefore, the seam was not accessible to the N and S of this ramp. The fieldwork included examination of the localisation and distribution of the sand bodies, their morphology, grain size, the presence of sedimentary structures, as well as measurements of their orientation. The positions of all of the analysed sand bodies were measured with GPS (see Fig. 2-5). Also examined was the relationship between the sand body occurrence and the morphology of the boundary between the Frimmersdorf Seam and the overlying and underlying sand units.

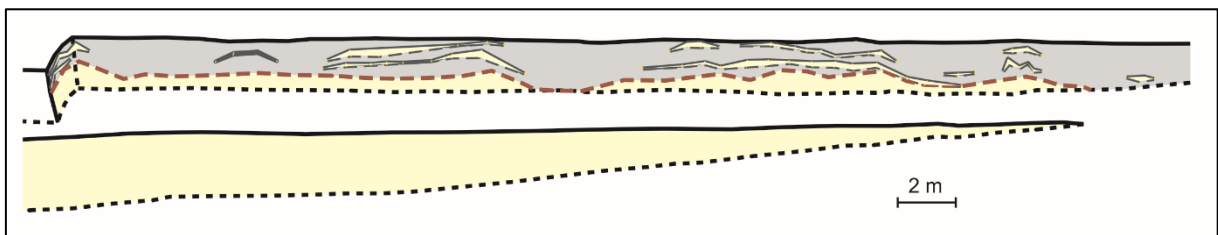


Fig. 2-5: High-resolution GPS-measurements of sand bodies (yellow) within an outcrop of the Frimmersdorf Seam (grey). The boundary between the Frimmersdorf Seam and the underlying Frimmersdorf Sand is indicated by the brown, dashed line.

2.3.2 Analytical approaches

Laboratory analyses commenced in August 2014, and continued through to November 2015. In addition to the analyses carried out as part of this thesis, the internal archives of the Department of Deposit Geology (RWE Power AG) were also data-mined and as such the current thesis includes work extending back over 30 years. Data used included grain size analyses as well as the geochemical composition of numerous sand bodies (all available from the RWE archives).

The analytical approaches also included geochemical, micropetrographical and coal petrological analyses, which were conducted at the LEK laboratories of the RWTH Aachen. The ash yields, major element compositions, humic substances distribution and the maceral compositions of a total of 79 samples were examined as part of this particular study.

2.3.3 3D model

The three-dimensional reconstruction of the Frimmersdorf Seam in the Garzweiler mining area is based on data from the RWE reservoir model. This model is based on geophysical well log data and drilling cores and also includes highly detailed field measurements (GOC-L). The 3D reconstruction is based on contour line sets from that reservoir model, representing the lignite boundaries, lignite thicknesses and known sand contents, and includes also information on the distribution and orientation of fault systems in the Garzweiler mining area. These data were supplemented by fieldwork measurements carried out as part of the present study, and including lignite-sand boundaries and the orientation of the sand bodies.

3 Geological framework

The Cenozoic-age Lower Rhine Embayment in NW Germany is part of the 1100 km long European Cenozoic Rift System, which is associated with the Variscan, Alpine and Pyrenean orogenic phases (Zagwijn, 1989; Ziegler, 1992; Schumacher, 2002; Sissingh, 2003; Dèzes et al., 2004; Ziegler & Dèzes, 2007; Rasmussen et al., 2010). The European Cenozoic Rift System consist of numerous subordinate graben systems, and extends from the Massif Central-Rhône Valley rift systems in S France, through to the Upper Rhine Graben in Germany. Near Frankfurt, the rift system bifurcates into two arms at the Rhenish Triple Junction (Schumacher, 2002; Sissingh, 2003; Dèzes et al., 2004; Ziegler & Dèzes, 2005, 2007). N of the Rhenish Triple Junction, the Hessen-Leine Depression extends to the SE, while the NW arm crosses the Rhenish Massif, passes into the Lower Rhine Embayment, and extends into the West Netherlands Basin and the S North Sea Basin (Prodehl et al., 1992; Ziegler, 1992; Geluk et al., 1994; Sissingh, 2003; Michon et al., 2003).

The Lower Rhine Embayment (Fig. 3-1) is one of the still active basins of the European Cenozoic Rift System. In the following sections, the evolution of the Lower Rhine Embayment from Palaeozoic to Quaternary times is described, including the tectonic evolution (chapter 3.1) and the depositional history (with particular attention to the German part, i.e. the Lower Rhine Basin; chapter 3.2).

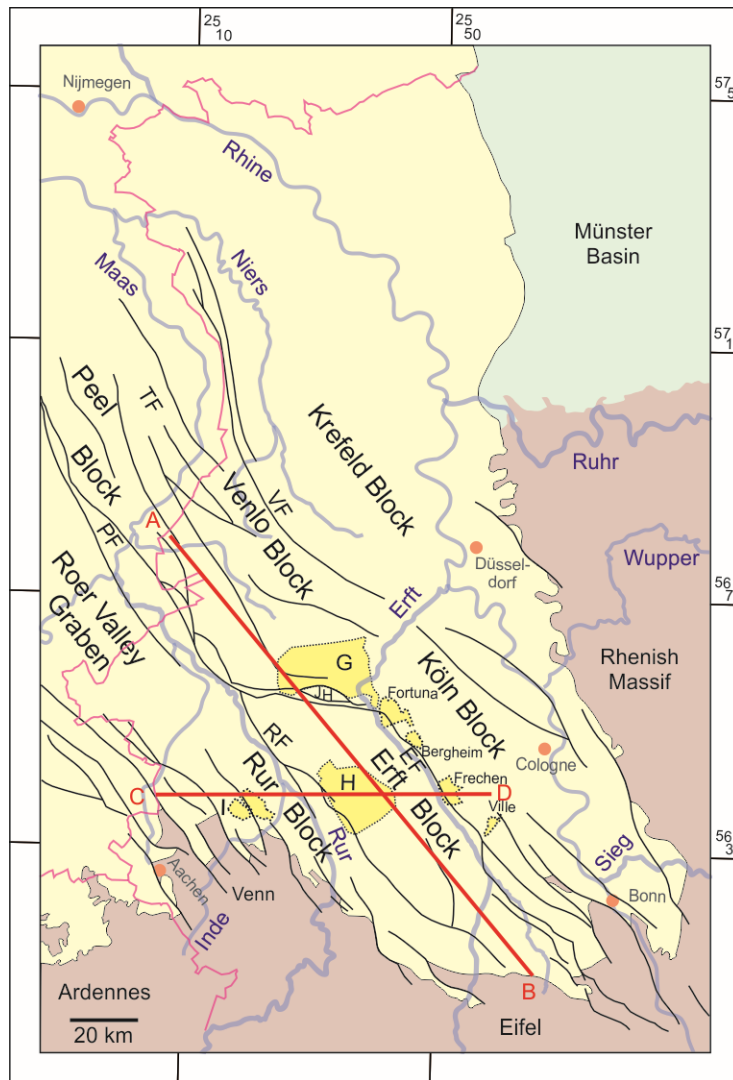


Fig. 3-1: A structural map of the Lower Rhine Embayment (after Schäfer et al., 1996; Houtgast & van Balen, 2000; Klett et al. 2002; Schäfer & Utescher, 2014). EF: Ertf Fault, FF: Feldbiss Fault, JH: Jackerath Horst, PF: Peel Fault, RF: Rur Fault, TF: Tegelen fault, VF: Viersen Fault. The former and active open-cast mines (RWE Power AG) are indicated by the yellow areas (G: Garzweiler, H: Hambach, I: Inden open-cast mines). The red lines (A-B, C-D) indicate the position of two cross sections, which are shown in Fig. 3-2).

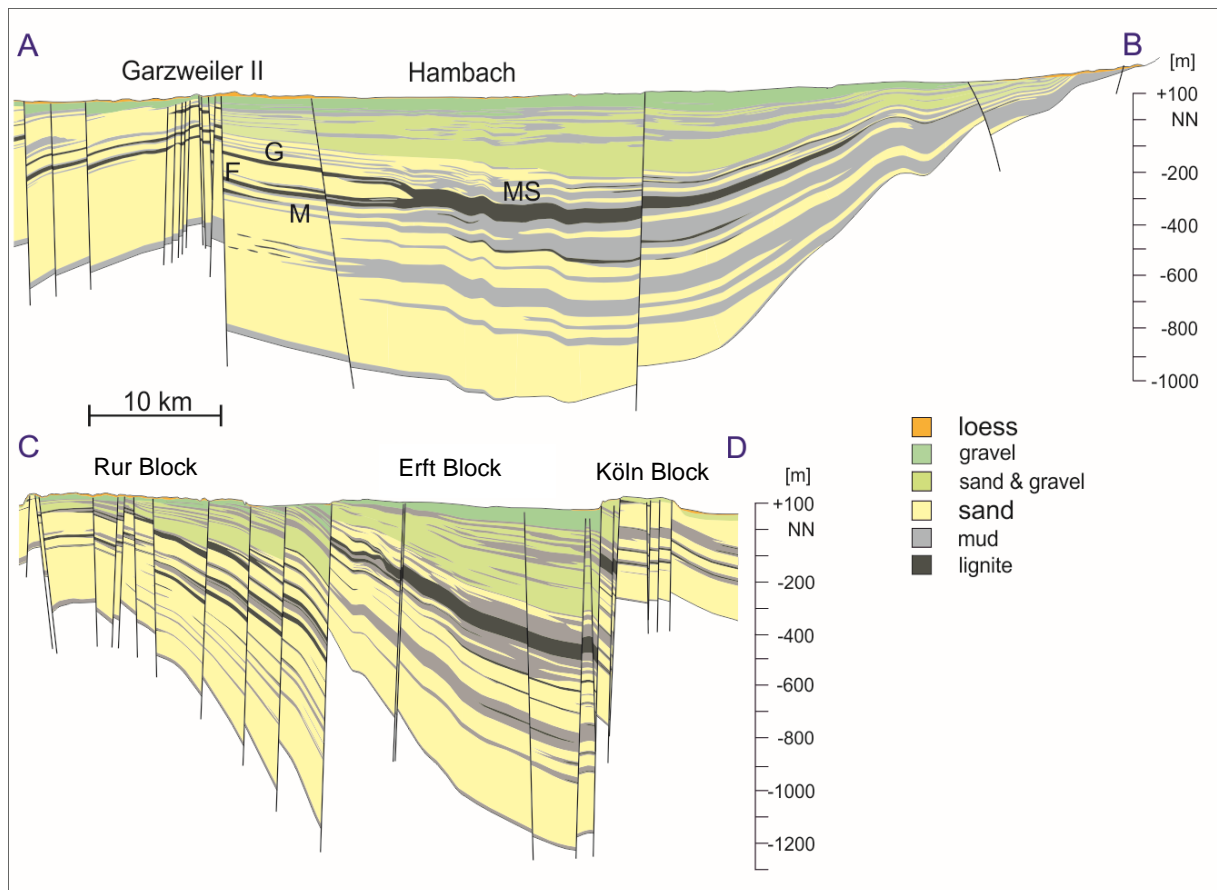


Fig. 3-2: Cross section A-B (NW-SE) and C-D (W-E; as indicated in Fig. 3-1). MS: Main Seam; M: Morken Seam, F: Frimmersdorf Seam, G: Garzweiler Seam.

3.1 Tectonic evolution of the Lower Rhine Embayment

In the Lower Rhine Embayment, the Cenozoic basin infill (see Fig. 3-2) rests unconformably on the Palaeozoic- and Mesozoic-age basement. The basement rocks can be directly correlated with the adjacent Rhenish Massif, which is part of the Rhenohercynian Zone of the Central European Variscan fold-and-thrust-belt (Dallmeyer et al. 1995; Franke, 1992; Oncken et al. 1999; Stets & Schäfer 2009). From Palaeozoic through to Mesozoic times, the evolution of the two adjacent areas (i.e. the basement of the Lower Rhine Embayment, and the Rhenish Massif) can be regarded as coherent.

The rocks forming the basement of the Lower Rhine Embayment and those of the adjacent Rhenish Massif were deposited in Devonian and Carboniferous times in a shallow to deep marine basin between Laurussia in the N, and Gondwana in the S (Dallmeyer et al., 1995; Stets & Schäfer, 2009, 2011). Within this so called Rhenohercynian Basin, mainly sandstones, siltstones and mudstones (Ribbert & Wrede, 2005) were deposited. The subsequent

shortening, folding and uplift of the Rhenohercynian Basin infill in early Carboniferous times was the result of the convergence between Laurussia and Gondwana (Dallmeyer et al., 1995; Stets & Schäfer, 2009, 2011).

In late Carboniferous and Permian times, the Variscan fold-and-thrust-belt was already eroded, with sediment being transported northwards towards the evolving Southern Permian Basin (McCann et al., 2006). Thus, the rocks which would subsequently form the basement rocks for the Lower Rhine Embayment and the Rhenish Massif were eroded to form a flat plain (Dallmeyer et al., 1995; Ziegler & Dèzes, 2007).

The tectonic evolution of the Lower Rhine Embayment and the adjacent Rhenish Massif in Cenozoic times was mainly controlled by the convergence of the Alpine and the European plates. During the main and late phases of the Alpine orogeny and the main folding phase of the Pyrenees, NW-directed, intra-plate, compressional stresses extended from the N Alpine foreland region through to the study area (Ziegler, 1992; Dèzes et al., 2004; Ziegler & Dèzes, 2007). As a result of these compressional stresses, a series of older Carboniferous and Mesozoic-age fault systems were reactivated in middle to late Eocene times (Ziegler, 1992; Zijerfeld et al., 1990; Winstanley, 1993; Geluk et al., 1994; Michon et al., 2003; Dèzes et al., 2004).

The NW-directed compressional stresses affecting the European crust resulted in lateral evasion movements of individual crustal segments to the W and, therefore, regional extensional regimes were established in NW Europe. These extensional stresses resulted in the formation of the numerous connected graben structures of the European Cenozoic Rift System. The positions of these subordinate grabens were pre-defined by the positions of the reactivated Carboniferous and Mesozoic-age fault systems (Ziegler, 1990; Zijerfeld et al., 1992; Winstanley, 1993; Geluk et al., 1994; Michon et al., 2003; Dèzes et al., 2004).

In the Lower Rhine Embayment at the NW end of the European Cenozoic Rift System, the initial rifting period began in Late Eocene times due to the reactivation of pre-existing faults at the NW margin of the Rhenish Massif (e.g. Ziegler, 1992; Sissingh, 2003, 2006; Schäfer & Utescher, 2014). Within the extensional tectonic regime, the Lower Rhine Embayment was separated into numerous (half-) graben and horst structures (Schäfer, 1994; Houtgast & van Balen, 2000; Houtgast et al., 2002; Bense & van Balen, 2004; Michon & van Balen, 2005; Schäfer et al., 2005; Schäfer & Utescher, 2014). These separated (half-) graben and horst structures are the Rur, Erft, Köln, Venlo and Krefeld blocks in the German part of the Lower Rhine Embayment (i.e. in the Lower Rhine Basin), as well as the Roer Valley Graben and the Peel Block in the Netherlands and Belgium forming the Roer Valley Rift System (according to e.g. Michon et al., 2003; see also Fig. 3-1).

The subsidence velocities of the numerous (half-) graben and horst structures in the Lower Rhine Embayment are variable. While the Erft Block subsided to a maximum depth of 1300 m, the Roer Valley Graben subsidence has been measured at 2000 m (Klett et al., 2002). In contrast, the Köln Block showed a degree of uplift when compared to the adjacent Erft Block. The Roer Valley Graben and the Erft Block form the deepest parts of the Lower Rhine Embayment. However, they are not in prolongation to one another, but the Erft Block is shifted to the SE.

In the Lower Rhine Embayment, the subordinate (half-) graben and horst structures are separated from one another by a series of major fault systems (Fig. 3-1). In the S part of the Lower Rhine Embayment, the Rur Block is separated from the Erft Block by the Rur Fault system, while the Erft Fault System separates the Erft from the NE Köln Block. In the NW part of the Lower Rhine Embayment, the Feldbiss (SW) and Peel fault systems (NE) bound the Roer Valley Graben. To the NW, the Tegelen Fault separates the Peel Block from the Venlo Block. The Venlo Block is bounded from the NW Krefeld Block by the Viersen Fault System

The various fault systems separating the numerous tectonic blocks in the Lower Rhine Embayment are mainly syn-sedimentary, and predominantly trend from NW-SE. Each major fault system consists of numerous subordinate faults, which are generally normal faults (Schäfer et al., 1996, Nickel, 2003; Sissingh, 2003). The fault activity varied over time as a result of the changing convergence rates between the African and European plates (Ziegler, 1992; Prodehl et al., 1992; Ziegler et al., 1995; Schumacher, 2002; Dèzes et al., 2004; Ziegler & Dèzes, 2005, 2006, 2007). Periods of increased subsidence in Oligocene times were followed by a decrease in fault activity in Miocene times, resulting from the W-directed shift of the Alpine orogeny (Klostermann et al., 2005). From Pliocene times onward, tectonic activity increased once more. This latter phase was related to the increased convergence rates between the African and European plates, and resulted in a period of uplift in the adjacent Rhenish Massif (Dèzes et al., 2004).

Tectonic activity in the Lower Rhine Embayment has persisted up to the present day. Indeed, the present-day NW-directed maximum horizontal stresses (caused by the ongoing NW-directed collisional stresses of the Alpine orogeny) and ongoing extension in the Lower Rhine Embayment caused some significant earthquakes in the recent history of the study area (Ziegler, 1992; Geluk et al., 1994; Hinzen, 2003, Sissingh, 2003, 2006; Schäfer et al., 2005; Ewald et al., 2006; Reicherter, 2008; Schäfer & Utescher, 2014; Grützner et al., 2016). The most prominent earthquakes occurred in Roermond 1992 ($M_b = 5.8$, see Michon & van Balen, 2005) and in Aachen 2002 ($M_L = 4.9$, see Hinzen & Reamer, 2007). In total, 2500 earthquakes, ranging from $M_L = 1.0$ to 6.1 were recorded from 1976 to 2002 (Hinzen, 2003).

3.2 Depositional history of the Lower Rhine Basin

The depositional history in this thesis focuses on the German part of the Lower Rhine Embayment, i.e. the Lower Rhine Basin. The stratigraphic history of the adjacent parts in Belgium and the Netherlands (i.e. of the Roer Valley Rift System) differ to varying degrees, largely as a result of their more distal position. In order to do these distal areas justice, an additional stratigraphic chapter would be necessary, but this would go beyond the scope of this work.

The depositional environment of the Lower Rhine Basin from Palaeogene times onward was controlled by a combination of tectonic activity (subsidence and fault activity, see chapter 3.1), and global sea-level and climatic fluctuations (Hager, 1993; Schäfer, 1994; Schäfer et al., 1996, 2005; Utescher et al., 2000; Zachos et al., 2001; Klett et al., 2002; Becker & Asmus, 2005; Schäfer & Utescher, 2014).

The sea-level fluctuations in the Lower Rhine Basin (and the adjacent Roer Valley Rift System), which were reconstructed from the sedimentary record, can be correlated with global sea level fluctuations (Haq et al., 1987; Zagwijn & Hager, 1987; Hager, 1993). More recently, they have been integrated into a sequence stratigraphic framework (Schäfer & Utescher, 2014).

The climatic conditions in the Lower Rhine Basin in Cenozoic times were reconstructed using wood remains as well as palynological data, and are correlated with a global cooling trend (Figueiral et al., 1999; Utescher et al., 2000; 2002; Zachos et al., 2001; Mosbrugger et al., 2005). Mean annual temperatures of 23-25 °C have been noted for Oligocene and Miocene times, decreasing to 13-14°C in late Pliocene times (Figueiral et al., 1999; Utescher et al., 2000; Mosbrugger et al., 2005) and further decreasing to 11°C in early Pleistocene times (Schäfer & Utescher, 2014). Precipitation rates in the depositional environment did not show any significant variations, and were relatively constant at 1000 mm/yr during most of the Cenozoic (Van der Burgh, 1973; Figueiral et al., 1999; Utescher et al., 2000).

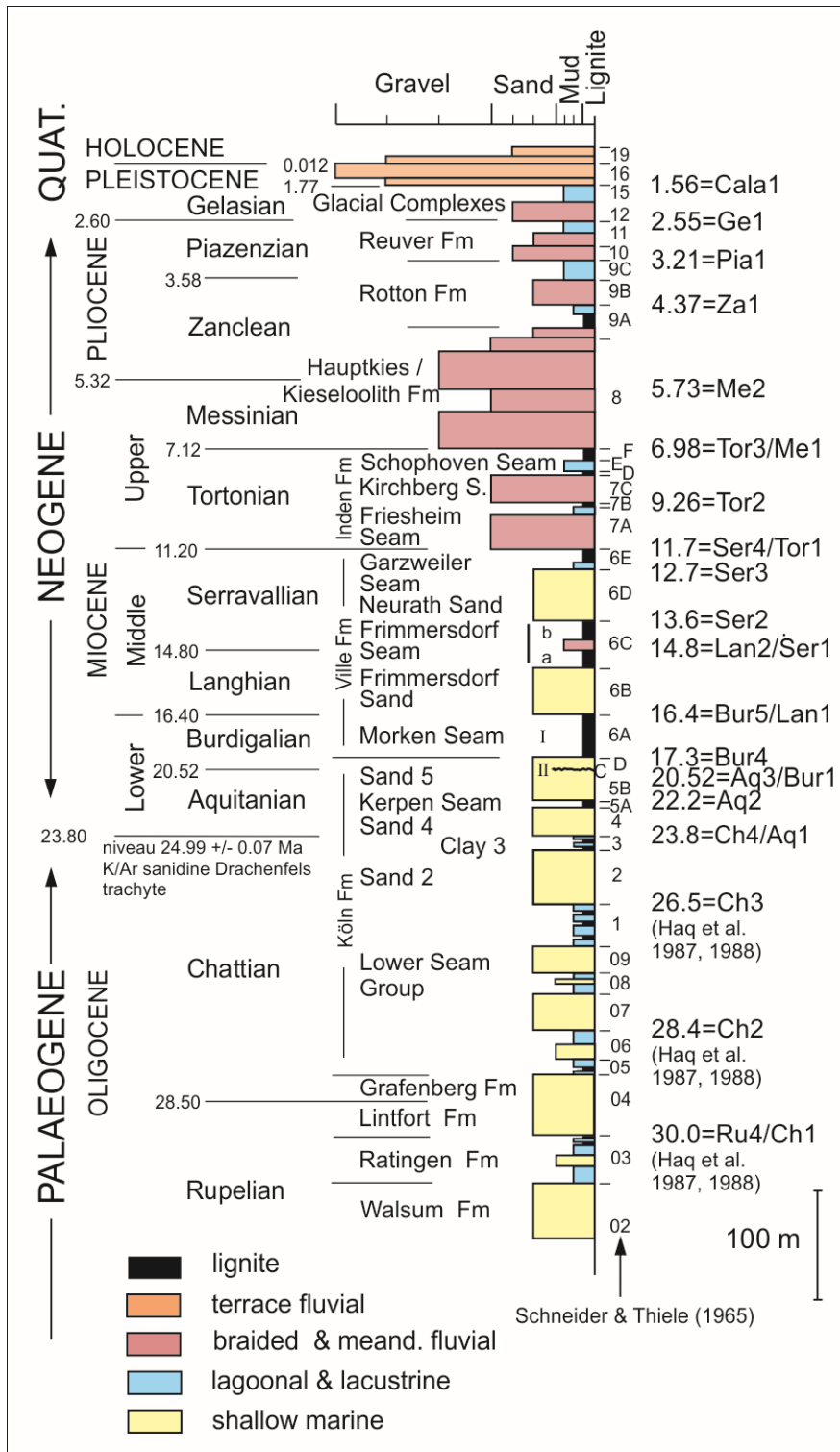


Fig. 3-3: Stratigraphic log of the Lower Rhine Basin (modified after Klett et al. 2002; Schäfer et al. 2004, 2005; Schäfer & Utescher 2014; Prinz et al. 2018). The log is based on two well logs (RWE Power AG), and represents the stratigraphy in the centre of the Erft Block (see Fig. 3-1). The lithostratigraphical code was established by Schneider & Thiele (1965). Biostratigraphical ages (Ma, left) after Berggren et al. (1995), cycle ages (Ma, right) after Haq et al. (1987, 1988) & Hardenbol et al. (1998).

3.2.1 Palaeogene

The initial subsidence of the Lower Rhine Basin in early Oligocene times allowed the Cenozoic-age North Sea to transgress onto the flat Palaeozoic and Mesozoic basement (Schäfer et al., 1996). In the funnel-shaped Lower Rhine Basin, an extended estuary formed due to the interaction of tides and waves in the North Sea on the one hand, and rivers entering the basin from the adjacent Rhenish Massif on the other (Hager, 1993; Schäfer et al., 1996; Schäfer & Utescher, 2014).

In Rupelian times, sands and clays were deposited in an estuarine setting under subtidal to supratidal conditions (Petzelberger, 1994; Schäfer et al., 1996; Klett et al., 2002; Schäfer & Utescher, 2014). The Rupelian-age estuarine sand deposits of the Walsum, Ratingen and Lintfort fms (Fig. 3-3) pass laterally into the so called Rupel Clay Member, which is distributed throughout the complete present-day onshore area of the Netherlands (Vis et al., 2016) and represents the distal shelfal areas in Oligocene times (Klett et al., 2002). These Rupelian-age deposits (i.e. both sands and the overlying clays) of the Walsum, Ratingen and Lintfort fms are considered to represent a transgressive system tract (TST), including a maximum flooding surface within the deposits of the Lintfort Fm (Schäfer & Utescher, 2014; see also Fig. 3-3). In the southern part of the Lower Rhine Basin, the depositional environment becomes increasingly continental/nearshore and here the estuarine sands are replaced by mud deposits which were deposited in a back-barrier tidal environment (Klett et al., 2002).

The deposition of the Köln Fm sediments commenced in Chattian times, (Fig. 3-3). These sands were deposited in the high-energy part of the estuarine setting. Coeval clay deposits represent fluvial input from several small rivers (Hager, 1993; Schäfer et al., 2004; Klett et al., 2002; Schäfer & Utescher, 2014). Due to a decrease in basin subsidence and a short-term retreat of the coastline, small mires became established in the S part of the Lower Rhine Basin (Hager, 1993; Becker & Asmus, 2005; Schäfer & Utescher, 2014). The accumulation of peat (the present-day Lower Seam Group; see Fig. 3-3), however, was intermittent, and the thin peat layers were regularly covered by fluvial sediments derived from the SE, or marine sediments transported from the NW as a result of marine flooding (Becker & Asmus, 2014).

A basin-wide transgression (correlated with a global eustatic sea level rise; see Hardenbol et al., 1998; Utescher et al., 2002) of the North Sea in late Chattian times resulted in the development of a sea-way connecting between the North German Basin and the Upper Rhine Graben as well as the flooding of the adjacent Rhenish Massif (Ziegler, 1992; Utescher et al., 2000). In the Lower Rhine Basin, the so-called 'Sand 2' (according to the Schneider & Thiele nomenclature from 1965; see also Utescher et al., 2002) was deposited. The deposition of this sand body is considered to represent a sea-level highstand (HST). This particular highstand in

the Lower Rhine Basin was associated with a global sea-level rise (i.e. Ch3 after Hardenbol et al. 1998), and the 'Late Oligocene Warming' period (Zagwijn & Hager, 1987; Utescher et al., 2002; Schäfer & Utescher, 2014).

3.2.2 Neogene

The Miocene-age depositional environment was mainly controlled by the marked sea-level variations which occurred at that time. Periods of sea-level rise alternated with periods of sea-level fall correlating with the development of extensiver mires spreading across the southern and central parts of the Lower Rhine Basin (Haq et al., 1987; Zagwijn & Hager, 1987; Hager, 1993; Schäfer et al., 2004, 2005; Klett et al., 2002; Schäfer & Utescher, 2014).

In Aquitanian times, the peats of the Kerpen Seam accumulated in the central part of the Lower Rhine Basin. To the S, the peats passed laterally into muds that were deposited in fluvial and lacustrine depositional environments (Schäfer et al., 2004; Becker & Asmus, 2005). The Kerpen Seam, and the overlying Aquitanian-age shallow-marine sand deposits are still considered to form part of the Köln Fm, since the conditions in the depositional environment were quite similar to those of late Oligocene times.

Whereas the formation of mires in the Lower Rhine Basin thus far was locally restricted and comparably short-lived, in Burdigalian times paralic environments became established – for the first time – across the entire basin. The reason for this was mainly due to a partial regression of the North Sea and a basin-wide rise of the groundwater level (Becker & Asmus, 2014). In the central part of the basin, up to 270 m of peat accumulated over a time span of 9-10 Ma (from Burdigalian through to Serravallian times; Hager, 1993). Subsequent to their compaction and initial coalification, these peats form the present-day, up to 100 m thick Main Seam of the Ville Fm (Hager et al. 1981; Hager 1993). However, continuous peat accumulation was only possible in the central part of the basin. To the NW, the North Sea repeatedly transgressed onto the mire, and, here, the Main Seam was subdivided into three subordinate seams, namely the Morken, Frimmersdorf and Garzweiler seams (Figs. 3-2 & 3-3). The lowermost Morken Seam was deposited in Burdigalian times.

In Langhian times, the Morken Seam was covered by the shallow-marine to coastal Frimmersdorf Sand. This sandy unit was deposited as a result of the North Sea flooding the mire. The Frimmersdorf Sand mainly consists of fine- to medium-grained, white-coloured quartz sands (Petzelberger, 1994). At the top of this sand unit, well-preserved root horizons mark the transition from the shallow-marine conditions, which prevailed during the accumulation of most of the present-day Frimmersdorf Sand, through to the coastal and paralic

conditions which followed. The roots represent the in situ vegetation of the mire which was established subsequent to the retreat of the North Sea. The root horizons extend into the Frimmersdorf Sand from the overlying Frimmersdorf Seam, which accumulated at the transition from Langhian to Serravallian times.

A subsequent transgression of the North Sea in mid-Serravallian times resulted in the deposition of the up to 60 m thick Neurath Sand (see Appendix A). This sand unit comprises a succession from subtidal through to supratidal sediments that accumulated in a high-energy estuarine setting in the Langhian-age Lower Rhine Basin.

The Burdigalian to Mid-Serravallian succession of estuarine sands and lignites that accumulated in the Lower Rhine Basin, correlate with a peak in the warming period that was ongoing during Oligocene times. During the Middle Miocene Climatic Optimum (17-15 Ma), mean annual temperatures were about 20°C, and these warm and humid conditions facilitated an acceleration in the growth of the peat-forming vegetation (Lücke et al., 1999; Utescher et al., 2000; 2002, 2009; Schäfer & Utescher, 2014; Stock et al., 2016).

In late Serravallian times, the peats of the present-day Garzweiler Seam were deposited on top of the Neurath Sand. The lignites of the Garzweiler Seam comprise noticeable contents of fossil wood remains, mainly from gymnosperm taxa (Taxodiaceae and Cupressaceae, Lücke et al., 1999). This period was related to a globally correlatable cooling trend (Hardenbol et al., 1998; Utescher et al., 2002) following the Middle Miocene Climatic Optimum. This cooling was also associated with a major eustatic sea-level fall.

The sea-level fall noted above, resulted in the retreat of the North Sea from the Lower Rhine Basin at the Serravallian/Tortonian transition (Boersma et al., 1981; Abraham, 1994; Valdivia-Manchego, 1994; Schäfer & Utescher, 2014). From earliest Tortonian times onward, and coeval with a period of extreme sea-level lowstand (Haq et al., 1988; Utescher et al., 2000, 2002, 2009; Stock et al., 2016), a new river system, draining the Rhenish Massif to the S, became established. This new fluvial system crossed the central part of the Lower Rhine Basin carrying sediment from the uplifting Rhenish Massif into the coastal environments to the N. The fluvial system comprised a high-sinuosity meandering river and has been interpreted as representing a predecessor of the present-day Rhine River (Gliese & Hager, 1978; Hager, 1993; Schäfer et al., 2004). The rapid accumulation of clastic fluvial sediments in the Lower Rhine Basin resulted in significant compaction of the underlying peat deposits of the Ville Fm (Hager, 1993).

In the western part of the basin, sediment accumulation rates were comparatively low (in comparison with the fluvial-dominated succession to the E) and, thus, locally restricted mires

were established (Schäfer et al., 2004). Within these mires, the peat accumulations of the present day Friesheim, Kirchberg and Schophoven seams (Upper Seam Group) formed. Together, these seams have a total thickness of 38 m (Schäfer et al. 2004). The peat accumulation, however, was repeatedly interrupted by periods of river channel avulsion, and, thus, clastic sediments were deposited within the peats as channels, crevasse splays or oxbow lakes (Boersma et al., 1981; Abraham, 1994; Schäfer et al., 1994). This succession, i.e. the so called Inden Fm represents a regressive system tract (RST) within the Lower Rhine Basin, resulting from the retreat of the North Sea. The regressive phase was associated with a fall in global temperatures (Utescher et al. 2000). Several features, e.g. ice-rafted debris, benthic foraminiferal isotope records or planktonic $\delta^{18}\text{O}$ records indicate, that the stepwise cooling of the Northern Hemisphere from Late Miocene times on was associated with early glaciations events (Utescher et al., 2000), interrupted by numerous interglacial periods.

In Messinian times, coarse-grained sand and gravel deposits were deposited under high-energy conditions in braided river systems in the subsiding Rhine Basin (Abraham, 1994; Valdivia-Manchego, 1996; Klett et al., 2002; Schäfer & Utescher, 2014). The sediments which comprise the Messinian-age Hauptkies Fm was associated with an early glaciation event (6.3-6.2 Ma glacial event) related to the ongoing temperature decrease (Utescher et al., 2000). A subsequent increase of mean annual temperatures at the Messinian/Zanclean transition was correlated with an interglacial period (Utescher et al., 2000).

In Zanclean times, the depositional environment was still dominated by river systems. However, the sediments which were deposited were increasingly fine-grained, in comparison to those of the underlying Messinian-age Hauptkies Fm. (Klett et al., 2002; Schäfer et al., 2004; Schäfer & Utescher, 2014). The Zanclean-age Rotton Fm and the stratigraphically overlying Piazenzian-age Reuver Fm comprise sediments (sands and muds) that were deposited in deltas, lakes and meandering rivers (Schäfer & Utescher, 2014). The Pliocene-age deposits of the Lower Rhine Basin are associated with a stepwise cooling to mean annual temperatures of 15°C in late Pliocene times (Mosbrugger et al., 2005; Utescher et al., 2012).

3.2.3 Quaternary

Tectonic activity, and major climatic changes largely controlled the depositional environment in Quaternary times (e.g. Zagwijn, 1975; Zachos et al., 2001; Busschers et al., 2007). The climatic change in NW Europe, sea-level fluctuations, and glaciations (Busschers et al., 2007) are related to the repeated expand and disintegration of the Scandinavian, Baltic and British ice masses (Clark et al., 2004; Mangerud, 2004; Svendsen et al., 2004; Busschers et al., 2007). In Pleistocene times, subsidence of the Lower Rhine Basin accelerated. Associated with this phase of basin subsidence was a period of uplift of the adjacent Rhenish Massif (Fuchs et al., 1983; Meyer & Stets, 1998; Klett et al., 2002). In the Lower Rhine Embayment, the glaciations of the Northern Hemisphere, in combination with the tectonic activity within the basin, resulted in a re-organisation of the depositional environment.

The deterioration of vegetation due to the climate cooling and continuous permafrost resulted in an increased supply of coarse-grained sediments (van Balen et al., 2010). This, combined with an extreme sea-level lowstand during glacial periods (up to 100 m below the present-day sea-level), and highly peaked discharge regimes during snowmelt events (van Balen et al., 2010) resulted in the formation of extended systems of braided rivers (Rhine and Maas rivers) that spread across the entire Lower Rhine Basin (Klett et al., 2002).

In the German part of the Lower Rhine Embayment (the Lower Rhine Basin), a succession of sand and gravel formed in the extended braided river system in Pleistocene times, and these so called Rhine River terraces are interpreted to represent a lowstand system tract (LST, Schäfer & Utescher, 2014). The gravel-rich sediments of the so called Main Terraces, which accumulated in Middle Pleistocene times, are the result of the final uplift of the Rhenish Massif to its present-day elevation (Fuchs et al., 1983; Meyer & Stets, 1998; Klett et al., 2002), and the resultant formation of an outwash-fan by the Rhine River (Boenigk, 1978, 1990, 1995 a, b; Schirmer, 1994; Klett et al., 2002).

During the maximum glaciation period, the Drenthe stage of the Saalian glaciations period, ice tongues of the Scandinavian ice sheet extended as far as the northern part of the Lower Rhine Embayment. Relicts of these glacial periods can be found in the present-day morphology, including ice-push ridges, sandurs, ice-marginal fluvial terraces (Mosbrugger et al., 2005), as well as ice wedges and thick loess deposits (Thome, 1959).

Due to the uplift of the Vile in Mid Pleistocene times, a prominent ridge crossing the Lower Rhine Basin from SE to NW, the Rhine River was forced to shift to the E, and subsequently, the Middle (Mid Pleistocene-age) and Lower Terraces (late Pleistocene times) accumulated (Boenigk, 1990; Fischer, 2010). To the NW, in the Netherlands, the glacial deposited fluvial and aeolian sediments are intercalated with marine beds, each of which represents short term interglacial periods (Zagwijn, 1975).

4 The geometry, distribution and development of sand bodies in the Miocene-age Frimmersdorf Seam (Garzweiler open-cast mine), Lower Rhine Basin, Germany: Implications for seam exploitation.

Linda Prinz, Tom McCann, Andreas Schäfer, Sven Asmus, Peter Lokay

Originally published online in Geological Magazine 2018 (Published online: 23 November 2016), Volume 155, Issue 3, pp. 685-706.

4.1 Abstract

The Cenozoic-age Lower Rhine Basin is located in the NW part of the European Cenozoic Rift System. In Miocene times, a combination of warm climatic conditions and basin subsidence resulted in the deposition of up to 100 m of lignite (i.e. Main Seam of the Ville Fm). The Main Seam can be subdivided into the Morken, Frimmersdorf and Garzweiler seams, separated by two intercalated transgressive sand units, namely the Frimmersdorf and Neurath sands, deposited in a shallow-marine, tide-dominated environment.

The lignite seams of the Ville Fm are currently worked by RWE Power AG, in the Garzweiler II open-cast mine. In the Frimmersdorf Seam (between the Frimmersdorf Sand and the Neurath Sand), the presence of small-scale sand bodies, together with their variable dimensions affects the industrial exploitation of the seam. Moreover, their irregular distribution complicates their precise and early recognition. Indeed, so-called barren lignite ($\geq 17\%$ of sand) and completely clean units can occur within a few metres of each other.

Initial classification of these highly variable sand bodies suggests a variety of both syn- and post-depositional causal mechanisms, providing evidence of an extremely complex depositional and post-depositional system. Syn-depositional sand bodies were deposited in a swamp area that was located in the fluvial-dominated subenvironment of an extended tidal estuary. The post-depositional formation of sand bodies is related to the intrusion of fluidized sands from the underlying Frimmersdorf Sand. These sand injectites within the Frimmersdorf Seam are considered to be linked to seismic activity within the Lower Rhine Basin.

4.2 Introduction

The Lower Rhine Basin is part of the European Cenozoic Basin (Fig. 4-1) which extends ca. 1100 km from the Mediterranean to the North Sea (e.g. Zagwijn, 1989; Ziegler, 1992; Sissingh, 2003; Dèzes et al., 2004). The European Cenozoic Basin formed as a result of passive rifting in late Eocene times, related to the reactivation of late Variscan, Permo-Carboniferous and Mesozoic fracture systems (Dèzes et al., 2004). The 100 km long and 50 km wide (Klett et al., 2002), triangular-shaped Lower Rhine Basin extends from the Netherlands in the NW to Bonn in the SE and cuts into the NW margin of the Rhenish Massif (Fig. 4-1).

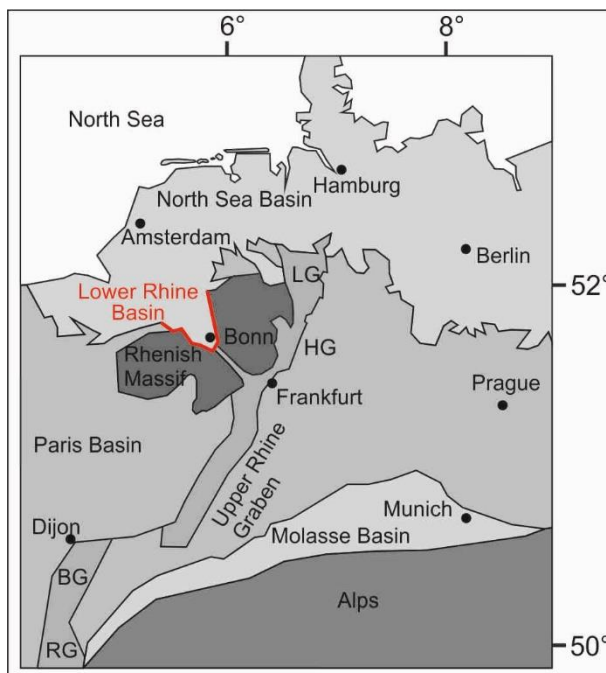


Fig. 4-1: A structural map of the NW European Cenozoic Rift System. At its northern end the Upper Rhine Graben bifurcates into the Hessen and Leine grabens to the NE, and the Lower Rhine Basin in the NW (Rhenish Triple Junction in the area of Frankfurt; after Schumacher, 2002; Sissingh, 2003 and Rasser et al., 2008).

The German part of the Lower Rhine Basin contains c. 1300 m of Oligocene- to Pleistocene-age siliciclastic sediments with associated lignite seams (Schäfer et al., 1996; Klett et al., 2002). The depositional succession records a transgressive-regressive trend beginning with marine deposits overlying Palaeozoic- and Mesozoic-age basement (Klett et al., 2002) in Rupelian times, through to a continental-marine environment from Chattian to Messinian times (late Oligocene to late Miocene) and a final phase of continental sedimentation from Zanclean times (early Pliocene) onward (Sissingh, 2003; Schäfer & Utescher, 2014).

During Miocene times regression of the North Sea and warm and temperate climatic conditions (Utescher et al., 2000, 2009; Zachos et al., 2001) in combination with ongoing subsidence (Hager, 1993; Schäfer et al., 1996) favoured the accumulation of up to 270 m of peat deposits

in the centre of the basin (Hager et al., 1981; Hager, 1986; Schäfer et al., 1996). These thick peat accumulations formed the Main Seam of the Ville Fm (present-day thickness: up to 100 m; Figs. 4-2- & 4-3). In the NW part of the Lower Rhine Basin the Main Seam is subdivided by two transgressive marine sand units (Frimmersdorf and Neurath sands) into the Morken, Frimmersdorf and Garzweiler seams (Figs. 4-2 & 4-3).

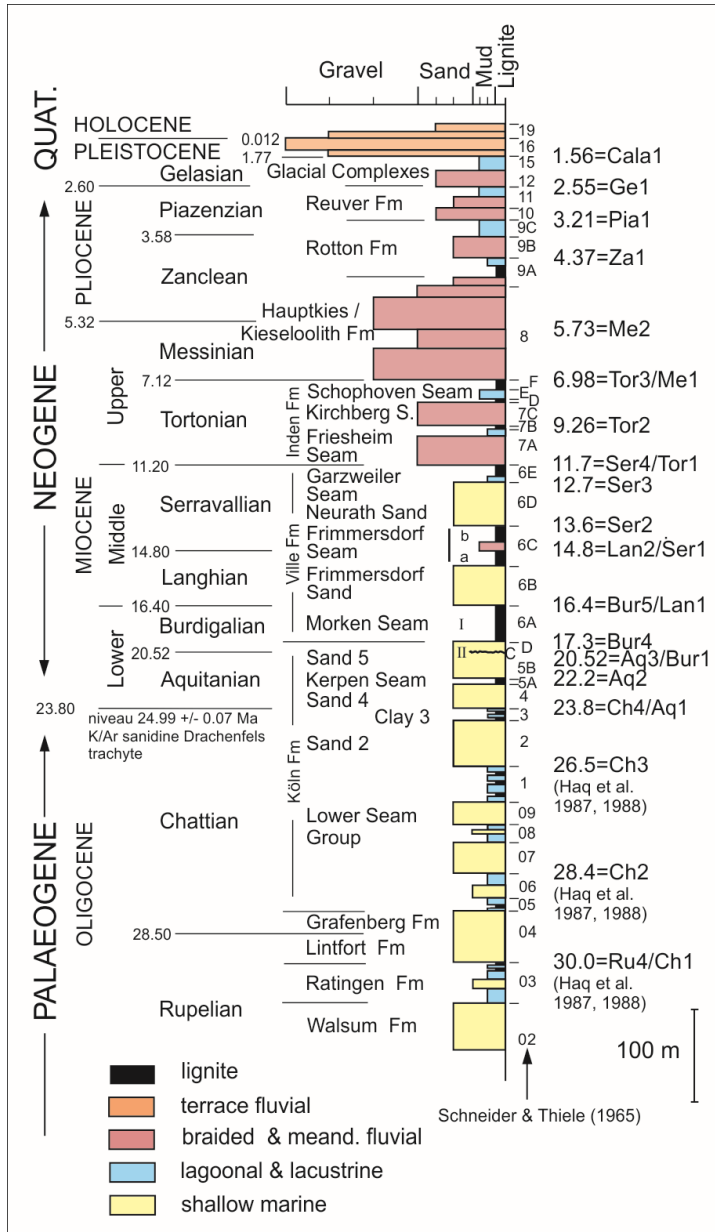


Fig. 4-2: Stratigraphic log of the Lower Rhine Basin (after Klett et al., 2002; Schäfer et al., 2004, 2005; Schäfer & Utescher, 2014). The lithostratigraphy is a synthesis based on the SNQ 1 (Erft Block) and Efferen (Köln Block) wells (RWE Power AG), and taken to represent the stratigraphy at the centre of the Erft Block (lithostratigraphical code established by Schneider & Thiele, 1965). Biostratigraphical ages [Ma] on the left after Berggren et al. (1995), cycle ages [Ma] after Hardenbol et al (1998).

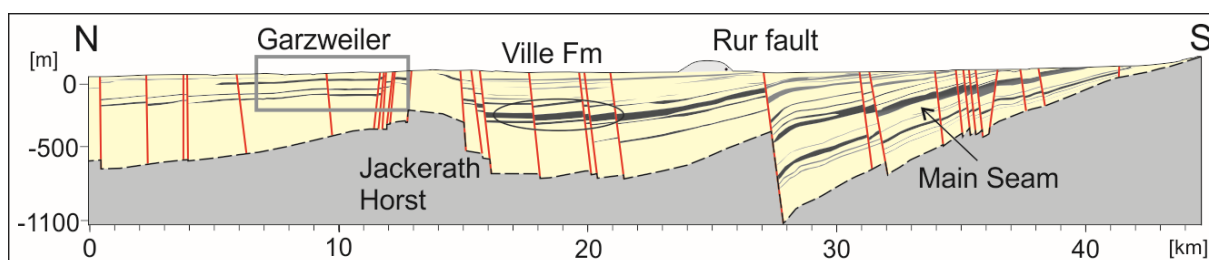


Fig. 4-3: N-S-oriented cross section of the Lower Rhine Basin (N-S line in structural map, Fig. 4-4), cross cutting the Jackerath Horst, the Garzweiler open-cast mine (rectangle) and a series of normal and reverse faults. The Main Seam is present in the SE, subdividing into the Morken, Frimmersdorf and Garzweiler seams in the NW (Ville Fm indicated by oval; stratigraphy based on RWE data).

The Lower Rhine Basin has been the subject of increased scientific and economic interests in the 20th century, resulting in a wide range of stratigraphic, sedimentological, palaeoclimatic and palaeontological studies (Teichmüller, M., 1958; Teichmüller, R., 1958, 1974; Utescher et al., 1992; Hager, 1993; Schäfer et al., 1996, 2005; Klett et al., 2002; Becker & Asmus, 2005; Schäfer & Utescher, 2014). The thick lignite accumulations in the Lower Rhine Basin have been exploited since the 19th century, when industrial open-cast mining first commenced. Today, there are three active open-cast mines run by RWE Power AG in the region, namely Hambach, Inden and Garzweiler (Fig.4-4). The Garzweiler open-cast mine (this study), NW of Cologne, was developed in 1983 as the northwestern extension of the older Frechen, Bergheim, Fortuna-Garsdorf and Frimmersdorf open-cast mines (RWE Power AG). In the Garzweiler II open-cast mine, the seams of the Ville Fm with an initial lignite amount of 1.2 billion of tons are currently mined, mainly for electricity generation (RWE Power AG, internal reports).

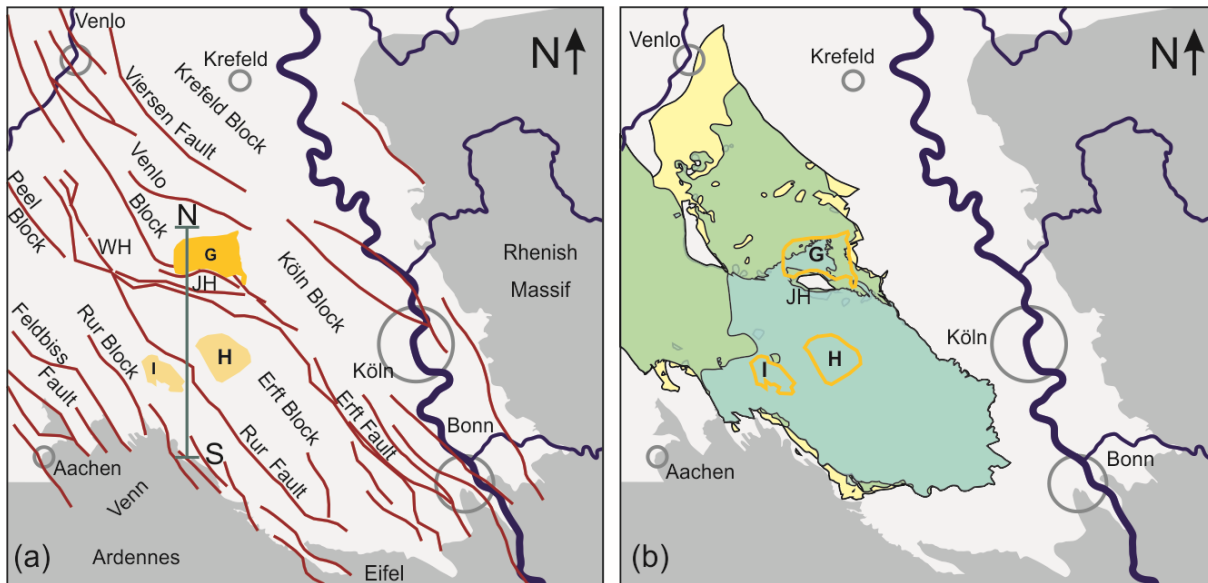


Fig. 4-4: Structural maps of the Lower Rhine Basin. a) The NW part of the Lower Rhine Basin comprises the Peel, Venlo and Krefeld blocks in the N and the Rur, Ert and Köln blocks in the S (after Schäfer & Utescher, 2014; RWE Power AG); each of the blocks are separated by major fault systems; section N-S: see Fig. 4-3. b) Distribution of lignite within the Lower Rhine Basin (yellow Morcken Seam; green: Frimmersdorf Seam; blue: Garzweiler Seam; based on RWE data). JH = Jackerath Horst; G = Garzweiler open-cast mine; H = Hambach open-cast mine; I = Inden open-cast mine.

The Langhian/Serravallian-age Frimmersdorf Seam in the Garzweiler open-cast mine contains sand bodies, which are broadly distributed throughout the entire Garzweiler mining area, and which have been recognised for over 30 years (RWE Power AG internal report). Their irregular distribution as well as their extremely variable nature has detrimentally affected both the mining and processing of the lignite. Indeed, the increase in the occurrence of sand bodies within the seam, as well as their extent has – since 2008 – complicated mining in the area, so that up to 1.5 million of tons of lignite per year has had to be discarded during this period (RWE Power AG, internal report). Currently the economic loss is significantly reduced as a result of additional processing in coal preparation plants. The situation would be greatly eased by early recognition of the entire sand volume in any future mining areas. However, this is difficult, largely due to the fact that most sand bodies are restricted in their thickness (centimetres up to metres). The distances between the exploration wells and the resolution (sand bodies have to be at least 10 cm thick) of geophysical logs (e.g. gamma ray, density, resistivity) impede the precise location of sand bodies and, therefore, the medium to short-term disposal of lignite volumes which, as noted above, is an important aspect for future planning and mining.

The origin and emplacement of these sand bodies has, to date, not been examined. This study is the first to provide a detailed classification of the highly variable sand bodies, with the aim

of reconstructing their origin and emplacement mechanisms as well as providing a temporal framework for these processes.

4.3 Geological Setting

The Lower Rhine Basin is located at the NW end of the European Cenozoic Rift System, which extends c. 1100 km from the Mediterranean via the Upper Rhine Graben to the North Sea Basin (Ziegler, 1992; Sissingh, 2003) (Fig. 4-1). Initiation and Cenozoic-age evolution of this extensive rift system appear to be related to the Alpine Orogeny, i.e. the collision of the anti-clockwise rotating African with the European plates (Schumacher, 2002; Sissingh, 2003; Dèzes et al., 2004; Ziegler & Dèzes, 2007; Rasmussen et al., 2010).

Rifting within the European Cenozoic Rift System was initiated in middle to late Eocene times, and induced by intra-plate, compressive tectonics (Ziegler et al., 1995; Dèzes et al., 2004; Ziegler & Dèzes, 2007). The rift system consists of two main parts, the Massif Central-Rhône Valley rift systems in the S and the Rhine Rift System in the N, both of which comprise numerous, subordinate, graben systems (Schumacher, 2002; Sissingh, 2003; Dèzes et al., 2004; Ziegler & Dèzes, 2007). The initiation of the subsidiary rift systems within the European Cenozoic Rift System resulted from compressional and regional tensional stresses in the Alpine Foreland (Ziegler, 1992). Rifting was associated with intra-plate magmatism and volcanism (Ziegler et al., 1995; Dèzes et al., 2004; Ziegler & Dèzes, 2007).

Within the Rhine Rift System, the N-S-trending Upper Rhine Graben bifurcates into the Hessen-Leine Depression in the NE and the Lower Rhine Basin in the NW (Prodehl et al., 1992; Ziegler, 1992; Sissingh, 2003). These three subordinate graben systems form the Rhenish Triple Junction (Sissingh, 2003), located at the SE end of the Rhenish Massif (Fig. 4-1). The Rhenish Triple Junction was the central point of volcanic activity during Cenozoic times (Ziegler, 1992).

Subsidence in the Lower Rhine Basin commenced in Oligocene times (Schäfer et al., 1996; Klett et al., 2002) at the NW margin of the Rhenish Massif, initiated at reactivated SW-NE-trending Variscan thrusts that influenced rifting from Rupelian times onwards (Nickel, 2003; Sissingh, 2003). Subsidence continued along several NW-SE-trending fault systems (Schäfer et al., 1996), including the Rur, Erft, Peel and Viersen faults, together with their numerous subsidiary faults (Figs. 4-3 & 4-4). These fault systems subdivide the Lower Rhine Basin into a series of grabens and horsts, comprising six main blocks. These include the Rur, Erft and Köln blocks to the SE of the Lower Rhine Basin, and the Peel, Venlo and Krefeld blocks to the NW (Figs. 4-3 & 4-4). The six main blocks subsided at different rates, for example, the Erft

Block to a maximum of 1300 m, while the Peel Block subsided to a depth of 2000 m (Klett et al., 2002).

The study area, within the Garzweiler open-cast mine, is surrounded by several tectonic features, some of which are still active (Ziegler, 1992; Hinzen, 2003; Sissingh, 2003; Ewald et al., 2006). Of these, the most important (in terms of this study) are the Erft Fault System (which separates the Erft and Köln blocks) and the Jackerath Horst at the southern margin of the Garzweiler open-cast mine (Figs. 4-3 & 4-4). The Erft Fault System comprises a series of broadly NW-SE-trending normal faults with an average dip of 70-80° to the SW (Schäfer et al., 2004). However, in the area S of the Garzweiler open-cast mine the strike direction of the faults within the Erft Fault System changes from the usual NW-SE orientation to broadly WNW-ESE and W-E trends, with a subsidiary ENE-WSW orientation, as well as the formation of a small horst structure (Fig. 4-4a). The WNW-ESE-striking step faults of this horst, termed the Jackerath Horst, form the S boundary of the present-day open-cast mine and were initially active in early Rupelian times. Therefore, the Jackerath Horst can be considered to be one of the oldest Cenozoic-age tectonic elements in the Lower Rhine Basin (Nickel, 2003).

The Cenozoic evolution of the Lower Rhine Basin was influenced by major climatic changes (Utescher et al., 2000, 2009; Zachos et al. 2001), characterised by a cooling trend from mean annual temperatures of 23-25°C in Oligocene and Miocene times down to 14°C in late Pliocene times (Utescher et al., 2000; Mosbrugger et al., 2005). The warmest Cenozoic-age climatic conditions in the Lower Rhine Basin have been observed in middle/late Eocene to early Oligocene times, with temperature peaks at the Late Oligocene Warming (late Chattian-age) and the Mid-Miocene Climatic Optimum (late Burdigalian-age; Zachos et al., 2001; Utescher et al., 2009; Grein et al., 2013). These temperature peaks are associated with sea level highstands in the Lower Rhine Basin (Schäfer & Utescher, 2014). Warm and temperate (at least subtropical) climatic conditions became increasingly cold and temperate in late Miocene times (Utescher et al., 2000, 2009; Zachos et al., 2001). In Pliocene times a further marked temperature decrease with mean annual temperatures of 14°C has been observed (Utescher et al., 2000; Mosbrugger et al., 2005), heralding the Pleistocene glaciation (Mosbrugger et al., 2005).

Sedimentation in the Lower Rhine Basin was influenced by constantly changing depositional environments which were controlled by subsidence, sea level changes and river channel avulsion (Becker & Asmus, 2005). The ingress of the North Sea onto the Palaeozoic and Mesozoic basement in early Oligocene-times marked the beginning of marine sedimentation in the North Sea region (Schäfer & Utescher, 2014). In the centre of the Lower Rhine Basin, sub- to supratidal sediments were deposited (Petzelberger, 1994; Schäfer et al., 1996) in a

high-energy estuarine embayment with a meso-tidal range (Schäfer et al., 1996; Schäfer & Utescher, 2014). Sediment input at this time was mainly clastic, derived from fluvial systems located to the S (Boersma et al., 1981; Schäfer & Utescher, 2014), draining the Rhenish Massif (Hager, 1993). It has also been suggested that a secondary clastic component was derived from coastal currents transporting material from the NW (Hager, 1993) as well as redistributing previously-deposited fluvial sediment.

At the Oligocene-Miocene transition, a decrease in the rate of basin subsidence resulted in partial regression of the North Sea (Becker & Asmus, 2005), and a northwesterly shift in the shoreline. Subsequently, the fluvial system became more extensive, traversing the newly-exposed coastal plain. Subsidence was also accompanied by the onset of peat formation (Schäfer et al., 2004; Becker & Asmus, 2005). Repeated marine transgressions resulted in the deposition of basin succession comprising alternating beds of clays, silts, peat and marine sediments (Schäfer et al., 2004; Becker & Asmus, 2005), the so called Köln Fm (Lower Seam Group; Aquitanian – early Burdigalian).

From early Burdigalian to late Serravallian times, coastal swamps with associated peat bogs and marshes became widespread (Teichmüller, M., 1958; Teichmüller, R., 1958; Mosbrugger et al., 1994; Schäfer et al., 1996; Klett et al., 2002). The thick peat accumulations from this period were the result of optimal climatic conditions, reduced subsidence and a decrease in sediment input from the Rhenish Massif. Up to 270 m of peat were accumulated over a period of 9 Ma (Hager et al., 1981; Hager, 1993), and subsequently compacted to form a lignite seam (up to 100 m) in the centre of the Lower Rhine Basin (Hager et al., 1981; Hager, 1986; Mosbrugger et al., 1994, 2005). This Main Seam (Burdigalian –Serravallian) extends from the SE of the Lower Rhine Basin up to an NE-SW-trending boundary in the area of the Hambach and Inden open-cast mines (Fig. 4-4). NW of this line, two NW-SE-directed transgressions resulted in the deposition of thick marine sand intercalations within the Main Seam of the Ville Fm (Petzelberger, 1994), resulting in its subdivision into three lignite units (Figs. 4-3 & 4-4).

Stratigraphically the lowest lignite is the Morken Seam (c. 10-12 m; average seam thicknesses within the Garzweiler open-cast mine; derived from internal RWE Power AG reports) and this is overlain by the marine Frimmersdorf Sand (c. 20 m). Subsequent regression resulted in a period of peat growth, forming the present-day Frimmersdorf Seam (c. 12 m). The boundary of the Frimmersdorf Sand with the overlying Frimmersdorf Seam is commonly planar or slightly wavy and may be marked by the presence of well-developed root horizons. These roots are up to 0.5 cm in diameter and extend down (up to 1 m) into the Frimmersdorf Sand. The Frimmersdorf Seam is overlain by the marine Neurath Sand (15-40 m), which accumulated during a period of transition from sub- to supratidal conditions. The uppermost Garzweiler

Seam (Serravallian) is the youngest part of the Ville Fm. At the contact of the Garzweiler Seam and the underlying Neurath Sand root horizons are rarely developed.

The Ville Fm was erosively capped by the sediments of the Inden Fm at the end of Serravallian times (Fig. 4-2). These were mainly deposited in meandering fluvial systems (Abraham, 1994; Klett et al., 2002; Schäfer et al., 2004). The Inden Fm also contains thin lignite seams, the so called Upper Seam Group (Figs. 4-2 & 4-4), which accumulated in locally restricted swamp environments (Schäfer et al., 2004) over a period of 2 Ma (Hager, 1993). The alternation of peats and fluvial deposits in the Inden Fm marks the final retreat of the North Sea from the Lower Rhine Basin (Boersma et al., 1981; Abraham, 1994; Valdivia-Manchego, 1994; Schäfer & Utescher, 2014).

At the late Miocene/Pliocene transition, sand and gravel as well as thick clay beds were deposited in lacustrine and fluvial environments on top of the Inden Fm (Schäfer & Utescher, 2014). Fluvial deposition changed from meandering to braided river systems during Pliocene times (Schäfer & Utescher, 2014). These clastic Messinian to Piacenzian-age sediments are termed the Hauptkies, Rotton and Reuver fms (Fig. 4-2). In Pleistocene times, the drastic climatic changes were marked by the deposition of thick fluvial units (terrace sediments; Schäfer & Utescher, 2014), accumulated in braided systems (precursors of the Rhine, Meuse, Mosel, Sieg and Wupper rivers; Boenigk, 1981; Klett et al., 2002).

4.4 Classification of sand bodies in the Frimmersdorf Seam

Sand bodies within the Frimmersdorf Seam exhibit strong variations related to their appearance, as well as their frequency or position within the seam. Sand bodies in fresh outcrops commonly vary from black to grey, or brown to reddish brown in colour. In older cut faces (days to one-two weeks old), the weathered sand bodies bleach to light grey, beige or white. Many sand bodies show evidence of vertical or horizontal bleaching. Colour changes and bleaching occurs independent of any variations in grain size or internal sedimentary structures. The classification of the sand bodies is based on six criteria: 1) position, 2) morphology, 3) orientation, 4) composition, 5) grain size, and, 6) sedimentary structures.

4.4.1 Position

The frequency and position of the sand bodies within the Frimmersdorf Seam show strong lateral and vertical variations. Sand bodies may be either isolated or grouped (up to 10). They can be concentrated 1) at the seam base, 2) at the top of the seam, 3) distributed throughout the seam or, indeed, 4) absent. Sand bodies occurring at the seam base can be isolated or concentrated. These latter occurrences consist of a variety of sand bodies, both laterally and vertically extensive.

Isolated sand bodies in the lower 50 cm of the seam are often connected to the underlying Frimmersdorf Sand. More extensive sand bodies are distributed in the lower 2 m of the seam, and these may also be connected to the underlying sand. The boundary between the Frimmersdorf Seam and the Frimmersdorf Sand is commonly marked by well-established root horizons. However roots are absent in areas with sand bodies at the base of the seam, connected to the Frimmersdorf Sand.

Sand bodies at the top of the seam are generally isolated and may be connected to the overlying Neurath Sand. These sand bodies may also contain rare chert nodules. Similar cherts are commonly found in the Garzweiler open-cast mine, occurring as an extended bed in the lower metres of the overlying Neurath Sand.

Most sand bodies are distributed throughout the Frimmersdorf Seam without any apparent concentration at a certain level and lacking visible connections to both the Frimmersdorf and Neurath sands. However, the vertical, as well as lateral, extent of the sand bodies can change over only a few metres, so that barren ($\geq 17\%$ sand, up to 30% in total) parts of the Frimmersdorf Seam and sand-free units may be juxtaposed over short distances.

4.4.2 Morphology

The sand bodies show a high degree of variation in terms of morphology (Fig. 4-5). This is further complicated by the fact that the various morphologies may be connected with one another, thus leading to composite forms. Four main morphologies have, to date, been recognised, including 1) layers/beds, 2) channel-like bodies, 3) irregular bodies, and, 4) reticulate or net-like bodies formed from combinations of 1-3. These shapes do not take into account vertical/ subvertical bodies with a dyke-like character (these will be examined below, under orientation). All recognized shapes can occur within one single vertical profile.

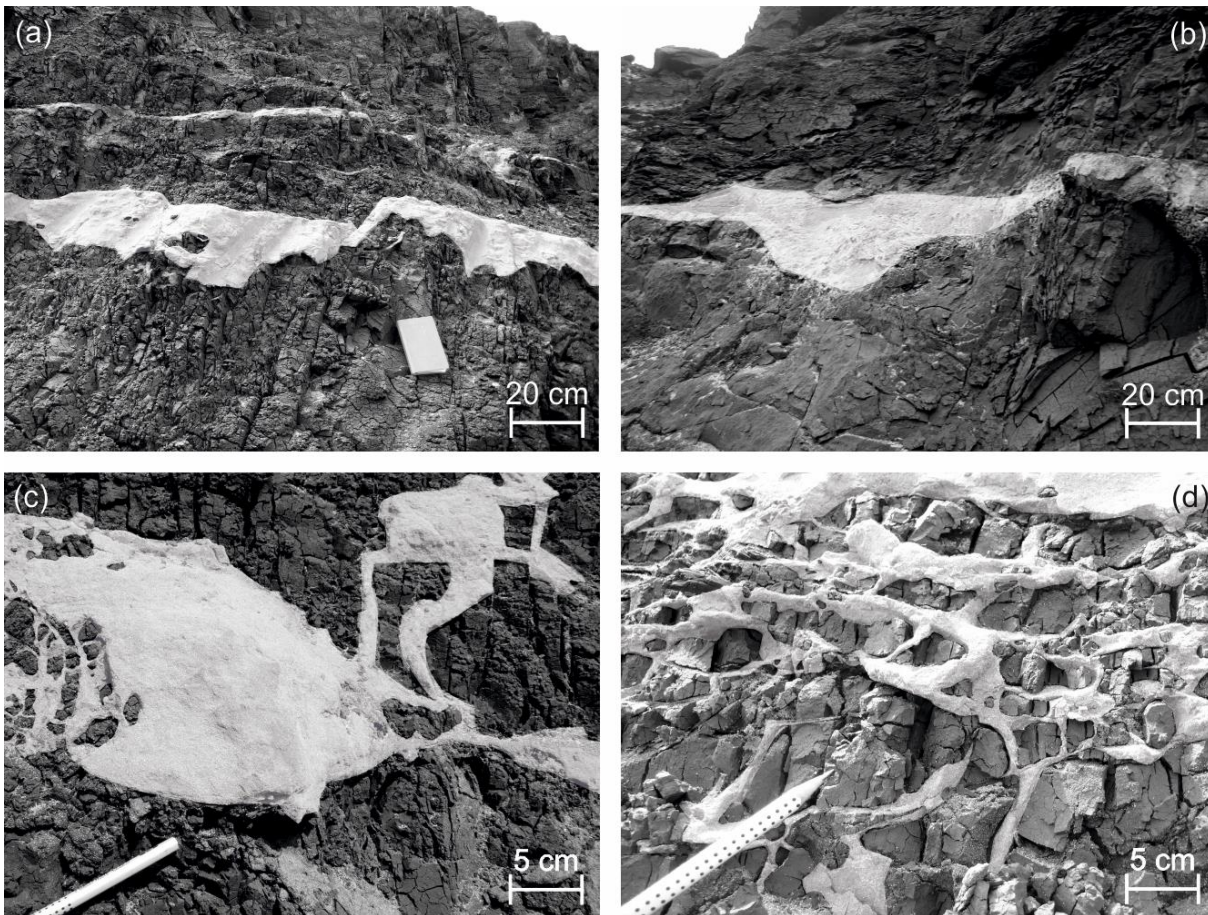


Fig. 4-5: Sand bodies within the Frimmersdorf Seam illustrating the different morphologies present: a) concordant sand beds, with even upper and wavy lower boundaries; b) thick (up to 1.8 m) channel-like sand body, c) irregular shaped sand body, and, d) reticulate sand bodies.

The horizontal layers/beds (1; Fig. 4-5a) are very variable in terms of thickness, ranging from 2 mm up to 1.0 m. Thicknesses are also laterally variable over distances of centimetres to tens of metres. The individual layers may thin and taper laterally, dying out over metres to tens of metres or they may end abruptly, and for no apparent reason, with a sharp cutoff. Individual layers may show constant thicknesses laterally, or they may be lenticular, with lateral thinning and thickening. Bifurcation may also occur within individual layers – with one bed splitting into two or more separate beds. Indeed, these beds may laterally rejoin to form one continuous bed again – thus resulting in a series of lignite pods separated by horizontal layers of continuous sand. The boundaries of these sand layers vis-à-vis the lignite are usually sharp. However, the upper and lower boundaries of the sand layers are variable, the former being wavy while the latter show a more pronounced wavy or irregular character.

Lenticular or channel-like sand bodies (2) (Fig. 4-5b) are much thicker than the layers and beds, ranging from 50-200 cm. They are never present as isolated sand bodies, but are always connected to horizontal (i.e. sills) or vertical (i.e. dykes) sand bodies. The boundaries with the

surrounding lignite are commonly sharp, although they resemble the sand layers (1, above) in that the lower boundaries are often wavy while the upper boundaries are less wavy. The lignite in both the sand beds/layers and the channel-like bodies is generally more compact and undisturbed than in areas with sand bodies of other shapes (see (4), reticulate sand bodies).

Irregular sand bodies (3; Fig. 4-5c), where present, generally have angular to roughly circular to ovoid forms, and range in diameter from c. 10-60 cm. The contacts with the lignite are sharp. Irregular sand bodies never occur isolated but always in combination with one of the other four recognised shapes, as well as with sand sills and/or dykes (Fig. 4-5c).

Reticulate sand bodies (4; Fig. 4-5d) are widespread, often with a poorly-defined net-like shape. However, given that they are often combined with other morphologies (1-3 above), as well as sand sills and dykes, they can be highly irregular (Fig. 4-5c). These sand bodies can extend laterally over 3-4 m, and have a general thickness of 50-150 cm. The individual veins of the net structure range in thickness from millimetres to centimetres. Of particular note is that the lignite within these reticulate structures is less compacted than that adjacent to, or within the other morphologies (1-3). Additionally, the isolated lignite fragments vary in shape from roughly rectangular to roughly ovoid.

4.4.3 Orientation

Although there is a degree of overlap between the morphological characteristics used above, the clear directional aspect of the sand bodies discussed within this category has led us to consider them as a descriptive feature in their own right. Three main bodies can be recognised – concordant sand bodies (beds/layers (1), morphology above), broadly horizontal, sill-like bodies and broadly vertical, dyke-like bodies (Fig. 4-6a). Detailed examination of the existing photographic material (RWE Power AG Archive) has revealed that sills are much more common than dykes (2:1 ratio). Both of these bodies will be discussed in more detail below.

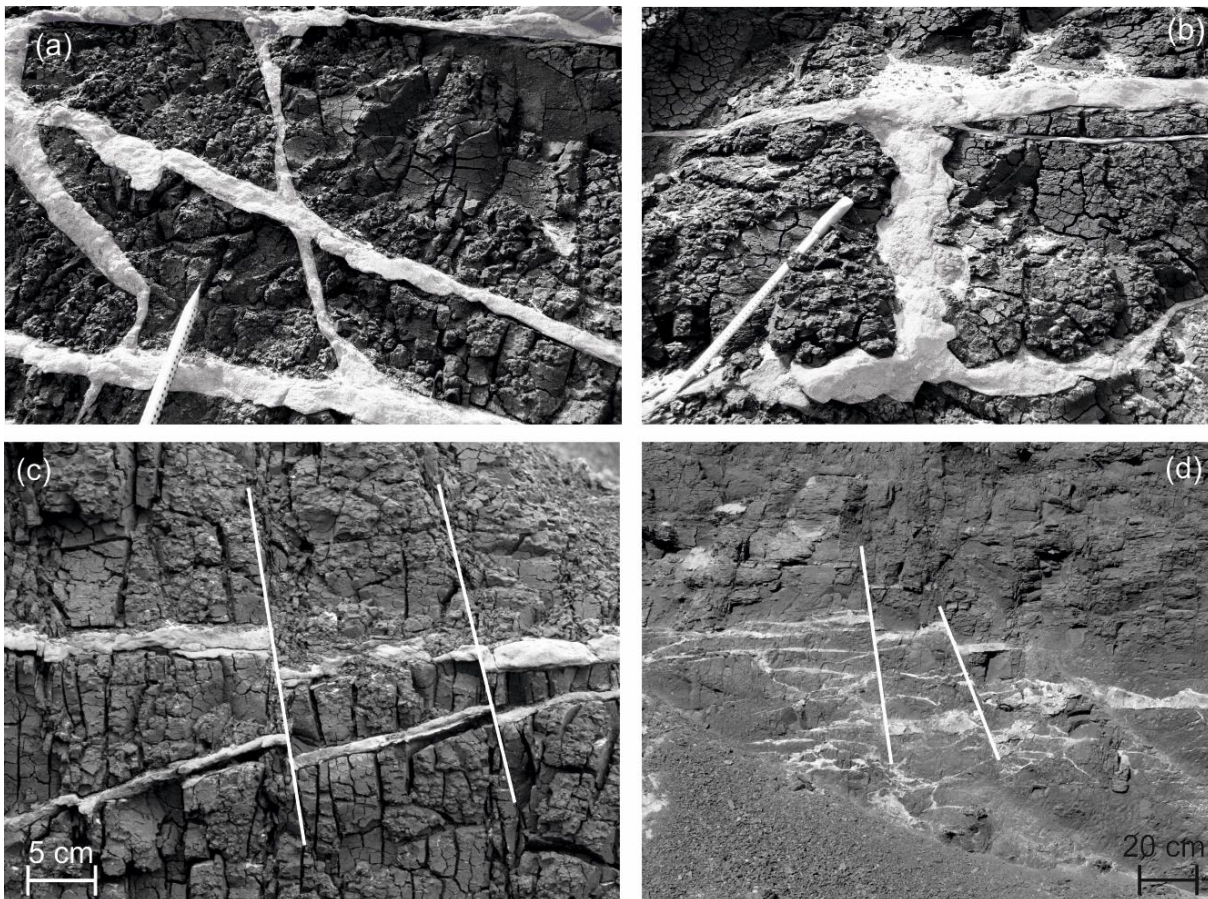


Fig. 4-6: Sand bodies illustrating the orientation; a) combination of sills and dykes, b) vertical dyke between to sills c) sills with vertical offset of 1-2 cm; and, d) sills with vertical offsets of up to 10 cm.

Sill-like sand bodies may be straight or slightly wavy and extend over distances of 10s of metres. The sill thickness varies between 1 and 50 cms (although the majority range between 1-20 cms). Unlike the bedded/layered morphology (1) above, the sills are not concordant with bedding, but are instead slightly discordant (with angles of up to c. 15°). Sills may be isolated or can occur in “swarms” with a series of up to 10 parallel or subparallel sill bodies. Additionally, individual sills may form convex upward bodies within the lignite. The various sills are often linked with dykes, particularly where there are a series of parallel or subparallel sills present (Fig. 4-6b).

Sills may show evidence of normal faulting (Figs. 4-6c, d). Offsets of 1-20 cm have been observed, and the faults may extend through a group of adjacent sills (over a distance of c. 2 m).

Sand dykes are vertical or subvertical (16-90°) bodies of sand which extend upwards within the lignite linking other sand bodies together, although isolated dykes (extremely rare) may also occur. The dykes vary in thickness from 5 mm up to 20 cm and can be traced over a scale

of metres across the outcrop. As mentioned above, sills and dykes of varying inclinations may commonly occur in combination with one another.

Dykes may extend into the Frimmersdorf Seam from the underlying Frimmersdorf Sand (these also comprise the majority of the observed dykes which are connected to the surrounding strata), or downwards from the overlying Neurath Sand (these dykes are extremely rare). Dykes intruding from the Frimmersdorf Sand into the Frimmersdorf Seam often merge into sills, and these latter may bifurcate and/or thin laterally. One particular dyke extending c. 2 m downwards from the Neurath Sand had a listric/curved form and thinned laterally. (Interestingly, this dyke also contained pebbles of chert in its upper part, i.e. that part which was closest to the Neurath Sand).

The orientations of both sills ($n = 29$) and dykes ($n = 61$) were measured within the Frimmersdorf Seam. The orientations of a range of concordant sand bodies (i.e. 1 above) were also measured ($n = 16$). Additionally, bedding orientations of both the lignite and the sand bodies bracketing it were measured, as well as a range of fractures within the lignite itself (Fig. 4-7). The predominant fracture orientations measured within the lignite were NW-SE, NE-SW and less commonly E-W. These three directions are also present in the sand bodies, although the NE-SW direction is more common (Fig. 4-8).

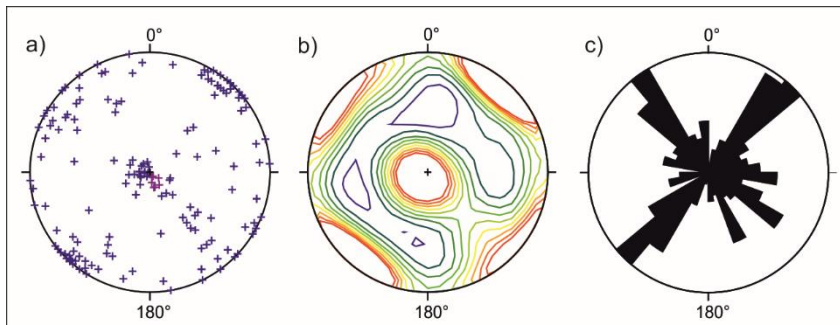


Fig. 4-7: Stereographic projection of lignite surfaces, a) symbol '+' illustrating fault planes, 'x' reflecting bedding surfaces; b) Density diagram; c) Rose plot.

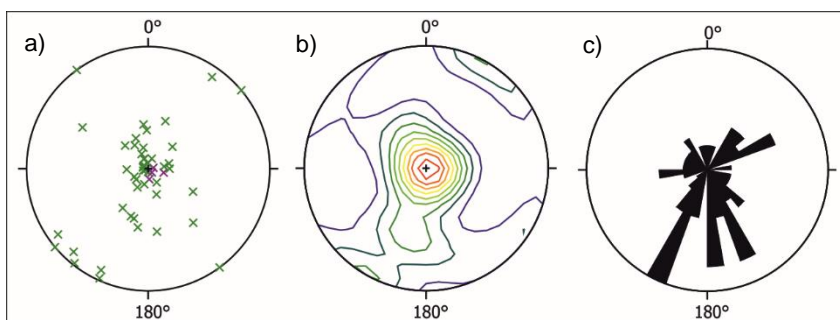


Fig. 4-8: Stereographic projection of sand surfaces, a) symbol '+' illustrating sills and dykes, 'x' reflecting bedding surfaces; b) Density diagram; c) Rose plot.

4.4.4 Composition

Petrographically, the sand bodies within the Frimmersdorf Seam predominantly consist of quartz (mainly monocrystalline) and K-feldspar, subordinate plagioclase and rarer amphibole, pyroxene, muscovite and zircon, in decreasing order of abundance. The white- or light grey-coloured sand grains are surrounded by dark-coloured humic substances which give the sand bodies a dark red, brown or even black colour.

Two clast types, namely lignite (as well as wood fragments) and mud are common within the sand bodies (Figs. 4-9a-c). Such clasts are only present in sand bodies which are > 10 cm thick. Lignite clasts (1; Figs. 4-9a & 4-9b) are the most frequent clasts present and range in shape from angular to well rounded, with diameters of 1-20 cm, although the majority are subangular to subrounded and < 20 cm in diameter. Lignite clasts are generally isolated and irregularly distributed throughout the sand bodies, although they also tend to be concentrated in the central parts of the sand bodies, rather than along the boundary areas with the surrounding lignite.

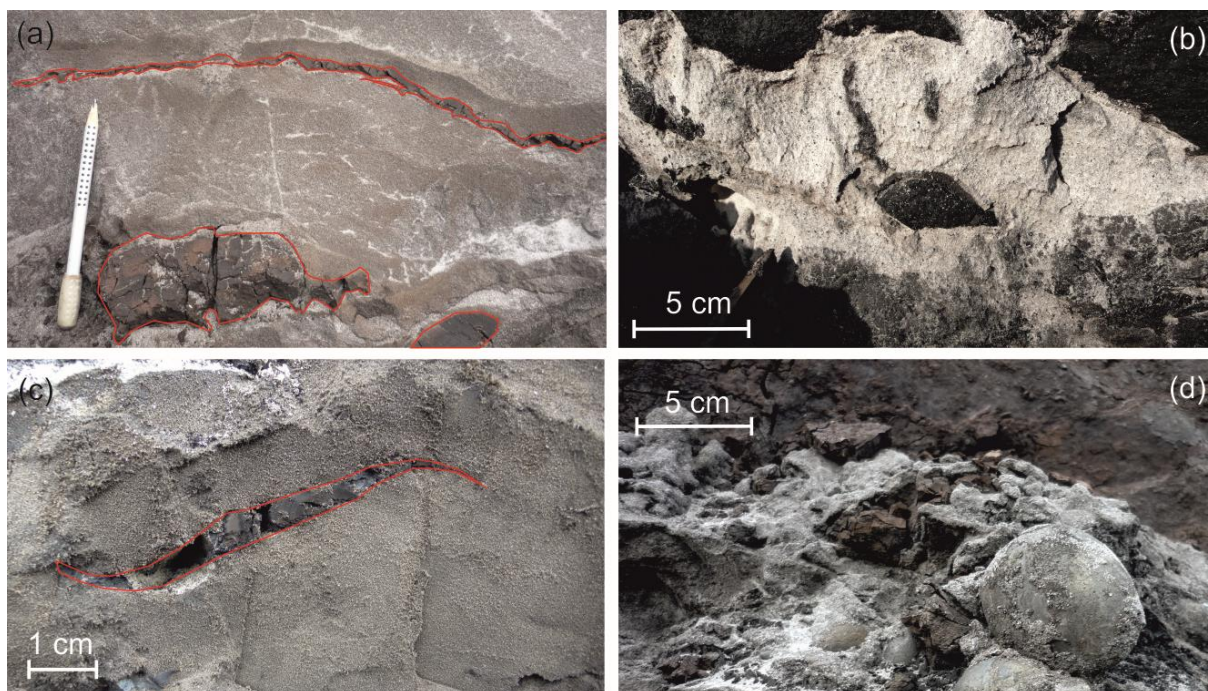


Fig. 4-9: Composition of the sand bodies; a) lignite lens at the top, lignite clasts at the bottom of a sand body; b) subrounded lignite clasts; c) mud lens, and, d) chert pebbles.

Thin sigmoidal-shaped lenses of lignite (Fig. 4-9a) were noted in three different sand bodies. These lenses are 1-3 cm thick and extend over a distance of up to 20 cm. The individual lenses are oriented broadly perpendicular to bedding. These lenses occur in sand bodies which also contain subrounded lignite clasts (up to 10 cm long; Fig. 4-9a).

Within one of the largest of the observed sand bodies (10 m wide and up to 1 m thick) there was a lens of concentrated lignite clasts close to the top of the sand, and parallel with the sand-lignite contact. Individual clasts were subangular to rounded. In addition, two large wood fragments (up to 20 cm in diameter and 30 cm long) were also present. The smaller of the wood fragments (c. 10 cm diameter) was located adjacent to the lignite-clast lens, whereas the larger fragment occurred at the upper boundary of the sand body and the lignite.

Mud in the form of lenses (2) and beds (3) is also present within the sand bodies. The lenses, dark grey or black in colour, are generally 1-2 cm thick and are often sigmoidal deformed (Fig. 4-9c). Thicker mud beds may also occur within individual sand bodies. In such cases, individual mud beds may be up to 10 cm thick, with sharp boundaries with the surrounding sand. These mud beds may occur at the top or bottom of horizontal sand bodies.

At seven different locations within the Garzweiler open-cast mine, sand bodies containing chert pebbles were noted (Fig. 4-9d). As noted above, isolated chert pebbles occurred rarely in sand dykes; these dykes migrating downwards from the overlying Neurath Sand. In addition, lenses or clusters of chert pebbles (up to 50 cm thick) may be concentrated either at the bottom, the centre or the top of concordant sand bodies and sills. Isolated chert pebbles may also occur within the lignite. However, thus far they have only been noted in lignites which are in close proximity to sand bodies also containing chert clasts.

4.4.5 Grain size and sorting

The sands within the Frimmersdorf Seam are commonly fine- to medium grained, and medium to well sorted, as well as being remarkably uniform (silt+clay < 10%, coarse-grained sand < 5%). Individual grains are subangular to rounded. Both the underlying Frimmersdorf Sand and the overlying Neurath Sand, were also examined, indicating that the grain size distribution of the sampled sand bodies was most similar to that of the upper part of the Frimmersdorf Sand, although there was enough overlap between the sand bodies within the lignite and the two bounding sand units to suggest that the sand across the region was similar in terms of grain size. In contrast to the sands, the chert clasts range in size from pebble through to small cobbles and are generally subrounded to well rounded.

4.4.6 Sedimentary structures

Sedimentary structures were observed within some of the sand bodies, including concordant sand bodies, sills and channel-like sand units (up to 2 m thick). The sedimentary structures can be classified as cross lamination (1) and trough cross lamination (2).

Cross lamination (1) has been noted in concordant sand bodies and sills with the individual laminae highlighted by colour changes related to different proportions of humic substances within the sand. The sand units are up to 50 cm thick and extend laterally for tens of metres.

Trough cross lamination (2) is present in concordant sand bodies, sills and channel-like bodies, where the grain sizes of the individual laminae ranges from fine- to coarse-grained sand (although the sand bodies themselves are not graded). Lamination is not always visible throughout the entire sand body.

Thin section analyses of samples from cross laminated sills have revealed that lamination is related to grain size variations (90-450 μm) and grain packing (Fig. 4-10a). Humic substances fill the interstitial space between individual mineral grains (Fig. 4-10b), and these substances are enriched in the coarser grained laminae (230-430 μm). Additionally, the alignment of elongate particles of organic matter (up to 3 mm in length) also accentuates the lamination (Fig. 4-10a).

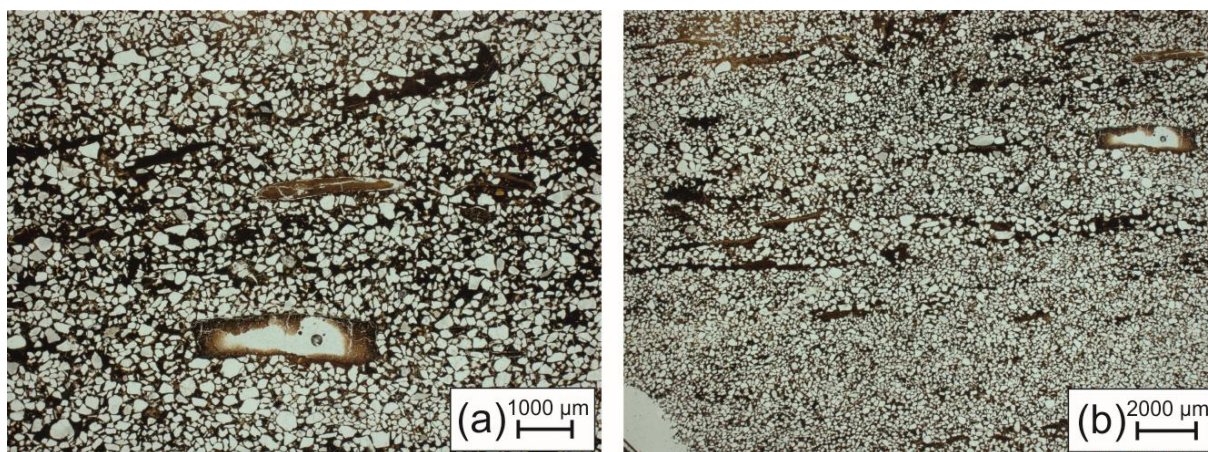


Fig. 4-10: Petrographic view of sand from a sill-like sand body. The sorting of the quartz grains results from a variation of grain sizes and grain packing; the pore space is filled by dark humic substances. Note the presence of elongated organic particles oriented parallel to lamination.

In two locations, planar (see section 4.4.7.) and trough cross lamination are present within thin, alternating sand-lignite beds. The trough cross lamination was observed in the basal part of a thick (up to 3 m thick) sand body.

4.4.7 Sand body complexity

The various features noted above may occur together, resulting in the generation of sand bodies of extraordinary complexity. One particular example comprises a sand body (20-40 cm thick and laterally extensive over c. 5 m) underlain by laminated lignite (i.e. part of the Frimmersdorf Seam). The boundary of the sand and lignite is sharp, but when traced laterally in 2D, the sand and lignite interdigitate with one another, at least at the base of the contact between them (Fig. 4-11). In the upper third of the sand body, there is well-developed trough cross lamination (thickness 2 cm) which passes laterally into a cluster of chert clasts. Individual laminae surfaces may contain small, isolated pebbles of lignite. The chert clasts within the cluster range in size from 0.5-3 cm, while the entire cluster is c. 5 cm thick and laterally extensive over at least 10 cm. A summary of the various sand body types, classified on the basis of the above noted criteria, is shown in Figure 4-12.



Fig. 4-11: Thick sand body underlain by laminated lignite. The sand body also contains a variety of chert pebbles and lignite clasts.

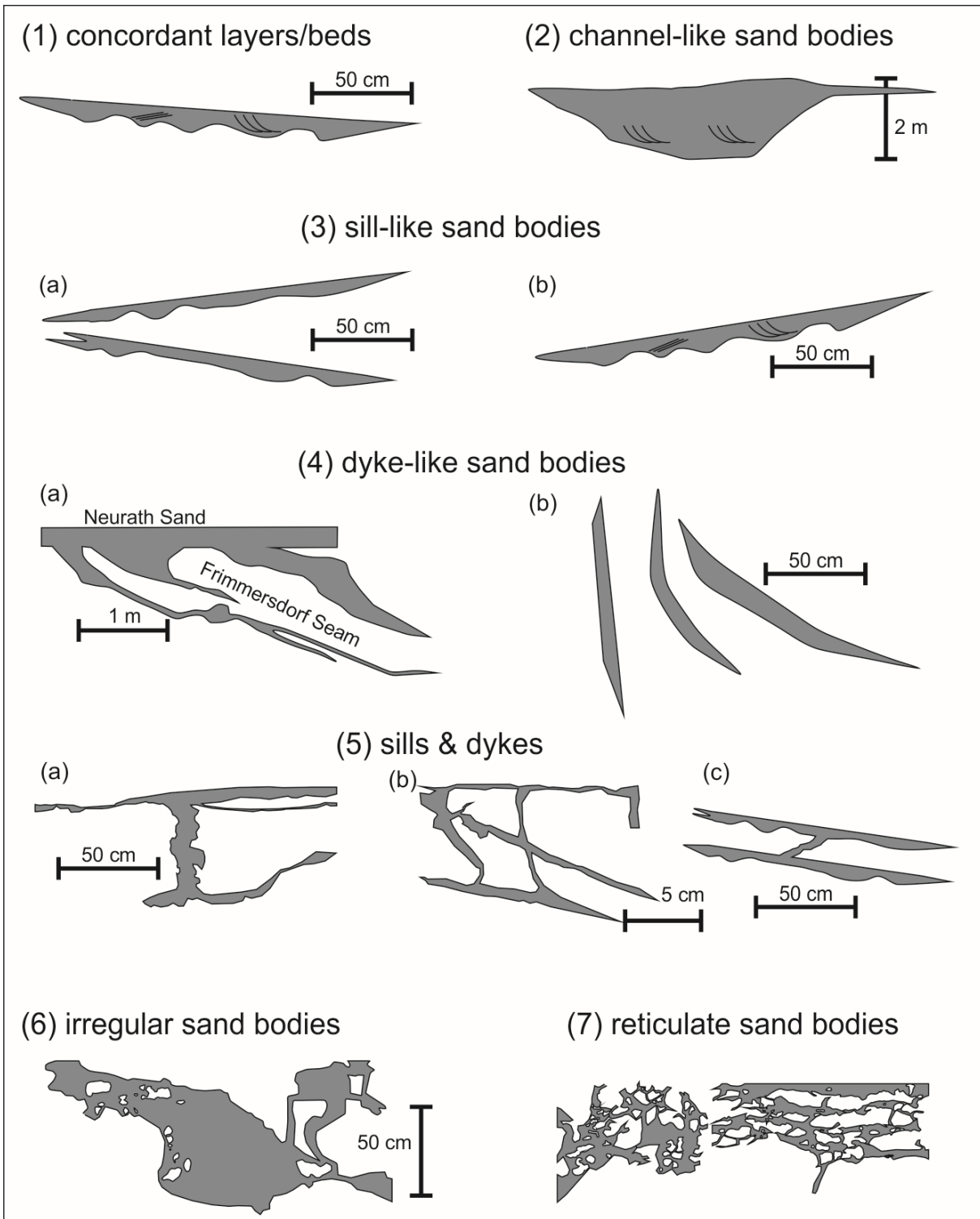


Fig. 4-12: Classification of sand bodies; 1) concordant layers/beds (tabular); 2) channel-like sand bodies; 3) sill-like sand bodies (tabular), a) isolated or several parallel sills, b) sill-like sand bodies with cross lamination; 4) dyke-like sand bodies, a) isolated dykes on top of the Frimmersdorf seam with connection to the overlying Neurath Sand, b) isolated or parallel dykes within the seam, without connection to the Neurath or Frimmersdorf sands; 5) combination of sills and dykes, a) dykes intruding into the Frimmersdorf Seam from the underlying Frimmersdorf Sand, b) symmetric sills and dykes within the seam; c) dykes connected to tabular sand bodies; 6) sand bodies with irregular morphology; 7) reticulate sand bodies.

4.4.8 Frimmersdorf Seam and Frimmersdorf Sand Boundary

The Frimmersdorf Seam is bounded by two sand units. The lowermost boundary (i.e. with the Frimmersdorf Sand) is widely exposed within the Garzweiler open-cast mine, while the uppermost boundary with the Neurath Sand is rarely accessible (being covered by mine tailings or exposed at locations where it is difficult to access). This latter boundary, however, has been interpreted as broadly erosional. The nature of the lower boundary, in contrast, is unclear and of particular interest in terms of the development of the sand bodies within the lignite unit.

As noted above, the lower boundary of the Frimmersdorf Seam is commonly marked by extensive root horizons, extending down into the Frimmersdorf Sand. However, the morphology of this lower boundary would appear to be affected by the presence and quantity of sand bodies within the lower six metres of the seam. Well-defined root horizons are common in areas with no or few sand bodies in the overlying seam, whereas in areas with extensive sand bodies, the boundary would appear to be more diffuse. Four criteria have been used in this study to describe the three boundary variations observed. These are 1) density of roots, 2) the presence of sedimentary structures, within the upper metre of the Frimmersdorf Sand, as well as 3) the quantity, and, 4) the types of sand bodies occurring in the overlying seam. The different boundary types are laterally restricted and may change over a few metres.

The first and most frequent boundary type between the lignite and sand is commonly sharp and slightly uneven. This boundary type appears to be restricted to areas of sand-free lignite or rare isolated, mainly concordant or sill-like sand bodies in the overlying seam. It is also marked by up to 1 m long roots. The roots are embedded in white-coloured and planar-laminated fine-grained sands.

The second boundary type is characterised by increasing amounts of sand bodies in the lignite, and the boundary between the lignite and sand becomes increasingly undulatory. Additionally, the amount, length and diameter of the roots present in the upper part of the Frimmersdorf Sand decreases. In this boundary type, the sand immediately below the lignite often contains larger wood fragments (trunks or branches), up to 20 cm in diameter. The sands are partly laminated and often dark-coloured.

The boundary type forming beneath barren (i.e. relatively sand rich) lignite, containing sills and dykes, irregular and reticulate sand bodies, changes significantly. The boundary is extremely undulatory with height differences of up to 1 m between the wave peaks and troughs. Roots or wood fragments as well as sedimentary structures are all absent.

4.5 Discussion

A variety of different sand bodies occur within the Frimmersdorf Seam in the Garzweiler open-cast mine. These sand bodies have been described according to a number of different criteria mainly based on their morphologies and compositions (cf. Table 4-1). This study provides a classification of the highly variable sand bodies within the Frimmersdorf Seam and suggests a variety of possible emplacement mechanisms, which may act in isolation or conjunction, resulting in the complexity of the present-day sand body pattern.

Table 4-1: List of the criteria used for the classification of the sand bodies, their description and interpretation

feature	description	interpretation
position	base	injection
	seam	syn-depositional & injection
	top	crack fills
morphology	tabular sand bodies, channel fills, irregular, reticulate	variety of syn- and post-depositional mechanisms
orientation	beds	fluvial/estuarine, storm events
	sills	injection, reflecting the regional stress field
	dykes	injection, reflecting the regional stress field
composition	clasts of lignite & mud	erosive
	lenses of lignite & mud	erosion during peat stage
	chert pebbles	high energy deposits; possible tidal influence
	wood fragments	erosion of the swamp area, transport in currents
grainsize	fine- to medium-grained sands, medium to well sorted;	remarkably uniform, possible origin from Neurath Sand as well as from Frimmersdorf sands
sedimentary structures	cross lamination, trough cross lamination, planar lamination	syn-depositional, formed by currents in an aqueous setting; ripples

4.5.1 **Syn-depositional features**

A number of features within the sand bodies have been used to suggest a syn-depositional origin. In particular, we refer to the presence of sedimentary structures or depositional/erosional morphologies which are best interpreted in terms of depositional processes. Thus, evidence for a syn-depositional origin of the sand bodies is based on a) the internal structure within some of the sand beds/units, indicative of the action of wave and/or current activity, and, b) the concordance of the sand beds/units within the lignite seam suggesting stratigraphic continuity and thus linking the processes governing deposition.

As noted above, channel-like sand bodies are present within the lignite. These channels (with depths of up to 200 cms) are clearly erosional, cutting down into the lignite. As such they were formed subsequent to peat formation, albeit not necessarily of the entire seam. Indeed, the

presence of these channels would suggest that peat formation occurred in stages, each stage marked by periods of increased sand deposition across the swamp area. Thus the lignite body (i.e. Frimmersdorf Seam) can be best categorised as an amalgamated unit, formed over a period of time, but with significant (days, months, years?) periods when fluvial systems prograded across the partially-indurated organic layers.

The presence of trough cross lamination within the channel-like sand bodies within the Frimmersdorf Seam would suggest deposition from unidirectional currents within an aqueous setting. Such lamination, mainly located at the bases of the channel-like units, forms due to the migration of fluvial ripples or dunes located at the channel bottom. The fact that these bodies contain evidence of unidirectional current activity would militate against their being small ponds within the swamp landscape, since such ponds would not have ripples within them (lacking currents, ripples could only be generated by wind energy, which in such cases is too weak to form ripples). However, the fact that the trough cross bedding is partly formed by alternating lignite and sand laminae may be interpreted as resulting from variations in the current velocity within the system.

The channel-like bodies also contain clasts of lignite, wood and mud. Such intraclasts may be typical in fluvial systems (e.g. Collier, 2002). Indeed, Feldman et al. (2008) have reported common concentrations of mud clasts (i.e. intraclasts conglomerates), suggesting that they result from bank collapse. The relatively isolated nature of the mud clasts in the channel-like sand bodies, however, would preclude such an origin. The isolated mud clasts would suggest that they may be derived from local mud lenses within the lignite, rather than bank collapse, or have been transported into the channels from elsewhere within the system. Indeed, such wholesale bank collapse would be less likely within an environment where the banks are formed from relatively compacted organic matter rather than less compacted sediment. In such situations, lignite intraclasts would be more prevalent, which is precisely the situation observed here, where both isolated mud clasts as well as lignite intraclasts concentrations were noted.

Both lignite intraclasts as well as wood fragments (including branches and trunks, up to 30 cm in diameter and up to 1-1.5 m long, although they are frequently smaller) are often aligned concordant to bedding, suggesting that they were derived as a result of erosion of the swamp vegetation and rapidly buried. Some larger fragments, however, show an orientation parallel to the current direction suggesting a degree of transport prior to final burial.

Although channel-like sand bodies are a useful indicator for the reconstruction of deposition of the sand bodies in a fluvial setting, thinner sand beds with lateral extents of tens of metres are much more frequent within the Frimmersdorf Seam. Tabular sand bodies with planar lamination, cross and trough cross lamination indicate that their deposition was controlled by

currents. Such planar bodies are common in floodplain environments, which to date have been the object of relatively less detailed study (see Miall, 1996). Both Ethridge et al. (1981) and Gersib & McCabe (1981) have subdivided floodplain areas within coal-bearing swamps into a number of different sub-environments, including crevasse splays and levees. Meanwhile, Wing (1984) noted that the presence of tabular bodies, similar to those recorded here, were related to the gradual aggradation of swamps (presumably with the incorporation of lignite intraclasts, as noted here), with the channel-like sand bodies representing active channel fill. Indeed, the overall fine-grained nature of the tabular and channel-fill sand bodies would suggest that the fluvial system which developed within the swampland of the present-day Frimmersdorf Seam was a low-gradient, meandering channel and floodplain system (cf. Madon et al., 2010). Flooding of the low-lying areas across the swamp was controlled either by rising levels within the channel systems (most probably seasonal), or as a result of tidal/marine incursions from the adjacent North Sea. Such latter incursions, however, would be marked by the presence of mud drapes (in the case of tidal incursions; cf. Hovikoski et al., 2005), or fossils in the case of more extensive marine incursions. Mud drapes were, however, not noted within the tabular sand bodies, while any fossils which may have been present within the sediments have been long since dissolved by the humic acids derived from the lignite units. Thus, it cannot be determined with absolute certainty whether the tabular sand bodies are the result of purely fluvial activity or whether a degree of marine influence occurred.

As noted above, chert pebbles may be present within both the channel-like and tabular sand bodies. These pebbles are concordantly arranged, parallel to bedding, and form flat-pebble conglomerates ranging in thickness from one clast thick through to 20 cm thick. The origin of these chert pebbles, however, is problematic. Deposits within the Lower Rhine Basin containing chert pebbles are, to date, only known from marine strata. Indeed, a significant and widespread chert-pebble-rich marker bed is well known from the marine Neurath Sand (stratigraphically overlying the Frimmersdorf Seam), and interpreted by Utescher et al. (2012) as a transgressive surface, deposited within a possible shoreface environment (Petzelberger, 1994), although such beds could also be interpreted as basal channel lags (cf. Andsbjerg et al., 2001). Therefore, the pebble origin is of significance in determining the precise depositional relevance of these deposits. Chert-pebble beds have also been identified in the Morken Sands, a marine sand unit between the Morken I and Morken II seams and which is stratigraphically lower than the Frimmersdorf and Neurath sands (Petzelberger, 1994). Therefore, it is possible that the chert pebbles may have been eroded from older beds and redeposited as channel lags in the Frimmersdorf swamp setting. Provenance studies, however, would suggest the chert pebbles were eroded from the Aachen-Limburg carbonate plateau and distributed within the Lower Rhine Basin by marine currents (Albers & Felder, 1981). If this was the case, their

presence within sand bodies in the Frimmersdorf Seam may be indicative of the extensive influence of tides and tidal currents within the swamp area, given that these pebbles would need to be transported parallel to the palaeocoastline and carried upstream within the estuarine setting. In such a situation, the tidal limit (i.e. the maximum upstream tidal influence; Dalrymple et al., 1992) could have been located up to c. 25 km landward from the coastline (i.e. the coastline in Miocene times, based on estimates in Utescher et al., 1992). Certainly, tidal influence may reach hundreds of kilometres upstream, depending on tidal range and coastal morphology (cf. Dalrymple & Choi, 2007; Gong & Shen, 2009). If, however, these chert pebbles were indeed transported by tidal currents along the coastline and upstream within the estuarine setting, it must also be presumed that the transporting currents carried significant amounts of sand-sized sediment in a bedload/suspension mix. This would then suggest that the channel-fill and tabular sands could be tidal deposits. However, there is a lack of any features suggestive of tidal influence (e.g. herringbone cross stratification, paired mud/silt drapes, see Shanley et al., 1992 and Hovikoski et al., 2005 for details). Another possible explanation is that these deposits may have been transported onshore by storm surges. These high-energy events would have transported coarse-grained material upstream. Storm abatement would have been followed by the reestablishment of the fluvial regime, and the subsequent seawards transport of sediment, with the conglomerates representing a form of storm residue.

Tidal range and the effect on the depositional setting within the swamp area can increase significantly during spring or storm tides. Major storm events, supported by high temperatures of a subtropical climate (Zagwijn & Hager, 1987; Utescher et al., 2000; Mosbrugger et al., 2005) may, as noted above, have resulted in widespread flooding of the swamps. Further evidence for the occurrence of flooding caused by storm surges is the presence of so-called groden bedding (i.e. alternating beds of sand and concentrated organic debris; cf. Schäfer et al., 2004; Bungenstock & Schäfer, 2009; Schäfer, 2010, p. 248) at the top of the Frimmersdorf Sand (Fig. 4-13), and the alternating sand-lignite succession in the overlying seam. Groden bedding develops as a result of flooding of salt marshes during storm tides, and may be identified from the juxtaposition of sands above halophyte vegetation (cf. Schäfer et al., 2004; Bungenstock & Schäfer, 2009; Schäfer, 2010, p. 248). In the study area, the high content of organic material within the bedding indicate the initial settlement of beach plants on top of the marine Frimmersdorf Sand following regression of the North Sea. In the lignite overlying these groden beds, a unit of alternating thick, concordant sand beds and lignite was developed. These layers may be indicative of repeated local flooding of the swamps.

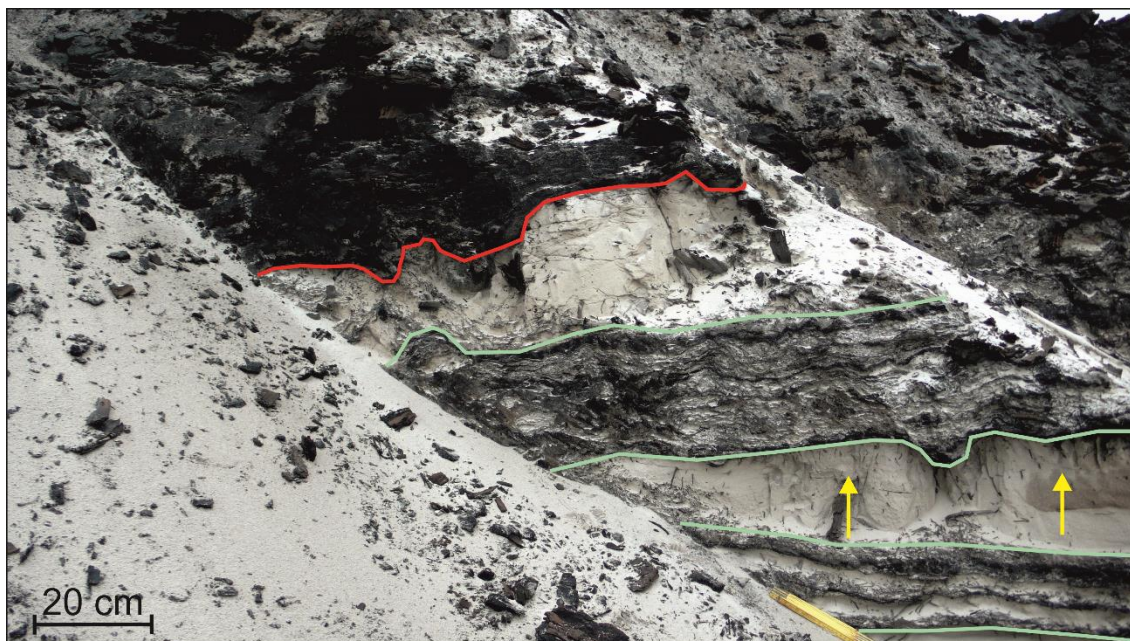


Fig. 4-13: Groden bedding (within the green lines), formed as a result of storm-controlled flooding of the swamp area, in the upper metres of the Frimmersdorf Sand. The red line marks the boundary between the Frimmersdorf Sand and the Frimmersdorf Seam above. Note the presence of the root horizon at the sand-groden boundary (yellow arrows).

Sandstone dykes, extending downwards from the Neurath Sand into the Frimmersdorf Seam or from sand bodies (e.g. tabular sands and channel fills), have also been noted. The position of these dykes would suggest that they formed either due to desiccation or as a result of tectonic activity. The fact that in the region groundwater levels were constantly rising, and that the organic-rich swamp (which ultimately formed the lignite seam) was more or less constantly under water would militate against a desiccation crack origin. The measured orientation of some of these dykes would appear to be broadly conform to the regional tectonic trend, but the measured sample is too small to be definitive. However, what is clear is that some of these cracks were passively filled from above, most probably during periods of overbank flow or storm surges (e.g. those dykes extending downwards beneath tabular sands). The dykes at the top of the seam, and extending downwards from the Neurath Sand were filled during the period of marine transgression and erosion which marked the cessation of swamp conditions (cf. Jolly & Lonergan, 2002). This supposition is supported by the presence of cherts within one of the observed dykes; cherts, as noted above, are common in shoreface deposits at the base of the overlying Neurath Sand (Petzelberger, 1994).

The concurrence of fluvial, tidal and marine processes that may have formed the sand bodies within the Frimmersdorf Seam indicate a complex depositional environment controlled by river systems and the North Sea. As noted above, the Lower Rhine Basin in Mid-Miocene times formed an estuarine embayment (Schäfer et al., 1996; Schäfer & Utescher, 2014). Estuarine

depositional settings are characterized by the interaction of fluvial and marine processes (Dalrymple et al., 1992; Hori et al., 2001). Based on the dominant controlling processes, estuarine embayments comprise three facies zones: the inner reach, the mixed-energy central part, and the outer reach (Dalrymple et al., 1992). The inner reach is dominated by fluvial processes and extends to the landward limit of tidal influence. In the central zone of an estuary, the interaction of tides and river currents result in a mixed-energy facies environment. The influence of rivers decreases seawards, so that the outer reach is dominated by marine processes (Dalrymple et al., 1992).

Based on the dominant marine processes, estuaries can be further distinguished. Wave-dominated estuaries (e.g. the Eastern Shore estuaries, Nova Scotia, Canada; Boyd & Honig, 1992) are bordered by barrier sands separating the mixed-energy central zone from the purely marine shoreface. In tide-dominated estuarine environments (e.g. the South Alligator River, Australia; Woodroffe, 2000) the marine-dominated reach is characterized by tidal sand bars, whereas the mixed-energy zone is marked by tidal-fluvial channels (Dalrymple et al., 1992). The tidal influence may reach hundreds of kilometres landwards, depending on the tidal range and the coastal gradient (Dalrymple & Choi, 2007). Additionally, the tidal energy increases landwards due to the funnel-shaped geometry of estuaries (Dalrymple et al., 1992). This may result in tidal bores moving upstream (e.g. the up to 2 m high wave in the Severn Estuary, SW UK (Uncles, 2010).

Sedimentary processes in an estuarine environment are regulated by periodic cycles, for example, tides and seasonal variations on the one hand, and spontaneous and aperiodic events (river flooding and storm surges) on the other hand (Gong & Shen, 2009). Within the Lower Rhine Basin fluvial influence from at least one river in the S (Hager, 1993) interacted with meso- to macrotidal tidal ranges and minor swells of the North Sea (Schäfer et al., 1996). In Miocene times, the precursor of the present-day Sieg River entered the Lower Rhine Basin from the Rhenish Massif and crossed the central part of the swamp environment (Hager, 1993). Minor fluvial channels within the Main Seam have been interpreted as river networks dewatering the swamp area (Petzelberger, 1994). In the southeastern area of the Lower Rhine Basin, an extended fluvial unit within the Frimmersdorf Seam has been identified (Schäfer et al., 1996; Schäfer & Utescher, 2014). Sand and clay were deposited in a highly sinuous meandering river, which eroded parts of the peat (Schäfer et al., 1996). The sinuous course of the river may be an indicator, that deposition was located in the meandering zone of a tide-dominated estuary (Dalrymple & Choi, 2007). This hypothesis is supported by the presence of a thick sand body (up to 10 m) within the uppermost Garzweiler Seam (Garzweiler open-cast mine), that comprised tidal bundles (Prinz et al., 2017).

According to Dalrymple et al. (1992) and Dalrymple & Choi (2007), estuarine environments only form under transgressive conditions. The lignite deposits of the Ville Fm are interpreted as base level rise half cycles (Schäfer & Utescher, 2014). Additionally, the fluvial unit within the Frimmersdorf Seam (noted above) was associated with the Mid-Miocene Unconformity (MMU; Schäfer & Utescher, 2014), a marked transgressive surface that extends across the Lower Rhine Basin and the adjacent North Sea Basin (cf. Huuse et al., 2001; Thöle et al., 2014). An eustatic origin for this basinwide transgression has been suggested (Schäfer & Utescher, 2014), although Thöle et al. (2014) suggest a combination of climatic change and increased basin subsidence. In the German North Sea Basin, the transgressive surface of the MMU is overlain by deltaic sediments of the Eridanos Delta (Thöle et al., 2014). The onset of delta progradation was due to a significant increase in sediment input (Michelsen et al., 1998), and a change in the sediment input direction from NE to E (Thöle et al., 2014). This increase in sediment supply may also have been responsible for the relatively large amount of sand bodies within the Frimmersdorf Seam, since the Morken and the Garzweiler seams only contain sporadic sand bodies.

4.5.2 Post-depositional emplacement mechanisms

The presence of various features (e.g. the discordance or faulting of sand bodies), have led us to consider post-depositional causal mechanisms, which may have been responsible for the emplacement and deformation of the sand bodies. In a broad sense, differential compaction across the region most probably resulted in thickness (and other?) variations occurring within both the sand and lignite units. Indeed, studies on the Main Seam (Hager et al., 1981) have shown, for example, that the gentle folding of the lignite may have resulted from the settlement characteristics of the peat. Hager et al. (1981) have suggested that the original thickness of the peat in the basin centre was c. 270 m, and that this was reduced over time and as a result of compaction, to a thickness of 100 m. In contrast, the sand units both above and below the Main Seam are considered to be close to their depositional thicknesses (with only minor changes in density and porosity). The broad but gentle folding of the sedimentary units, however, does not explain the origin of the smaller features within the lignite bed, which is the subject of the present study, although it most probably resulted in additional post-depositional deformation/movement of some of the features.

The Lower Rhine Basin region in Pleistocene times was influenced by both glacial and periglacial activity, with relics of moraines, ice wedges or thick loess deposits being recorded (e.g. Thome, 1959). These are generally associated with the Drenthe stage of the Saale glaciation (e.g. Golte & Heine, 1980). Indeed, permafrost conditions (associated with this or

other glacial episodes) may have been responsible for the formation of fractures within the peat/lignite, that later could have been filled by fluidized sands. In Late Pleistocene times climatic conditions favoured the formation of continuous permafrost in the area of the Rhine catchment (van Balen et al., 2010). However, ice wedges resulting from the seasonal thawing and freeze of the periglacial soils are, as far as known, in the Lower Rhine Basin restricted to the Pleistocene-age fluvial deposits (Thome, 1959). Moreover, any characteristics (e.g. wedge-parallel lamination) of pseudomorphic ice wedge replacements are absent within the sand bodies of the Frimmersdorf Seam.

The presence of large ice bodies across the region of the Lower Rhine Basin, meant that it was subjected to glacio-isostatic rebound subsequent to the retreat of the Weichselian-age Scandinavian & British ice sheets (e.g. Steffen et al., 2006; van Balen et al., 2010). Therefore, an isostatic response (5-10 m of relative uplift along the Rhine; van Balen et al., 2010) would most probably have influenced the depositional setting. On the other hand, the general subsidence of the basin reached a maximum in Quaternary times (e.g. Grützner et al., 2016), at a time when rebound was occurring. Given that the degree of uplift (c. 5-10 m) occurred over a time span of 115 ka years, the precise amount of uplift which occurred during the period of basin subsidence would have been of the order of submillimetres, and probably not enough to influence the development of fractures within the lignite (which, as noted above, tend to be of the order of centimetres).

The evidence for post-depositional mechanisms resulting in the formation of some of the sand bodies include, a) the discordance of the sand bodies (dykes, some sill-like sand bodies, irregular and net-like sand bodies) with regard to bedding, reflecting stratigraphic discontinuity, b) the preferred orientation of some sand bodies reflecting the regional stress field (Figs. 4-7 & 4-8), and, c) the connection of some sand bodies either to the overlying Neurath Sand (see above) or the underlying Frimmersdorf Sand.

Sand bodies directly linked to the underlying Frimmersdorf Sand may have formed as a result of upward-directed intrusion. In lignite seams within the Lower Rhine Basin, upward-directed transport of sands into overlying lignite seams have previously been described (Bajor, 1958; Berger, 1958). Both of these authors noted the presence of redistributed sand deposits within lignite seams of the Ville Fm in former open-cast mines. Bajor (1958) described sand intrusions (up to 15 m thick), as well as fan-like arrangements of sand-filled cracks (where the sands contained lignite clasts) in a location (former Neurath open-cast mine) where the Morken and Frimmersdorf seams are joined to form one thick lignite seam. Emplacement of these intrusions was interpreted as being related to the presence of confined groundwater (Bajor, 1958). Similarly, in the Morken Seam of the Frimmersdorf-Süd open-cast mine a channel

deposit with low-angle sand dykes radiating outwards from the channel top into the lignite was described (Berger, 1958). The emplacement of these channel-related sand dykes was interpreted as resulting from sand movement related to hydraulic pressure (Berger, 1958). Hager et al. (1981) concluded that these various intrusions formed as a result of disequilibrium between hydraulic pressure within the pore waters of the sediment below the lignite seam and settlement of the peat forming these seams. Pore fluids within the underlying sand beds were trapped and led to the generation of overpressure (Hager et al., 1981).

The presence of some of the sand bodies within the lignite may possibly be related to similar emplacement processes related to overpressuring. Recent work on sand injectites has recognised a series of interrelated processes, namely, (1) liquefaction, (2) fluidization, and, (3) hydraulic fracturing (e.g. Mazzini et al., 2003; Duranti & Hurst, 2004; Jonk et al., 2005; Braccini et al., 2008; Cartwright et al., 2008; Scott et al., 2009; Hurst et al., 2011). These three processes, acting in conjunction, can lead to the formation of complex patterns of sand distribution within the lignite. The preconditions for the formation of sand injectites are the deposition of low-permeability host strata above unconsolidated sands, causing the generation of overpressure within the parent sand body (Jolly & Lonergan, 2002; Jonk et al., 2005; Braccini et al., 2008).

The Frimmersdorf Sand (in this system representing the parent sand body) consists of well sorted and fine- to medium-grained, unconsolidated sand beds (Petzelberger, 1994). Overpressure in these sands, as noted above, may have been generated by their rapid burial and sealing by low-permeability organic deposits (Jonk et al., 2005). Peat accumulation rates on top of the Frimmersdorf Sand have been estimated at 0.1-2 mm per year (Hager, 1986). This is comparable to the sedimentation rates of sediments in the South Viking Graben of the North Sea which have also been subjected to sand intrusion (i.e. 50-100 m/Ma; Jonk et al., 2005). Peat commonly has a high hydraulic permeability, depending on its composition and level of maturity. However, during subsidence the porosity of the peat decreases due to overburden pressure (cf. Taylor et al., 1998; p. 93). Additionally the permeability of lignite may be influenced by external stresses, for example, compressional forces (Somerton et al., 1975; Jasinge et al., 2011). In the Lower Rhine Basin, external stresses may have been related to tectonic movement along the numerous fault systems.

Overpressure in unconsolidated sands can also be generated as a result of so-called disequilibrium compaction (Jolly & Lonergan, 2002; Duranti & Hurst, 2004; Braccini et al., 2008; Hurst et al., 2011). In such a situation, when the fluid pressure in the pore spaces increases due to the sealing of the sediments, overpressuring may occur (Jolly & Lonergan, 2002; Braccini et al., 2008). During compaction, the pore water is expelled from the overlying (and

sealing) host strata, and drained into the permeable parent sand body (Jolly & Lonergan, 2002), increasing the amount of pore fluid present. The trapping of these fluids within the pore space precludes an even compaction of the sand body (Braccini et al., 2008), and the degree of disequilibrium which ensues can lead to the formation of sand injectites resulting from the forced emplacement of remobilized sand into fractures in the overlying unit (cf. Duranti & Hurst, 2004; Scott et al., 2009).

Disequilibrium compaction may also be an explanation for the lack of any comparable sand bodies within the underlying Morken and overlying Garzweiler seams, when compared with the frequency and extensive distribution of sand bodies in the Frimmersdorf Seam. The Morken and Garzweiler seams are covered by permeable deposits, i.e. the marine Frimmersdorf Sand on top of the Morken Seam, and the coarse-grained sands and gravels of the Hauptkies Fm covering the Garzweiler Seam. These permeable deposits would have facilitated compactional pressure within the underlying lignite beds and the concomitant release of pore water from the peat deposits as a result of ongoing (and increasing) compaction (cf. Hager et al., 1981). The Frimmersdorf Seam, on the other hand, was capped by the marine sediments of the Neurath Sand. The lowermost metres of the Neurath Sand contain high amounts of clays and silt, which make this unit a sealing rather than a permeable layer. This may have resulted in the development of a degree of disequilibrium compaction and resultant pressure in the underlying peat accumulations (e.g. Hager et al., 1981).

As noted above, a series of processes are required for the formation of sand injectites commencing with the liquefaction and fluidization of the sediments within the parent unit (e.g. Lowe, 1975; Owen, 1996; Hurst & Cronin, 2001; Duranti & Hurst, 2004; Braccini et al., 2008; Hurst et al., 2011). Liquefaction occurs when increased pore-fluid pressure transforms a saturated granular material from a solid into a liquefied state (Duranti & Hurst, 2004). Liquefaction of sediments results in the loss of primary sedimentary structures within the parent sand unit (Braccini et al., 2008; Hoffmann & Reicherter, 2012). This homogenization of primary sedimentary structures can be observed within the uppermost metres of the Frimmersdorf Sand (cf. chapter 4.4.8) and may also result in the disintegration or redistribution of wood fragments possibly belonging to former root horizons. The remobilization of this liquefied material (= fluidization) occurs via the upwards-moving pore fluids which follow the hydraulic gradient towards the sediment surface (Jolly & Lonergan, 2002; Cartwright et al., 2008).

The presence of cracks within the host sediment body is considered to be the result of hydraulic fracturing (e.g. Jolly & Lonergan, 2002; Mazzini et al., 2003; Duranti & Hurst, 2004; Jonk et al., 2005; Cartwright et al., 2008), generated when the overpressure within the pore-water filled sediment is greater than the fracture strength of the host sediment. When passing a plane of

minor competence contrast (Cartwright et al., 2008), such as bedding planes, the pressure may be directed parallel to the bedding, resulting in vertical dykes that merge into sills (Fig. 4-6b).

Commonly, sand injection occurs at pre-existing, dilated fractures (e.g. Jolly & Lonergan, 2002; Mazzini et al., 2003; Duranti & Hurst, 2004; Jonk et al., 2005; Cartwright et al., 2008). The orientations of these pre-existing fractures may thus reflect the regional stress directions (Jolly & Lonergan, 2002; Figs. 4-4a, 4-7 & 4-8).

Fluidization of water-saturated sands and their transport within fracture systems may result in significant erosion of the host strata (Duranti & Hurst, 2004; Hurst et al., 2011). The erosion of the bounding peat during the transport of the fluidized sands may lead to the intermixture of fine particles of organic detritus with the sand grains. The enrichment of peat detritus in the pore spaces of the sand bodies has been observed in thin section (cf. Fig. 4-10). Additionally peat and wood fragments that are present within the sand bodies may have been derived from wall erosion as the fluidized sand moved within the dyke.

The deposition of fluidized sands may form a type of lamination, which forms due to grain size variations, as well as variations in grain packing, and is orientated parallel to the margins of the sand bodies (Scott et al., 2009; Hurst et al., 2011). Within the sampled sill-like sand bodies, the presence of this lamination is emphasised by the elongate orientation of the sand grains and wood fragments parallel to the sill margins.

Though fluidization would commonly appear to be restricted to sands (generally fine- to medium grained sands; (Lowe, 1975; Hurst et al., 2011), gravel-sized sediments can also become liquefied and remobilized (Fontana et al., 2015). Therefore, syn-sedimentary sand bodies which contain chert pebbles may also have been reworked as a result of liquefaction and fluidization processes.

Liquefaction and fluidization processes may also have influenced syn-depositional sand bodies in the Frimmersdorf Seam. The combination of apparently syn-depositional, cross-laminated sand bodies with upward or laterally spreading dykes can be explained by the remobilization of the unconsolidated sands. The reworking of the syn-sedimentary sand bodies may result in the homogenization of former sedimentary structures (Braccini et al., 2008; Hoffmann & Reicherter, 2012), which may explain why sedimentary structures are relatively rare within the majority of the sand bodies in the Frimmersdorf Seam.

The generation of overpressure in water-saturated sands, and the final remobilization of the sediments, may also have been initiated by seismic activity (e.g. Obermeier, 1996; Jolly & Lonergan, 2002; Duranti & Hurst, 2004; Jonk et al., 2005; Braccini et al., 2008). Fault activity

can lead to rapid and sudden increases in pore pressure in unconsolidated sediments, resulting in hydraulic fracturing and the remobilization of sands within the parent unit (Duranti & Hurst, 2004). The possibility that earthquakes may have been, at least, partly responsible for the emplacement of sand bodies within the seam is supported by the fact that the region is one of ongoing active seismicity (Ziegler, 1992; Klostermann et al., 1998; Hinzen, 2003; Sissingh, 2003; Ewald et al., 2006). Tectonic activity in the Lower Rhine Basin occurs along the numerous fault systems, generated from the extensional forces which formed the rift basin, as well as forming the main faults for the ongoing subsidence of the basin (Nickel, 2003; Schäfer et al., 2005). In particular, the Erft Fault System is considered to have been a major centre for seismic activity, since it has controlled the uplift (hundreds of metres) of the western Köln Block. Small-scale evidence of tectonically-induced deformation of sand bodies include the presence of normal faults within associated concordant or sill-like sand bodies which have vertical offsets of several centimetres (Figs. 4-6c & 4-6d).

Sand injectite studies have, to date, mainly concentrated on consolidated sandstone injectites in mudstone host strata, and exposed in outcrops (Petersen, 1968; Ewald et al., 2006; Braccini et al., 2008; Scott et al., 2009; Hurst et al., 2011), although injectite complexes in subaqueous deposits of the North Sea are increasingly reported in the literature (Duranti & Hurst, 2004; Jonk et al., 2005; Cartwright et al., 2008; Scott et al., 2009). Studies of subaqueous sand injectites, however, are difficult since only small sections of drill core can be sampled and analysed. Therefore, it is difficult to distinguish between syn-sedimentary and injected sand bodies within the basins (Duranti & Hurst, 2004). Since injection structures can affect oil and gas reservoirs, for example, in allowing leakage of hydrocarbons, these sand bodies are of great scientific and economic interest (Jolly & Lonergan, 2002; Braccini et al., 2008). Sand bodies in the Garzweiler open-cast mine, due to their accessibility, provide the possibility to study unconsolidated sand injectites in outcrops which are constantly being renewed, since it is an active mine, as well as allowing a 3D view of these sand bodies. In addition, the relation of the parent unit, i.e. the Frimmersdorf Seam, with the sand bodies within the host strata can be analysed.

4.5.3 Time frame

The current results do not allow the formation of the sand bodies to be accurately located within the formational time frame, apart from a broad assignment as either syn- and post-depositional (cf. Table 4-2). However, there are certain aspects which do shed more light onto the interaction of sand emplacement and lignite formation, for example a) the chronology of tectonic activity within the Lower Rhine Basin, b) the properties of peat and lignite during

subsidence and settlement or c) the ductile deformation of peat clasts within some of the post-depositional sand bodies.

Table 4-2: Broad time frame for the development of the various structures observed within the lignite of the Frimmersdorf Seam.

1	peat formation
2	syn-depositional formation of sand bodies, fluvial/ estuarine, storm events
3	cessation of swamp conditions
4	transgression and deposition of the Neurath Sand
5	sand injection + post-depositional deformation of pre-existing sand bodies, deformation of sand bodies due to peat compaction

Tectonic activity (a), which is considered to represent one possible mechanism for the formation of sand injectites, was particularly high during Oligocene times, decreased in importance during Miocene times, and again increased from Messinian times onward (Schäfer et al., 2005). The reduction in tectonic activity in Miocene times (Sissingh, 2003), resulting from the west-directed shift of the Alpine Orogeny (Klostermann et al., 1998), may indicate that formation of sand injectites was coeval with the renewed seismic activity in the Messinian.

The settlement and compaction of peat (b), which influences its sealing properties, is primarily dependent on its initial thickness. Comparatively thick peat accumulations (e.g. the Main Seam, with a thickness of c. 100 m of lignite) commonly undergo increased compaction due to their own weight, whereas thinner peat accumulations (e.g. the Morken or the Frimmersdorf seams, c. 15 m lignite) only undergo significant compaction when overburden pressure increases as a result of the deposition of thick sediment units above (Hager et al., 1981). This may suggest that the formation of the sand injectites in the Frimmersdorf Seam was related to the increase in overburden due to the deposition of the Neurath Sand and Garzweiler Seam (and possibly including the overlying upper Miocene, Pliocene and Pleistocene-age deposits).

The presence of rounded lignite clasts (c) and, in particular, ductilely-deformed lignite lenses indicates, however, that the emplacement of the sand bodies containing these lenses occurred during the peat generation stage. If the organic material had attained the lignite stage any redistributed material would have shown brittle behaviour.

4.6 Conclusions

The highly variable sand bodies present within the Frimmersdorf Seam of the Garzweiler open-cast mine suggest that a variety of causal mechanisms may have been responsible for their emplacement. Both syn- and post-depositional processes, acting in isolation or in combination can be used to provide a suitable model for the formation of all of the described sand bodies.

Coeval with peat formation, the sand bodies were deposited in an estuarine environment. Within this Miocene-age estuary, sand bodies were formed by the interaction of river and tidal influences, supplemented by aperiodic events, e.g. fluvial flooding or storm surges.

The post-depositional sand bodies may have formed due to the injection of fluidized sand into the peat accumulations. The liquefaction and fluidization of the parent sand body, as well as the hydraulic fracturing of the sealing host strata (i.e. lignite) were related to the generation of overpressure within the sands, while fracturing was also possibly linked to seismic activity within the Lower Rhine Basin.

Acknowledgements

We acknowledge the funding for this study from the RWE Power AG. Thanks to the staff members of the department GOC-L, especially the field crew of the Garzweiler open-cast mine, as well as Dr. Thomas Thielemann and Sonja Weiler for editing datasets. Special thanks to Dr. Friederike Bungenstock (NIhK Wilhelmshaven) for providing an insight in recent swamp environments around the Jadebusen (North Sea). The manuscript benefited greatly from the comments of Gösta Hoffmann and an anonymous reviewer.

5 Channel deposits in the Miocene-age Frimmersdorf Seam

5.1 Abstract

Sand bodies in the Garzweiler open-cast mine affect the mining activities, and were analysed in terms of e.g. their distribution and orientation within the Miocene-age Frimmersdorf Seam. Former studies (see above) have shown, that these sand bodies are partly related to syn-depositional emplacement mechanisms. Fluvial and estuarine sand bodies were deposited in the extensive Miocene-age mires, which were also affected by episodic flooding events from the adjacent North Sea. The laser scanning and sedimentological interpretation of one large sand body, which was exposed in the Garzweiler open-cast mine in November 2015, give evidence of the complex interaction of fluvial and tidal currents in the mires of the Miocene-age Lower Rhine Embayment.

5.2 Introduction

The presence of sand bodies within the Miocene-age Frimmersdorf Seam has significantly complicated mining activity within the Garzweiler open-cast mine for more than 10 years. These sand bodies are extremely difficult to detect and highly irregular in their distribution. The uncontrolled input of sand-rich lignites to the combustion process reduces the efficiency of the coal-fired power plants and, therefore, up to 1.5 Mio tons of lignite had to be discarded in the past. This study aims to improve the understanding of the occurrence and distribution of sand bodies in the Frimmersdorf Seam.

During the fieldwork for this thesis, numerous sand bodies were observed and analysed in the outcrops of the Garzweiler open-cast mine. Due to the mining activity, the outcrops are constantly refreshed, providing a three-dimensional outcrop situation over time. However, due to the exploitation slope geometry, only a two dimensional section view of individual sand bodies is possible. Moreover, the distance of at least 10 m between two consecutive sections cut by the bucket-wheel excavator in the mining progress is too large to correlate individual sand bodies over time. In order to overcome this problem, as well as providing a detailed analysis of one particular sand body, a section was chosen in the Frimmersdorf seam for scanning with laser scanners. Thus, in November 2015, one comparably large sand body that was exposed in the upper part of the seam, was scanned in seven closely spaced outcrop sections in order to provide a three dimensional overview of its morphology and geometry.

5.3 Geological framework

The Garzweiler open-cast mine, which is in the focus of this study, is located on the Venlo Block in the German part of the Lower Rhine Embayment (i.e. the Lower Rhine Basin). In Miocene times, the depositional environment was affected by a combination of sea-level fluctuations, subsidence, and subtropical climatic conditions (Utescher et al. 2002, 2009, Schäfer et al. 1996). In the area of the Garzweiler open-cast mine, intercalated sand and lignite units were deposited (Fig. 5-1). The c. 15 m thick Morken Seam, which was accumulated in Burdigalian times, was subsequently overlain by the shallow-marine to coastal sediments of the Frimmersdorf Sand (Langhian-age, c. 15 m), deposited in the estuarine setting of the North Sea. Following the retreat of the North Sea, extensive mires developed across the Lower Rhine Basin. These mires were the source of the peat deposits of the present day Frimmersdorf Seam (c. 15 m). In Serravallian times, the North Sea coastline shifted once more to the SE (i.e. landwards), and the up to 60 m thick Neurath Sand was deposited in a high-energy, estuarine depositional environment. The overlying Garzweiler Seam (c. 10 m) was deposited in middle to late Serravallian times (Fig. 5-1).

The mires that developed across the Lower Rhine Basin in Miocene times have been the focus of numerous studies in the past (e.g. Teichmüller, M. 1958; Teichmüller, R. 1958; Figueiral et al., 1999; Lücke et al., 1999; Utescher et al. 2000; Mosbrugger et al., 2005). It was suggested that the peats formed in topogenous mires that gradually evolved into raised bogs with ombrogenous conditions (Cameron et al., 1989; Borren et al., 2004; Stock et al., 2016). The mires were dewatered by several small rivers, and one of them was probably an early precursor of the present-day Sieg River (Hager, 1993). In the SE parts of the Frimmersdorf Seam, deposits of a meandering fluvial river have been observed in the Hambach open-cast mine (Mörs, 2002; Schäfer et al., 2004, 2005; Schäfer & Utescher, 2014).

5.4 Methods

The analyses of the exposed sand body include both the characterization of various sedimentary parameters as well as the high-resolution laser scanning. The sedimentological approach included grain size analyses, as well as the recognition and interpretation of the various sedimentary structures and the composition of the sand body, for example, in terms of the presence of particular clasts (e.g. provenance, current energy) or organic (i.e. wood) fragments. The scanning (optical measurement instruments Riegl, Leica Geosystems) of the

sand and lignite surfaces, and the graphical evaluation of the scanned information was carried out in close cooperation with the RWE Power AG (Fig. 5-1).

In order to facilitate the high-resolution scanning of the sand body, the slope was peeled off by the shovel of a small excavator to sharpen the lignite and sand surfaces. After scanning the slope, a new surface was cut at a distance of c. 1-3 m, and this new surface was subsequently scanned. In total, seven consecutive sections were measured over two days of fieldwork, thus providing seven detailed laser scans. In addition, as noted above, the exposed sand bodies were also examined in detail, noting the various sedimentary structures, while samples were also taken for grain size analysis.



Fig. 5-1: Laser scanning of one sand body in the upper part of the Frimmersdorf Seam (11.11.2015).

5.5 Results

The graphical interpretation of the laser scans results from the different reflectivity values of sand and lignite (see figure 5-2). The green and yellow areas represent lignite, while the darker blue and violet colours mark sand surfaces.

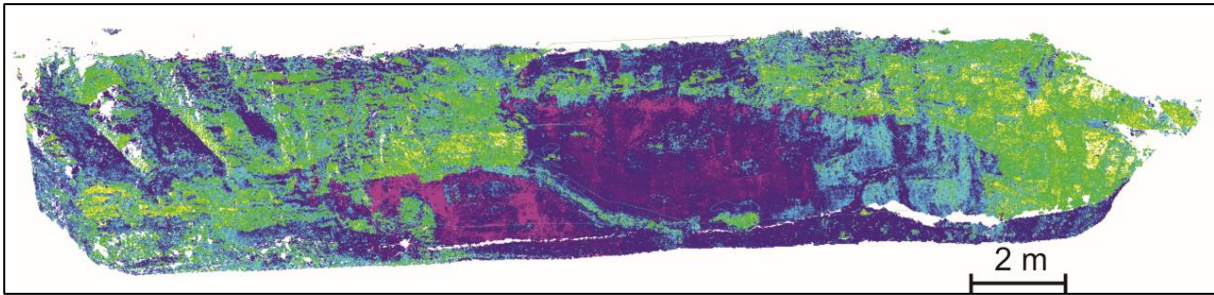


Fig. 5-2: High-resolution image of the laser scanning, based on the different reflectivity of sand and lignite.

The c. 3 m thick scanned sand body is one of the thickest sand bodies observed within the Frimmersdorf Seam in the Garzweiler open-cast mine over the three years of fieldwork. Indeed, this sand body is even thicker than 3 m, since its lower parts were not exposed. The sand body dips to the NW, i.e. parallel to the general dip direction of the Miocene-age strata in the Lower Rhine Basin. Due to the fact that the sand body gradually disappears below working floor level, the base of the sections could not be measured. There is also clear decrease in thickness to the NW, and, therefore, the sand body thins out from SE to NW (see Fig. 5-4).

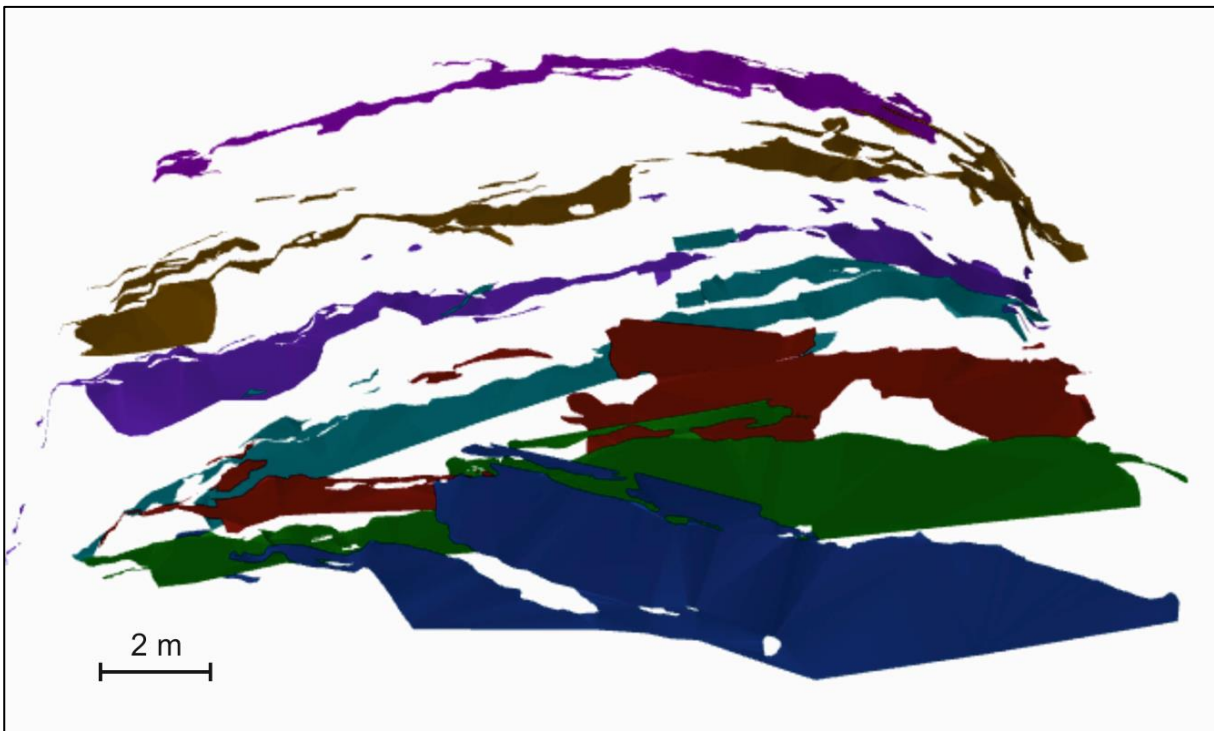


Fig. 5-3: Graphical interpretation of the seven consecutive sand body sections; from SE (blue section) to NW (violet section).

The sand body is predominantly structureless and has mainly sharp boundaries to the adjacent lignite. However, in some areas, even parallel or trough cross bedding/lamination could be rarely observed. Additionally, two sand sections revealed trough cross laminated sand-lignite alternations (Fig. 5-4) at the base of the sand body.

The sands are predominantly fine- to medium-grained, and contain 2.2 to 7.0% of mud. The grain size distributions from samples taken from each of the seven different sections do not vary significantly. The sand sample which was taken from the second section was partly blue coloured, while the other 7 samples were all brownish to grey coloured. The blue colours of the sand would suggest that the sand comprise glauconitic minerals.

The sand body contains 0.5-50 cm thick chert pebble beds that are found within fine- to medium-grained sand layers, which alternate with pure sand layers. Individual pebbles (which were excluded from the grain size analyses outlined above) range from 0.5 to 5 cm in diameter. Both the thicknesses of the individual pebbles as well as those of the pebble-sand layers increase from the first section through to the third section. These chert pebble beds occur predominantly in the basal parts of the sand body. Individual cherts, however, are also incorporated into the lignite directly underlying the sand body. These chert pebbles were embedded into a matrix of sand-rich lignites (Fig. 5-4).

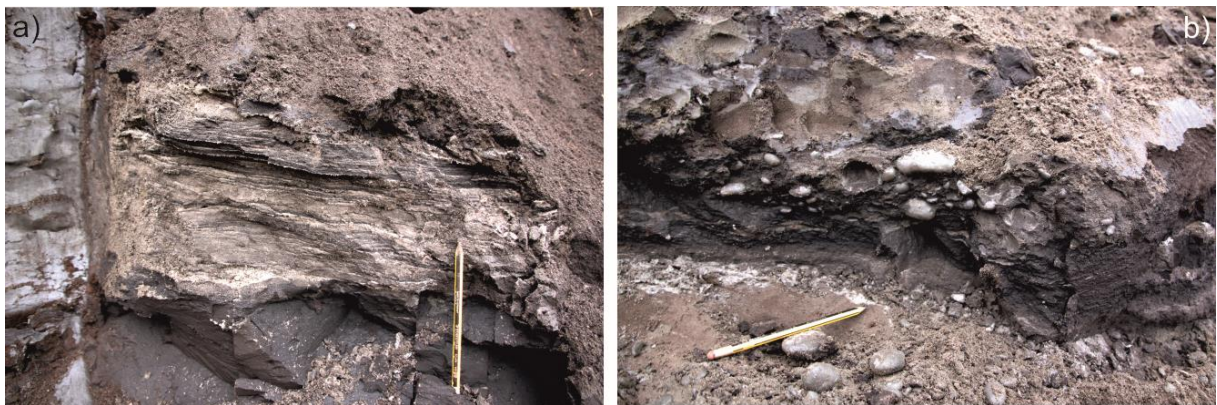


Fig. 5-4: a) Sand-lignite alternations at the base of the sand body; b) Chert pebbles at the base of the sand body, and within the underlying lignite (pencil for scale).

The measured sand body also included numerous wood fragments, which are exposed within the various outcrop sections. These wood fragments ranged in size from 1 mm to 3 m, and represent possible tree stumps, trunks, branches and roots. The fragments are oriented horizontally (for the most part) within the sand body, and thus broadly parallel to the depositional surface. (Sub-) horizontal trunks (up to 50 cm in diameter) or smaller branches are also present within the adjacent lignite (i.e. lateral to the sand body). They often cover the upper boundary of the sand body, and were deposited parallel to the sediment surface.

Additionally, tree trunks and stumps (up to 30 cm) are present within the lignite which have an upright position.

At the base of the measured sand body, lignite clasts are preserved. These clasts, with diameters of 0.5-2 cm, were rounded and concentrated near the basal sand-lignite boundary. Lignite clasts also occurred at the top of the sand body. Within the first and second section, large (up to 20 cm in diameter), angular to subangular lignite clasts were incorporated into the sands at the top of the sand body.

From the top and the sides of the sand body, sand dykes and sills extend into the adjacent lignite. The dykes range in thickness from 2-5 cm and extend over a distance of 2 m. The sills are 1-10 cm thick, and can laterally extend over 3 m.

5.6 Interpretation & Discussion

The orientation of the sand body parallel to the lignite bedding, and some of the features that have been observed within the individual sections of the measured sand body are clearly representative of a syn-depositional origin. Though the sand deposits in most of the measured sections are mainly structureless, the rare presence of primary sedimentary structures facilitates the interpretation of possible emplacement mechanisms, which were responsible for the sand body formation. The planar and trough cross lamination structures can be certainly associated with current activity on sedimentary surfaces.

In general, the position of the sand body in the central part of the Lower Rhine Embayment (i.e. c. 25 km landward from the Miocene-age coastline; based on estimates in Utescher et al., 1992), and the channel-like geometry of the sand body, would suggest, that it represents the channel fill of a comparably small-scale river system, and eroding into the underlying lignite. The small-scale planar/trough cross lamination structures were probably deposited in the river bed, by the passage of ripples or small-scale dunes (e.g. Bridge & Tye, 2000).

The channel deposit is very thick (>3 m) and laterally restricted (<10 m), when compared to the numerous sand bodies observed during the past 3 years of fieldwork. According to a classification on the dimensions of fluvial channel bodies (Gibling, 2006), the measured sand body can be classified as very narrow (<10 m), and thin (1-5 m). However, Gibling (2006) also noted in his study on the dimensions on fluvial channels that the channel body deposits in an outcrop are commonly larger than the original river bed.

The isolated nature of this channel body segment would suggest that the sand body was deposited in an abandoned channel belt (e.g. Giblin, 2006; Bridge & Tye, 2000). However, due to a decrease in current velocity, deposition in abandoned channels is mainly dominated by very fine grained sediments and suspended organic matter (e.g. Bridge et al., 1986). In the measured sand body the entire succession from base to the top comprises fine- to medium-grained sands. However, an active channel can also be filled, e.g. due to a landslide or repeated flood events (Giblin, 2006).

The alternations of chert-sand beds with sand beds, as well as the sand-lignite alternations at the base of the sand body are indicative of changing current velocities, possibly as a result of seasonal variations (e.g. Bridge & Tye, 2000). The intercalated lignite beds at the base of the sand body result from the erosion of the peat during channel incision. The lignite clasts at the base and the top of the sand body are also indicative of the erosional forces of the stream, and were most probably eroded from the surrounding channel banks. Indeed, the presence of intraclasts, resulting from bank collapse, is a common feature in fluvial systems (Collier, 2002; Feldman et al., 2008).

Whereas the channel geometry of the sand body, and its position within the central parts of the former mire, indicate a fluvial origin, the blue coloured, glauconitic sand within the second section would also suggest that the depositional environment was influenced by marine waters (Chafetz & Reid, 2000; Bal & Lewis, 1994). As noted above, the depositional environment of the Miocene-age Lower Rhine Embayment was largely influenced by the high-energy processes of the adjacent North Sea (including wave and tidal currents, as well as periodic flooding events), and by the presence of numerous small-scale meandering river channels crossing the paralic mires (e.g. Boersma et al., 1981; Boenigk, 1981; Hager & Prüfert, 1988; Hager, 1993; Schäfer, 1994; Schäfer et al., 1996; Klett et al., 2002; Schäfer et al., 2004; Schäfer & Utescher, 2014), and formed an extended estuary (Schäfer et al., 1996; Prinz et al., 2017a).

The presence of chert pebbles within the sand body and the underlying lignite beds may be also indicative of a marine influence on the mire, because chert pebbles have, thus far, only been noted in marine strata (Petzelberger, 1994). At the base of the shallow marine to coastal Neurath Sand, for example, an extensive chert pebble bed (which is distributed throughout the entire Garzweiler mining area, and can be up to 1.5 m thick) was interpreted to represent a transgressive surface (Utescher et al., 2012). Within the measured sand body, the chert pebbles may be indicative of an estuarine origin, i.e. the interaction of fluvial and tidal currents. The tidal range of the North Sea in Miocene times was at least mesotidal (2-4 m; Schäfer & Utescher, 2014) and, thus, the tidal influence could have extended several kilometres

landwards, especially during spring or storm tides (e.g. Dalrymple & Choi, 2007). Additionally, the tidal range can increase significantly as a result of funnelling within embayments such as the Lower Rhine Embayment (Mazumder & Arima, 2005; Dalrymple & Choi, 2007; Longhitano et al., 2012), and tidal waves may move upstream for several kilometres (Dalrymple et al., 1992; Dalrymple & Choi, 2007; Uncles, 2010). Thus, tidal activity might be responsible for the transport of chert pebbles into the river-dominated segments of the estuary (e.g. Dalrymple & Choi 2007), as well as the formation of the lamination and bedding structures.

On the other hand, in general chert pebbles could have been also distributed by pure fluvial systems. Gravel sheets, like the chert pebble beds within the lignite and the overlying sand body, commonly form as river channel-floor lags, and are suggested to be transported from eroded banks or bars upstream as a lag in an active channel (Miall, 2006). These gravel sheets are accumulated at a point of channel shallowing or flow expansion. Horizontally bedded gravel beds are suggested to form in channels with rapid gravel transport (Hein & Walker, 1977; Miall 2006), resulting in a low-relief gravel sheet (Miall, 2006), similar to those observed within the measured sand body. Gravel deposits, however, are more common in braided rivers, forming channel bars or basal lags (Bal & Lewis, 1994). In meandering rivers, the formation of gravel sheets is associated with major short-term changes in flow regimes, e.g. a flooding event (Bal & Lewis, 1994). However, at that time the meandering fluvial systems within the Lower Rhine Embayment were comparably small (see Hager, 1993), and their source area (i.e. the Rhenish Massif) was a relatively flat plain, prior to its uplift in Quaternary times (e.g. Fuchs et al., 1983). Additionally, the mire was covered by a dense vegetation. Therefore it is questionable if the transport energy of river systems in the Langhian/Serravallian-age mire was sufficient to transport chert pebbles of that size.

The wood remains observed within the sand body, and the adjacent lignite, are perfect indicators of the Miocene-age peat forming vegetation. Some of the tree trunks and branches that were deposited parallel to the sand body bedding were probably transported within the fluvial/estuarine stream, and aligned parallel to the current direction. The trunks and stumps within the lignite, however, represent the vegetation that grew directly on the channel banks or, subsequent to channel abandonment, on top of the channel deposits. The horizontally orientated wood remains probably represent trees and bushes which were blown over and fell onto the mire surface, whereas the (sub-) vertical tree trunks and stumps were presumably incorporated in situ. Former studies have shown that larger wood fragments from the Ville Fm were coniferous trees, mainly gymnosperms such as *Sequoia* and *Sciadopitys* (Teichmüller, M. 1958; Teichmüller, R., 1958; Teichmüller & Thomson, 1958; Mosbrugger et al., 1994; Schäfer et al., 1996; Figueiral et al., 1999; Klett et al., 2002; van der Burgh, 1973; von der

Brelie, 1981). However, palms (Arecaceae) have also been reported, albeit sporadically (Mosbrugger et al., 1994).

As noted above, the sand body was located in the central part of the Frimmersdorf Seam, and was probably formed in the fluvial-dominated segment of a meandering, estuarine system. Similar observations have been made in the Hambach open-cast mine. Here, a prominent sand channel fill was noted in the central part of the Frimmersdorf Seam in the Hambach open-cast mine (Schäfer & Utescher, 2014; Fig. 5-5). It was suggested that this channel fill, which formed in a small meandering river (Mörs, 2002; Schäfer et al., 2004, 2005; Schäfer & Utescher, 2014), can be correlated with the Mid-Miocene Unconformity (c.15 Ma). The sand body, which have been measured in this study was located on the same stratigraphic level as the channel fills in the Hambach open-cast mine, and, therefore, can also be related to the Mid Miocene Unconformity. The globally correlatable Mid Miocene Unconformity was associated with a eustatic sea-level rise in the North Sea Basin (Huuse & Clausen, 2001; Rasmussen, 2004), probably controlled by tectonic activity and increased subsidence of the North Sea Basin (Michelsen et al., 1998; Clausen et al., 1999; Rasmussen, 2002, 2004) and climatic changes (Huuse & Clausen, 2001).

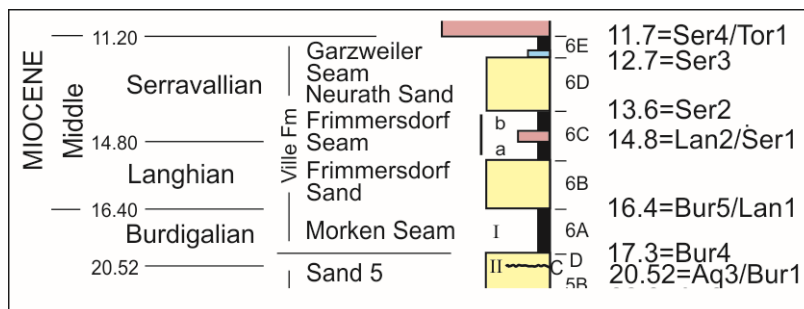


Fig. 5-5: Section of the stratigraphical log of the Lower Rhine Basin. The fluvial sand bed, which is indicated by the red bar within the lignite, separates the seam into Frimmersdorf a and Frimmersdorf b. This sand bed, which was exposed in the Hambach open-cast mine, was associated with the Mid-Miocene Unconformity.

The sand dykes and sills extending vertically and horizontally from the sand body into the adjacent lignite are indicative of injection processes that later affected the syn-depositional channel deposits the measured sand body. Liquefaction and fluidization may have resulted in the homogenization of former syn-sedimentary structures and may be responsible that syn-sedimentary structures within the clearly fluvial-estuarine channel deposit are only sporadically preserved within the measured sand body.

5.7 Conclusions

The sand body, which was observed within the Miocene-age Frimmersdorf in the Garzweiler open-cast mine, and which have been measured with high-resolution laser instruments, was probably of a syn-depositional origin. The features indicative of a syn-depositional origin include the presence of a variety of sedimentary structures (e.g. even parallel, or trough cross lamination), sand-lignite alternations, as well as the orientation of the sand body concordant to the lignite bedding.

The sand body was probably deposited in a small, meandering river draining the mires which formed along the coastline of the North Sea in middle Miocene times. It is also possible that the river may have been subjected to estuarine influences – particularly in its lower reaches and which may also have been controlled by an estuarine input. The sand body may be correlated to the Mid Miocene Unconformity, an erosive surface, which has been identified throughout the entire North Sea Basin. The progradation of river systems in the mires of the Lower Rhine Basin can be related to an eustatic sea-level rise of the adjacent North Sea.

6 Syn- and post-depositional sand bodies in lignite – the role of coal analysis in their recognition. A study from the Frimmersdorf Seam, Garzweiler open-cast mine, western Germany

Linda Prinz, Laura Zieger, Ralf Littke, Tom McCann, Peter Lokay, Sven Asmus

Originally published online in International Journal of Coal Geology 2017 (Published online: 08 June 2017), Volume 179, pp. 173-186.

6.1 Abstract

The Lower Rhine Basin is a Cenozoic-age rift basin at the NW end of the European Cenozoic Rift Basin. In Middle Miocene times, fluctuating sea-levels in the North Sea and the repeated spreading of paralic mires resulted in the deposition of marine sand units (Frimmersdorf and Neurath sands), alternating with thick lignite beds (Morken, Frimmersdorf and Garzweiler seams). Within the Frimmersdorf Seam, the presence of sand bodies has been interpreted both in terms of syn-depositional emplacement in an estuarine setting, as well as post-depositional sand injection and soft-sediment deformation partly linked to tectonic activity within the Lower Rhine Basin. While understanding of the causal mechanisms has improved, early recognition of sand concentrations in future mine area remains difficult. Therefore, organic petrological and inorganic geochemical analyses of sand and lignite samples were carried out in order to assess their efficacy as proxies for such studies. The results reflect the complexity of the depositional environment, which was influenced by both fresh and marine waters. Ash yields of the lignite samples are variable and sulphur contents as well as Ca/Mg ratios depend on the distance from the overlying marine Neurath Sand. Humic substance values of the lignites are dependent on the sampling position within the seam, and may be related to sand body deposition. Moderate contents of gelified macerals and the small size of huminite particles reflect the depositional environment during peat formation, but are not influenced by sand body deposition, not even when in close proximity to the sands. While the geochemical and petrological methods provide much information on the depositional environment of the Miocene-age Lower Rhine Basin, and also on marine versus freshwater deposition of the sands, they do not facilitate the differentiation of syn- and post-depositional sand emplacement in the Frimmersdorf Seam.

6.2 Introduction

The Lower Rhine Basin is a triangular-shaped rift system in NW Germany. The 100 km long and 50 km wide basin extends from the Netherlands in the NW to Bonn in the SE and cuts into the NW margin of the Rhenish Massif (Fig. 6-1; Schäfer et al., 1996; Klett et al., 2002). From the Oligocene through to the Pleistocene, up to c. 1300 m of siliciclastic sediments accumulated within the German part of the basin (Schäfer et al., 1996; Klett et al., 2002).

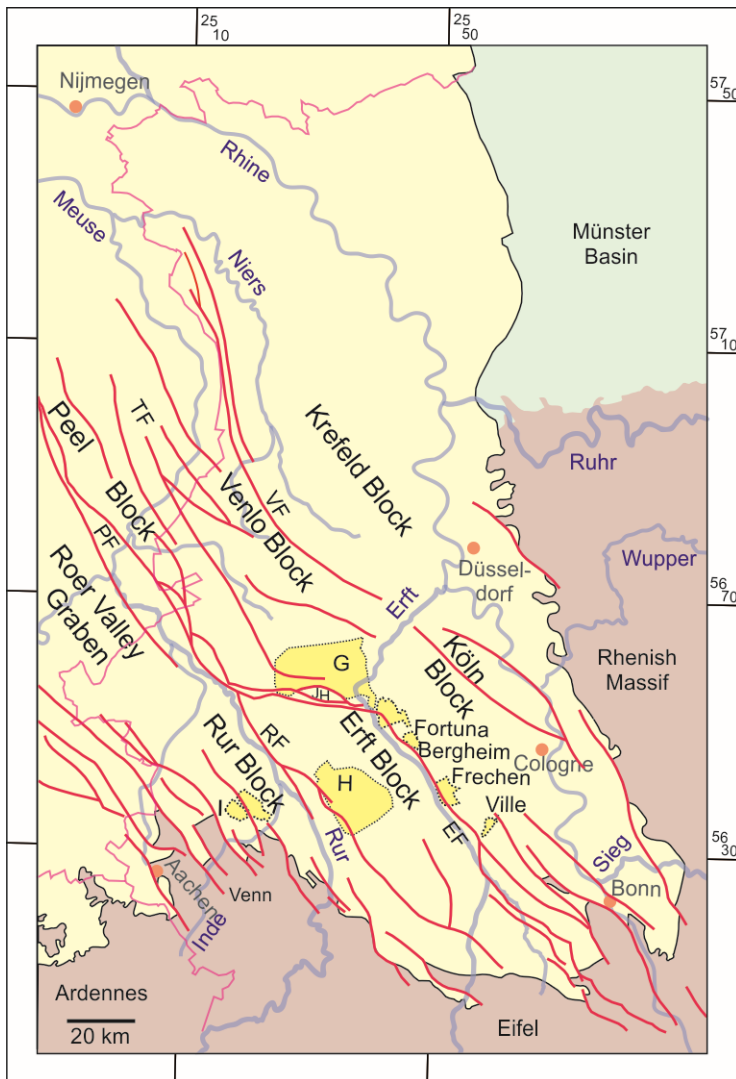


Fig. 6-1: A structural map of the Lower Rhine Embayment in the NW of the Rhenish Massif (after Houtgast and van Balen, 2000; Klett et al., 2002; Prinz et al., 2018; Schäfer et al., 1996; Schäfer and Utescher, 2014). Red lines mark the position of the fault systems, which separate the basin into six main tectonic blocks. Key: EF Ertf Fault, JH Jackerath Horst, PF Peel Fault, RF Rur Fault, TF Tegelen Fault, VF Viersen Fault. Pink line: Germany-Netherlands-Belgium borders. The Rur Block (Germany) extends into the Roer Valley Graben in the Netherlands. The figure also includes the position of the three active open-cast mines: G Garzweiler, H Hambach, and I Inden, as well as former open-cast mines and pits (Fortuna, Bergheim, Frechen and Ville).

In early to late Miocene times, marine and fluvial sediments with associated lignite seams were deposited (Schäfer et al., 1996; Klett et al., 2002). These lignite seams accumulated during three main phases of peat growth comprising, respectively, the Köln, Ville and Inden fms. Peat growth was favoured by ongoing basin subsidence (Hager, 1993; Schäfer et al., 1996), as well as optimal climatic conditions throughout the period of accumulation (Utescher et al., 2000; Zachos et al., 2001), with up to 270 m of peat being deposited in the basin centre (Mid-Miocene-age Main Seam of the Ville Formation, Fig. 6-2; Hager et al., 1981; Hager, 1986; Schäfer et al., 1996).

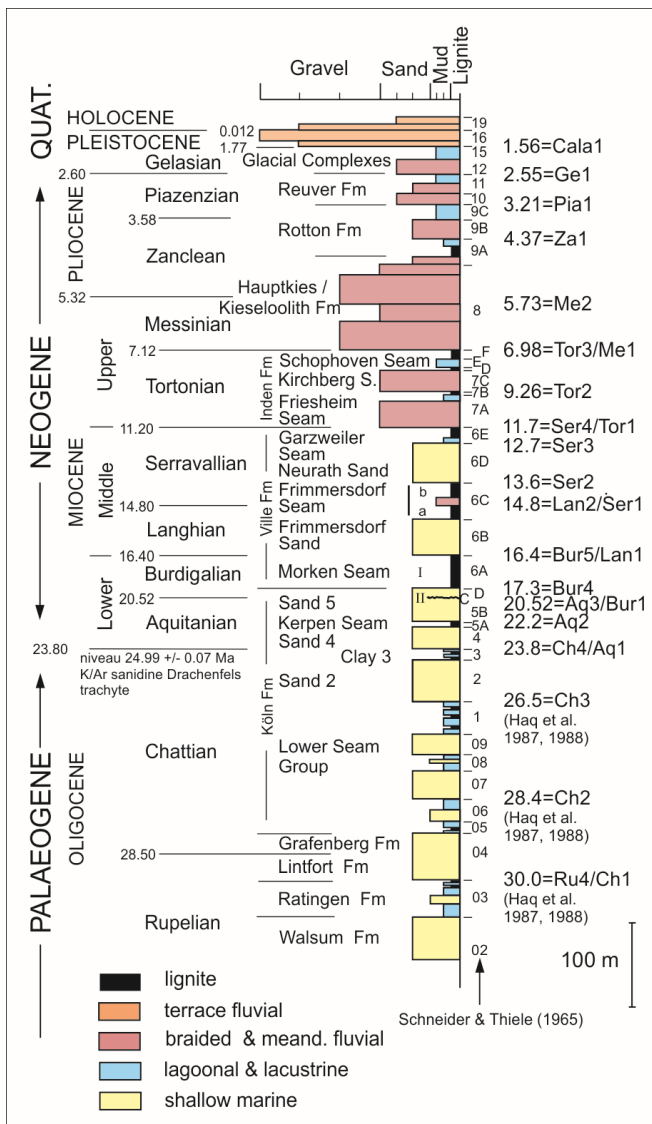


Fig. 6-2: Stratigraphic log of the Lower Rhine Basin (modified after Klett et al., 2002; Schäfer et al., 2004, 2005; Schäfer and Utescher, 2014; Prinz et al., 2018). The lithostratigraphic log represents the stratigraphy of the Lower Rhine Basin in the centre of the Ertf Block (based on two well logs, SNQ 1 on the Ertf Block, and Efferen on the Köln Block; RWE Power AG); lithostratigraphical code established by Schneider and Thiele (1965). Biostratigraphical ages (Ma; left) after Berggren et al. (1995), cycle ages (Ma; right) after Haq et al. (1987; 1988) & Hardenbol et al. (1998).

The lignites of the Ville Fm are of great economic interest, due to the seam thicknesses and the generally low ash and sulphur contents. Currently, they are worked in two open-cast mines (Hambach and Garzweiler open-cast mines) run by RWE Power AG (Fig. 6-1). The Garzweiler open-cast mine, the location for this study, is situated to the NW of Cologne, Germany (Fig. 6-1). It can be subdivided into the Garzweiler I and the currently active Garzweiler II fields, the latter containing c. 1.3 billion tons of lignite, which are exploited for electricity generation.

The mining of the Langhian/Serravallian-age Frimmersdorf Seam (on average 12 m in thickness), is complicated by the presence of fine- to medium-grained sand bodies. These irregularly-distributed sand bodies with variable thicknesses (mm's – c. 2 m) and morphologies have a negative effect on both the mining and processing of the lignite. Up to 1.5 million tons of lignite per annum could not be used for electricity generation in the past, since lignite containing $\geq 17\%$ sand is classified as barren. At present, the lignite is treated in coal preparation plants, reducing the waste significantly. However, due to the distances between the exploration wells, and the relatively low resolution of geophysical logs (sand bodies have to be at least 10 cm thick), high-resolution detection within future mining areas and the calculation of future lignite volumes remain a challenge.

A detailed knowledge of the sand body emplacement mechanisms within the area of the present-day Garzweiler II mining area will help both to improve the calculation of lignite volumes as well as gain insight into the Miocene-age palaeoenvironment. An initial classification of the sand bodies present within the lignites of the Frimmersdorf Seam suggested that a variety of syn- and post-depositional mechanisms were responsible for their emplacement (see Fig. 6-3) (Prinz et al., 2018). Syn-depositional emplacement mechanisms involve the deposition of sand in fluvial and tidal channels (Fig. 6-3a), as well as aperiodic events such as flooding of the Miocene-age mire. Subsequent to peat accumulation, overpressuring within the unconsolidated Frimmersdorf Sand led to sand injection into the Frimmersdorf Seam (Fig. 6-3b). Additionally, soft-sediment deformation of existing syn-depositional structures (e.g. due, for example, to peat compaction), may have been responsible for the morphology of some of the sand bodies (Prinz et al., 2018).

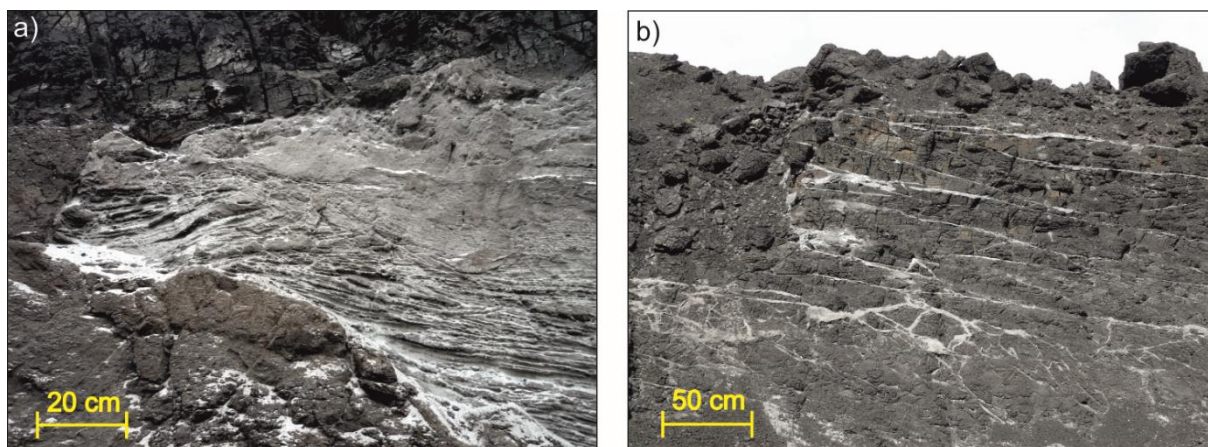


Fig. 6-3: Sand bodies in the Frimmersdorf Seam, Garzweiler open-cast mine. a) A syn-depositional sand body comprising (trough) cross lamination; this sand body was deposited in a fluvial-estuarine environment; b) A variety of post-depositional sand bodies, including sills and dykes.

In this present study, the initial classification of the sand bodies (see Prinz et al., 2018) is integrated with geochemical, coal petrological and micropetrographical analyses, in order to further clarify possible emplacement mechanisms for the sands. To maximise our understanding of the Miocene-age depositional setting and any possible relationship with the emplacement of sand bodies within the Frimmersdorf Seam, all palaeoenvironmental aspects controlling its evolution, including tectonics, sedimentology, climate evolution and the types of peat-forming vegetation present (i.e. classification of the type of mire) must be considered. The correlation of syn-, and post-depositional sand bodies, respectively, with the results of the methods noted above aims to facilitate the classification of future sand bodies within the Frimmersdorf Seam.

6.3 Geological background

6.3.1 Geological setting

The Lower Rhine Basin is part of the extensive European Cenozoic Rift System (ECRS), which was active in middle to late Eocene times (Ziegler, 1992; Ziegler et al., 1995; Dèzes et al., 2004; Ziegler & Dèzes, 2007). The ECRS extends c. 1100 km from the Mediterranean via the Upper Rhine Graben to the North Sea Basin (Ziegler, 1992, Sissingh, 2003).

The formation of the Lower Rhine Basin commenced in Oligocene times at the NW margin of the Rhenish Massif (Schäfer et al., 1996). The basin subsided to a maximum of 1300 m along the NW-SE-trending Rur, Erft, Peel, Tegelen and Viersen fault systems (Schäfer et al., 1996, Houtgast & van Balen, 2000). Basin infill, from the onset of subsidence in the Oligocene,

consisted of clastic sediments, both marine and fluvial, controlled by sea-level changes in the North Sea, and precipitation in the Rhenish Massif area (Schäfer et al., 1996; Becker and Asmus, 2005). Thus, the stratigraphically-oldest deposits within the Lower Rhine Basin are early Oligocene-age marine siliciclastic sediments, which accumulated following the transgression of the North Sea onto the flat, peneplained Palaeozoic and Mesozoic basement (Schäfer and Utescher, 2014).

With the retreat of the North Sea at the Oligocene-Miocene transition, coastal mires with constantly shifting fluvial systems were established on the coastal plain between the shoreline to the NW and the Rhenish Massif to the SE (Schäfer et al., 2004; Becker and Asmus, 2005). In this area, the sediments of the so-called Köln Fm, comprising thin lignite seams (Lower Seam Group, Aquitanian – early Burdigalian, Fig. 6-2), were deposited (Schäfer et al. 2004; Becker and Asmus, 2005).

From early Burdigalian to late Serravallian times, a combination of optimal climatic conditions (see chapter 6.3.2), repeated long-term retreats of the North Sea from the Lower Rhine Basin, and a decrease in basin subsidence, favoured the establishment of extensive mires (Teichmüller, 1958; Teichmüller and Thomson, 1958; Schäfer et al., 1996; Klett et al., 2002). As noted above, locally up to 270 m of peat was deposited over a time span of c. 9 Ma (Hager et al., 1981; Hager, 1993). The peat accumulations within the Lower Rhine Basin were initially formed in topogenous mires that gradually evolved into raised bogs (Schäfer, 1994; Stock et al., 2016). Organic petrological, geochemical and carbon isotope analyses of lignite samples from the Garzweiler open-cast mine allowed the reconstruction of a nutrient depleted paralic depositional environment (Stock et al., 2016). Low sulphur and ash yields, in combination with low GWI (groundwater index; see section 6.5.1) and VI (vegetation index) values indicated a depositional setting within a raised mire, with floral assemblages that developed under stable environmental conditions above the general groundwater level (Stock et al., 2016). Petrographical and organic geochemical studies have shown, that the peat-forming vegetation in the Miocene-age mires mainly comprised herbaceous plants and deciduous trees (Stock et al., 2016), and major vegetation changes from angiosperm- to gymnosperm-dominated taxa (Lücke et al., 1999).

Peat accumulation was repeatedly interrupted by marine transgressions, two of which were extensive enough to result in the deposition of the marine Frimmersdorf and Neurath sands (Petzelberger, 1994). These, up to 60 m thick, transgressive sands subdivide the up to 100 m thick Main Seam (Ville Fm, Fig. 6-2) into three subordinate seams in the NW. The stratigraphically lowest lignite within the NW part of the Ville Fm is the Morken Seam (c. 15 m; mean seam thicknesses within the Garzweiler open-cast mine), which is overlain by the marine

Frimmersdorf Sand (c. 15 m). The overlying Frimmersdorf Seam (c. 15 m) is erosively capped by the marine Neurath Sand (up to 60 m). The uppermost unit of the Ville Fm is the Garzweiler Seam (c. 10 m).

The Serravallian/Tortonian transition marked the end of marine influence in the Lower Rhine Basin (Boersma et al., 1981; Abraham, 1994; Valdivia-Manchego, 1994; Schäfer and Utescher, 2014). The succession (Inden Fm, Fig. 6-2) comprises fluvial sediments deposited from meandering river systems (Abraham, 1994; Klett et al., 2002; Schäfer et al., 2004), as well as peat accumulations from locally restricted mires (= Upper Seam Group; Schäfer et al., 2004). Similar conditions prevailed during the Messinian extending through to Pliocene and Pleistocene times, when meandering systems were gradually replaced by braided ones (Boenigk, 1981; Klett et al., 2002; Schäfer and Utescher, 2014).

6.3.2 Climate and sea level fluctuations

As noted above, sedimentation within the Lower Rhine Basin was largely influenced by major climatic changes and sea-level fluctuations (Fig. 6-4; Utescher et al., 2000, 2009; Zachos et al., 2001). Indeed, the climatic evolution of the basin can be characterised as a general cooling trend from almost tropical conditions in middle Eocene times, through to mean annual temperatures (MAT) of 16-25 °C in Oligocene and Miocene times. The sea-level highstand in Upper Oligocene times can be correlated with global warming and a eustatic sea level rise (Zagwijn and Hager, 1987; Schäfer and Utescher, 2014). The warm and humid conditions continued into the Miocene warm interval, this latter phase representing the warmest period in the Neogene, and extended up to Early Serravallian times (Mid-Miocene climatic optimum, 17-14 Ma, latest Burdigalian to early Serravallian; Utescher et al., 2002, 2009; Schäfer and Utescher, 2014). Deposition of the Morken Seam, the Frimmersdorf Sand, the Frimmersdorf Seam and the basal part of the Neurath Sand occurred during this warm period (Utescher et al., 2002).

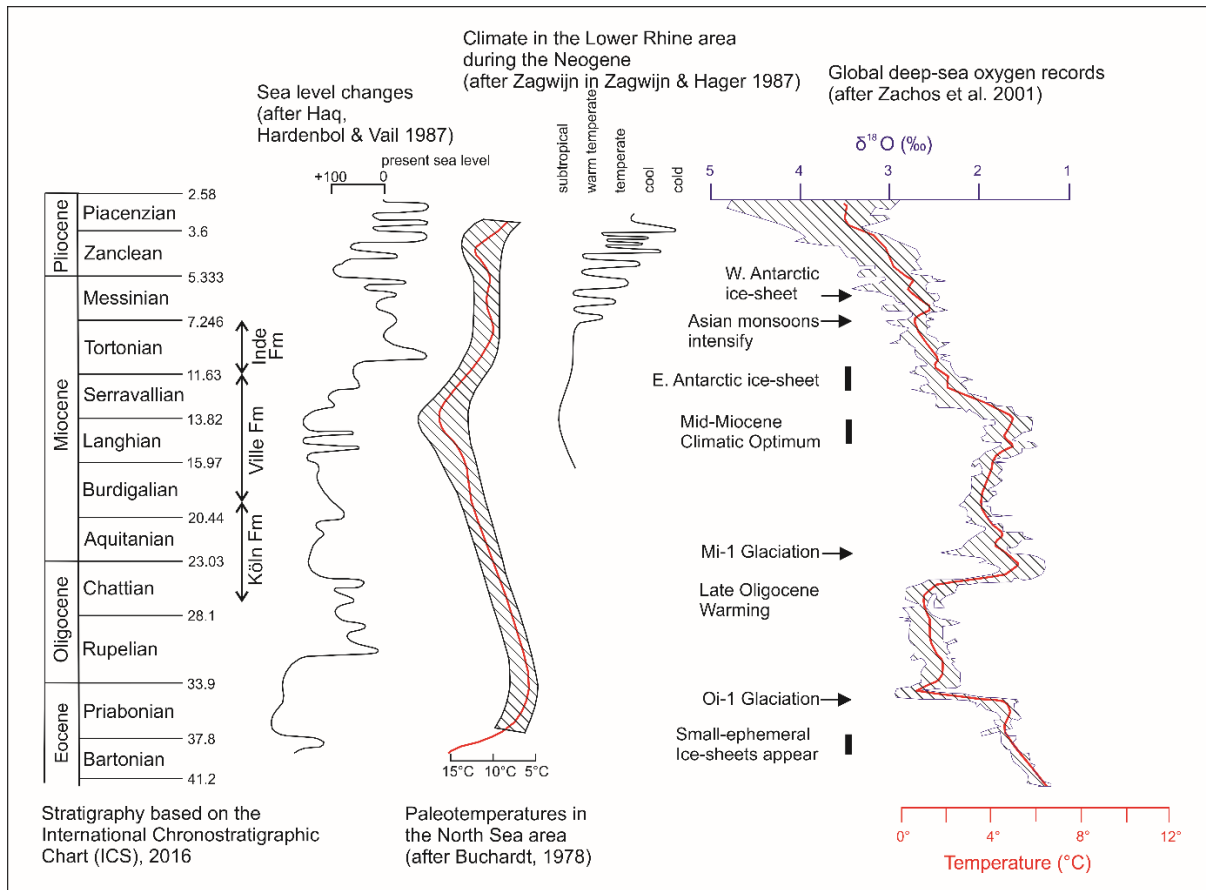


Fig. 6-4: Sea level fluctuation and climatic variations in the North Sea (after Bucharadt, 1978; Haq et al., 1987; Zagwijn and Hager, 1987; Hager & Prüfert, 1988; Hager, 1993), compared to global climatic changes (after Zachos et al., 2001). International chronostratigraphic chart after Cohen et al. (2013; updated).

A marked regression, related to a major eustatic sea-level fall, occurred during the globally correlatable Middle Miocene cooling (14.1-14.8 Ma; Hardenbol et al., 1998; Utescher et al., 2002). The temperature decrease is recognised in the Late Serravallian-age Garzweiler Seam (Lücke et al., 1999; Utescher et al., 2000; Stock et al., 2016). From Late Miocene times onward, the weakening oceanic influence (coastal offlap, global regression from 14 Ma onwards; Haq et al., 1988), was characterized by a marked increase in seasonality (Utescher et al., 2000), combined with 2-3°C of cooling (Utescher et al., 2009; Stock et al., 2016). Evidence of ongoing cooling has been observed in the Tortonian-age Upper Seam Group (Inden Fm), and this was coeval with an extreme sea-level lowstand (Utescher et al., 2002).

At the Miocene/Pliocene transition, the deposition of the coarse-grained Hauptkies Fm in a braided river system was related to a decrease in temperature and a sea-level lowstand that can be correlated to an early glacial event (Messinian). In Pliocene times, temperatures continued to fall, down to MATs of <15°C (Utescher et al., 2000; Mosbrugger et al., 2005; Utescher et al., 2012), marking the onset of the Pleistocene glaciation (Mosbrugger et al., 2005).

6.4 Methods

6.4.1 Sampling strategy

Sampling of coals in proximity to a variety of different sand bodies was carried out at six different locations in the Garzweiler open-cast mine. In total, 79 samples (55 lignite, 20 sand, 2 mud and 2 wood samples) were taken. The samples from Locations 1, 2 and 3 represent the lowermost 6 m of the Frimmersdorf Seam. At Location 1, a vertical profile of 4.5 m above seam base was sampled. 15 lignites were taken, as well as one sand sample from the underlying Frimmersdorf Sand, and one sand sample from one of two parallel sand beds within the lignite. At Location 2, a total of 26 samples were taken, including 19 lignite, 1 mud and 6 sand samples, covering the clastic deposits of an irregular shaped sand body, and lignites at varying distances to this sand body. Samples from Location 3 comprise 5 sand and 10 lignite samples, including 2 lignite samples from lignite clasts, which were embedded in the sand bodies. Samples from Locations 4 and 5 represent the uppermost two metres of the Frimmersdorf Seam, while those from Location 6 were derived from the central part of the seam. At Location 4, 1 piece of wood, 2 sand and 3 lignite samples were taken at the top of the Frimmersdorf Seam and from three parallel sand beds within the seam. At Location 5, 3 samples from a sand body immediately below the Neurath Sand (see Prinz et al. 2017 for more details on the Neurath Sand), as well as 1 lignite sample and 1 wood sample were sampled. Location 6 was positioned in the central part of the seam. Here, 1 mud and 2 sand samples from a laterally extended sand body, and 7 lignite samples from the contact areas between the lignite and sand have been taken.

6.4.2 Sample preparation

Prior to the geochemical analyses, the lignite samples were lyophilised. The dry samples were cut and prepared in order to manufacture polished sections; preparation of the sections followed the procedure of DIN (Deutsches Institut für Normung/ German Institute for Standardization) 22020-2 (1998) as described in Littke et al. (2012). The remaining dried sample aliquots were ground to a fine powder, using a disc mill, as an initial step for the geochemical analyses. Two clay and one sand samples were treated with hydrogen peroxide in order to remove any organic material prior to X-ray diffraction analysis.

6.4.3 Ash yield and elemental analysis

The ash yields of the lignite samples (54 samples; as described in Taylor et al. 1998 and following the DIN 51719, 1997 procedure) were measured in triplicate from 1 ± 0.1 g ground and water-free samples which were heated in a muffle furnace at a constant heating rate of $8.33^\circ\text{C}/\text{min}$ to 500°C . Subsequently, the sample was heated to a temperature of 850°C for 60 min. After cooling to room temperature in a desiccator, the incinerated sample was weighed. The loss of ignition (LOI) of four sand samples (Location 2) was measured in triplicate according to DIN 18128 procedure (DIN 18128, 2002). The water-free and ground samples, weighing 1 ± 0.1 g (weighed in a preheated porcelain crucible) were heated in a muffle furnace at 550°C for at least 2h. After cooling in a desiccator, the samples were reweighed.

Total organic carbon (TOC) and total inorganic carbon (TIC) were measured using a LiquiTOC II-device with a solid matter module. The device was calibrated with a 47.10% total carbon (TC) standard for lignite and a 5.31% standard for sand. Oxygen served as the carrier gas. The total sulphur content (TS) was measured using a Leco S-200 elemental analyser, calibrated with a Leco Sulphur standard, containing $0.313 \pm 0.015\%$ sulphur. Pulverised and homogenised samples were weighed in a ceramic crucible (20 mg of lignite or 100 mg of sand), and mixed with iron fillings to ensure complete combustion. In the high-frequency induction furnace, the sample evaporated at a temperature of 1800°C . The resulting SO_2 was transported to an IR-detector with oxygen as carrier gas.

6.4.4 Humic substances

In total, 23 lignite samples were analysed, derived from Locations 1 (n=3), 2 (n=12), 3 (n=5) and 4 (n=3). At Location 2, 4 sand samples were also collected for analysis.

The fractionation of the humic substances was performed using a modified three-stage method, based on differences in the solubility of humin, humic acid and fulvic acid. In order to leach the acidic fraction from the coal substance, c. 3 g of the pulverised and dry lignite samples and 4 g of the sand samples were mixed with a few drops of acetone and 50 ml of 0.5 M KOH in a small vessel which was initially placed for 5 min in an ultrasonic bath and then centrifuged for 10 min at 8500 rpm. The humin, together with any inorganic components of the sample precipitated due to the insolubility of humin in alkaline environments. The leachate, containing the readily soluble fulvic and humic acid fractions was transferred to a new centrifuge vessel and 4 ml of 30% HCl were added. Subsequently, 1 M HCl was added to the solution until it attained a pH of 1. Following a reaction time of at least 12h, all of the humic acid contained in the sample was precipitated. The suspension was once again centrifuged for

20 min at 8500 rpm. The precipitated humic acid was then dried in an oven at a moderate temperature for at least two days. Subsequently, the solid humic acid fraction was weighed. The remaining leachate, containing the fulvic acid, was transferred into a new centrifuge vessel and 1 M NaOH was added until a pH 7 was attained, and at which point the fulvic acid precipitates. Once again, the sample was set aside for at least 12h and then centrifuged again for 20 min at 14000 rpm (following 5 min in an ultrasonic bath). The precipitate was dried in an oven at moderate temperatures for at least two days, at which point the solid fulvic acid fraction could be weighed. The results for the sand samples were normalised with their LOI results.

6.4.5 Coal petrography

The micro-petrographic composition of coal samples is based on maceral counting and classification (ICCP, 2001; Sýkorová et al. 2005; Pickel et al. 2017). The analysis was conducted at a Zeiss Axio Imager microscope (automatic point counting instrument; software Fossil; Technisches Büro Carl H. Hilgers), with 500 points counted per section. Maceral counting was performed under incident light with 500 x total magnification, using a 50 x oil immersion objective. The identification of liptinites was facilitated by the use of a UV-light source and a 50 x Epiplan-NEOFLUAR objective.

6.4.6 Inorganic geochemistry and mineralogy

The XRF analysis of 15 lignite samples (Locations 1-5) was performed at the Sybilla laboratory of RWE Power AG. The lignites were dried at 130°C, filled into a grinding vessel of wolfram carbide, and then treated in a disc mill (following the DIN 51701 standard sample preparation procedure). Analyses were conducted in a S8 TIGER (Bruker) with sequential wavelength dispersive X-ray fluorescence (WDXRF). The oxides (SiO_2 , TiO_2 , Al_2O_3 , Fe_2O_3 , MnO , MgO , CaO , Na_2O , K_2O , P_2O_5 , SO_3 and BaO) were determined following slow ashing of the lignite samples.

Bulk mineralogical compositions were derived from the X-ray diffraction patterns measured on randomly oriented powders of the < 10 μm fraction of the organic free samples (14/488 and 14/489). This grain size fraction was separated by sedimentation in deionized water, washed, dried and milled in a McCrone Micronising mill to assure uniform crystallite sizes. Milling was done in ethanol to avoid dissolution of water-soluble components, strain and heat damage. An internal standard (corundum, 20 wt%) was added to improve the accuracy of the analysis. Sample holders were prepared by means of a side filling method to minimize preferential

orientation. The measurements were done on a Huber MC9300 diffractometer using CoK α -radiation produced at 40 kV and 30 mA. During the measurement, the sample was illuminated through a fixed divergence slit (1.8 mm, 1.45°), a graphite monochromator and a 58 mm, 0.3 mm spacing soller slit. The diffracted beam was measured with a scintillation detector at a counting time of 10 s for each step of 0.02° 2 θ . Diffractograms were recorded in the 2 θ range from 2° to 82°. Quantitative phase analysis was performed by Rietveld refinement using the Profex-BGMN software (Doebelin and Kleeberg, 2015), with customized clay mineral structure models (Ufer et al., 2008, 2012 & 2015). All reported mineral compositions relate to the crystalline content of the analysed samples. Detailed identification of clay minerals was done on oriented mounts on porous ceramic tiles. These were measured from 2 to 42° 2 θ , with a step size of 0.02° and counting time of 5 s, in air-dried, glycolated and heated (500 °C) states.

6.5 Results and discussion

The analytical tools that were used to examine the lignites and sands from the different locations include the ash yield (Fig. 6-5), the Loss of Ignition (LOI), the carbon content and maceral analyses. The results of the analyses are shown in tables 6-1-6-3.

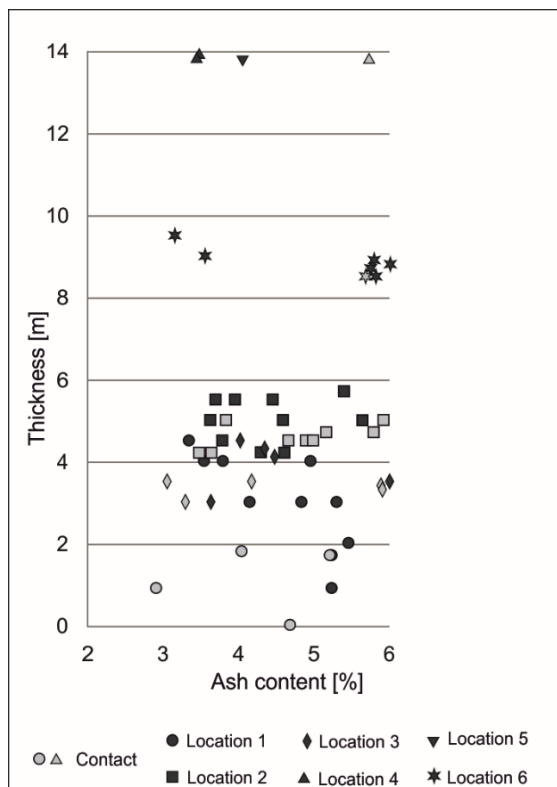


Fig. 6-5: Plot of the ash yields of the lignite samples from Locations 1-6, which are distributed on a nearly vertical section from the bottom to the top of the Frimmersdorf Seam. The light grey marks indicate lignite samples that were taken from contact areas with sand bodies.

6.5.1 Syn-depositional sand features

Syn-depositional emplacement mechanisms within the Miocene-age peat environment include deposition in river or stream channels (Gersib & McCabe, 1981; Hager, 1993), as well as deposition related to occasional inundations, e.g. during storm events (Goodbred et al., 1998), or river floods (Kalkreuth et al., 1991). The various features produced from these events can be subdivided into a) broadly concordant sand beds (Locations 1, 4 and 6) and b) channel-like units (Location 5), which were sampled at the base (Location 1), in the central part (Location 6), and at the top of the Frimmersdorf Seam (Locations 4 & 5).

Table 6-1: Carbon, sulphur and ash contents at Locations 1-6; s: sample type, L: Location, n: number of samples.

s	L	n	TOC [wt.%]			TIC [wt.%]			TC [wt.%]			TS [wt.%]			ash [wt.%]		
			min	max	Ø	min	max	Ø	min	max	Ø	min	max	Ø	min	max	Ø
lignite	1	14	50,02	66,80	60,52	0,99	1,90	1,41	51,20	68,27	61,93	0,52	0,88	0,70	2,91	5,44	4,46
	2	19	57,20	63,58	61,72	0,53	2,38	1,17	58,17	64,55	62,44	0,76	1,82	1,32	3,47	5,9	4,53
	3	10	58,36	62,30	60,20	0,70	1,73	1,18	59,73	63,54	61,38	0,59	0,91	0,72	3,05	5,98	4,47
	4	3	46,14	60,56	54,65	1,24	1,54	1,38	47,51	61,80	65,03	2,83	3,53	3,18 (n=2)	3,44	5,7	4,2
	5	1	54,32	54,32	54,32	3,62	3,62	3,62	57,94	57,94	57,94	3,44	3,44	3,44 (n=1)	4,04	4,04	4,05
	6	7	56,87	62,39	60,45	0,92	3,54	1,47	60,42	63,59	61,92	0,95	1,89	1,38	3,15	5,99	5,09
sand	1	2	2,35	4,38	3,37	0,24	0,29	0,27	2,60	4,67	3,64	0,15	0,15	0,15 (n=1)	n.a.	n.a.	n.a.
	2	6	0,45	4,39	2,78	0,18	0,20	0,18	0,62	4,57	2,96	0,15	0,32	0,27 (n=4)	n.a.	n.a.	n.a.
	3	5	3,32	5,74	4,39	0,18	0,31	0,26	3,63	6,03	4,65	0,15	3,29	1,02 (n=5)	n.a.	n.a.	n.a.
	4	2	1,22	1,61	1,42	0,21	0,22	0,22	1,43	1,83	1,63	3,48	3,48	3,48 (n=1)	n.a.	n.a.	n.a.
	5	3	0,41	2,54	1,25	0,18	0,19	0,19	0,59	2,72	1,43	n.a.	n.a.	n.a.	n.a.	n.a.	n.a.
	6	2	0,89	2,54	1,72	0,18	0,18	0,18	1,07	2,63	1,85	n.a.	n.a.	n.a.	n.a.	n.a.	n.a.
clay	2	1	36,63	36,63	36,63	10,95	10,95	10,95	47,58	47,58	47,58	n.a.	n.a.	n.a.	n.a.	n.a.	n.a.
	6	1	4,82	4,82	4,82	0,25	0,25	0,25	5,06	5,06	5,06	n.a.	n.a.	n.a.	n.a.	n.a.	n.a.
wood	5	1	47,39	47,39	47,39	3,32	3,32	3,32	50,71	50,71	50,71	6,53	6,53	6,53	n.a.	n.a.	n.a.

In terms of the ash yield, the values range from 2.91 to 5.99% (on average 4.59%; Table 6-1) for the lignites adjacent to syn-depositional sand bodies (Fig. 6-5). These ash yields, when compared with other mining areas, are comparably low (Ballisoy and Schiffer, 2001; Stock et al., 2016; RWE internal report). Additionally, no trend in terms of ash yield relative to the lignite's position in relation to the sand bodies has been observed, e.g. samples from the direct contact between the lignites and sand may show lower ash yields than lignites at a distance of a few centimetres. The lignite sample from Location 5, i.e. the channel-like sand body, had a slightly lower ash yield (4.04%) than the sand beds from Locations 1 (4.46 %), 4 (4.21%) and 6 (5.09%). However, due to the low sample density this result cannot be considered conclusive. The LOI values of the analysed sand samples vary between 3.99% and 7.96%, with an average of 5.60% (Table 6-2).

Table 6-2: distribution of humic substances and Loss of Ignition (LOI); n = 27 samples; L = Location.

L	Sample	material	LOI [wt%]	humic acid + ash [wt%]	humic acid [wt%]	fulvic acid [wt%]
1	14/417	lignite	n.a.	64,54	33,70	1,76
	14/418	lignite	n.a.	76,62	21,39	1,99
	14/422	lignite	n.a.	85,71	12,51	1,78
2	14/433	lignite	n.a.	81,95	16,60	1,45
	14/435	lignite	n.a.	91,18	7,63	1,19
	14/438	lignite	n.a.	90,51	8,13	1,36
	14/440	lignite	n.a.	92,61	6,22	1,18
	14/441	lignite	n.a.	88,05	10,87	1,08
	14/442	lignite	n.a.	89,16	9,76	1,08
	14/443	lignite	n.a.	93,01	5,94	1,05
	14/444	lignite	n.a.	77,32	21,32	1,36
	14/445	lignite	n.a.	85,37	13,26	1,37
	14/446	lignite	n.a.	81,50	16,83	1,67
	14/447	lignite	n.a.	93,15	5,93	0,92
	14/451	lignite	n.a.	92,86	6,17	0,97
	14/452	sand	5,46	66,11	26,25	7,64
	14/453	sand	3,99	66,11	27,10	6,68
14/455	sand	5,00	66,22	25,85	12,60	
14/456	sand	7,96	61,56	28,94	7,79	
3	14/459	lignite	n.a.	63,26	7,15	1,72
	14/463	lignite	n.a.	89,61	8,66	1,73
	14/467	lignite	n.a.	90,38	8,41	1,22
	14/470	lignite	n.a.	80,22	18,17	1,61
	14/473	lignite	n.a.	83,00	15,46	1,55
4	14/476	lignite	n.a.	91,24	7,49	1,27
	14/477	lignite	n.a.	93,25	5,73	1,02
	14/479	lignite	n.a.	90,43	8,45	1,11

TOC contents (Table 6-1) of lignite samples surrounding the syn-depositional sand bodies would appear to correlate with seam depth. Within the lignite samples of the lower and the middle parts of the Frimmersdorf Seam (Locations 1, 60.52% and 6, 60.45%), TOC contents are higher than at the top of the seam (Locations 4, 54.65% and 5, 54.32%). TIC contents of the lignite samples adjacent to the syn-depositional sand bodies range from 0.92-3.62% (on

average 1.51%). The TOC (1.85%) and TIC (0.21%) values for the sand samples do not show any apparent correlation.

Sulphur values (Table 6-1, Fig. 6-6) of syn-depositional sand bodies show an upseam increase, ranging from 0.67% at the base (Location 1) through to 1.38% in the middle (Location 6), up to 3.28% at the top of the seam (Location 4). The lignite (n=1) from Location 5 had a sulphur content of 3.44% while a wood sample (14/483) from the same location, but in direct contact with the Neurather Sand had the highest recorded sulphur content for the area (6.53%).

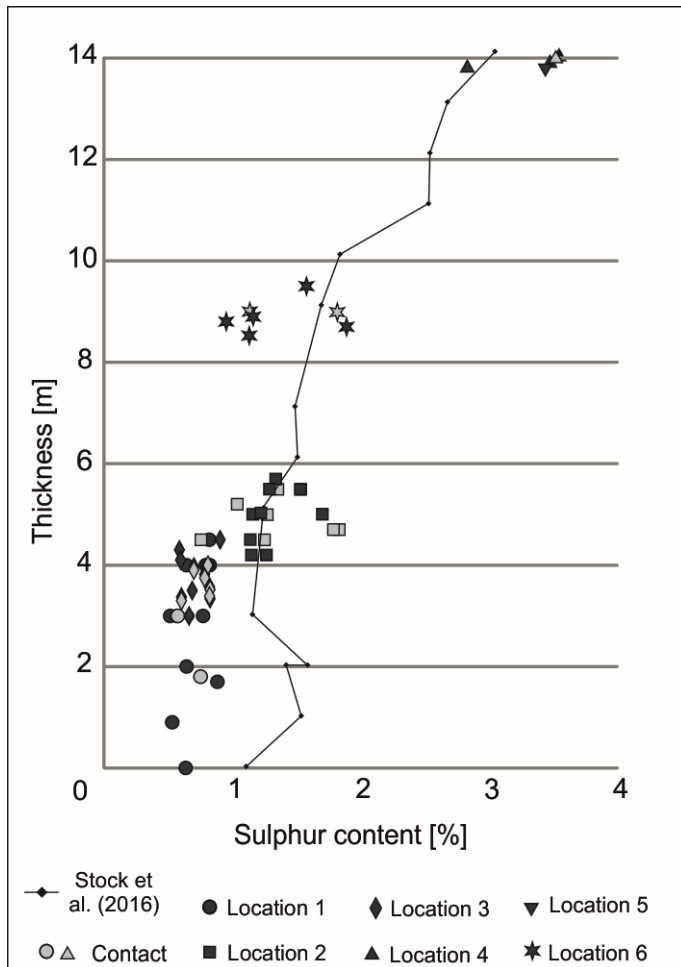


Fig. 6-6: Sulphur contents from lignite samples from Locations 1 to 6. The thin black line represents sulphur contents measured by Stock et al. (2016) in their study on the Frimmersdorf Seam.

The distribution of humic substances (humins, humic acids and fulvic acids; Table 6-2, Fig. 6-7) in the lignites adjacent to the syn-depositional sand bodies was also dependent on the sample position with the Frimmersdorf Seam. Humic and fulvic acids decrease from the base through to the top of the seam, and this trend most probably results from the downward leaching of the mobile humic fractions.

The 55 lignite samples, on average, comprise 87.77% huminite, 5.89% liptinite, 1.39% inertinite (e.g. Fig. 6-8), and 4.95% mineral matter. The most abundant submaceral of the lignite samples is humodetrinite, with an average content of 70.03%, ranging from 49.0 to 90.33%. Maceral analyses would suggest that liptinite and inertinite contents decrease from the seam base to the top, decreasing from 6-21 to 3.8% (liptinite), and 1.52 to 1.0% (inertinite), respectively.

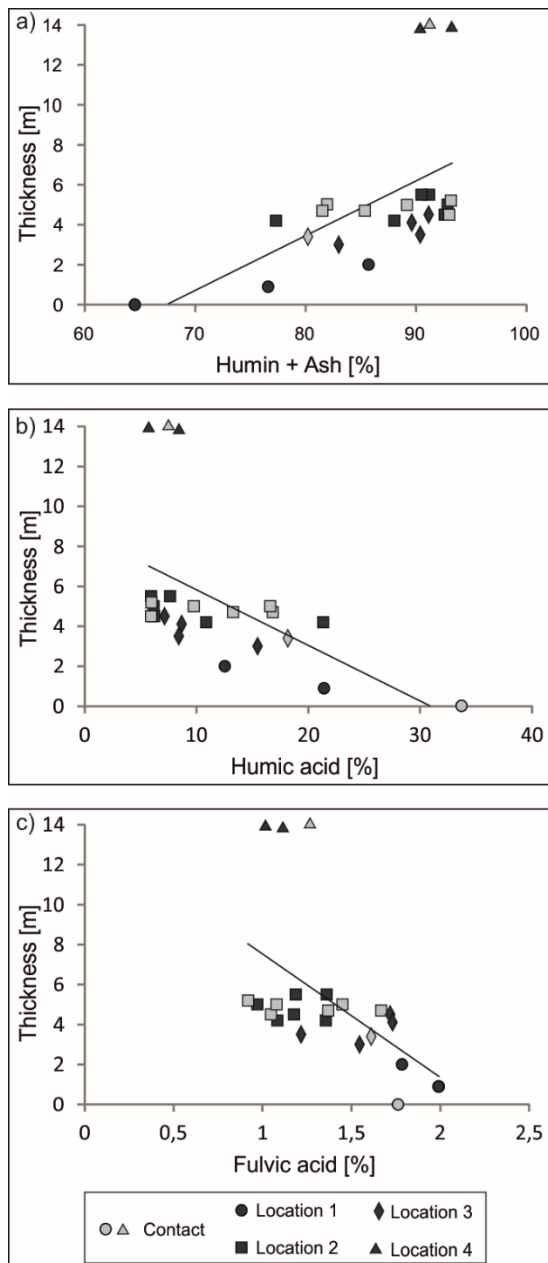


Fig. 6-7: Distribution of humic substances. a) Humin, b) Humic acid, c) Fulvic acid, in relation to the position of the sampled lignite within the Frimmersdorf Seam (see text for location details).

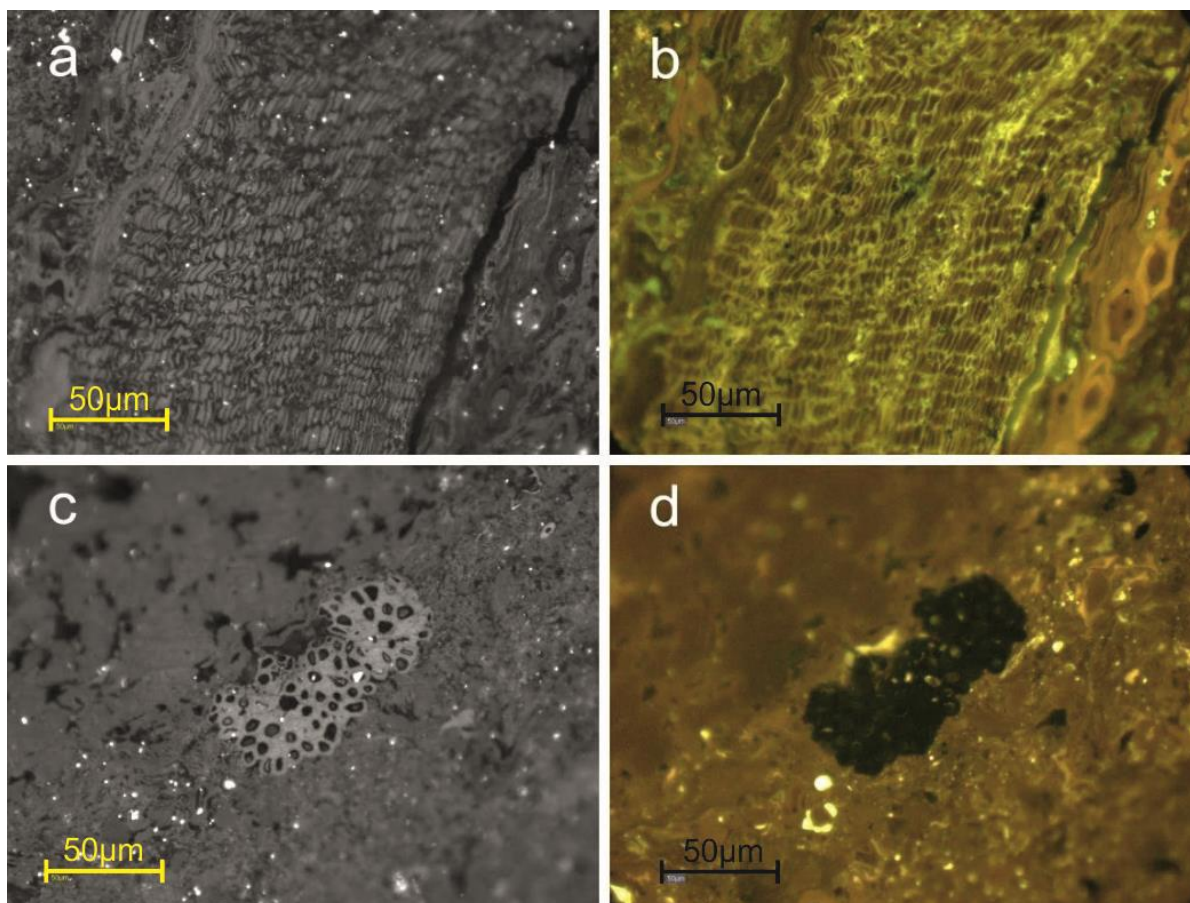


Fig. 6-8: Microphotographs of samples from Location 2 in incident- (a, c) and UV-light (b, d) showing examples of structured macerals: (a, b) ulminite (U) and corpohuminite (C) surrounded by suberin (S); (c, d) funginite (F) in a matrix of attrinite (A) and densinite (D). The yellow scale (lower left corner) is 50µm.

The maceral indices, i.e. the composition of the peat, as illustrated by the gelification index and the preserved plant tissue can be used for the classification of the depositional environment. The gelification index (GI) reflects the water availability within the mire; the tissue preservation index (TPI) represents the palaeovegetation, since lignin-rich plants, such as trees and shrubs, are more resistant to degradation and gelification than cellulose-rich, herbaceous plants (Diessel, 1992). GI and TPI ratios were calculated on the basis of equations (1) and (2), respectively (modified after Kalkreuth et al., 1991; Diessel, 1992), and adapted for lignites:

$$(1) \text{GI} = \frac{(\text{huminite} - \text{attrinite} - \text{textinite}) + \text{macrinite}}{\text{textinite} + \text{attrinite} + \text{semifusinite} + \text{fusinite} + \text{inertodetrinite}}$$

$$(2) \text{TPI} = \frac{\text{humotelinite} + \text{semifusinite} + \text{fusinite}}{\text{macrinite} + \text{detrohuminite}}$$

The ratios of the vegetation index and the groundwater index (VI/GWI; Calder et al., 1991; Flores, 2002) can be used as an indicator of the water supply to the mire, with two types recognized - ombrotrophic (fed by rainwater) or rheotrophic/topotrophic (groundwater). VI and GWIAC are calculated following equations (3) and (4) (modified after Hacquebard, 1993 and Stock et al., 2016):

$$(3) VI = \frac{\text{humotelinite} + \text{semifusinite} + \text{fusinite} + \text{suberinite} + \text{resinite}}{(\text{huminite} - \text{humotelinite}) + \text{inertodetrinite} + \text{liptodetrinite} + \text{sporinite} + \text{cutinite}}$$

$$(4) GWI_{AC} = \frac{\text{gelohuminite} + \text{densinite} + \frac{\text{ash content}}{2}}{\text{humotelinite}}$$

The main ash constituents of the lignite samples are either SiO₂ (40% of the sampled lignite) or CaO (53%, see Table 6-3). Within one sample (Location 2, 14/443), SiO₂ (30.7%) and CaO (26.0%) contents are almost identical. Maximum CaO contents of CaO-dominated lignites range from 33.1-43.5% (on average 38.6%). High CaO values are associated with high SO₃ contents (range 24.5-36%; on average 27.6%). Within the 15 lignite samples, Fe₂O₃ contents range from 1.29%-11.8% (on average 7.58%). The highest Fe₂O₃ contents (>8%) were observed in CaO-dominated lignite ashes.

Table 6-3: Major element distribution from lignite samples from Locations 1-5, based on XRF analysis of 15 lignite samples; L: Location, n: sample ID.

L	n	SiO ₂ [wt%]	TiO ₂ [wt%]	Al ₂ O ₃ [wt%]	Fe ₂ O ₃ [wt%]	MnO [wt%]	MgO [wt%]	CaO [wt%]	Na ₂ O [wt%]	K ₂ O [wt%]	P ₂ O ₅ [wt%]	SO ₃ [wt%]	BaO [wt%]
1	417	93,40	<0.1	0,45	1,29	<0.1	0,42	2,75	0,16	<0.1	<0.2	1,85	<0.1
	422	2,35	0,11	1,07	11,60	0,16	3,47	43,50	0,23	<0.1	<0.2	25,10	0,22
	431	2,21	0,12	4,05	8,92	0,11	3,42	41,10	0,23	<0.1	<0.2	28,70	0,20
2	434	17,30	0,25	5,20	7,37	0,11	2,84	33,10	0,20	<0.1	<0.2	26,70	0,18
	443	30,70	0,14	3,02	9,71	0,11	2,42	26,00	0,18	<0.1	<0.2	25,30	0,12
	444	68,00	0,22	1,10	4,44	<0.1	1,22	12,60	0,17	<0.1	<0.2	8,58	<0.1
	447	65,60	0,37	2,14	4,54	<0.1	1,30	12,10	0,19	0,10	<0.2	10,40	<0.1
	450	5,44	0,10	1,97	9,50	0,16	3,50	40,50	0,25	<0.1	<0.2	30,50	0,20
3	461	1,32	<0.1	3,77	10,20	0,17	3,33	39,90	0,21	<0.1	<0.2	29,00	0,22
	463	0,82	0,11	3,32	10,60	0,18	3,29	38,30	0,22	<0.1	<0.2	36,00	0,24
	466	68,60	0,17	1,56	4,25	<0.1	1,27	12,80	0,18	<0.1	<0.2	8,30	<0.1
	467	0,92	0,13	3,67	11,80	0,18	3,44	42,20	0,21	<0.1	<0.2	24,90	0,26
	473	2,67	0,14	2,15	11,20	0,21	3,49	42,60	0,22	<0.1	<0.2	24,50	0,26
4	476	66,70	0,11	1,93	2,30	<0.1	1,26	11,40	0,18	<0.1	<0.2	13,60	<0.1
5	184	72,80	0,28	2,56	5,95	<0.1	1,20	5,46	0,17	0,15	<0.2	8,72	<0.1

Major element analysis (XRF), i.e. the measurements of the occurrence of oxides within the lignites, can be used to ascertain the composition of the water influencing the peat (seawater/freshwater), as well as any possible interactions between the water and the peat (Foscolos et al., 1989; Diessel, 1992). The Ca/Mg ratio is a useful indicator for the freshwater/seawater differentiation, since Miocene-age seawater (like modern seawater) was enriched in Mg compared to freshwater (Hardie, 1996; Zimmermann, 2000; Lowenstein et al., 2001). The distribution and values of SiO₂, CaO and Al₂O₃ can be used to classify the silicates within the lignites. Ash samples dominated by SiO₂ suggest that the quartz grains originated from precipitation during the peat stage. The presence of clay minerals, on the other hand can indicate authigenic deposition. Furthermore, the ratios of FeO/TiO₂ and MnO/TiO₂ (compared to a sample set of shale that is used as standard) can be used to measure the relative transport energy on the mire surface (Kolditz et al., 2012). The silicate compositions of the lignite ash samples from Locations 1 at the base of the seam, and 4 and 5 at the top of the seam, do not show any correlation between SiO₂, or CaO-dominance, nor with the position of the sample within the seam (base/top), or in terms of the proximity of syn-depositional sand bodies.

The results of the XRD analyses from one clay sample (14/488) and one sand sample (14/489) from Location 6 are described below. Sample 14/488 mainly consists of 10 Å clays and micas (45.28%; consisting of muscovite, illite and glauconite), quartz (24.22%) and kaolinite (23.49%), with minor amounts of microcline (4.65%), anatase (2.09%) and siderite (0.27%). The clay fraction from the sand sample (14/489) showed a clearly visible green colour subsequent to the removal of organic material. Since this sample was measured on an oriented aggregate mount, the results represent only a qualitative mineral composition. The calculated muscovite 1Mt in sample 14/489, as well as the muscovite 1Md and 2M1 in sample 14/488 represent 10 Å clays and mica (TOT minerals). These consist of muscovite, illite, and glauconite as well as possible glauconite-containing mixed layer clays, such as glauconite-illite and glauconite-smectite, which were not identified or qualified separately.

The clay fractions sampled from the sand beds at Location 6 contained glauconite (XRD analyses). The formation of glauconite is restricted to marine environments at shallow water depths (Chafetz and Reid, 2000). The presence of glauconite with the sand beds at Location 6 would, therefore, suggest that these sands were originally deposited in a shallow-marine setting.

6.5.2 Post-depositional sand features

The sand bodies at Locations 2 and 3 have been interpreted in terms of post-depositional sand injection (see Prinz et al., 2018 for more details). Sills and dykes at Location 3 most probably result from liquefaction and re-mobilisation of sand, followed by its injection and re-deposition within the lignite (Braccini et al., 2008; Hurst et al., 2011; Fontana et al., 2015). The classification of the sand body at Location 2 is more ambiguous, although the absence of sedimentary structures, the irregular morphology and the wavy lower and upper boundaries, would suggest a post-depositional origin. Sampling Locations 2 and 3 are positioned at the same seam level, and only a few meters distant from one another.

The measured ash yields at Location 2 range from 3.47 to 5.90% (on average 4.53%; Fig. 6-5). Ash yields from lignites sampled at the upper boundary decrease (from 5.90 to 4.44%; and 3.83 to 3.69%) with increasing distance (max 3 cm) to the sand body. In contrast, at the lower boundary ash yields increase with increasing distance (max 50 cm) from the sand bodies, ranging from 3.63% and 3.47% at the direct contact, to 4.29% and 4.59%, respectively, at a distance of 50 cm. At Location 3, ash yields range from 3.05 to 5.98%. The highest ash yields have been measured from two lignite clasts, one embedded in the sands (5.86%), and one (5.88%) sampled at 10 cm distance to the sand body. In summary, lignite sampled at some

distance to the sand body show slightly higher ash yields in comparison with samples taken from the direct lignite-sand contact.

TOC (60.90%) and TIC (1.18%) values for the lignite samples show little variation. However, it should be noted, that there is a considerable variability in the TOC contents of the sands (n=6) from Location 2 which range between 0.45% and 4.39%. The TOC and TIC of a clay sample from the same location are remarkably high (36.63 and 10.95%, respectively). Samples from within the sand body at Location 3 have slightly higher TIC contents (0.31%) than those taken from the horizontal sand layers (i.e. sills, beds; 0.18%).

Sulphur values from the lignite samples at Location 2 range from 0.76 to 1.82% (1.31% on average; Fig. 6-6), while the sand samples from the same location range from 0.15 to 0.32% (0.27% on average). Based on the sulphur distribution within the sand body and the adjacent lignite, it would appear that there is no noticeable trend in sulphur values in relation to the sand body. At Location 3, lignite sulphur contents range from 0.59 to 0.91% (average 0.72%). Within the measured sands, the range of sulphur values (0.15 to 3.29%) is comparably high. However, both within the sand and the lignite samples, no vertical or other trend have been observed.

The values of soluble humic substances from lignite samples at Location 2 show significant variations, ranging from 6.85 to 22.68%. At Location 3, soluble humic substances range from 8.87 to 19.87%. At Locations 2 and 3, a vertical decrease of humin from the top to the bottom of the sampling locations, as well as an increase in both humic and fulvic acids was observed (Fig. 6-7).

In terms of the maceral group distribution, samples of Location 2 show slightly lower values of huminites (85.72%) and inertinites (1.01%) than those from Location 3 (88.48% and 1.58%, respectively), while liptinite contents are nearly identical (6.68 and 6.80%). The mineral content of lignites at Location 2 (6.59%) is more than twice that of Location 3 (3.14%). At Location 3, the lignite ashes are mainly CaO-dominated, and also show the highest Fe₂O₃ values. Only one sample from the direct contact between lignite and sand showed a SiO₂ dominated silicate composition. At Location 2, the number of SiO₂ dominated samples (n= 2) equals the number of CaO dominated lignite ashes.

6.5.3 Evaluating the coal petrology and inorganic geochemistry in terms of syn-depositional and post-depositional processes

As noted above, a range of geochemical, mineralogical and coal petrographical factors were measured within the Frimmersdorf Seam of the Garzweiler open-cast mine. Comparing and contrasting these analyses, and their possible relationship with the causal mechanisms which controlled the formation of the sand bodies within the Frimmersdorf Seam may help to elucidate the origin (syn/post-depositional) as well as help to differentiate such bodies from one another.

The ash yield values are broadly similar across the region, and between Locations 1-6. The average ash yield of the syn-depositional sand bodies of 4.59% is quite similar to those of the post-depositional sand bodies (4.51%). This would suggest that the ash yield of lignites adjacent to these sand bodies is broadly independent of the causal mechanisms, in that there are only minor increases in lignite ash values with decreasing distance to the sand bodies. In terms of the syn-depositional emplacement of the sand bodies, these results are unexpected, since the input of sand into a peat usually results in higher ash yields (Whateley and Tuncali, 1995). For example, peats from the Mississippi delta adjacent to a clastic source contain about 50% ash (McCabe, 1987). Low ash yields for the post-depositional sand bodies, however, would suggest that the emplacement of the sand bodies occurred subsequent to any compaction of the peat, or even at the lignite formation stage. Due to the presence of numerous syn-depositional sand bodies within the Frimmersdorf Seam (see Prinz et al., 2018), a higher ash yield within the lignites of the Frimmersdorf Seam would be expected. However, the comparably low lignite ash yields from the sampling locations are characteristic for all of the lignite seams within the Lower Rhine Basin (Stock et al., 2016; RWE internal report). As such, the low ash yield, as well as the overall sharp contacts between the lignite and sand, are probably the result of the peat structure, rather than the absence of clastic sources.

The sulphur (organic or pyritic) content and its distribution within a lignite seam may be an indicator of any possible marine influence on the peat or lignite. The total sulphur content in coals consists of an organic and an inorganic component. One of the common inorganic constituents in lignite is pyrite (Ward, 2002, 2016). The presence of pyrite in coals may reflect both a syn-depositional (e.g. framboids, euhedral crystals), as well as a post-depositional origin (e.g. massive, fracture filling and dendritic pyrite; Dai et al., 2015). In the studied lignites, mainly syn-depositional pyrite is present. This form of pyrite (or possibly marcasite) is formed during the peat stage by anaerobic sulphate-reducing bacteria in the presence of iron (III) according to the following equations (Berner, 1984):

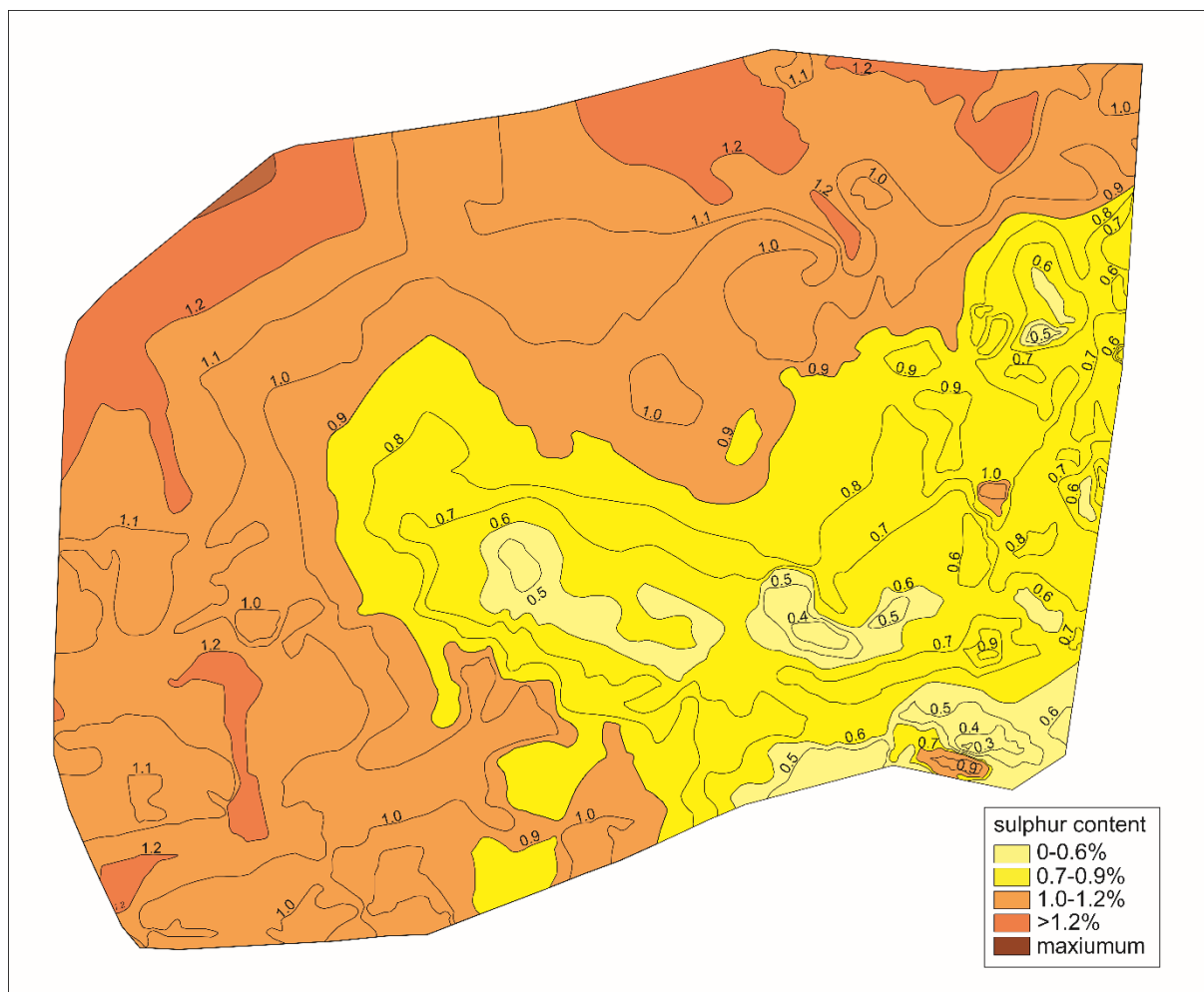


Fig. 6-9: Contour map of the sulphur content of the Frimmersdorf Seam in the Garzweiler open-cast mine (RWE Power AG; see Fig. 6-1 for location).

In terms of humic substances fractionation, the increase in the contents of both humic and fulvic acids from lignites and sands sampled from the top of the seam, in comparison to those sampled from the bottom, in addition to the decrease in humin from seam top to base, may both have resulted from the downward leaching of the mobile soluble humic fractions within the seam. However, marked variations in humic and fulvic acid contents from Locations 2 and 3 (post-depositional) suggest that it may be possible to differentiate between syn- and post-depositional sand bodies. The markedly variable humic and fulvic acid contents within a locally restricted sand body may result from the liquefaction and fluidization of the re-deposited sands, and, therefore, may be indicative of post-depositional sand bodies. However, for more precise assessment of the correlation between the sand injection and variations in the contents of soluble humic substances, a detailed study examining this hypothesis would be necessary.

In terms of the carbon content of the lignite and sand samples, the position of the sampling locations would appear to be the decisive factor. Additionally, the carbon content correlated with the colour of the sand samples. Micropetrographical analyses have shown that the dark

brownish colours of the sand bodies result from organic substances, which coat the lighter sand grains. These humic substances migrate into the sands from the surrounding peat and/or lignite, and, thus, TOC values can not be used to determine the timing of sand deposition within the seam. However, TIC contents of lignites adjacent to post-depositional sand bodies are slightly lower compared to those of lignites adjacent to syn-depositional sand bodies. On the other hand, the internal variations of TIC within both of the sand bodies exceed the variance between syn- and post-depositional sand body types; more detailed examination would be necessary to properly evaluate this.

The maceral composition of the lignites do not correlate with the syn- or post-depositional origin of the sand bodies but rather with the position of the sampling location within the seam. Additionally, microscopic analyses of the direct contact areas between lignite and sand indicate that the contacts are mainly sharp. The silicate composition of lignite ashes adjacent to the syn- and post-depositional sand bodies do not show any correlation with the sand bodies and, thus, can not be used to subdivide the sand bodies within the Frimmersdorf Seam.

Examination of the various results presented above would suggest that, in general, the classification and differentiation of the sand bodies based purely on geochemical or coal petrographical analyses is not possible. Some analytical techniques, however, do show a degree of promise. For example, marine and non-marine sands can be clearly differentiated (see below). Furthermore, it would appear that the TIC contents, as well as the observed variations in the contents of soluble humic substances may be indicative of post-depositional emplacement mechanisms, although this hypothesis would require further (and more detailed) analysis. However, the analytical results do provide much information with regard to the general depositional environment during Miocene times and, therefore, elucidate the conditions under which the syn-depositional sand bodies were deposited.

6.5.4 Depositional environment

As noted by Taylor et al. (1998, see also Gore, 1983), the term “mire” has been used since the early eighties as a generic word for wetlands (such as moors, swamps, fens etc.) in which peat accumulates. Mires can be classified as a) topogenous mires, where peat formation is caused by high levels of groundwater, and where the peats are often richer in plant nutrients (eutrophic) and higher in inorganic content, and b) ombrogenous mires where the water is provided by rainfall, and the resultant peats are poorer both in terms of plant nutrients (oligotrophic, ombrotrophic) and inorganic content. Thus, determining the type of water present within a peat-forming ecosystem (i.e. rainwater, groundwater) is of fundamental importance in

interpreting the depositional setting. As part of this, the ash and mineral contents of the lignites can be useful since they provide information on the eutrophic/oligotrophic nature of the waters which passed through the mires (Taylor et al., 1998; Iordanidis and Georgakopoulos, 2003; Stock et al., 2016).

The ash yield of the lignite is generally low, when compared to lignites from other mining areas (see Ballisoy and Schiffer, 2001; Stock et al., 2016; RWE internal report). Higher ash yields at the base of the Frimmersdorf Seam were interpreted as being indicative of permanent water cover at the onset of peat formation, related to peat accumulation in a topogenous mire or low moor (cf. Iordanidis and Georgakopoulos, 2003). The low ash-yield values within the rest of the seam would suggest that this low moor, over time, gradually changed into a raised bog (cf. Borren et al., 2004), characterized by ombrogenous conditions (Cameron et al., 1989; Stock et al., 2016), and with peat accumulation occurring above the general groundwater level (Stock et al., 2016). However, the unexpectedly low ash yields which were measured from the lignite samples in direct contact with syn-depositional sand bodies (fluvial/estuarine) are problematic, suggesting that the determination of topogenous/ombrogenous conditions based on ash yields from the Frimmersdorf Seam is questionable.

Humic substances fractionation can be used to provide information on the mineralisation of the water influencing the seam during the peat or lignite stage. The appearance and distribution of the different macerals within lignite samples can be used as an indicator for the hydrological (marine, brackish or freshwater) and vegetational conditions within the palaeoenvironment (Diessel, 1986; Kalkreuth et al. 1991). During the peat- and lignite stages, biochemical gelification (a physico-chemical process, in which solid, humic material is transformed into a plastic phase), occurred (Teichmüller, 1975). The degree of gelification is dependent on the depositional conditions, e.g. the water supply (Teichmüller, 1989). The moderate to low degree of gelification of the macerals, as indicated by the GI ratios would suggest that there was periodic flooding of the otherwise mainly ombrogenous mire (Diessel, 1986; Crosdale, 1993; Kalkreuth et al., 1991), and this flooding may have also been responsible for the deposition of the adjacent sand bodies. The higher degree of gelification in some samples (Fig. 6-10) would support the hypothesis that the sand bodies were deposited in river systems or from flooding events, as well as from the injection of liquefied sands into the seam.

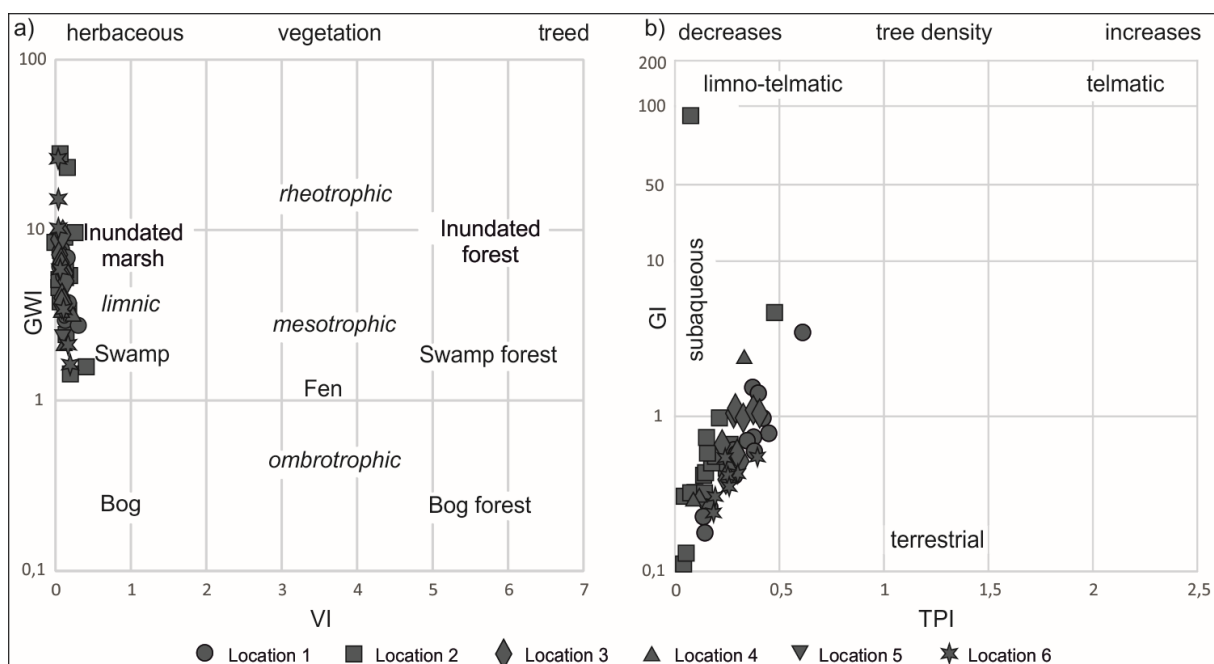


Fig. 6-10: GWI/VI-, and GI/TPI ratios of samples from Locations 1 to 6. The GWI/VI ratios (a) were plotted onto the mire palaeoenvironment diagram of Calder et al. (1991). b) Classification of the paleo-mire type after Diessel (1986), in which the TPI are plotted against GI values.

The water level within the peat-forming environment (i.e. above or below the groundwater level) can also be determined by the GWIAC/VI ratios (Fig. 6-10a). The GWIAC values of most samples would suggest that deposition occurred within a limnic swamp or marsh milieu (mesotrophic, i.e. transitional between ombrogenous/topogenous conditions). Additionally, some of the plot positions (Fig. 6-10a) would support the idea of periodic flooding. Deposition in a subaqueous setting is also supported by the GI and TPI values (Fig. 6-10b, cf. Diessel 1986), although it is possibly that both the GI and GWIAC values may have been affected by the post-depositional flow of water within the peat/lignite system. Such changes in the GI and GWIAC values (Fig. 6-10, cf. Calder et al. 1991) may have resulted in the environment being designated as mesotrophic rather than ombrotrophic. Thus, the GWIAC/VI ratios do not necessarily reflect the water supply during peat formation, since they can be easily “reset” by subsequent fluid movement within the depositional setting. The post-depositional influence of water on the maceral ratios is also reflected by the fact that similar VI values are present in lignite samples taken from the same stratigraphic level whereas the GWIAC values (from the same samples) are highly variable.

These initial results (see above), would suggest that the lignites of the Frimmersdorf Seam were deposited in a mire under mesotrophic to ombrotrophic conditions. The vegetation was dominated by small, herbaceous plants (indicated by VI values, cf. Stock et al. 2016), and the mire was characterized by a low to moderate water table, while also being influenced by strong

flooding events. The marked impact of these short term, intense flooding events may have affected the organic petrology, in particular those results related to gelification (GI values).

The chemistry of the water present within the depositional setting (i.e. marine, brackish or freshwater) can be determined using a number of indices, e.g. the TOC/TS ratios, the sulphur content, or Ca/Mg ratios (Werner, 1958; Ward, 1991; Bechtel et al., 2008). The TOC/TS ratios of the lignites in the Frimmersdorf Seam would suggest that the depositional setting was dominated by freshwater. Berner (1984) and Casagrande (1987) have noted that marine, organic-rich sediments show a linear relation between the S and TOC contents, resulting from pyrite formation due to microbial activity. The TOC/TS ratios of the lignite samples from the Frimmersdorf Seam show significantly lower ratios when compared to those of the “Normal Marine” standard (cf. Berner, 1984 and Casagrande, 1987), suggesting that the pore waters were fresh.

The generally low ash and moderate sulphur contents from the samples of the Frimmersdorf Seam both suggest that the sand bodies were deposited under freshwater conditions (cf. Taylor et al. 1998), with the sulphur contents subsequently modified by the deposition of the overlying marine Neurath Sand. In general, decreasing ash and sulphur contents towards the top of lignite seams coincide with the natural evolution of a mire towards increasingly less groundwater-controlled conditions (i.e. drier conditions, cf. Kalkreuth et al., 1991). However, the fact that an opposing trend has been observed in the Frimmersdorf Seam (i.e. towards wetter conditions) may be related to the post-lignite deposition of the Neurath Sand (Fig. 6-6, Stock et al., 2016; Prinz et al. 2017). Indeed, the observed variations in the TOC/TS ratios at the top of the lignite, as well as the increase in the observed TS values from the base to the top (Fig. 6-6), would both support the idea of marine flooding of the depositional setting (see also Prinz et al. 2017)

Werner (1963) suggested that a Ca/Mg ratio of <8 was indicative of a possible marine influence on lignites from the Lower Rhine Basin. The ratios for 15 lignite samples taken adjacent to the sand bodies from Locations 2 to 5 range are all >8 (i.e. between 11.94 and 14.86) and would, thus, suggest that there was no marine influence. The apparent contrast with the sulphur contents above, where the values would suggest post-depositional alteration due to the subsequent deposition of the Neurath Sand can be explained by the fact that the dissolved Mg and Ca are bound to the organic material within the mire. Here, part of the non-crystalline inorganic particles are attached to carboxylates and similar functional groups and remain in the peat in an ion-exchangeable state (Ward, 1991). Additionally, the sorption of Ca-cations in sediment decreases with the increasing salinity of the transport fluid (Müller, 1964).

The Ca/Mg ratios of two samples taken from contacts of the Frimmersdorf Sand-Frimmersdorf Seam and the Frimmersdorf Seam-Neurath Sand, respectively, have values of ≤ 8 , thus possibly indicating the influence of the marine signal on the Ca/Mg ratios. An additional sample (14/476) from the latter contact (Location 4) has a higher value (10.72). A possible explanation for this higher value may be the reduction in the amount of Mg as a result of subsequent dilution by rainwater.

6.6 Transport energy

Kolditz et al. (2012) have suggested that the FeO/TiO_2 and MnO/TiO_2 ratios can be used to indicate the relative energy levels of fine-grained sediments within tidal flat settings. FeO/TiO_2 ratios higher than those of an average shale standard (after Wedepohl, 1971) are indicative of a low-energy transport, while higher transport energies are suggested for sediments with ratios similar to the stoichiometric composition of ilmenite (Fig. 6-11a). The MnO/TiO_2 ratios may also reflect the prevailing energy level during sand transport within the mire, with particular values for the redeposition of sand within the setting being suggested (i.e. the “relocation” of sand according to Kolditz et al., 2012; Fig. 6-11b). The FeO/TiO_2 and MnO/TiO_2 ratios measured for 15 samples from various sand bodies within the lignite all show values which are higher than those of the standard average shale (or relocated sand). This would suggest low energy transport of the sands prior to their deposition within the peat-forming system.

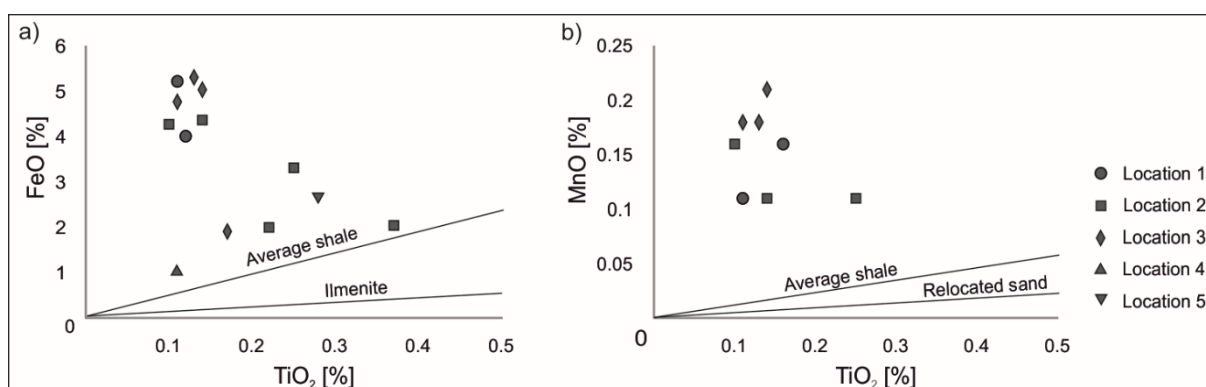


Fig. 6-11: FeO/TiO_2 and MnO/TiO_2 ratios are used as indicators for the energy level of sediment transport in tidal flat marshes (Kolditz et al., 2012). a) Plot of FeO/TiO_2 ratios of the analysed lignites in comparison to the ratios of an “Average shale” and ilmenite after Wedepohl (1971). b) Plot of MnO/TiO_2 ratios of the analysed lignites, compared to the ratios of the “Average shale” and “Relocated sand” (after Kolditz et al., 2012).

6.7 Conclusions

In Miocene-times, the Lower Rhine Basin formed a large embayment, which was controlled by shallow-marine conditions in the NW, and the establishment of extensive mires, dewatered by

several small river systems to the SE. Within the peat and lignites of the present-day Frimmersdorf Seam, numerous sand bodies have been observed. The present study has confirmed, that several causal mechanisms may have been responsible for the emplacement of sand bodies within the seam. Though various analyses, for example of sulphur and ash yields, indicate deposition within a freshwater-controlled depositional environment, other results such as the presence of glauconite within one channel-like sand body, and rarely observed lower Ca/Mg ratios, would suggest possible marine influence. Thus, the depositional environment would appear to have been one broadly characterized by freshwater conditions, with rare marine flooding events.

These results correlate with a depositional model of the Lower Rhine Basin representing an extended estuarine setting, controlled by the interaction of fluvial and tidal-marine processes. The development of small fluvial systems, which drained the peat environment, led to the deposition of channel deposits, as well as possible crevasse splays. The tidal influence of the adjacent North Sea may have resulted in the deposition of glauconite-bearing sands (possibly channelized) within the mire, as well as increased Ca/Mg ratios in lignites adjacent to the sand bodies. Subsequently, post-depositional sand injection led to the formation of a series of highly-variable sand bodies, and these are associated with highly gelified macerals within the adjacent peats. Marked variations within the humic substances fractions may have resulted from the liquefaction, fluidization, and re-deposition of the sands within the injection structures.

Though the various geochemical and petrographical analyses on lignite samples from the Frimmersdorf Seam provide very useful information on the Miocene-age depositional environment and the post-depositional effects of the overlying marine Neurath Sand, a classification of the sand bodies based purely on the presented analytical methods would appear to be questionable. Though some indicators, such as the TIC content or the observed variations in soluble humic substances within the post-depositional sand bodies would appear to be useful in terms of classifying the sand bodies, it is clear that further work is necessary.

Acknowledgements

We are thankful for the theoretical support and suggestions of P. Weniger (BGR) and A.T. Stock (LEK). We acknowledge project funding of the first author from RWE Power AG. Thanks to the staff members of the department GOC-L, especially the field crew of the Garzweiler open-cast mine. The manuscript benefited greatly from the comments of Shifeng Dai and an anonymous reviewer.

7 Sand injectites - from source to emplacement: an example from the Miocene-age Frimmersdorf Seam, Garzweiler open-cast mine, Lower Rhine Embayment.

Linda Prinz & Tom McCann

Submitted at Subsurface Sand Remobilization and Injection. Special Volume of the Geological Society of London

7.1 Abstract

Sand injectites are exposed in a Miocene-age lignite seam in the Lower Rhine Embayment, which is exploited in the Garzweiler open-cast mine, Germany. Due to the ongoing mining of the seam, the sand injectites were analysed over a timespan of three years. The combination of fieldwork, geophysical and drilling well data, as well as a 3D reconstruction of the host unit revealed that the sand injectites within the Frimmersdorf Seam (=host unit) are highly variable, and include sills, dykes, reticulate and irregular-shaped sand bodies. The injectites may be connected to the underlying Frimmersdorf Sand (=parent sand unit), the overlying Neurath Sand (=parent sand unit), or distributed throughout the seam. Sand injectites often contain lignite intraclasts that are indicative of the erosive forces that affected the host unit during the injection processes. The differentiation of sand injectites from syn-depositional sand bodies is largely based on the orientation (discordant/concordant), and the presence of primary sedimentary structures in the latter.

The formation of the sand injectites was partly related to seismic activity along the numerous and still active syn-sedimentary fault systems of the Lower Rhine Basin. The remobilisation of fault-parallel oriented sand injectites was largely controlled by the prevailing stress field during injection processes.

7.2 Introduction

The Lower Rhine Embayment is a Cenozoic-age rift system which extends from the NW border of the Rhenish Massif into the West Netherlands Basin (Geluk et al., 1994). It consists of numerous (half-) graben and horst structures in NW Germany, The Netherlands and Belgium. The main elements of this rift are the Lower Rhine Basin (Schäfer et al., 1996, 2004) in the NW of the Rhenish Massif, and the Roer Valley Rift System to the NW (Houtgast & van Balen, 2000; Bense & van Balen, 2004; Camelbeeck et al., 2007).

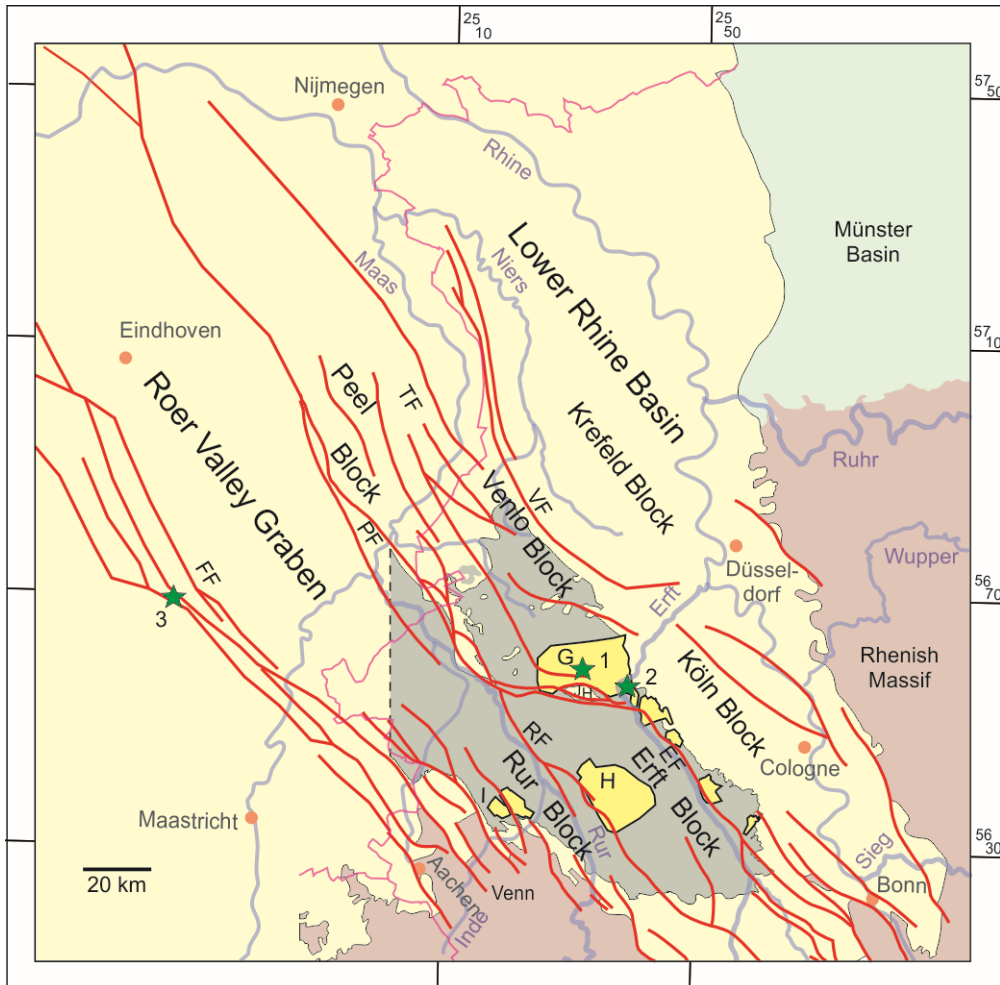


Fig. 7-1: A structural map of the Lower Rhine Embayment (Germany/Belgium/The Netherlands), comprising the Roer Valley Graben and the Lower Rhine Basin. The red lines represent the major fault systems within the Lower Rhine Embayment (EF: Erft Fault, FF: Feldbiss Fault, JH: Jackerath Horst, PF: Peel Fault, RF: Rur Fault, TF: Tegelen fault, VF: Viersen Fault). The yellow areas mark the positions of former and active open-cast mines (G: Garzweiler, H: Hambach, I: Inden open-cast mines). The green stars indicate locations where sand injectites have been observed (1: present study location, 2: see Bajor (1958) and Berger (1958), 3: see Vanneste et al. (1999)). The grey area represents the distribution of the Frimmersdorf Seam (RWE Power AG; western border is not specified). After Schäfer et al. (1996); Houtgast & van Balen (2000); Klett et al. (2002); Schäfer & Utescher (2014); Prinz et al. (2018).

The study area is located in the central part of the Lower Rhine Basin on the so-called Venlo Block (Fig. 7-1). In the active Garzweiler open-cast mine (RWE Power AG), lignites of the so-called Ville Fm (Mid Miocene-age, Fig. 7-2) are exploited. Mining of the Langhian/Serravallian-age Frimmersdorf Seam has been affected by the presence of numerous sand bodies for some years, and thus understanding their location and origin is of great economic importance.

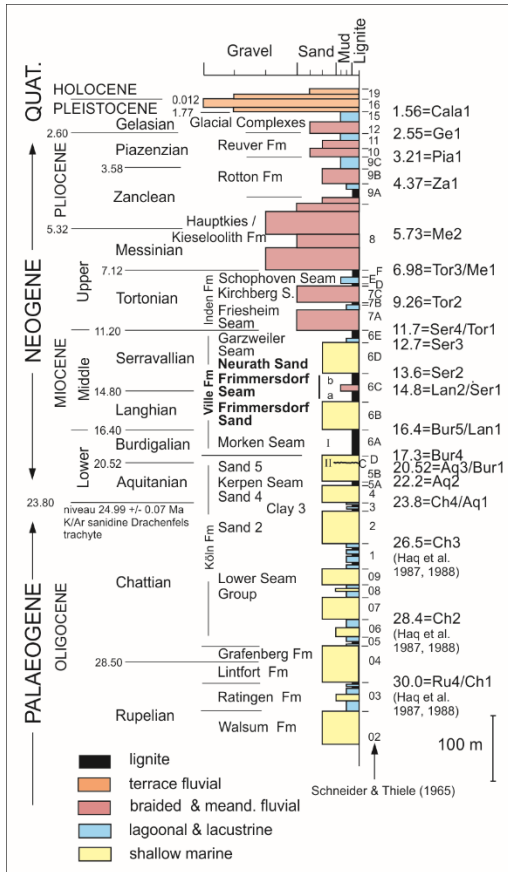


Fig. 7-2: Stratigraphic log of the Lower Rhine Basin (modified after Klett et al. 2002; Schäfer et al. 2004, 2005; Schäfer & Utescher 2014; Prinz et al. 2018). The log is based on two well logs (RWE Power AG), and represents the stratigraphy in the centre of the Erft Block (see Fig. 1). The lithostratigraphical code was established by Schneider & Thiele (1965). Biostratigraphical ages (Ma, left) after Berggren et al. (1995), cycle ages (Ma, right) after Haq et al. (1987, 1988) & Hardenbol et al. (1998).

Initial studies on these sand bodies have revealed that emplacement occurred by a variety of mechanisms and at different times within the depositional/post-depositional system. Syn-depositional sand bodies were deposited in river channels or during flood events within extended coastal mires (Prinz et al., 2018). Post-depositional sand bodies were identified as sand injectites (Prinz et al., 2018, 2017b), and these occur both more frequently than the syn-depositional sand bodies, as well as being much more variable. Typical morphologies include sills, dykes, reticulate and irregularly-shaped sand bodies (Fig. 7-3a and 7-3b).

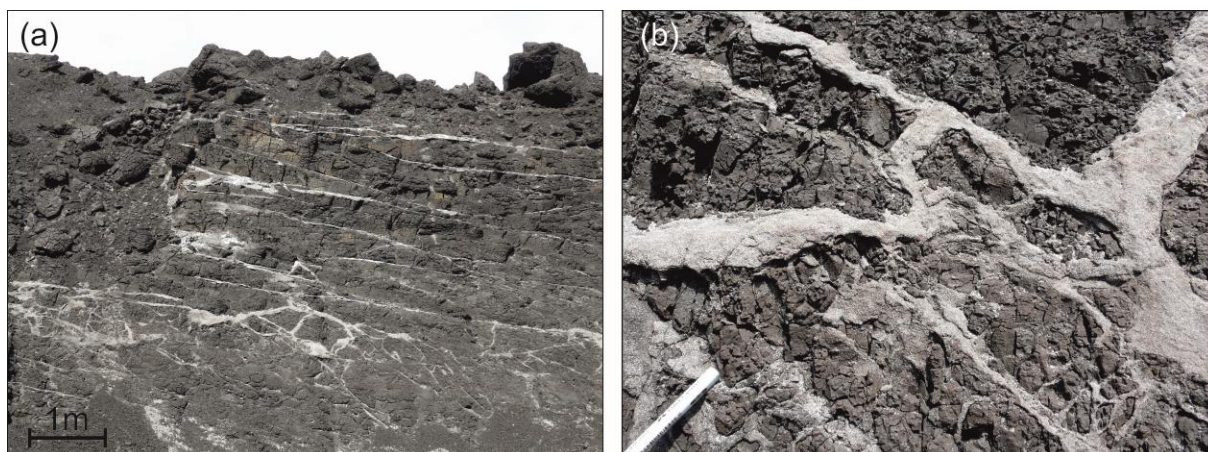


Fig. 7-3: Sand injectites within the Frimmersdorf Seam, (a) Sills and dykes within the Frimmersdorf Seam. Though sand injectites may be very thin, when compared to the entire seam thickness, their occurrence in swarms result in a noticeable decrease in economic value of the lignite. (b) Sand injectites within the Frimmersdorf Seam are highly variable, both in terms of their morphology and orientation (pencil for scale).

The sediments of the parent sand bodies (i.e. Frimmersdorf Sand, Neurath Sand) and associated sand channels within the Frimmersdorf Seam, as well as the lignites of the latter, were all deposited within a shallow-marine to paralic environment which was characterised by frequently-changing sea levels (Schäfer et al., 1996, 2005; Schäfer & Utescher, 2014). Though sand injectites have also been documented in glacial (Johnston 1993; van der Meer et al., 2009; Hoffmann & Reicherter, 2012), lacustrine (Aspler & Donaldson, 1986; Martel & Gibling, 1993; Taşgın, 2011), aeolian (Netoff, 2002; Huuse et al., 2005), fluvial (Plint, 1985; Aspler & Donaldson, 1986), deltaic (Reimnitz & Marshall, 1965; Davies, 2003), tidal (Reimnitz & Marshall, 1965), estuarine (Plint, 1983), and shallow-marine (Thompson et al., 2007) environments (Jolly & Lonergan, 2002; Ross et al., 2011), they are most frequently found in clastic deep-water marine settings (Jolly & Lonergan, 2002; Huuse et al., 2003, 2005; Duranti & Hurst, 2004; Hurst et al., 2005; Hurst & Cartwright, 2007). In comparison, sand injectites in lignite deposits have been rarely noted in the literature. Indeed, only two authors, Bajor (1958) and Berger (1958) commented on the presence of intrusive sand bodies within the Morken and Frimmersdorf seams in small sand and lignite pits (Fig. 7-1), which were eventually subsumed into the Garzweiler open-cast mine, while Demoulin (1996), working on earthquake-related clastic dykes (E Belgium), introduced the term “sand dykes” for these intrusions.

Sand injectites, which occur worldwide in sediments ranging in age from Neoproterozoic through to Holocene (Obermeier, 1996; Williams, 2001; Rodrigues et al., 2009), are of great economic interest since they can both positively and negatively influence the quality of oil and gas reservoirs (Huuse et al., 2003; Hurst et al., 2003, 2005; Hurst & Cartwright, 2007). Due to their often highly porous and permeable nature, sand injectites may form significant conduits for fluid migration (Huuse et al., 2003; Hurst et al., 2003, 2005). For this reason, studies

focussing on these structures have increased (Hurst et al., 2003, 2011, 2016; Duranti & Hurst, 2004; Hurst & Cartwright, 2007; Braccini et al., 2008), with much of the work concentrated on subsurface hydrocarbon reservoirs (in particular in the North Sea Basin; Jonk et al., 2003, 2005; Duranti & Hurst, 2004; Hurst et al., 2005, 2011; Davies et al., 2006; Cartwright et al., 2008; Scott et al., 2009; Jackson et al., 2011), and in outcrop (Peterson, 1968; Hurst & Cronin, 2001; Jonk et al., 2003; Hurst et al., 2005, 2016; Davies et al., 2006; Braccini et al., 2008; Scott et al., 2009; Vigorito & Hurst, 2010; Palladino et al., 2016). In most studies the sand injectites were observed within mud/mudstone and shale deposits (e.g. Huuse et al., 2003; Jonk et al., 2003; Duranti & Hurst, 2004; Vigorito et al., 2008; Braccini et al., 2008; Kane, 2010; Hurst et al., 2011, 2016; Cobain et al., 2017), although they have also been reported from sand-rich host units (e.g. Vanneste et al., 1999; Neuwerth et al., 2006; Hoffmann & Reicherter, 2012; see also Fig 7.1).

Sand injectites, in general, form by the fluidisation and remobilisation of unconsolidated sand subsequent to the failure and natural hydraulic fracturing of a low permeability sealing unit during relatively shallow burial (< 500 m below the seafloor; Obermeier, 1996; Lonergan et al., 2001; Jolly & Lonergan, 2002; Mazzini et al., 2003; Hurst et al., 2003, 2005, 2011; Duranti & Hurst, 2004; Rodrigues et al., 2009; Vigorito & Hurst, 2010). The generation of overpressure, controlled by the sealing capacity of the host strata, and fluid migration into the parent sand unit, is considered to be essential for the formation of sand injectites (Vigorito & Hurst, 2010). However, it is also widely accepted that triggering events (e.g. seismicity, rapid loading, thermal pressurization or fluid migration; see Hurst et al., 2011) are also required (Huuse et al., 2003, 2005; Duranti & Hurst, 2004; Hurst et al., 2005, 2011; Braccini et al., 2008). Injectites probably do not form as a single event, but instead tend to be multi cyclic (Hurst et al., 2003).

In comparison with many other studies on injectites, where the primary focus is on their recognition in terms of fluid conduits and/or migration barriers, the economic impulse for the study of sand bodies (including injectites) in lignite seams of the mining areas of the Lower Rhine Basin was based on the fact that the sand is an impurity within the lignite seams and, as such, needs to be avoided if the lignite produced is to be of value. Indeed, the variable nature and irregular distribution of the various sand bodies has complicated mining within the Garzweiler open-cast mine, so that in the past, up to 1.5 million tons of lignite per annum could not be used for electricity generation within the coal-fired power plants. Thus, the early and precise recognition of injectites (as well as other sand bodies) within future mining areas was the main focus of this work.

Fieldwork within an active open-cast mine has a number of clear advantages in comparison to traditional methods of geological investigation in that the mining activity provides a constant

flux of new outcrops. Though the Garzweiler open-cast mine advances at 300 m per year, the actual area of fieldwork over the last 3 years is relatively small due to problems of access and mine safety. To the N and S of the lignite access ramp, the lignite seam could be seen, and a variety of sand structures observed, but they were too high from the ground to be seen in detail. Therefore, in this study outcrop results are combined with data (including sand content maps, seam thickness maps, structural maps) from the RWE Power AG reservoir model, in order to analyse sand injectites across the entire Garzweiler II mining area. While as noted above, sand injectites have been previously reported from lignites (Bajor, 1958; Berger, 1958; Demoulin, 1996) and sand (i.e. Roer Valley Graben; Vanneste et al., 1999; see Fig. 7-1) in the area, to date, there has been no comprehensive examination of their occurrence and formation. Indeed, the present study is the first comprehensive analysis of sand injectites within a lignite seam, exposed within an active open-cast mine.

7.3 Geological background

The Lower Rhine Embayment is part of the European Cenozoic Rift System, a major system of interrelated and interlinked basins which formed within the Alpine and Pyrenean foreland (Prodehl et al., 1992; Sissingh, 2003; Dèzes et al., 2004). The rift system extends c. 1100 km from the Mediterranean in the S (offshore), through to the Massif Central – Rhône Valley rift systems, the Upper Rhine Graben and the Lower Rhine Embayment (onshore), as far as the North Sea Basin in the N (Ziegler, 1992; Prodehl et al., 1992; Sissingh, 2003; Michon et al., 2003; Dèzes et al., 2004).

Initial rifting of the European Cenozoic Rift System in late Eocene times was related to the main and late orogenic phases of the Alpine and Pyrenean collision phases (Ziegler, 1992; Sissingh, 1997, 1998, 2001, 2003; Schumacher, 2002; Dèzes et al., 2004; Ziegler & Dèzes, 2007; Rasmussen et al., 2010), as well as with the opening of the North Atlantic (Ziegler, 1992; Zijerveld et al., 1992; Michon et al., 2003; Rasmussen et al., 2010). The evolution of the European Cenozoic Rift System can be subdivided into 4 stages, commencing with an (1) early rifting stage in late Eocene times, followed by the (2) main (Oligocene) and (3) late rifting stages (from late Aquitanian times onward), and finally, (4) a phase of neotectonic activity from Pliocene times onward (Ziegler, 1992; Prodehl et al., 1992; Ziegler et al., 1995; Schumacher, 2002; Sissingh, 2003; Dèzes et al., 2004; Ziegler & Dèzes, 2005, 2006, 2007; Cloetingh et al., 2010).

The collision of the African plate, which was rotating in an anti-clockwise direction, with the Eurasian plate resulted in the formation of a series of passive, intra-continental foreland rift

systems (Schumacher, 2002; Sissingh, 2003; Dèzes et al., 2004; Ziegler & Dèzes, 2005, 2005, 2007). These foreland basins are also associated with increased volcanic activity, caused by mantle plumes that rise from the core/mantle boundary and evoke a partial melting of the upper asthenosphere and lower lithosphere (e.g. Wilson & Downes, 1992; Ziegler, 1992; Wilson et al., 1995; Ziegler et al., 1995; Dèzes et al., 2004; Ziegler & Dèzes, 2007). Subsidence of the intra-continental foreland rift systems is considered to have been controlled by repeated stress field changes in the Alpine foreland (Prodehl et al., 1992; Ziegler, 1992; Sissingh, 2003; Dèzes et al., 2004; Ziegler & Dèzes, 2005, 2006, 2007; Cloetingh et al., 2010). These changing compressional and tensional stress fields reflect the final stage of the Pyrenean orogeny, as well as the intensified coupling of the Alpine collision zone with its foreland (Prodehl et al., 1992; Ziegler, 1992; Sissingh, 2003; Dèzes et al., 2004; Ziegler & Dèzes, 2005, 2006, 2007; Cloetingh et al., 2010). Rifting processes were also associated with thermal uplift of the adjacent Variscan Massifs, induced by plume-related thermal thinning of the mantle-lithosphere (Prodehl et al., 1992; Ziegler, 1992; Sissingh, 2003; Dèzes et al., 2004; Ziegler & Dèzes, 2005, 2006, 2007; Cloetingh et al., 2010). The intra-continental foreland rift systems propagated along older reactivated Variscan, Permo-Carboniferous and Mesozoic crustal discontinuities (Ziegler, 1992; Chorowicz & Deffontaines, 1993; Schumacher, 2002; Michon et al., 2003; Sissingh, 2003; Dèzes et al., 2004).

One major element within the European Cenozoic Rift System is the Rhine Rift System (Ziegler, 1992; Prodehl et al., 1992; Sissingh, 2003; Dèzes et al., 2004; Ziegler & Dèzes, 2005, 2007; Cloetingh et al., 2010). This rift system consists of three grabens, i.e. the Upper Rhine Graben, the Lower Rhine Embayment and the Hessian Graben. All three of these basins converge in the area of Frankfurt to form the so-called Rhenish Triple Junction (Ziegler, 1992; Prodehl et al., 1992; Sissingh, 2003; Dèzes et al., 2004; Ziegler & Dèzes, 2005, 2007; Cloetingh et al., 2010). The Lower Rhine Embayment thus forms the NW end of the Rhine Rift System and extends in a NW-SE direction towards the North Sea Coast (Ziegler & Dèzes, 2005). However, the Lower Rhine Embayment can also be subdivided into two discrete areas, namely the Roer Valley Graben (Netherlands) and the Lower Rhine Basin (Germany). While these two elements would appear to be subsumed into the Lower Rhine Embayment, there is one important distinguishing factor, namely, the presence/absence of lignite. The Roer Valley Graben (RVG) has extremely limited lignite deposits, whereas the Lower Rhine Basin (LRB) includes the rich lignite deposits to the NW of Cologne (Fig. 7-1).

The initial subsidence phase within the Lower Rhine Embayment is thought to be related to the main rifting stage of the European Cenozoic Rift System in early Oligocene times (Geluk et al., 1994; Ziegler, 1994; Schäfer et al., 1996; Houtgast & van Balen, 2000; Klett et al., 2002). The Lower Rhine Embayment subsided along several, NW-SE-trending fault systems under

extensional conditions (Geluk et al., 1994; Schäfer et al., 1996, 2004; Houtgast & van Balen, 2000; Michon et al., 2003; Michon & van Bale, 2005; Ewald et al., 2006; Schäfer & Utescher, 2014; Grützner et al., 2016). These NW-SE-trending syn-sedimentary fault systems separate the Lower Rhine Embayment into a series of (half-) graben and horst structures (Schäfer, 1994; Houtgast & van Balen, 2000; Houtgast et al., 2002; Bense & van Balen, 2004; Michon & van Balen, 2005; Schäfer et al., 2005; Schäfer & Utescher, 2014).

The Lower Rhine Embayment is orientated parallel to the present-day, NW-directed maximum horizontal stress, and is, therefore, still undergoing extension perpendicular to the main direction of the major regional faults (Geluk et al., 1994; Ewald et al., 2006). The fact that tectonic activity is still ongoing is reflected by the fact that significant earthquakes still occur within the Lower Rhine Embayment (Ziegler, 1992; Hinzen, 2003; Sissingh, 2003, 2006; Schäfer et al., 2005; Reicherter, 2008; Schäfer & Utescher, 2014; Grützner et al., 2016). For example the 1992 Roermond earthquake measured $M_b = 5.8$, see Michon & van Balen (2005), while in 2002, an earthquake with $M_L = 4.9$ occurred (Aachen; Hinzen & Reamer, 2007). From 1976 to 2002, c. 2500 earthquakes, ranging from $M_L = 1.0$ to $M_L = 6.1$ have been recorded (Hinzen, 2003).

The study area, the Garzweiler open-cast mine, is located – as noted above – on the so called Venlo Block in the central part of the Lower Rhine Embayment. This is one of a series of fault-bounded blocks which are the Rur, Erft and Köln blocks in the SW, and the Roer Valley Graben and Venlo and Krefeld blocks in the NW. The Roer Valley Graben subsided to a maximum of 2000 m, while the Erft Block subsided to 1300 m (Klett et al., 2002). The individual blocks are separated by mainly NW-SE trending fault systems. The Venlo Block is bounded by several major fault systems, including the Erft Fault System in the SW, and the Jackerath Horst in the S (see Fig. 7-1). This latter is one of the oldest Cenozoic-age tectonic elements in the LRB (Nickel, 2003) and shows a different, E-W fault orientation.

7.3.1 Stratigraphic record

The stratigraphy of the LRB, from Oligocene times onward, records a history characterised by a combination of subsidence, and global climatic and sea level fluctuations (Schäfer, 1994; Schäfer et al., 1996, 2005; Utescher et al., 2000; Zachos et al., 2001; Becker & Asmus, 2005; Schäfer & Utescher, 2014). Commencing with the initial North Sea transgression onto the Palaeozoic- and Mesozoic-age basement in early Oligocene times, thick sub- to supratidal siliciclastic sediments were deposited in a shallow-marine depositional environment (Petzelberger, 1994; Schäfer et al., 1996; Klett et al., 2002).

A partial regression of the North Sea in Miocene times, coupled with optimal climatic conditions (Zagwijn & Hager, 1987; Utescher et al., 2000, 2009; Mosbrugger et al., 2005), facilitated the establishment of extensive coastal mires in the SE part of the Lower Rhine Embayment (Teichmüller, M. 1958; Schäfer et al., 1996; Klett et al., 2002). In the study area (i.e. Garzweiler area), peat accumulation was interrupted by repeated local transgressions of the North Sea (Burdigalian to Serravallian times), resulting in the development of a stratigraphy characterized by alternating strata of lignite and marine sands (Petzelberger, 1994; Schäfer et al., 1996, 2005; Schäfer & Utescher, 2014). This lignite-sand succession, termed the Ville Fm (see Fig. 7-2) is the focus of this study. The Morken Seam (Burdigalian, c. 10-12 m) is the stratigraphically lowest lignite of the Ville Fm. It is overlain by the Langhian-age Frimmersdorf Sand (c. 20 m, parent sand unit), and subsequently the Frimmersdorf Seam (Langhian/Serravallian; c. 12 m, host strata). The Neurath Sand (10-40 m thick) overlies the Frimmersdorf Seam, while the succession is capped by the Serravallian-age Garzweiler Seam (c. 10 m), the uppermost unit of the Ville Fm (see Fig. 7-2).

At the Serravallian/Tortonian transition, the North Sea finally retreated from the study area (Boersma et al., 1981; Abraham, 1994; Valdivia-Manchego, 1994; Schäfer & Utescher, 2014), which was associated with a global cooling trend (Utescher et al., 2000). From Tortonian times onward, the depositional environment was controlled mainly by fluvial deposition. Initially, the river systems were meandering ones, with braided systems developing later (Boersma et al., 1981; Abraham, 1994; Valdivia-Manchego, 1994; Klett et al., 2002). The change in the type of fluvial system occurring in the Lower Rhine Embayment area was related to a marked decrease in temperature from Pliocene times onward (Boenigk, 1981; Abraham, 1994; Utescher et al., 2000; Zachos et al., 2001; Klett et al., 2002; Schäfer et al., 2004; Mosbrugger et al., 2005; Schäfer & Utescher, 2014).

7.4 Sand injectites in the Frimmersdorf Seam

The analysis and interpretation of sand injectites in this study is mainly based on fieldwork in the Garzweiler open-cast mine. Due to the mining activity, outcrops are constantly cut back, thus revealing new aspects of the lignite bed as well as its relationship with both the underlying and overlying sand bodies. Therefore, as noted above, it was possible to examine a variety of sand injectites over a period of three years. The field studies included measurements of the orientations of the various sand injectites, as well as measurements of bedding, joints and faults within the surrounding lignites. The database gathered from the field studies was supplemented by a 3D reconstruction of the seam based on geophysical well log data, analysis of drilling cores, and fieldwork measurements as part of a reservoir model prepared by the

RWE Power AG for the Garzweiler open-cast mine. From this reservoir model, contour maps with line sets at 1 m intervals were exported that reflect the altitudes of lower and upper boundaries of the Frimmersdorf Seam. These contour maps were transformed into 3D surfaces (using MOVE 2015 modelling software). The datasets also include information on the fault distribution across the region, as well as fault orientations and offsets. In addition, seam thicknesses were included. The sections below examine the injectites from a number of aspects, including a) the parent sand bodies, b) the intrusive complex (i.e. injectites and host unit), and c) emplacement mechanisms (see discussion).

7.5 Parent sand units

Within the Garzweiler open-cast mine a variety of sources have been identified as possible parent sand units for the various injectites (e.g. sills, dykes) present within the lignite. These include, a) syn-sedimentary sand bodies, albeit as a subordinate source (Prinz et al., 2018), b) the Frimmersdorf Sand, directly underlying the host unit, and, subordinately, c) the overlying Neurath Sand (see Fig. 7-4). The syn-sedimentary sand bodies were deposited in i) fluvial or estuarine channel systems (Fig. 7-5), or ii) as beds related to flooding events within the extended Miocene-age mires. Both of these sand body types can be easily differentiated from sand injectites by the presence of primary sedimentary structures (e.g. trough cross/ cross lamination, Fig. 7-5), and mm-thin alternations of sand and lignite at the base of some of the sand bodies. These laminae formed as a result of deposition under changing current velocities (see Prinz et al., 2018 for more details). These channels and flood event beds may also contain chert pebbles which are indicative of high velocity currents. All of the channel and flood deposits in the Frimmersdorf Seam were influenced by the post-depositional remobilisation of sands, which resulted in the formation of sills and dykes that spread upwards or laterally into the lignite from the syn-sedimentary sand bodies.

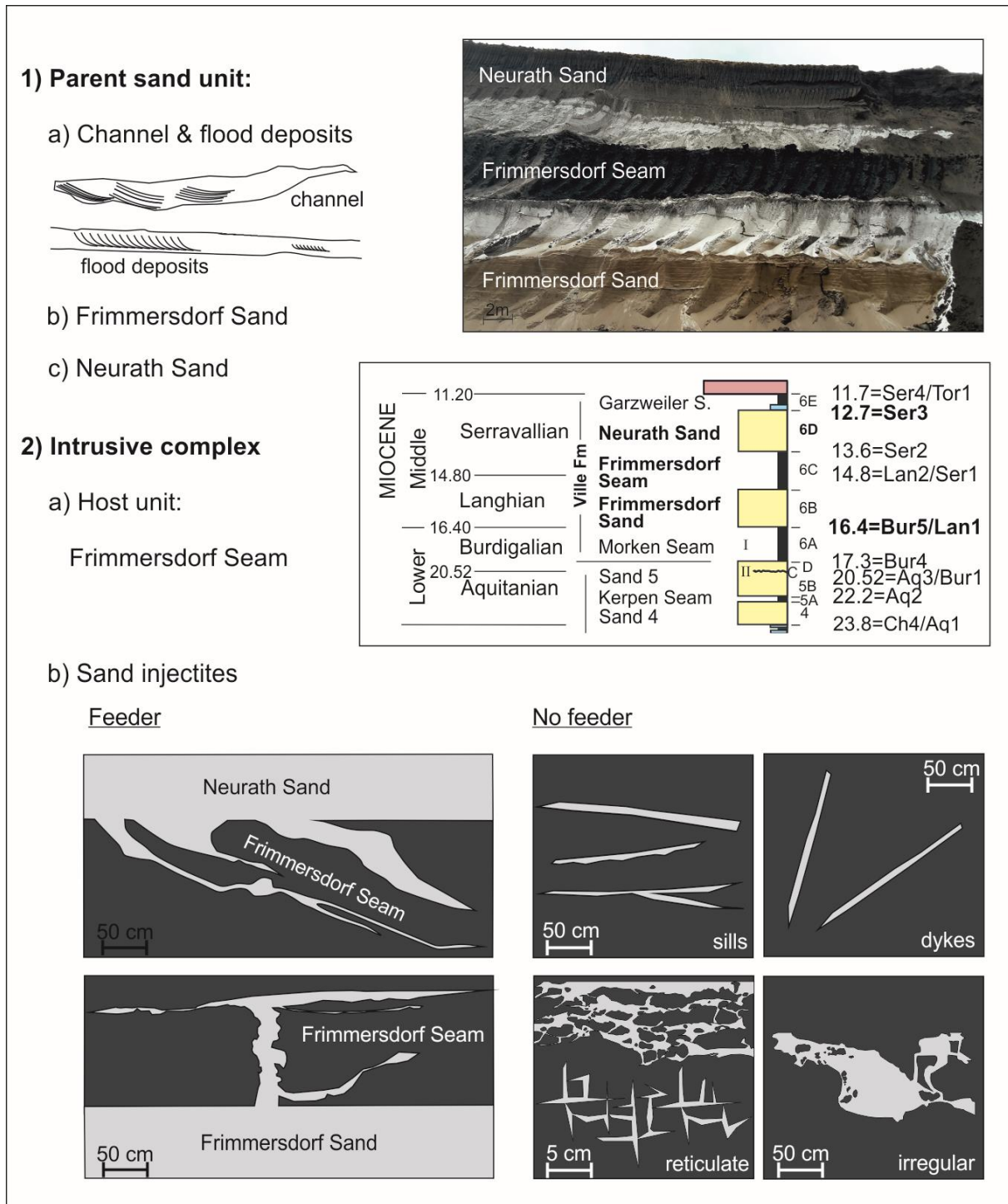


Fig. 7-4: Classification of the parent sand unit (1) and intrusive complex (2), comprising the host unit (2a) and the sand injectites (2b).

The Frimmersdorf Sand, directly underlying the host unit (i.e. Frimmersdorf Seam), has been identified as the second most important parent sand unit, with several dykes extending from this unit into the overlying seam. The Frimmersdorf Sand comprises c. 20 m of fine-to medium-grained sands, which were deposited in a nearshore shallow-marine environment (Petzelberger, 1994; Schäfer et al., 2005; Schäfer & Utescher, 2014). The stratigraphy of the Frimmersdorf Sand records the deposition of a succession ranging from subtidal through to intratidal sediments (Petzelberger, 1994). The sediments were deposited in early to mid Langhian times.

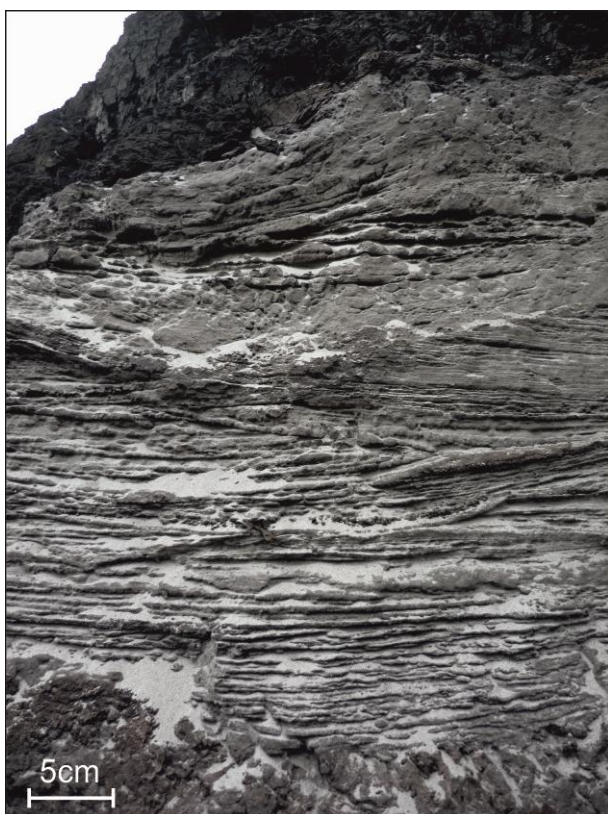


Fig. 7-5: Syn-depositional channel fill at the base of the Frimmersdorf Seam, comprising trough cross lamination. Individual laminae may contain mm-fine organic remains, as well as cm-large wood fragments.

At the top of the Frimmersdorf Sand, well-defined root-horizons may be exposed (see Fig. 7-6a). These roots extend from the base of the lignite down into the parent sand unit, for up to 1.5 m. The upper few metres of the Frimmersdorf Sand are characterised by the presence of a variety of sedimentary structures (mainly planar parallel lamination) which are interpreted as representing inter- to supratidal deposition in an environment characterised by the retreating North Sea. However, in areas where sand injectites are present in the overlying seam, both the root horizons between the host and parent units, as well as the fine-grained lamination are both missing (Fig. 7-6b). Additionally, angular lignite clasts and wood fragments (up to 20 cm) were reworked into the upper few metres of the Frimmersdorf Sand. These areas of

disturbance within the Frimmersdorf Sand are also associated with upwards directed bulges (convex up) of the boundary between the parent sand and the host unit.

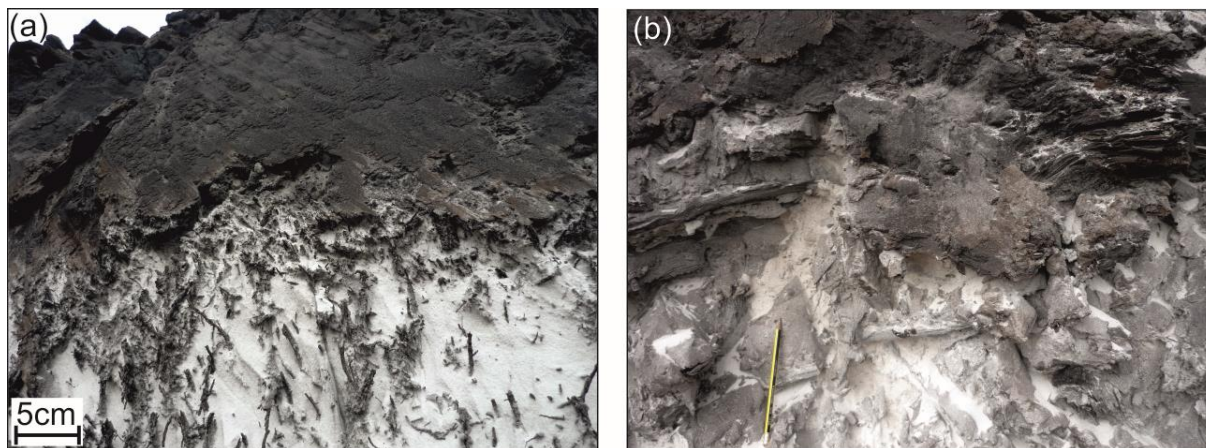


Fig. 7-6: Boundaries between the Frimmersdorf Sand (parent sand unit) and the Frimmersdorf Seam (host unit). (a) Well-defined root horizons, extending down into the Frimmersdorf Seam; (b) Roots, as well as syn-sedimentary structures are missing, sand, lignite and larger wood remains were probably reworked.

The Neurath Sand, directly overlying the Frimmersdorf Seam, comprises subtidal to supratidal sands up to 40 m thick (Prinz et al., 2017a). The sediments were deposited in an estuarine environment in Serravallian times. The sand body has also been interpreted as a possible parent sand unit, though only two locations with sand injectites extending down from this source had been observed. The dykes are initially high angle, levelling out into sill-like structures at depth.

7.6 Intrusive complex

7.6.1 Sand injectites

In general, the sand injectites which occur within the Frimmersdorf Seam comprise fine- to medium-grained well-sorted quartz-rich sands. When freshly cut by the bucket-wheel excavator, the injectites are very hard to observe, since the dark colour of the sands is similar to that of the surrounding lignite. The dark colour results from the presence of finely-dispersed humic substances that fill the pore volume between the individual sand grains as well as coating them. After some days exposure (and with the appropriate weather conditions), the humic substances are washed or blown away, and the now light-coloured injectites can be clearly distinguished from the surrounding red, brown or black coloured lignite.

The sand injectites within the Frimmersdorf Seam are highly variable both in terms of their external geometry and their orientation (see Fig. 7-4). Recognised morphologies include sills,

high- and low-angle dykes, reticular sand bodies as well as discordant, irregularly-shaped bodies, and these often occur in combination with each other (see Fig. 7-4 and 7-7; and also Prinz et al., 2018 for more details). The injectites range in thickness (or width) from small-scale structures (which may be only a single grain thick) through to larger features which can be up to 1 m thick. However, there is a great degree of variability in the thickness/width of the injectites, both from base to tip as well as along their length. The injectites also vary considerably in terms of their length from a few centimetres to 20 m. Within the group of injectites, the sills range in thickness from 1-50 cm, and dip from up to 15°. The dykes have widths of 5-20 cm, and dip from 15-30° (low angle dykes, <math><30^\circ</math>) and from 30-90° (high angle dykes). The injectites occur both singly as well as in groups (up to 20-50 in number, particularly if they are small scale), up to the point where individual injectite morphology (i.e. dyke, sill) may become lost as the structure becomes increasingly reticulate.

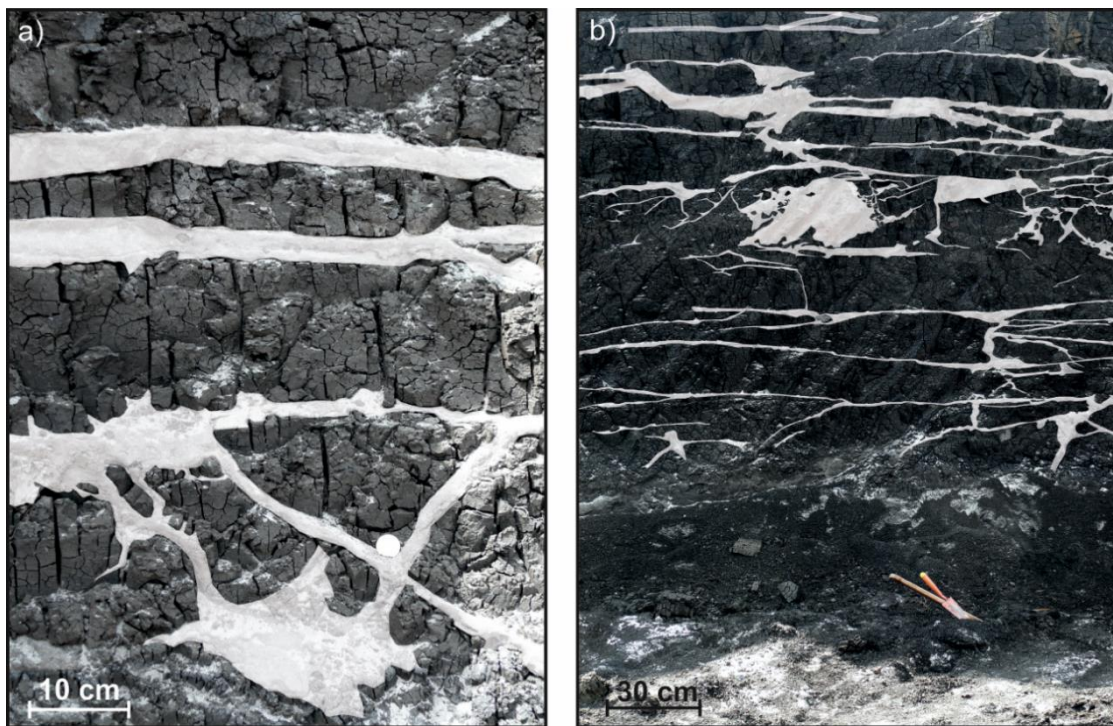


Fig. 7-7: Sand injectites within the Frimmersdorf Seam. (a) Sills (upper part) and high-angle dykes (lower part); (b) Sills (which may divide and reconnect along their length), dykes and irregularly-shaped injectites.

Individual dykes frequently show connections with the underlying Frimmersdorf Sand while the connections to the overlying Neurath Sand are more rare. Sand dykes that are fed either by the overlying Neurath Sand, or the underlying Frimmersdorf Sand are often curved in form, commencing as vertically-oriented dykes and becoming asymptotic as the dip angle is reduced and they merge laterally into sills. Sills and dykes within the Frimmersdorf Seam may be stepped and faulted and frequently show sudden changes in their orientation or thickness. Indeed, sills may split into several segments that may subsequently rejoin along the sill length.

Reticulate sand bodies are complex systems of vertical and horizontal components, showing a high degree of connection and comprising a series of mm- to cm-thick sills and dykes that may spread over several metres within the seam.

Sand injectites within the Frimmersdorf Seam may contain rounded to angular lignite intraclasts (mm-20 cm) or, less frequently, unconsolidated clay clasts, as well as wood fragments (Prinz et al., 2018). Elongate lignite intraclasts are often sorted parallel to the injectite margins, and may occur within the whole seam.

7.6.2 Host unit

The Frimmersdorf Seam of the Garzweiler open-cast mine dips to the NW, from +84 m.a.s.l. in the SE part of the mining area, to -110 m.a.s.l. in the NW. The seam thickness varies from 0 m (completely eroded) in the area of the Jackerath Horst, to a maximum of 20 m in the central part of the open-cast mine. The areas of maximum seam thickness would appear to correlate with the areas of maximum sand content within the seam. The Frimmersdorf Seam is overlain by up to 150 m of mainly clastic deposits, and this overburden thickness represents, according to Stock et al (2016), the maximum burial depth of the lignite. The lignite has relatively low ash and sulphur contents (on average 4.47 wt%, and 1.79 wt%, respectively, see Prinz et al., 2017b), and consists mainly of huminite macerals (Prinz et al., 2017b).

On initial examination, the seam morphology (represented by the upper and lower boundaries of the seam, see Fig. 7-8a and 7-8b) would appear to show little variability in terms of thickness or relief. However, when a vertical exaggeration of c. 20 is implemented, it is clear that there is a marked correlation between seam morphology and the presence of sand bodies within the seam. Indeed, the presence of sand bodies within the Frimmersdorf Seam result in a variety of effects on the seam morphology. These include the formation of bulges (convex-up structures) or depressions (concave structures) along the upper and lower boundaries of the seam (Fig. 7-9). Indeed, 40% of the observed sand bodies are seen to coincide with the presence of a convex bulge on the upper boundary of the seam (Fig. 7-9e, g, h). Additionally, the lower boundary of the seam below 46% of the sand bodies shows an upward-directed bulge (Fig. 7-9c, f, h). In 28.35% of all boundary types, the combination of convex-up bulges of both the lower and upper boundaries is the most common type of deformation observed (Fig. 7-9h).

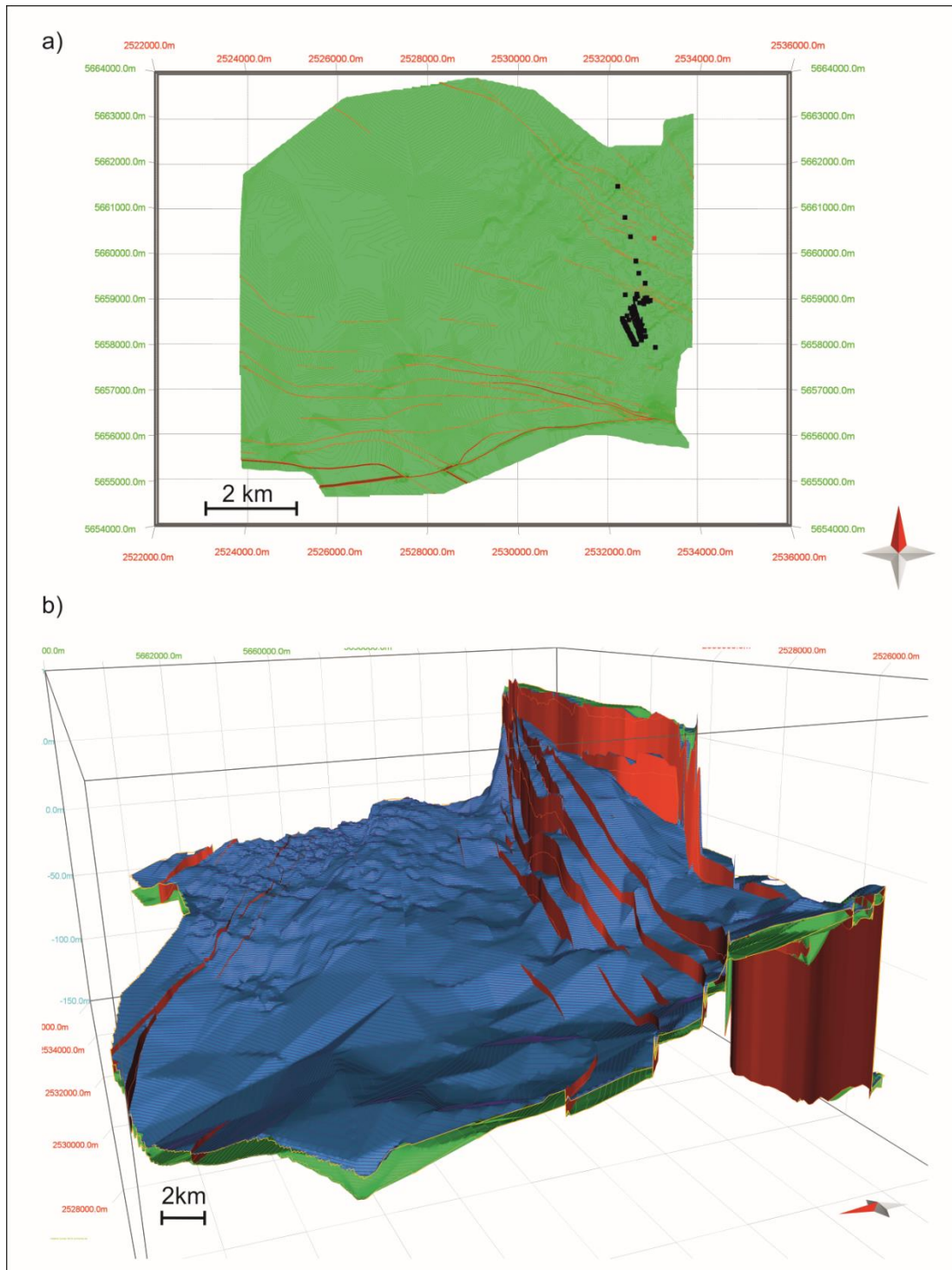


Fig. 7-8: 3D model of the Frimmersdorf Seam within the Garzweiler open-cast mine. (a) Top view with study locations (black points) and faults (red lines). Interestingly, the SW-NE-trending prominent depressions noted on the lower boundary (and which also occur on the upper boundary, see 8b) exactly parallel the orientation of the Variscan-age Aachen Fault, a notable thrust which faulted the Palaeozoic-age basement of the Lower Rhine Embayment (see Ribbert & Wrede 2005). (b) Lower (green) and upper (blue) boundaries of the lignite seam (vertical exaggeration x20), fault planes (red). The E-W trending Jackerath Horst faults show offsets of up to 100 m, while those of the faults to the N of the open-cast mine (NW-SE-trending) have offsets of only c. 1-15 m. The area to the E of the seam has a greater concentration of exploratory wells (being close to the exploration slope), thus providing a much more detailed picture of the geology of this particular zone.

In addition to the presence of convex and concave structures of the seam boundaries, the 3D reconstruction of the seam also provides detailed data on the orientation of faults within the open-cast mine (including dip angles and directions, see Fig. 7-7 and 7-10). Two main fault directions can be observed within the area of the Garzweiler open-cast mine (see Fig 7-8a and Fig. 7-10). In the NE part of the mine, the (mainly normal) faults predominantly strike NW-SE, which is the dominant strike direction in the Lower Rhine Embayment. Offsets of these faults range from cm-m. However, in the S part of the Garzweiler open-cast mine the fault direction is markedly different, and shows an almost E-W orientation. These E-W-oriented linking faults form part of the Jackerath Horst system, and show offsets of up to c. 100 m (see Fig. 7-8b). The observed sand injectites in the Garzweiler area are generally located in areas without any obvious faults. Despite this apparent lack of fault activity close to the injectite locations, the orientations of the injectites mirror those of the faults - both in terms of the dominant Lower Rhine Embayment fault direction (NW-SE) and the Jackerath Horst (E-W) (Fig. 7-8).

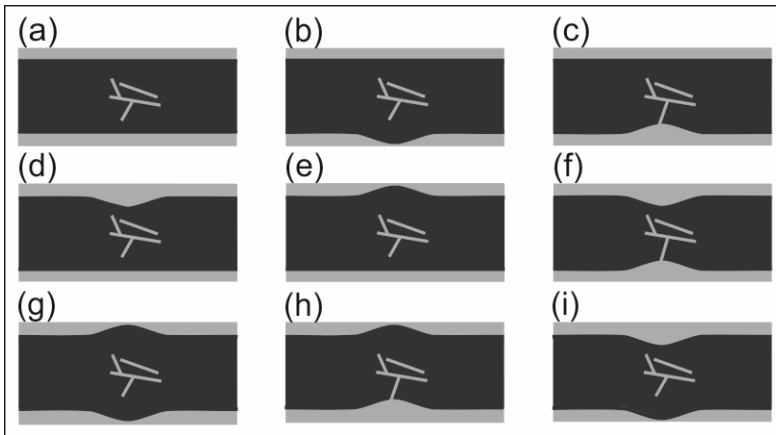


Fig. 7-9: (a-i) Boundary types of the Frimmersdorf Seam (in areas where sand injectites occur) and their expression in the under- and overlying Frimmersdorf and Neurath sands, respectively.

The contact boundaries between the sand injectites and the surrounding lignite are always extremely sharp. Indeed, not even single sand grains penetrate into the surrounding lignite. Additionally, geochemical, coal petrological and micropetrographical studies on injected sands and related lignites from the Frimmersdorf Seam have suggested that the presence of sand injectites does not influence the surrounding lignite in terms of its geochemical composition and coal petrology (Prinz et al., 2017b). Despite this, and as noted above, there is a clear relationship between the presence of injectites and the bulges observed along the lignite-sand boundaries.

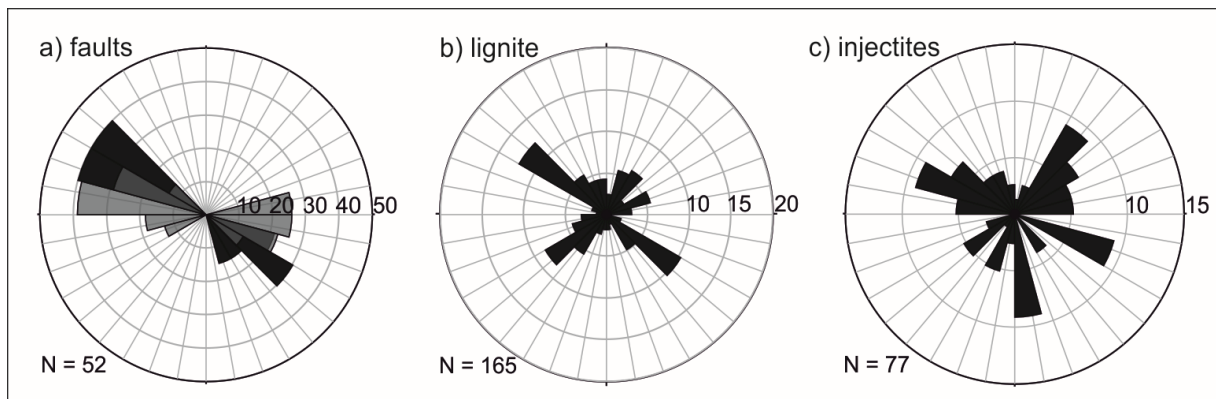


Fig. 7-10: Rose diagrams of (a) the faults within the Garzweiler open-cast mine, (b) lignite surfaces from outcrops in the Frimmersdorf Seam, and (c) injectites that were exposed within the Frimmersdorf Seam.

7.7 Discussion

Sand injectites within the Frimmersdorf Seam are, as noted above, extremely variable, in terms of their external geometry, their orientation and their distribution. Their presence within the seam (Fig. 7-11) resulted in a significant decrease in economic value of the lignites in the past, although their occurrence is also of great scientific value. Combining these two aspects (economic vs scientific) has been the focus of the present study. Having described the injectites above, the following sections will investigate, in detail, the mechanisms related to our understanding of their distribution and concentration within the Frimmersdorf Seam. In particular, this study will focus on the source-to-sink aspect of the injectites, examining the parent sand bodies, the host unit and the injectites themselves in order to achieve an overview of the source to emplacement continuum.

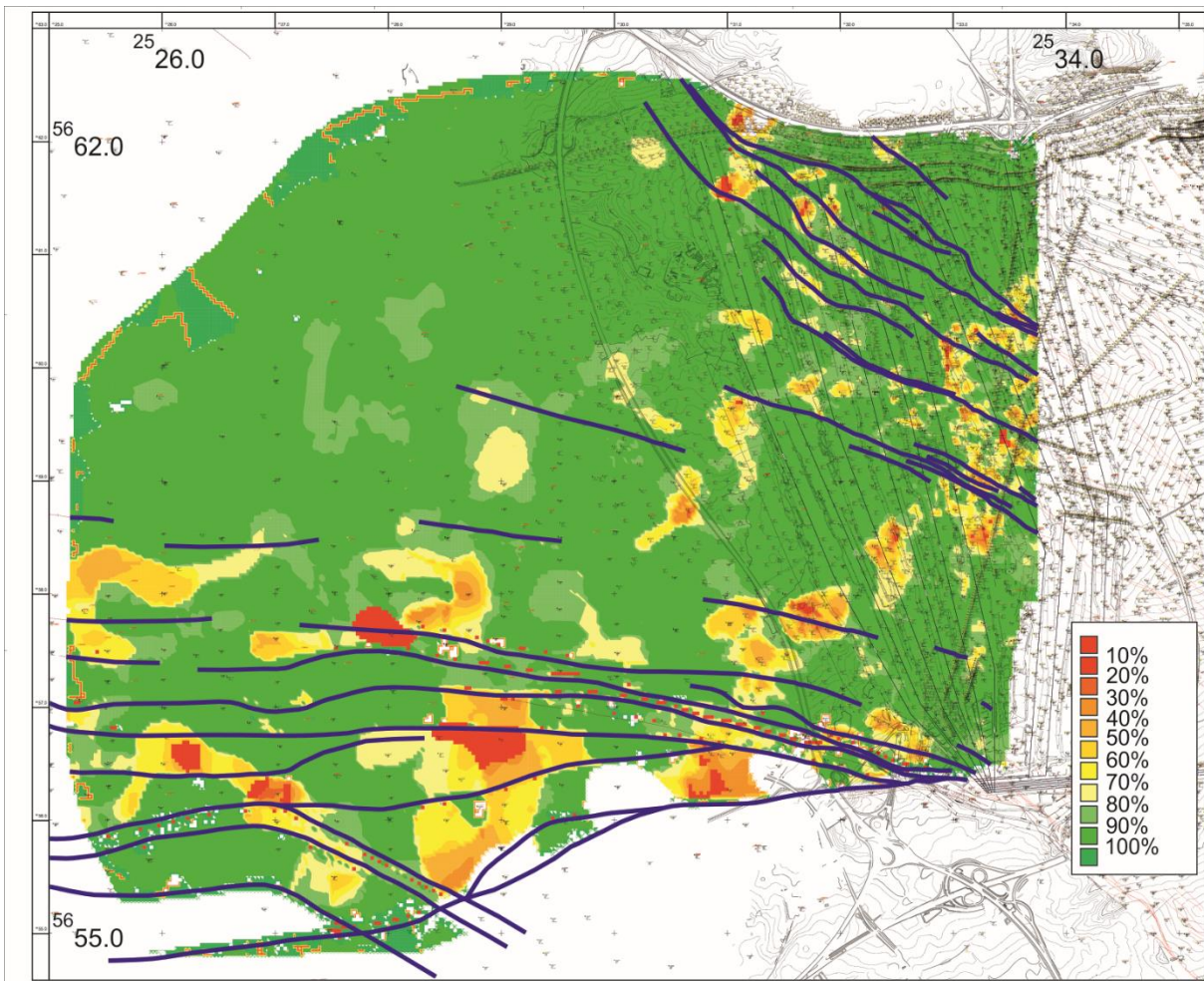


Fig. 7-11: Map of the Frimmersdorf Seam within the Garzweiler open-cast mine. Modified after a RWE reservoir model (status 2016). The colour trends from green to red represent the lignite contents (green areas: no sand within the seam, lignite completely exploitable; red areas: less than 10% of the seam usable for electricity generation). The blue lines represent the positions of the faults in the mining area.

7.7.1 From source...

As noted above, three different sources of sand injectites have been observed: 1) syn-depositional channels and beds, 2) the underlying Frimmersdorf Sand (the main parent sand body), and, 3) the overlying Neurath Sand. Syn-depositional channels and beds are only rarely present within the seam (only three locations were observed). However, where present, they are always associated with sills and dykes. As noted above, sand channels and beds may be distinguished from injectites by the presence of sedimentary structures or intercalated sand and lignite laminae (Fig. 7-5). Both of these are indicative of the action of currents (fluvial/estuarine) on the peat surface, as well as of variations in current velocity. However, fluidization and remobilization of channels and beds can lead to homogenisation of the original sedimentary structures (Duranti et al., 2002; Duranti & Hurst, 2004), and, thus, impede the identification of syn-depositional parent sand bodies. Additionally, the external geometry of channel deposits may be intensely deformed by the fluidisation and remobilisation of sand, so that the original channel geometry is not recognisable (Vigorito & Hurst, 2010).

However, numerous sand injectites were directly fed by the underlying sand unit, with the sands moving upward through the lignite along cracks and fissures generated within the seam. The sheer number of injectites (e.g. dykes, sills) which are clearly connected to the Frimmersdorf Sand would suggest that it is this sand body, rather than the subordinate synsedimentary sands and the overlying Neurath Sand, which is the dominant source of sand injectites.

Sand injectites which are fed by the overlying Neurath Sand are rare with only two observed in this study. These dykes, clearly derived from the overlying sand body, suggest formation from a downward directed injection process. That top-sourced sand injectites are so rare is partly related to the outcrop situation within the mine. However, this cannot be considered as the only reason for the significant lack of top-sourced structures within the Frimmersdorf Seam, suggesting that other causes need to be investigated.

7.7.2 ...to emplacement.

The intrusive complex, comprising the lignites of the Frimmersdorf Seam and the various injected sand bodies, shows a variety of features, both within the complex itself as well as in conjunction with the under- and overlying sand units, which may be interpreted in terms of how the structures were emplaced. It is clear from both the morphological variation of the intrusive sand bodies as well as their variable orientations, that no single emplacement factor can be invoked for all of the observed structures. Instead, a series of factors need to be investigated

and these, acting individually, but probably more often in combination, have resulted in the complex configuration presently observed within the Frimmersdorf Seam. As noted above, fracturing of a low permeability sealing unit (i.e. the lignite seam) as a result of failure and/or natural hydraulic fracturing and related to fluid migration, changes in pore pressure and outside triggering all need to be investigated.

The overburden thickness of the Frimmersdorf Seam was never extensive, with a maximum thickness of c. 150 m being suggested. Thus, the lignite had a relatively shallow burial depth, enough to ensure compaction and loss of moisture within the concentrated organic material (a minimum of 36 m of vegetated matter, although this is only a minimum given that the upper part of the succession was probably eroded during the transgression of the North Sea; Schäfer & Utescher, 2014), but only enough for coalification to commence. This latter process, together with compaction, both resulted in a significant reduction of the pore volume within the peat, thus influencing its sealing capacity. Interestingly, geochemical studies have revealed the porous nature of the original peat, based on the high sulphur contents which suggest that the original pore water was replaced at least three times by sulphur-rich seawater during the deposition of the overlying Neurath Sand (Stock et al., 2016; Prinz et al., 2017b).

Several characteristics within the intrusive complex indicate that the formation of sand injectites (including hydraulic fracturing of the host unit, and the remobilisation of fluidized sands) was a highly erosive process. The lignite intraclasts which are present within numerous sand injectites were probably eroded from the host strata during some phase of the injection process, and were subsequently incorporated into the remobilised sands. Their orientation, which in the case of elongate lignite clasts, may be parallel to the sill margins would suggest that flow was clearly parallel to the injectite margins. The lignite fragments, which are up to 20 cm in length/diameter, are generally rounded (the majority) to angular in shape. The rounding would assume a degree of erosion occurring within the injectite, resulting in the loss of angularity in the fragment. This must have occurred relatively rapidly, given that the injectites within the Frimmersdorf Seam rarely achieve lengths of more than 10 m. The angular fragments tend to be more elongate in shape (blade form) and, as noted above, are often oriented parallel to the injectite margins. The angular shapes would suggest a degree of catastrophic or explosive failure of the low-permeability host lignite due to hydraulic fracturing (see Hurst et al., 2005).

Erosion also occurred on a smaller scale, as demonstrated by the presence of finely-dispersed humic substances filling the pore spaces of the sand injectites, while organic particles were seen to coat the sand grains, resulting in the dark colour of the injectites. These humic substances were derived both from erosion of the host strata due to the passage of the sand-

fluid mixtures of the injectites as well as from the microabrasion of the lignite clasts within the sand-fluid mixtures. Additionally, the enrichment of humic detritus within the pore space of the sands may have been related to souring of the lignite walls during hydraulic fracturing (Hurst et al., 2011). The presence of intraclasts (commonly mud clasts) and finely-dispersed fines within injectites has been previously noted, and interpreted by a number of authors as being indicative of the erosive nature of the injection processes (Obermeier, 1996; Kawakami & Kawamura, 2002; Duranti & Hurst, 2004; Hurst et al., 2005, 2011, 2016; Diggs, 2007; Braccini et al., 2008; Scott et al., 2009; Kane, 2010; Vigorito & Hurst, 2010).

Erosion, as part of the emplacement processes, occurred on a small-scale within the injectite, but also on a larger scale within some of the parent sand bodies. For example, the absence of roots or sedimentary structures in the upper part of the Frimmersdorf Sand would suggest a degree of erosion leading to the loss of root horizons, as well as homogenisation of the upper part of the bed during fluidisation and remobilisation of sand. Interestingly, these structure-free zones also contain lignite clasts, suggesting that erosion along the lignite-sand margins was also occurring. Furthermore, these zones of disturbance coincide with the locations where the lignite-sand boundary has a convex up morphology, related to the upwelling of fluids in the underlying sands, and prior to the hydraulic fracturing which resulted in shattering and intrusion of the injectites (see also Obermeier, 1996; Hurst & Cronin, 2001; Duranti & Hurst, 2004; Vigorito & Hurst, 2010). The erosive contact between the Frimmersdorf Sand (parent sand unit) and the Frimmersdorf Seam (host unit) may be indicative of high-velocity, erosive flow during sand injection, and such morphologies are a common feature of sand injectites (Hurst et al., 2011). Indeed, outcrop studies on sand injectites have shown that the boundaries between the depositional parent sand units directly feeding clastic dykes, and the host sediments, are often deformed (Vigorito & Hurst, 2010). Additionally, the upper boundary of the Frimmersdorf Seam was affected by the presence of sand injectites within the seam. Their emplacement resulted in a thickening of the host strata, which is associated with a convex-up bulge along the upper boundary (see Fig. 7-9). Similar morphologies, termed 'jack-ups', which are often associated with a significant thickening of the host unit, have been noted by numerous authors (e.g. Braccini et al., 2008; Cartwright et al., 2008; Kane, 2010; Palladino et al., 2016; Hurst et al., 2016).

The direction of sand injection is controlled by the hydraulic gradient; i.e. upward, lateral (Hurst et al., 2005) or downward (Kane, 2010). As noted above, dykes fed by the underlying Frimmersdorf Sand are indicative of upward moving pore fluids, while those extending down from the Neurath Sand result from downward directed fluid migration. The presence of both upward as well as downward directed fluid migration is supported by observations made on the bleaching processes, and related to the redistribution of humic acid within the succession.

At the top of the Frimmersdorf Sand, the fine-grained sands are apparently white coloured, while the colour of the underlying sand beds range between different shades of beige and brown. This colour distribution results from downwards-directed bleaching processes caused by the remobilisation of humic acid derived from the lignite seam. Therefore, the colouring of the sand beds is not a function of depositional, syn-sedimentary processes, but rather it is related to the post-depositional redistribution of humic acids. It should be noted, that the subtidal sand beds (1-2 m thick) directly overlying the Frimmersdorf Seam are also noticeably white coloured (see Fig. 7-4), whereas the up to 8 m thick overlying deposits (mud-rich sands deposited in the subtidal transition zone, Prinz et al., 2017a) are dark grey in colour. The boundary between the white- and grey-coloured sands is not a sedimentological boundary, for example based on grain size differences, but rather related to the difference in colour. Thus, if we assume that the colouration of the sand within this sand-lignite succession is a function of post-depositional processes, the extremely white colours of the lowermost Neurath Sand deposits may also be the result of humic acid bleaching. Since the grey beds above do not appear to have been affected by the humic acid, we can also assume that the bleaching of the lowermost metres of the Neurath Sand was not due to a downwardly-directed bleaching event and, therefore, that the humic acids were also possibly derived from the Frimmersdorf Seam. This would support the hypothesis, that both upward-, as well as downward-moving pore fluids influenced the diagenetic history of the parent sand units (i.e. Frimmersdorf Sand, Neurath Sand) and the intrusive complex (i.e. Frimmersdorf Seam), albeit presumably at different times.

The propagation of hydraulic fracturing within the host unit may also determine the geometry of the sand injectites present. Dykes extending into the Frimmersdorf Seam from either the Neurath Sand above, or the underlying Frimmersdorf Sand show similar external geometries, though they are formed by downward-directed and upward-directed hydraulic fracturing processes, respectively. Dykes, which are fed by the Frimmersdorf Sand, are very steep at their base, and then merge into flat dipping sills (see Fig. 7-12a). The same observation had been made with dykes extending down from the Neurath Sand. These dykes never cross the entire lignite seam, but rather pass at a depth of 4 m (maximum), and in an asymptotic fashion, into sills (Fig. 7-12a). Such a pattern has been interpreted by Vigorito & Hurst (2010) as being indicative of pressure release within the system. However, other dyke-sill systems also exist within the Frimmersdorf Seam. These tend to more angular in form, where the dyke-sill junction is at 90° (Fig. 7-12b). Such a configuration may be also indicative of pressure release. As noted above, hydraulic fracturing of the host unit (and the resultant emplacement of fluidized sands) is largely the result of overpressurized fluids (e.g. Duranti et al., 2002; Jolly & Lonergan, 2002; Duranti & Hurst, 2004; Jonk et al., 2005; Braccini et al., 2008; Hurst et al., 2011). If the pressure release (or certainly a decrease in pressure) occurs after the passage of a few metres

into the host unit (i.e. the zone of steep hydraulic fracturing), then the next phase of injection growth may be lateral, where movement is facilitated by the presence of bedding planes (e.g. Cartwright et al., 2008).

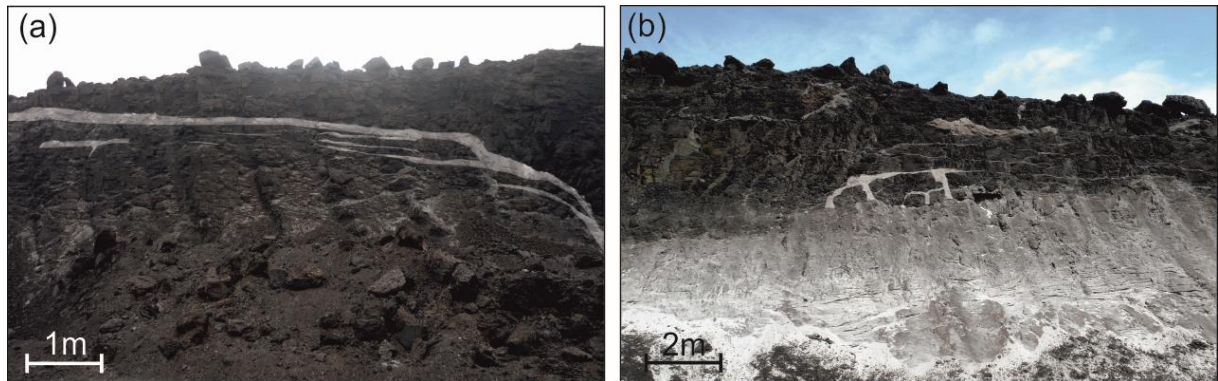


Fig. 7-12: Dykes which are fed by the underlying Frimmersdorf Sand. (a) Asymptotic injectites, (b) Injectites with dyke-sill junction of 90°.

While overpressuring and resultant hydraulic fracturing is clearly responsible for much of the observed deformation within the host unit, the question remains as to what external triggering factors may have resulted in the generation of such pressures. Hurst et al. (2003) have noted this conundrum, suggesting that pore pressure within the parent sand body alone cannot be responsible for the various observed sand injectites worldwide. Hydraulic fracturing subsequent to failure within the host units may also be related to a variety of triggering mechanisms, such as differential compaction (rapid loading/unloading; Osborne & Swarbrick, 1997; Hurst et al., 2003; Jonk et al., 2005), polygonal or tectonic faulting and folding (Lonergan et al., 2001; Hurst et al., 2003), or a rapid addition of overpressured fluids (Lonergan et al., 2001; Jonk et al., 2005).

Measurements of the orientation of sand injectites and lignite from the study area within the Garzweiler open-cast mine (cf. Prinz et al., 2018) revealed a clear relationship between the presence of sand injectites and the lignite fracture system. When the field data were compared to the fault orientation data for the entire Garzweiler open-cast mine as derived from the 3D model of the Frimmersdorf Seam, it was clear that there was a close correlation between the presence of sand injectites and the fault orientations. Sand injectites have both the NW-SE direction as observed from the faults in the northern part of the open-cast mine, as well as the E-W direction of the Jackerath Horst in the southern part of the mine (Figs. 7-8 & 7-11). The former reflect the dominant fault orientations of the Lower Rhine Embayment, while the latter is mainly restricted to the area S of the open-cast mine. The data from the reservoir model also indicate that numerous sand injectites are concentrated in the area of the Jackerath Horst in the S, where step faults may show offsets of up to 100 m (Fig 7-11).

Several studies have shown that sand injection often occurs along pre-existing zones of structural weakness, for example faults or fractures that may act as potential failure planes (e.g. Jolly & Lonergan, 2002; Hurst et al., 2003; Mazzini et al., 2003; Duranti & Hurst, 2004; Jonk et al., 2005; Cartwright et al., 2008). Seismic activity has been interpreted as a significant triggering mechanism (Hurst et al., 2011), since earthquakes may weaken the sealing host units (Huuse et al., 2003). The syn-sedimentary faults within the Lower Rhine Basin are indeed still active, and form epicentres of significant seismic activity (e.g. Ziegler, 1992; Sissingh, 2003; Hinzen, 2003; Ewald et al., 2006). Soft sediment deformation structures, such as sand intrusions and water escape structures, have been also reported from the area of the Feldbiss Fault (located within the Roer Valley Graben, see Fig. 7-1), and these were related to seismic activity along the fault system (Vanneste et al., 1999). Particularly in the area of the Jackerath Horst, seismic activity may have acted as a triggering mechanism resulting in the formation of sand injectites. This can be related to two aspects, namely, the high concentration of injectites in this region (Fig. 7-11) as well as the large offsets observed.

Seismic activity, therefore, would appear to be a significant trigger for injectite formation. However, close examination of fault planes within the Garzweiler open-cast mine during the fieldwork for this study did not show any evidence of sand fillings. Thus, though there is indeed a spatial correlation between the presence of sand injectites and faults (see Fig. 7-11), it is also clear that sand bodies are not necessarily concentrated directly on, or along, the fault planes, but also they may be present in close proximity to, or even at some distance to the faults (metres to 10s of metres). However, in the area where sand injectites were measured directly in outcrop (and, as noted, had orientations parallel to the dominant fault directions in the region), no fault planes were detected (neither in outcrop, nor in exploration well data). This would tend to support the idea that while the presence of injectites is, to a degree, fault controlled, the relationship between the two is far from clear.

A number of authors (e.g. Secor, 1965; Huang, 1988; Boehm & Moore, 2002; Jolly & Lonergan, 2002; Jonk et al., 2005; Monnier et al., 2015) have suggested that the nucleation and propagation of sand injectites may be controlled by the paleostress field that was active during the period of sand injection. This idea would suggest that the sand injectites within the area could form parallel to, but not necessarily on, fault planes. The stress field in the Lower Rhine Basin was mainly controlled by the Alpine collision, and the resultant propagation of the European Cenozoic Rift System. These NW-SE-directed, horizontally-oriented stress fields resulted in the generation of a NE-SW-directed extensional regime in the Lower Rhine Embayment (Ziegler, 1992; Michon et al., 2003; Westerhoff et al., 2008).

Tectonic activity within the Lower Rhine Embayment changed over time, from periods with rapid subsidence in the main rifting phase (Oligocene), through to periods characterized by decreased subsidence rates in Miocene times. This was related to a decrease in the convergence rates between the African and European plates during the Burdigalian (19.5 Ma, Rosenbaum et al., 2002; Dèzes et al., 2004) and related to a phase of decreased tectonic activity within the various grabens of the European Cenozoic Rift System (Sissingh, 2003). This period coincides with the deposition of the succession observed in the Garzweiler area. However, it is entirely possible that the injectites occurred later, coincident with the new onset of tectonic activity in the region which commenced in Messinian times, and has been ongoing up to the present day (Michon et al., 2003; Dèzes et al., 2004). This would be in contrast to many of the injectites observed in various graben systems of the North Sea Basin, which formed also due to the Alpine collision and the opening of the North Atlantic, in Mid Miocene times (i.e. simultaneously to the accumulation of the Frimmersdorf Seam) (Huuse et al., 2003; Hurst et al., 2003; Andresen et al., 2009).

The presence of fault planes may also have an additional effect on the formation of sand injectites within the Lower Rhine Basin. As noted above, peat and lignite are comparably permeable, though settlement and compaction, as well as external stresses may enhance the sealing capacities (Somerton et al., 1975; Taylor et al., 1998; Jasinge et al., 2011). A number of studies, however, have shown that fault planes within the Lower Rhine Basin are often covered by clay smears (Bense & van Balen, 2004), which formed as a result of dragging or ductile flow of clay beds within the sedimentary succession (Smith, 1980; Lindsay et al., 1993; Knipe, 1993; Fulljames et al., 1997). Within the Lower Rhine Basin, clay particles of fluvial and limnic accumulations are distributed on the planes of syn-sedimentary faults. These clay-smearred, low-permeability faults thus form strong barriers to fluid migration between the individual tectonic blocks (Bense et al., 2003; Bense & van Balen, 2004; Oswald, 2005). Thus, the sealing capacities of the fault systems and the subsequent compartmentalisation of the fluid flow system within the sand bodies, may have had a significant influence on the generation of pore pressures within the porous parent sand units. However, the associated presence of so-called 'relay zones' (see Bense et al., 2003; Bense & van Balen, 2004) within the fault system could greatly facilitate fluid flow in the sand-rich bodies. The relatively sudden influx of fluids into areas where the unconsolidated sands are already water saturated could lead to a sharp increase in pore pressure and fluid escape (and resultant hydraulic fracturing) resulting in the formation of sand injectites (e.g. Vigorito & Hurst, 2010).

There is one final point, which needs to be addressed, but which is somewhat problematic. Based on our current level of knowledge, the sand injectites in the lignites of the Frimmersdorf Seam are mainly restricted to this particular seam, and also to the area of the Garzweiler open-

cast mine (this also includes former pits in the SE, see Bajor, 1958 and Berger, 1958, from which the currently active open-cast mine developed; see also Fig. 7-1). The under- and overlying seams of the Ville Fm, as well as the seams of the Inden Fm that are exploited in the westerly-located Inden open-cast mine (see Figs. 7-1 and 7-2), do not show any comparable structures. Additionally, in the area of the Hambach open-cast mine, where the Frimmersdorf Seam is also exploited (there, the seam is combined with the overlying Garzweiler Seam), no sand injectites have been observed thus far. If we assume that the sealing capacity of the host unit, as well as pore fluid pressures control the generation of sand injectites, the irregular distribution of sand injectites within the Frimmersdorf Seam in the comparably small area of the Lower Rhine Basin raises some questions. One possibility is the fact that faults which control fluid migration within the stratigraphy are concentrated in the region to the south of the Garzweiler open-cast mine (as discussed above). Another possible reason, is the fact that the Frimmersdorf Seam in the area of the Garzweiler open-cast mine is bracketed by thick sand bodies (i.e. Frimmersdorf Sand, Neurath Sand), whereas in other parts of the Lower Rhine Basin, the seam (here termed the Main Seam, which comprises the Frimmersdorf and Garzweiler seams) is bracketed by thick mud deposits. Thus, one of the main requirements for the formation of sand injectites, namely, the presence of unconsolidated, water-saturated sand is lacking. Additionally, the muds seal the seam, thus preventing the passage of sands from units lower down in the stratigraphy.

7.8 Conclusions

Sand injectites within the Lower Rhine Basin, as well as the parent sand and host units, have been analysed from the three-dimensional outcrops of the Garzweiler open-cast mine. These outcrops are constantly changing as a result of it being an active working mine, thus providing ever-changing aspects of all three. A combination of fieldwork, data derived from an industry reservoir model, and a 3D reconstruction of the seam led to the following results:

- 1) Sand injectites within the Frimmersdorf Seam are fed from three different sources: a) syn-depositional channels and beds that were deposited in the extended coastal mires which subsequently were altered to form the seam, b) the Frimmersdorf Sand, a c. 20 m thick shallow marine deposit, which directly underlies the Frimmersdorf Seam, and c) the Neurath Sand, a 10-40 m thick shallow marine deposit, which directly overlies the seam.
- 2) Syn-depositional sand bodies may be differentiated from sand injectites by the presence of primary sedimentary structures that are indicative of currents flowing over a depositional surface. Additionally, the discordant nature of the sand injectites clearly distinguishes them from the concordant syn-depositional bodies.
- 3) The orientation of the sand injectites parallel to the regional fault systems cropping out within the open-cast mine are indicative of an emplacement controlled, or at least strongly influenced, by the tectonic evolution of the Lower Rhine Embayment. Sand injectites partly formed due to seismic activity along the major fault systems (e.g. the NW-SE oriented Lower Rhine Embayment faults, or the W-E oriented Jackerath Horst).
- 4) Not all of the sand injectites would appear to have a direct relationship to the prevailing fault systems, for example, those injectites which occur where no faults are present. It is probable that such injectites formed within the zone of the prevailing extensional stress field and are, therefore, oriented parallel to the main fault orientations (i.e. NW-SE, W-E) within the Garzweiler-open-cast mine.

- 5) The fault systems in the Lower Rhine Embayment are often covered by clay smears that prevent open fluid migration between the individual tectonic blocks. Water is thus confined to distinct "compartments", and when subsequent flow occurs (possibly related to relay fault zones), the subsequent sharp rise in pore pressure can result in injectite formation.

Acknowledgement

We acknowledge the funding for this study from the RWE Power AG. We would like to offer our special thanks to Peter Lokay (RWE Power AG) for his valuable support during the development and implementation of this study. Thanks to Sven Asmus, the field crew of the Garzweiler open-cast mine and the staff members of the department GOC-L, especially to Hans Münch and Michaela Schneider.

8 Conclusions

Sand bodies within the Frimmersdorf Seam (Garzweiler open-cast mine) in the Lower Rhine Embayment have been noted for more than 30 years. The sand contents within the lignites of the Frimmersdorf Seam are extremely high, when compared to the Morken or Garzweiler seams in the Garzweiler open-cast mine. Additionally, the sand bodies are generally restricted to the Garzweiler open-cast mine, while the lignites of the Frimmersdorf Seam in the Hambach open-cast mine are comparably sand-free. The uncontrolled input of lignites into the combustion processes in the coal-fired power plants has to be avoided. Though sand contents within the exploited lignite can be detected due to the introduction of new coal preparation plants, the calculation of future lignite volumes remains problematic. To improve the understanding of the sand body distribution within the Garzweiler mining area, it was essential to fully understand the mechanisms that resulted in the emplacement of the sands within the lignite.

The analysis and interpretation of the sand bodies are based on a combination of fieldwork, analytical methods and 3D reconstructions (using map data from the RWE reservoir model). A number of conclusions could be drawn, including:

1. An initial **classification** of the sand bodies has shown that they are extremely variable, in terms of their distribution, orientation and internal structures.
 - 1.1. The detailed examination of the sand bodies within the Frimmersdorf Seam in the three-dimensional outcrops of the Garzweiler open-cast mine, was based on sedimentological analyses, and included measurements of the orientation and their position (GPS measurements) over a timespan of three years. The study also includes archival data from the past 30 years which were provided by the RWE Power AG (Department of Deposit Geology), comprising detailed photographic documentation, as well as analyses on grain size distributions and the composition of the sand bodies.
 - 1.2. The following criteria were used to classify the sand bodies within the Frimmersdorf Seam:
 - (a) Position: Sand bodies may be concentrated at the seam base or at the top, distributed throughout the seam, or they are completely absent. Though most sand bodies do not show any visible connections, they may be connected to the underlying Frimmersdorf Sand, or the overlying Frimmersdorf Seam.

- (b) Morphology: Four main morphologies are present within the seam: horizontal layers and beds, channel-like, irregular or reticulate sand bodies. These morphologies may occur in isolation, or they are connected with one another, leading to an extremely wide range of different sand body types.
- (c) Orientation: in terms of their orientation, sand bodies can be differentiated into concordant layers/beds, and discordant sills (with angles of up to 15°) and dykes (16-90°).
- (d) Composition: the sand within the Frimmersdorf Seam mainly consists of monocrystalline quartz, and K-feldspar, subordinate plagioclase and rarer amphibole, pyroxene, muscovite and zircon. The pore space between the sand grains is filled with dark-coloured humic substances that also coat the individual lighter-coloured sand grains. The sand bodies also include lignite and clay clasts as well as chert pebbles.
- (e) Grain size and sorting: the sands are mainly fine- to medium-grained, medium to well sorted.
- (f) Sedimentary structures: internal syn-sedimentary structures are, though quite rare, an important feature for the classification of the sand bodies. Cross and trough cross lamination structures occur both in channel-like, as well as concordant sand bodies.

2. Based on the classification of the sand bodies within the Frimmersdorf Seam, two major **emplacement mechanisms** were determined. Syn-depositional sand bodies were formed by the interaction of river and tidal currents, landward of the estuary that formed within the Lower Rhine Embayment in Miocene times, and coeval with peat formation. Deposition occurred within channels or as a result of periodic inundations of the seam, for example, as a result of seasonal sea-level variations or storm surges. The marine influence of some individual channel deposits was evident from the presence of glauconitic sands.

Post-depositional liquefaction and fluidization processes, resulted in the formation of so called sand injectites. These form due to the generation of overpressuring in water-saturated sand deposits (parent sand units), which have been sealed by a host unit, i.e. the peat/lignite of the Frimmersdorf Seam. The hydraulic fracturing of the peat/lignite, which is induced by the overpressuring and an additional triggering event (which have are considered to be essential for the formation of sand injectites) results in pressure release and the remobilisation of the water-saturated sands. The sand injectites in the Frimmersdorf Sand were fed by different parent sand units, namely the underlying Frimmersdorf Sand, the overlying Neurath Sand, and syn-depositional sand bodies within

the lignite. The still coeval tectonic activity of the syn-sedimentary fault systems in the Lower Rhine Basin can be regarded as a possible triggering event: fault activity can lead to rapid and sudden increases in pore pressure, and, therefore, result in the hydraulic fracturing of the host unit and the remobilization of sands.

2.1. The current results allow timing of the sand body formation to be placed within a general framework. The syn-depositional sand bodies clearly formed in Langhian/Serravallian times coeval with the period of peat formation, while the post-depositional sand bodies (i.e. injectites) occurred later. However, the precise formational time of these sand injectites can be only broadly assigned. The formation of sand injectites, as noted above, is associated with the generation of overpressuring in unconsolidated sand deposits, which are sealed with a low permeability host unit. Peat deposits, in general, are comparably permeable, and this may suggest, that the peats underwent settlement and compaction, or even a degree of coalification, prior to the formation of the sand injectites.

Sand injectites which are fed by the overlying Neurath Sand, certainly formed subsequent to the transgression of the North Sea onto the mire. The generation of overpressure in the lower parts of the Neurath Sand is certainly related to their capping by thick supratidal, mud-rich sands, or even the entire Neurath Sand deposits and overlying lignites and gravels.

The close relationship between sand injectite orientation, and the orientation of fault systems in the Lower Rhine Embayment would suggest that the emplacement of sand bodies was related to fault activity. The tectonic activity of the numerous fault systems within the Lower Rhine Embayment was generally low in early and middle Miocene times, with fault activity increasing in late Miocene, Pliocene and Pleistocene times. Thus, if the formation of sand injectites was triggered by tectonic activity, they probably formed in late Miocene, Pliocene or Pleistocene times rather than in the middle Miocene.

2.2. Coal petrographical and geochemical analyses have shown that both syn-depositional sand body formation, as well as injection processes have surprisingly little effect on the adjacent lignite. The ash content of all of the lignite samples collected from the direct contact areas with sand bodies are always extremely low, and this is rather

unusual, especially in terms of syn-depositional sand body formation. Former studies have shown that sand deposition within mires results in significantly increased ash contents of the adjacent peats. Carbon and sulphur contents of the lignite are related to their relative position in the Frimmersdorf Seam, rather than to sand body emplacement.

In addition to the information on the sand-lignite boundaries, the geochemical, coal petrological and micropetrographical analyses of the lignite and sand samples from the Frimmersdorf Seam provided some useful information on the depositional environment within the Lower Rhine Embayment in Miocene times. Sulphur and ash contents of the lignites would suggest that the syn-depositional sand bodies formed in a freshwater-controlled depositional environment, while the presence of glauconite within one channel deposit, and lower Ca/Mg ratios provide evidence of an estuarine input.

3. Sand bodies within the Miocene-age Frimmersdorf Seam have complicated mining activity within the Garzweiler open-cast mine since 2008. Although the introduction of new coal preparation plants reduced the lignite waste significantly, the calculation of lignite volumes in future Garzweiler mining areas remains problematic, and, therefore, it was essential to improve the understanding of the sand body distribution within the Frimmersdorf Seam. Therefore, a three dimensional reconstruction, based on contour line map data from the RWE reservoir model, lignite thicknesses, and known sand contents, was established, and integrated with sand body positions and orientations.

3.1. Interpretation of the three dimensional reconstruction of the Frimmersdorf Seam has shown that there is a clear correlation between the presence of sand injectites and the seam morphology. The lower boundaries of the seam are often erosively deformed by fluidization processes, while the upper boundaries above sand injectites commonly shows a convex-up bulge. Therefore, the deformation of the seam boundaries above or below sand injectites, as reflected in the seam morphology, can help to improve the early recognition of sand bodies.

Additionally, there would appear to be a direct relationship between the sand injectites orientation/position with the regional, syn-sedimentary fault system within the Garzweiler mining area. Measurements have shown that the sand injectites are commonly orientated parallel to the orientation of the fault planes in the Garzweiler

open-cast mine. The fault systems in the Lower Rhine Embayment are commonly NW-SE oriented, and these fault orientations prevail also in the N part of the Garzweiler open-cast mine. However, in the S of the Garzweiler open-cast mine, W-E-orientated faults were also noted. The sand injectites measured within the Frimmersdorf Seam reflect both the common NW-SE-orientations, as well as the W-E-orientations. This relationship suggest that sand injectites were emplaced parallel to the prevailing stress field during hydraulic fracturing of the host strata.

The study on sand bodies within the Miocene-age Frimmersdorf Seam in the Garzweiler open-cast mine (Lower Rhine Embayment) can also help to improve the general understanding of the formation of sand injectites, which are currently of great scientific and economic interest. In the North Sea Basin, sand injectites may form significant conduits for oil and gas migration, and can both positively and negatively influence the quality of oil and gas reservoirs. In the oil and gas reservoirs of the North Sea, the identification of subsurface Miocene-age parent sand units is often difficult. Additionally, differentiation between syn- and post-depositional sand bodies in drill cores, as well as in geophysical or seismic data is problematic. Numerous recent studies focus on the relationship between sand injectites and their parent sand units on the one hand, and sand injectites and their host unit on the other. The fact that the Frimmersdorf Seam injectites provide clear evidence of the sources (i.e. the Frimmersdorf and Neurath Sands as well as syn-depositional sand bodies) of the injectites, as well as allowing the structures to be mapped in detail and to be distinguished from the adjacent syn-depositional sand bodies in the Frimmersdorf Seam, means that the study provides insights into all relevant processes that are related to sand injectite formation.

Further research in the Garzweiler open-cast mine should concentrate on thin section analyses, since former studies on sand injectites have shown, that the internal microstructures present within sand injectites may differ significantly from those of syn-depositional sand bodies. The differentiation between syn- and post-depositional sand bodies in the Frimmersdorf Seam, however, is often unambiguous, for example due to primary sedimentary structures. Therefore, the comparison of the microstructure of these clearly syn-depositional sand bodies with those of sand injectites, would possibly provide some distinctive features. Perhaps, these features would help to identify syn- and post-depositional sand bodies in different environment, for example the North Sea Basin. Though a direct relationship between the North Sea sand injectites and the Lower Rhine Embayment injectites is certainly questionable, there are, indeed, some common features. Sand injectites, which were studied

within the North Sea were often emplaced in Miocene-age sediments and formed in graben systems, which are also part of the European Cenozoic Rift System, i.e. which are structurally related to the Lower Rhine Embayment.

9 References

- Abraham, M., 1994. Untersuchungen zur sedimentologischen Entwicklung der fluviatilen Deckschichten (Miozän/Pliozän) der Rheinischen Braunkohle. *Bonner Geowissenschaftliche Schriften* 15, 227pp.
- Albers, H.J., Felder, W.M., 1981. Feuersteingerölle im Oligomiozän der Niederrheinischen Bucht als Ergebnis mariner Abrasion und Carbonatlösungsphasen auf der Kreide-Tafel von Aachen-Südlimburg, in: Reiche, E., Hilden, H. (Eds.), *Geologie und Lagerstättenerkundung im Rheinischen Braunkohlenrevier*. Fortschritte in der Geologie von Nordrhein und Westfalen 29, 469–482.
- Andresen, K.J., Clausen, O.R., Huuse, M., 2009. A giant ($5.3 \times 10^7 \text{ m}^3$) middle Miocene (c. 15Ma) sediment mound (M1) above the Siri Canyon, Norwegian-Danish Basin: Origin and significance. *Marine and Petroleum Geology* 26(8), 1640–1655.
- Andsbjerg, J., Nielsen, L.H., Johannessen, P.N., Dybkjær, K., 2001. Divergent development of two neighbouring basins following the Jurassic North Sea doming event: the Danish Central Graben and the Norwegian-Danish Basin, in: Martinsen, O.J., Dreyer, T. (Eds.), *Sedimentary environments offshore Norway - Palaeozoic to recent*. NPF Special Publication 10, 175–197.
- Aspler, L., Donaldson, J.A., 1986. Penecontemporaneous sandstone dykes, Nonacho Basin (early Proterozoic, Northwest Territories): horizontal injection in vertical, tabular fissures. *Can. J. Earth. Sci* 23, 827–838.
- Bajor, M., 1958. Beobachtungen über Fazies, synsedimentäre Tektonik und Schwimmsandintrusionen in der Grube Neurath (Niederrhein), in: Ahrens, W. (Ed.), *Die Niederrheinische Braunkohlenformation*. Fortschritte in der Geologie von Nordrhein und Westfalen 1 & 2, 119–125.
- Bal, A., Lewis, D.W., 1994. A Cretaceous - early Tertiary macrotidal estuarine-fluvial succession: Puponga Coal Measures in Whanganui Inlet, onshore Pakawau sub-basin, northwest Nelson, New Zealand. *New Zealand Journal of Geology and Geophysics* 37, 287–307.
- Ballisoy, N., Schiffer, H.-W., 2001. Braunkohle in Europa. RWE Braun Aktiengesellschaft, Köln, 50 pp.
- Bechtel, A., Gratzner, R., Sachsenhofer, R.F., Gusterhuber, J., Lücke, A., Püttmann, W., 2008. Biomarker and carbon isotope variation in coal and fossil wood of Central Europe through the Cenozoic. *Palaeogeography, Palaeoclimatology, Palaeoecology* 262(3-4), 166–175.
- Becker, B., Asmus, S., 2005. Beschreibung und Korrelation der känozoischen Lockergesteinsschichten der Grundgebirgsbohrung im Umfeld des Tagebaus Hambach, in: *Geologischer Dienst Nordrhein-Westfalen* (Ed.), *Der tiefere Untergrund der Niederrheinischen Bucht - Ergebnisse eines Tiefbohrprogramms im Rheinischen Braunkohlenrevier*. scriptum - Arbeitsergebnisse aus dem Geologischen Dienst Nordrhein-Westfalen 13, Krefeld, 61–74.
- Bense, V.F., van Balen, R., Vries, J.J. de, 2003. The impact of faults on the hydrogeological conditions in the Roer Valley Rift System: an overview. *Netherlands Journal of Geosciences - Geologie en Mijnbouw* 82(1), 41–54.
- Bense, V.F., van Balen, R., 2004. The effect of fault relay and clay smearing on groundwater flow patterns in the Lower Rhine Embayment. *Basin Research* 16(3), 397–411.
- Berger, F., 1958. Flözauswaschungen und Schwimmsand-Intrusionen im Tagebau frimmersdorf-Süd, in: Ahrens, W. (Ed.), *Die Niederrheinische Braunkohlenformation*. Fortschritte in der Geologie von Nordrhein und Westfalen 1 & 2, 113–118.
- Berggren, W.A., Kent, D.V., Swisher, C.C., Aubry, M.-P., 1995. A revised Cenozoic geochronology and chronostratigraphy, in: Berggren, W.A., Kent, D.V., Aubry, M.-P., Hardenbol, J. (Eds.), *Geochronology, time scales and global stratigraphic correlation*. SEPM Special Publication 54, 129–212.
- Berner, R.A., 1984. Sedimentary pyrite formation: An update. *Geochimica et Cosmochimica Acta* 48, 605–615.
- Boehm, A., Moore, J.C., 2002. Fluidized sandstone intrusions as an indicator of Paleostress orientation, Santa Cruz, California. *Geofluids* (2), 147–161.
- Boenigk, W., 1978. Gliederung der altquartären Ablagerungen in der Niederrheinischen Bucht. *Fortschritte in der Geologie von Rheinland und Westfalen*, 28: 135–212.
- Boenigk, W., 1981. Die Gliederung der tertiären Braunkohlendeckschichten in der Ville (Niederrheinische Bucht), in: Reiche, E., Hilden, H. (Eds.), *Geologie und Lagerstättenerkundung im Rheinischen Braunkohlenrevier*. Fortschritte in der Geologie von Nordrhein und Westfalen 29, 193–263.

9 References

- Boenigk, W., 1990. Die pleistozänen Rheinterrassen und deren Bedeutung für die Gliederung des Eiszeitalters in Mitteleuropa. In: Liedtke, H. (ed): *Eiszeitforschung*. 130-140, Darmstadt.
- Boenigk, W., 1995 a. Central Upland Margin Traverse. In: W. Schirmer (ed): *Quaternary Field Trips in Central Europe*, 10: 559-598, Pfeil (München).
- Boenigk, W., 1995 b. Terrassenstratigraphie des Mittelpleistozän am Niederrhein und Mittelrhein. *Mededelingen Rijks Geologische Dienst*, 52: 71-81.
- Boersma, J.R., van Gelder, A., Groot, T. de, Puigdefabregas, C., 1981. Formen fluvialer Sedimentation in neogenen und jüngeren Ablagerungen im Braunkohlentagebau Frechen (Niederrheinische Bucht), in: Reiche, E., Hilden, H. (Eds.), *Geologie und Lagerstätten erkundung im Rheinischen Braunkohlenrevier*. *Fortschritte in der Geologie von Nordrhein und Westfalen* 29, 275–307.
- Borren, W., Bleuten, W., Lapshina, E.D., 2004. Holocene peat and carbon accumulation rates in the southern taiga of western Siberia. *Quaternary Research* 61, 42–51.
- Boyd, R., Honig, C., 1992. Estuarine sedimentation on the eastern shore of Nova Scotia. *Journal of Sedimentary Research* 62(4), 569–583.
- Braccini, E., de Boer, W., Hurst, A., Huuse, M., Vigorito, M., Templeton, G., 2008. Sand injectites. *Schlumberger Oilfield Review*, 34–49.
- Bridge, J.S., Smith, N.D., Trent, F., Gabel, S.L., Bernstein, P., 1986. Sedimentology and morphology of a low-sinuosity river: Calamus River, Nebraska Sand Hills. *Sedimentology* 33, 851-870.
- Bridge, J.S., Tye, R.S., 2000. Interpreting the dimensions of ancient fluvial channel bars, channels, and channel belts from wireline-logs and cores. *AAPG Bulletin* 84(8), 1205-1228.
- Buchardt, B., 1978. Oxygen isotope palaeotemperatures from the Tertiary period in the North Sea area. *Nature* 275, 121–123.
- Bungenstock, F., Schäfer, A., 2009. The Holocene relative sea-level curve for the tidal basin of the barrier island Langeoog, German Bight, Southern North Sea. *Global and Planetary Change* 66(1-2), 34–51.
- Busschers, F.S., Kasse, C., van Balen, R.T., Vanderberghe, J., Cohen, K.M., Weerts, H.J.T., Wallinga, J., Johns, C., Cleveringa, P., Bunnik, F.P.M., 2007. Late Pleistocene evolution of the Rhine-Meuse system in the southern North Sea basin: imprints of climate change, sea-level oscillation and glacio-isostasy. *Quaternary Science Reviews* 26, 3216-3248.
- Calder, J.H., Gibling, M.R., Mukhopadhyay, P.K., 1991. Peat formation in a Westphalian B piedmont setting, Cumberland basin, Nova Scotia: implications for the maceral-based interpretation of rheotrophic and raised paleomires. *Bull. Soc. Géol. France* 162(2), 283–298.
- Camelbeeck, T., Vanneste, K., Alexandre, P., Verbeeck, K., Petermans, T., Rosset, P., Everaerts, M., Warnant, R., van Camp, M., 2007. Relevance of active faulting and seismicity studies to assessments of long-term earthquake activity and maximum magnitude in intraplate northwest Europe, between the Lower Rhine Embayment and the North Sea, in: Stein, S., Mazotti, S. (Eds.), *Continental intraplate earthquakes: Science, Hazard and Policy Issues*. *Geological Society of America Special Paper* 425, 193–224.
- Cameron, C.C., Esterle, J.S., Palmer, C.A., 1989. The geology, botany and chemistry of selected peat-forming environments from temperate and tropical latitudes. *International Journal of Coal Geology* 12(1-4), 105–156.
- Cartwright, J., James, D., Huuse, M., Vetel, W., Hurst, A., 2008. The geometry and emplacement of conical sandstone intrusions. *Journal of Structural Geology* 30(7), 854–867.
- Casagrande, D.J., 1987. Sulphur in peat and coal, in: Scott, A.C. (Ed.), *Coal and coal-bearing strata: Recent advances*. *Geological Society Special Publication* 32, 87–105.
- Chafetz, H., Reid, A., 2000. Syndepositional shallow-water precipitation of glauconitic minerals. *Sedimentary Geology* 136 (1-2), 29–42.
- Chorowicz, J., Defontaine, B., 1993. Transfer faults and pull-apart model in the rhinegraben from analysis of multisource data. *J. Geophys. Res.* 98(B8), 14339–14351.
- Clark, C.D., Gibbard, P.L., Rose, J., 2004. Pleistocene glacial limits in England, Scotland and Wales. In: Ehlers, J., Gibbard, P.L. (Eds.), *Quaternary Glaciations: Extent and Chronology*, vol. 1, Europe. *Developments in Quaternary Science*. Elsevier, Oxford, pp. 47–82.
- Clausen, O.R., Gregersen, U., Michelsen, O., Sørensen, J.C., 1999. Factors controlling the Cenozoic sequence development in the eastern parts of the North Sea. *Journal of the Geological Society (London)* 156, 809-816.

- Cloetingh, S., van Wees, J.D., Ziegler, P.A., Lenkey, L., Beekman, F., Tesauro, M., Förster, A., Norden, B., Kaban, M., Hardebol, N., 2010. Lithosphere tectonics and thermo-mechanical properties: An integrated modelling approach for Enhanced Geothermal Systems exploration in Europe. *Earth-Science Reviews* 102(3-4), 159–206.
- Cobain, S.L., Hodgson, D.M., Peakall, J., Shiers, M.N., 2017. An integrated model of clastic injectites and basin floor lobe complexes: Implications for stratigraphic trap plays. *Basin Res* 17, 272.
- Cohen, K.M., Finney, S.C., Gibbard, P.L., Fan, J.-X., 2013. The ICS International Chronostratigraphic Chart. *Episodes* 36(3), 199–204.
- Collier, B., 2002. Detailed stratigraphy and facies analysis of the Paleoproterozoic Athabasca Group along the Shea Creek-Douglas River transect, Northern Saskatchewan. Saskatchewan Geological Survey - Summary of Investigations 2, 16pp.
- Crosdale, P.J., 1993. Coal maceral ratios as indicators of environment of deposition: do they work for ombrogenous mires? An example from the Miocene of New Zealand. *Org. Geochem.* 20(6), 797–809.
- Dai, S., Yang, J., Ward, J.C., Hower, J.C., Liu, H., Garrison, T.M., French, D., O'Keefe, J., 2015. Geochemical and mineralogical evidence for a coal-hosted uranium deposit in the Yili Basin, Xinjiang, northwestern China. *Ore Geology Reviews* 70, 1–30.
- Dalrymple, R.W., Zaitlin, B.A., Boyd, R., 1992. Estuarine facies models: conceptual basis and stratigraphic implications. *Journal of Sedimentary Petrology* 62(6), 1130–1146.
- Dalrymple, R.W., Choi, K., 2007. Morphologic and facies trends through the fluvial–marine transition in tide-dominated depositional systems: a schematic framework for environmental and sequence-stratigraphic interpretation. *Earth-Science Reviews* 81(3-4), 135–174.
- Dalrymple, R.W., Mackay, D.A., Ichaso, A.A., Choi, K.S., 2012. Processes, morphodynamics, and facies of tide-dominated estuaries, in: Davis, R.A., Jr, Dalrymple, R.W. (Eds.), *Principles of Tidal Sedimentology*. Springer, 79-107.
- Davies, R.J., 2003. Kilometer-scale fluidization structures formed during early burial of a deep-water slope channel on the Niger Delta. *Geology* 31(11), 949–952.
- Davies, R.J., Huuse, M., Hirst, P., Cartwright, J., Yang, Y., 2006. Giant clastic intrusions primed by silica diagenesis. *Geol* 34(11), 917-920.
- Demoulin, A., 1996. Clastic dykes in east Belgium: evidence for upper Pleistocene string earthquakes west of the Lower Rhine rift segment. *Journal of the Geological Society* 153(5), 803–810.
- Dèzes, P., Schmid, S.M., Ziegler, P.A., 2004. Evolution of the European Cenozoic Rift System: Interaction of the Alpine and Pyrenean orogens with their foreland lithosphere. *Tectonophysics* 389(1-2), 1–33.
- DIN 51719, 1997: Testing of solid fuels - Solid mineral fuels - Determination of ash content.
- DIN 22020-2, 1998. Investigation of raw material in hard-coal mining - Microscopical examination of hard coal, coke and briquettes - Part 2: Preparation of Polished Surface from Lump Material and Particulate Blocks.
- DIN 18128, 2002. Soil - Investigation and Testing - Determination of Ignition Loss.
- Diessel, C., 1986. On the correlation between coal facies and depositional environments. *Proceeding 20th Symposium of Departement Geology, University of New Castle, New Sputh Wales*, 19–22.
- Diessel, C., 1992. *Coal-bearing depositional systems*. Springer, Heidelberg, 721 pp.
- Diggs, T.N., 2007. An outcrop study of clastic-injection structures in the Carboniferous Tesnus Formation, Marathon Basin, in: Hurst, A., Cartwright, J.A. (Eds.), *Sand injectites: implications for hydrocarbon exploration and production*. AAPG Memoir 87. The American Association of Petroleum Geologists.
- Doebelin, N., Kleeberg, R., 2015. Profex: a graphical user interface for the Rietveld refinement program BGMN. *Journal of Applied Crystallography* 48(5), 1573–1580.
- Duranti, D., Hurst, A., Bell, C., Groves, S., Hanson, R., 2002. Injected and remobilized Eocene sandstones from the Alba Field, UKCS: core and wireline log characteristics. *Petroleum Geoscience* 8, 99–107.
- Duranti, D., Hurst, A., 2004. Fluidization and injection in the deep-water sandstones of the Eocene Alba Formation (UK North Sea). *Sedimentology* 51(3), 503–529.
- Ethridge, F.G., Jackson, T.J., Youngberg, A.D., 1981. Floodbasin sequence of a fine-grained meander belt subsystem: the coal-bearing Lower Wasatch and Upper Fort Union formations, Southern Powder

9 References

- River Basin, Wyoming, in: Ethridge, F.G., Flores, R.M. (Eds.), Recent and ancient nonmarine depositional environments. SEPM Special Publication 31, 191–209.
- Ewald, M., Igel, H., Hinzen, K.-G., Scherbaum, F., 2006. Basin-related effects on ground motion for earthquake scenarios in the Lower Rhine Embayment. *Geophysical Journal International* 166(1), 197–212.
- Feldman, H.R., McCrimmon, G.G., Freitas, T.A. de, 2008. Fluvial to estuarine valley-fill models without age-equivalent sandy shoreline deposits, based on the Clearwater Formation (Cretaceous) at Cold Lake, Alberta, Canada, in: Hampson, G.J., Steel, R.J., Burgess, P.M., Dalrymple, R.W. (Eds.), Recent advances in models of siliciclastic shallow-marine stratigraphy. SEPM Special Publication 90, 443–472.
- Figueiral, I., Mosbrugger, V., Rowe, N.P., Ashraf, A.R., Utescher, T., Jones, T.P., 1999. The Miocene peat-forming vegetation of northwestern Germany: an analysis of wood remains and comparison with previous palynological interpretations. *Review of Palaeobotany and Palynology* 104, 239–266.
- Fischer, P., 2010. Zur mittel- und jungquartären Relief- und Bodenentwicklung der nordwestlichen Kölner Bucht - Detailuntersuchungen der lössbedeckten Mittelterrassenlandschaft. Published PhD thesis, University of Köln, 231pp.
- Flores, D., 2002. Organic facies and depositional palaeoenvironment of lignites from Rio Maior Basin (Portugal). *International Journal of Coal Geology* 48(3-4), 181–195.
- Fontana, D., Lugli, S., Marchetti Dori, S., Caputo, R., Stefani, M., 2015. Sedimentology and composition of sands injected during the seismic crisis of May 2012 (Emilia, Italy): Clues for source layer identification and liquefaction regime. *Sedimentary Geology* 325, 158–167.
- Foscolos, A.E., Goodarzi, F., Koukouzas, C.N., Hatziyannis, G., 1989. Reconnaissance study of mineral matter and trace elements in Greek lignites. *Chemical Geology* 76(1-2), 107–130.
- Franke, W., 1992. Phanerozoic structures and events in central Europe, in: Blundell, D., Freeman, R., Mueller, S. (Eds.), A continent revealed in the European geotraverse. Cambridge University Press, Cambridge, 164–179.
- Fuchs, K., von Gehlen, K., Mälzer, H., Murawski, H. & Semmel, A., (eds.) 1983. Plateau Uplift. The Rhenish Shield – a case history. 411 pp., Springer (Berlin, Heidelberg, New York, Tokyo).
- Dallmeyer, R.D., Franke, W., Weber, W. 1995. Pre-Permian Geology of Central and Eastern Europe. Springer, 604pp.
- Fulljames, J.R., Zijerveld, L., Franssen, R., 1997. Fault seal processes: systematic analysis of fault seals over geological and production time scales, in: Møller-Pedersen, P., Koestler, A.G. (Eds.), Hydrocarbon seals - Importance for exploration and production. Norwegian Petroleum Society Special Publications 7, 51–59.
- Geluk, M.C., Duin, E., Duser, M., Rijkers, R., van den Berg, M.W., van Rooijen, P., 1994. Stratigraphy and tectonics of the Roer Valley Graben. *Geologie en Mijnbouw* 73, 129–141.
- Gersib, G.A., McCabe, P.J., 1981. Continental coal-bearing sediments of the Port Hood Formation (Carboniferous), Cape Linzee, Nova Scotia, Canada, in: Ethridge, F.G., Flores, R.M. (Eds.), Recent and ancient nonmarine depositional environments. SEPM Special Publication 31, 95–108.
- Gibling, M.R., 2006. Width and thickness of fluvial channel bodies and valley fills in the geological record: a literature compilation and classification. *Journal of Sedimentary Research* 76, 731–770.
- Gliese, J., Hager, H., 1978. On brown coal resources in the Lower Rhine embayment. *Geol. Mijnbouw* 57, 517–525.
- Golte, W., Heine, K., 1980. Fossile Rieseneiskeilnetze als periglaziale Klimazeugen am Niederrhein, in: Aymans, G. (Ed.), Niederrheinische Studien. Arbeiten zur rheinischen Landeskunde 46, 95–108.
- Gong, W., Shen, J., 2009. Response of sediment dynamics in the York River Estuary, USA to tropical cyclone Isabel of 2003. *Estuarine, Coastal and Shelf Science* 84(1), 61–74.
- Goodbred, S.L., Wright, E.E., Hine, A.C., 1998. Sea-level change and storm-surge deposition in a late Holocene Florida salt marsh. *J. Sediment. Res.* 68 (2), 240–252.
- Gore, A., 1983. Introduction: Mires: Swamp, Bog, Fen and Moor, in: Gore, A. (Ed.), Mires: swamp, bog, fen, moor, 4A (General Studies). *Ecosystems of the World 4A*. Elsevier Scientif. Publ. Co., pp. 1–34.
- Grein, M., Oehm, C., Konrad, W., Utescher, T., Kunzmann, L., Roth-Nebelsick, A., 2013. Atmospheric CO₂ from the late Oligocene to early Miocene based on photosynthesis data and fossil leaf characteristics. *Palaeogeography, Palaeoclimatology, Palaeoecology* 374, 41–51.

- Grützner, C., Fischer, P., Reicherter, K., 2016. Holocene surface ruptures of the Rurand Fault, Germany—insights from palaeoseismology, remote sensing and shallow geophysics. *Geophys. J. Int.* 204(3), 1662–1677.
- Hacquebard, P.A., 1993. Petrology and facies studies of the carboniferous coals at Mabou mines and invernness in comparison with those of the Port Hood, St. Rose and Sydney coalfields of Cape Breton Island, Nova Scotia, Canada. *International Journal of Coal Geology* 24(1-4), 7–46.
- Hager, H., Kothen, H., Spann, R., 1981. Zur Setzung der rheinischen Braunkohle und ihrer klastischen Begleitschichten, in: Reiche, E., Hilden, H. (Eds.), *Geologie und Lagerstättenerkundung im Rheinischen Braunkohlenrevier*. Fortschritte in der Geologie von Nordrhein und Westfalen 29, 319–352.
- Hager, H., 1986. Peat accumulation and syngenetic clastic sedimentation in the Tertiary of the Lower Rhine Basin (F.R. Germany). *Mémoires de la Société Géologique de France* 149, 51–56.
- Hager, H., Prüfert, J., 1988. Tertiär, in: Hilden, H.D. (Ed.), *Geologie am Niederrhein*. Geologisches Landesamt NRW, Krefeld, 32–40.
- Hager, H., 1993. The origin of the Tertiary lignite deposits in the Lower Rhine region, Germany. *International Journal of Coal Geology* 23(1-4), 251–262.
- Haq, B.U., Hardenbol, J., Vail, P.R., 1987. Chronology of fluctuating sea levels since the Triassic. *Science* 235, 1156–1167.
- Haq, B.U., Hardenbol, J., Vail, P.R., 1988. Mesozoic and Cenozoic chronostratigraphy and cycles of relative sea-level change, in: Wilgus, C.K., Hastings, B.S., Kendall, G., Posamentier, H.W., Ross, C.A., van Wagoner, J.C. (Eds.), *Sea-level changes: An integrated approach*. SEPM Special Publication 42, 71–108.
- Hardenbol, J., Thierry, J., Farley, M.B., Jacquin, T., Graciansky, P.C. de, Vail, P.R., 1998. Mesozoic-Cenozoic sequence chronostratigraphy of European basins, in: Graciansky, P.C. de, Hardenbol, J., Jacquin, T., Vail, P.R. (Eds.), *Mesozoic-Cenozoic sequence stratigraphy of European basins*. SEPM Special Publication 84, 763–781.
- Hardie, L.A., 1996. Secular variation in seawater chemistry: An explanation for the coupled secular variation in the mineralogies of marine limestones and potash evaporites over the past 600 m.y. *Geology* 24(3), 279–283.
- Hein, F.J., Walker, R.G., 1977. Bar evolution and development of stratification in the gravelly, braided, Kicking Horse River, British Columbia. *Canadian Journal of Earth Sciences* 14(4), 562–570.
- Hinzen, K.-G., 2003. Stress field in the Northern Rhine area, Central Europe, from earthquake fault plane solutions. *Tectonophysics* 377(3-4), 325–356.
- Hinzen, K.-G., Reamer, S.K., 2007. Seismicity, seismotectonics, and seismic hazard in the northern Rhine area, in: Stein, S., Mazotti, S. (Eds.), *Continental intraplate earthquakes: Science, Hazard and Policy Issues*. Geological Society of America Special Paper 245, 225–242.
- Hoffmann, G., Reicherter, K., 2012. Soft-sediment deformation of Late Pleistocene sediments along the southwestern coast of the Baltic Sea (NE Germany). *Int J Earth Sci (Geol Rundsch)* 101, 351–363.
- Hori, K., Saito, Y., Zhao, Q., Cheng, X., Wang, P., Sato, Y., Li, C., 2001. Sedimentary facies of the tide-dominated paleo-Changjiang (Yangtze) estuary during the last transgression. *Marine Geology* 177, 331–351.
- Houtgast, R., van Balen, R., 2000. Neotectonics of the Roer Valley Rift System, the Netherlands. *Global and Planetary Change* 27(1-4), 131–146.
- Houtgast, R., van Balen, R., Bouwer, L., Brand, G., Brijker, J., 2002. Late Quaternary activity of the Feldbiss Fault Zone, Roer Valley Rift System, the Netherlands, based on displaced fluvial terrace fragments. *Tectonophysics* 352(3-4), 295–315.
- Hovikoski, J., Räsänen, M., Gingras, M., Roddaz, M., Brusset, S., Hermoza, W., Romero Pittman, L., Lertola, K., 2005. Miocene semidiurnal tidal rhythmites in Madre de Dios, Peru. *Geology* 33(3), 177–180.
- Huang, Q., 1988. Geometry and tectonic significance of Albian sedimentary dykes in the Sisteron area, SE France. *Journal of Structural Geology* 10 (5), 453–462.
- Hurst, A., Cronin, B.T., 2001. The origin of consolidation laminae and dish structures in some deep-water sandstones. *Journal of Sedimentary Research* 71(1), 136–143.

9 References

- Hurst, A., Cartwright, J.A., Huuse, M., Jonk, R., Schwab, A., Duranti, D., Cronin, B.T., 2003. Significance of large-scale sand injectites as long-term fluid conduits: evidence from seismic data. *Geofluids* 3, 263–274.
- Hurst, A., Cartwright, J.A., Duranti, D., Huuse, M., Nelson, M., 2005. Sand injectites: an emerging global play in deep-water clastic environments, in: Doré, A.G., Vining, B.A. (Eds.), *Petroleum Geology: North-West Europe and Global Perspectives - Proceedings of the 6th Petroleum Geology Conference*. Petroleum Geology Conferences Ltd. Geological Society, London, 133–144.
- Hurst, A., Cartwright, J.A., 2007. Relevance of sand injectites to hydrocarbon exploration and production, in: Hurst, A., Cartwright, J.A. (Eds.), *Sand injectites: implications for hydrocarbon exploration and production*. AAPG Memoir 87. The American Association of Petroleum Geologists, 1–19.
- Hurst, A., Scott, A., Vigorito, M., 2011. Physical characteristics of sand injectites. *Earth-Science Reviews* 106(3-4), 215–246.
- Hurst, A., Huuse, M., Duranti, D., Vigorito, M., Jameson, E., Schwab, A., 2016. Application of outcrop analogues in successful exploration of a sand injection complex, Volund Field, Norwegian North Sea. Geological Society, London, Special Publications 436(1), 75–92.
- Huuse, M., Clausen, O.R., 2001. Morphology and origin of major Cenozoic sequence boundaries in the eastern North Sea Basin: top Eocene, near-top Oligocene and the mid-Miocene unconformity. *Basin Research* 13(1), 17–41.
- Huuse, M., Lykke-Andersen, H., Michelsen, O., 2001. Cenozoic evolution of the eastern Danish North Sea. *Marine Geology* 177(3-4), 243–269.
- Huuse, M., Duranti, D., Guargena, C.G., Prat, P., Holm, K., Steinsland, N., Cronin, B.T., Hurst, A., Cartwright, J.A., 2003. Sandstone intrusions: Detection and significance for exploration and production. *FB 21*, 15–24.
- Huuse, M., Shoulders, S.J., Netoff, D.I., Cartwright, J., 2005. Giant sandstone pipes record basin-scale liquefaction of buried dune sands in the Middle Jurassic of SE Utah. *Terra Nova* 17(1), 80–85.
- International Committee for Coal and Organic Petrology (ICCP), 2001. The new inertinite classification (ICCP System 1994). *Fuel* 80, 459–471.
- Iordanidis, A., Georgakopoulos, A., 2003. Pliocene lignites from Apofysis mine, Amynteo basin, Northwestern Greece: Petrographical characteristics and depositional environment. *International Journal of Coal Geology* 54(1-2), 57–68.
- Jackson, C.A.-L., Huuse, M., Barber, G.P., 2011. Geometry of winglike clastic intrusions adjacent to a deep-water channel complex: Implications for hydrocarbon exploration and production. *AAPG Bulletin* 95(4), 559–584.
- Jasinge, D., Ranjith, P.G., Choi, S.K., 2011. Effects of effective stress changes on permeability of latrobe valley brown coal. *Fuel* 90(3), 1292–1300.
- Johnston, J.D., 1993. Ice wedge casts in the Dalradian of South Donegal: Evidence for subaerial exposure of the Boulder Bed. *Irish Journal of Earth Sciences* 12, 13–26.
- Jolly, R., Lonergan, L., 2002. Mechanisms and controls on the formation of sand intrusions. *Journal of the Geological Society, London* 159, 605–617.
- Jonk, R., Duranti, D., Parnell, J., Hurst, A., Fallick, A.E., 2003. The structural and diagenetic evolution of injected sandstones: examples from the Kimmeridgian of NE Scotland. *Journal of the Geological Society, London* 160, 881–894.
- Jonk, R., Hurst, A., Duranti, D., Parnell, J., Mazzini, A., Fallick, A.E., 2005. Origin and timing of sand injection, petroleum migration, and diagenesis in Tertiary reservoirs, south Viking Graben, North Sea. *Bulletin* 89(3), 329–357.
- Kalkreuth, W.D., Marchioni, D.L., Calder, J.H., Lamberson, M.N., Naylor, R.D., Paul, J., 1991. The relationship between coal petrography and depositional environments from selected coal basins in Canada. *International Journal of Coal Geology* 19(1-4), 21–76.
- Kane, I.A., 2010. Development and flow structures of sand injectites: The Hind Sandstone Member injectite complex, Carboniferous, UK. *Marine and Petroleum Geology* 27(6), 1200–1215.
- Kawakami, G., Kawamura, M., 2002. Sediment flow and deformation (SFD) layers: evidence for intrastratal flow in laminated muddy sediments of the Triassic Osawa Formation, Northeast Japan. *Journal of Sedimentary Research* 72 (1), 171–181.

- Klett, M., Eichhorst, F., Schäfer, A., 2002. Facies interpretation from well logs applied to the Tertiary Lower Rhine Basin fill, in: Schäfer, A., Siehl, A. (Eds.), *Rift tectonics and syngenetic sedimentation - the Cenozoic Lower Rhine Graben and related structures*. *Netherlands Journal of Geosciences* 81, 167–176.
- Klostermann, J., Kremers, J., Röder, R., 2005. Rezente tektonische Bewegungen in der Niederrheinischen Bucht, in: *Geologischer Dienst Nordrhein-Westfalen (Ed.), Der tiefere Untergrund der Niederrheinischen Bucht - Ergebnisse eines Tiefbohrprogramms im Rheinischen Braunkohlenrevier*, vol. 37. scriptum - Arbeitsergebnisse aus dem Geologischen Dienst Nordrhein-Westfalen 13, Krefeld, pp. 557–571.
- Knipe, R.J., 1993. The influence of fault zone processes and diagenesis on fluid flow, in: Horbury, A.D., Robinson, A.G. (Eds.), *Diagenesis and Basin Development*. *AAPG Studies in Geology* 36, 135–148.
- Kolditz, K., Dellwig, O., Barkowski, J., Bahlo, R., Leipe, T., Freund, H., Brumsack, H.-J., 2012. Geochemistry of Holocene salt marsh and tidal flat sediments on a barrier island in the southern North Sea (Langeoog, North-West Germany). *Sedimentology* 59, 337–355.
- Lindsay, N.G., Murphy, F.C., Walsh, J.J., Watterson, J., 1993. Outcrop studies of shale smears on fault surfaces, in: Flint, S.S., Bryant, I.D. (Eds.), *The Geological Modelling of Hydrocarbon Reservoirs and Outcrop Analogues*. *Special Publication of the International Association of Sedimentologists* 15, 113–123.
- Littke, R., Urai, J.L., Uffmann, A.K., Risvanis, F., 2012. Reflectance of dispersed vitrinite in Palaeozoic rocks with and without cleavage: Implications for burial and thermal history modeling in the Devonian of Rursee area, northern Rhenish Massif, Germany. *International Journal of Coal Geology* 89, 41–50.
- Lonergan, L., Lee, N., Johnson, H.D., Cartwright, J.A., Jolly, R., 2001. Remobilization and injection in deepwater depositional systems: implications for reservoir architecture and prediction, in: Weimer, P., Slatt, R.M., Coleman, J., Rosen, N.C., Nelson, H., Bouma, A.H., Styzen, M.J., Lawrence, D.T. (Eds.), *Deepwater Reservoirs of the World*. *GCSSEPM Foundation 20th Annual Bob F. Perkins Research Conference*, 515-132.
- Longhitano, S.G., Mellere, D., Steel, R.J., Ainsworth, R.B., 2012. Tidal depositional systems in the rock record: A review and new insights. *Sedimentary Geology* 279, 2-22.
- Lowe, D.R., 1975. Water escape structures in coarse-grained sediments. *Sedimentology* 22(2), 157–204.
- Lowenstein, T.K., Timofeeff, M.N., Brennan, S.T., Hardie, L.A., Demicco, R.V., 2001. Oscillations in Phanerozoic seawater chemistry: Evidence from fluid inclusions. *Science* 294(5544), 1086–1088.
- Lücke, A., Helle, G., Schleser, G.H., Figueiral, I., Mosbrugger, V., Jones, T.P., Rowe, N.P., 1999. Environmental history of the German Lower Rhine Embayment during the Middle Miocene as reflected by carbon isotopes in brown coal. *Palaeogeography, Palaeoclimatology, Palaeoecology* 154(4), 339–352.
- Madon, M., Abu Bakar, Z.A., Ismail, H.H., 2010. Jurassic-Cretaceous fluvial channel and floodplain deposits along the Karak-Kuantan Highway, Central Pahang (Peninsular Malaysia). *Bulletin of the Geological Society of Malaysia* 56, 9–14.
- Mangerud, J., 2004. Ice sheet limits on Norway and the Norwegian continental shelf. In: Ehlers, J., Gibbard, P.L. (Eds.), *Quaternary Glaciations: Extent and Chronology*, vol. 1, Europe. *Developments in Quaternary Science*. Elsevier, Oxford, pp. 271–294.
- Martel, A.T., Gibling, M.R., 1993. Clastic dykes of the Devonian-Carboniferous Horton Bluff Formation, Nova Scotia: storm-related structures in shallow lakes. *Sedimentary Geology* 87, 103–119.
- Mazumder, R., Arima, M., 2004. Tidal rhythmites and their implications. *Earth-Science Reviews* 69, 79-95.
- Mazzini, A., Jonk, R., Duranti, D., Parnell, J., Cronin, B., Hurst, A., 2003. Fluid escape from reservoirs: Implications from cold seeps, fractures and injected sands Part I. The fluid flow system. *Journal of Geochemical Exploration* 78-79, 293–296.
- McCabe, P.J., 1987. Facies studies of coal and coal-bearing strata, in: Scott, A.C. (Ed.), *Coal and coal-bearing strata: Recent advances*. *Geological Society Special Publication* 32, 51–66.
- McCann, T., Pascal, C., Timmerman, M.J., Krzywiec, P., López-Gómez, J., Wetzel, A., Krawczyk, C.M., Rieke, H., Lamarche, J., 2006. Post-Variscan (end Carboniferous-Early Permian) basin evolution in Western and Central Europe, in: Gee, D.G., Stephenson, R.A., *European Lithosphere Dynamics*. *Geological Society, London, Memoirs* 32, 355-388.

9 References

- Meyer, W. & Stets, J., 1998. Junge Tektonik im Rheinischen Schiefergebirge und ihre Quantifizierung. *Zeitschrift der Deutschen Geologischen Gesellschaft*, 149: 359-379.
- Miall, A., 1996. *The geology of fluvial deposits: Sedimentary facies, basin analysis, and petroleum geology*. Springer, Berlin, 582 pp.
- Miall, A.D., 2006. Reconstructing the architecture and sequence stratigraphy of the preserved fluvial record as a tool for reservoir development: A reality check. *AAPG Bulletin* 90(7), 989-1002.
- Michelsen, O., Thomsen, E. Danielsen, M., Heilmann-Clausen, C., Jordt, H., Laursen, G.V., 1998. Cenozoic sequence stratigraphy in the eastern North Sea, in: Graciansky, P.C. de, Hardenbol, J., Jacquin, T., Vail, P.R. (Eds.), *Mesozoic-Cenozoic sequence stratigraphy of European basins*. SEPM Special Publication 84, 91–118.
- Michon, L., van Balen, R.T., Merle, O., Pagnier, H., 2003. The Cenozoic evolution of the Roer Valley Rift System integrated at a European scale. *Tectonophysics* 367(1-2), 101–126.
- Michon, L., Van Balen, R.T., 2005. Characterization and quantification of active faulting in the Roer valley rift system based on high precision digital elevation models. *Quaternary Science Reviews* 24, 457–474.
- Mörs, T., 2002. Biostratigraphy and paleoecology of continental Tertiary vertebrate faunas in the Lower Rhine Embayment (NW Germany). *Netherlands Journal of Geosciences/ Geologie en Mijnbouw* 81(2), 177-183.
- Monnier, D., Gay, A., Imbert, P., Cavailhes, T., Soliva, R., Lopez, M., 2015. Sand injectites network as a marker of the palaeo–stress field, the structural framework and the distance to the sand source: Example in the Vocontian Basin, SE France. *Journal of Structural Geology* 79, 1–18.
- Mosbrugger, V., Gee, C.T., Belz, G., Ashraf, A.R., 1994. Three-dimensional reconstruction of an in-situ Miocene peat forest from the Lower Rhine Embayment, northwestern Germany—new methods in palaeovegetation analysis. *Palaeogeography, Palaeoclimatology, Palaeoecology* 110(3-4), 295–317.
- Mosbrugger, V., Utescher, T., Dilcher, D.L., 2005. Cenozoic continental climatic evolution of Central Europe. *Proceedings of the National Academy of Sciences of the United States of America* 102(42), 14964–14969.
- Müller, W., 1964. Unterschiede in den chemischen und physikalischen Eigenschaften von fluviatilen, brakischen und marinen Sedimenten, in: van Straaten, L. (Ed.), *Deltaic and shallow marine deposits*. *Developements in Sedimentology*, 293–300.
- Netoff, D., 2002. Seismogenically induced fluidization of Jurassic erg sands, south-central Utah. *Sedimentology* 49(1), 65–80.
- Neuwerth, R., Suter, F., Guzman, C.A., Gorin, G.E., 2006. Soft-sediment deformation in a tectonically active area: The Plio-Pleistocene Zarzal Formation in the Cauca Valley (Western Colombia). *Sedimentary Geology* 186(1-2), 67–88.
- Nickel, E., 2003. *Oligozäne Beckendynamik und Sequenzstratigraphie am Südrand des Nordwesteuropäischen Tertiärbeckens*. Dissertation, Bonn, 155 pp.
- Obermeier, S.F., 1996. Use of liquefaction-induced features for paleoseismic analysis - An overview of how seismic liquefaction features can be distinguished from other features and how their regional distribution and properties of source sediment can be used to infer the location and strength of Holocene paleo-earthquakes. *Engineering Geology* 44, 1–76.
- Oncken, O., von Winterfeld, C., Dittmar, U., 1999. Accretion of a rifted passive margin: The Late Paleozoic Rhenohercynian fold and thrust belt (Middle European Variscides). *Tectonics* 18(1), 75-91.
- Osborne, M.J., Swarbrick, R.E., 1997. Mechanisms for generating overpressure in sedimentary basins: a re-evaluation. *AAPG Bulletin* 81, 1023–1041.
- Oswald, T., 2005. Neue geohydrologische Erkenntnisse aus dem Umfeld des Braunkohle-Tagebaus Hambach (Niederrheinische Bucht, in: Geologischer Dienst Nordrhein-Westfalen (Ed.), *Der tiefere Untergrund der Niederrheinischen Bucht - Ergebnisse eines Tiefbohrprogramms im Rheinischen Braunkohlenrevier*. scriptum - Arbeitsergebnisse aus dem Geologischen Dienst Nordrhein-Westfalen 13, 91–120.
- Owen, G., 1996. Experimental soft-sediment deformation: structures formed by the liquefaction of unconsolidated sands and some ancient examples. *Sedimentology* 43, 279–293.

- Palladino, G., Grippa, A., Bureau, D., Alsop, G.I., Hurst, A., 2016. Emplacement of sandstone intrusions during contractional tectonics. *Journal of Structural Geology* 89, 230–249.
- Peterson, G.L., 1968. Flow structures in sandstone dikes. *Sedimentary Geology* 2(3), 177–190.
- Petzelberger, B., 1994. Die marinen Sande im Tertiär der südlichen Niederrheinischen Bucht. Sedimentologie, Fazies und stratigraphische Deutung unter Berücksichtigung der Sequenzstratigraphie. *Bonner Geowissenschaftliche Schriften* 14, Universität Bonn, 112 pp.
- Pickel, W., Kus, J., Flores, D., Kalaitzidis, S., Christanis, K., Cardott, B.J., Misz-Kennan, M., Rodrigues, S., Hentschel, A., Hamor-Vido, M., Crosdale, P., Wagner, N., 2017. Classification of liptinite – ICCP System 1994. *International Journal of Coal Geology* 169, 40–61.
- Plint, A.G., 1983. Liquefaction, fluidization and erosional structures associated with bituminous sands of the Bracklesham Formation (Middle Eocene) of Dorset, England. *Sedimentology* 30(4), 525–535.
- Plint, A.G., 1985. Possible earthquake-induced soft-sediment faulting and remobilization in Pennsylvanian alluvial strata, southern New Brunswick, Canada. *Can. J. Earth. Sci.* 22, 907–912.
- Prinz, L., McCann, T., Schäfer, A., Asmus, S., Lokay, P., 2018. The geometry, distribution and development of sand bodies in the Miocene-age Frimmersdorf Seam (Garzweiler open-cast mine), Lower Rhine Basin, Germany: implications for seam exploitation. *Geological Magazine*, 22 pp.
- Prinz, L., Schäfer, A., McCann, T., Utescher, T., Lokay, P., Asmus, S., 2017 a. Facies analysis and depositional model of the Serravallian-age Neurath Sand, Lower Rhine Basin (W Germany). *Netherlands Journal of Geosciences* 21, 1–21.
- Prinz, L., Zieger, L., Littke, R., McCann, T., Lokay, P., Asmus, S., 2017 b. Syn- and post-depositional sand bodies in lignite – the role of coal analysis in their recognition. A study from the Frimmersdorf Seam, Garzweiler open-cast mine, western Germany. *International Journal of Coal Geology* 179, 173–186.
- Prodehl, C., Glahn, A., Gutschera, M., Mueller, S., Haak, V., 1992. Lithospheric cross sections of the European Cenozoic rift system, in: Ziegler, P.A. (Ed.), *Geodynamics of Rifting. Volume 1. Case History Studies on Rift: Europe and Asia. Tectonophysics* 208, 113–138.
- Rasmussen, E.S., Dybkær, K., Piasecki, S., 2002. Miocene depositional systems of the eastern North Sea Basin, Denmark. *Danmarks og Grønlands Geologiske Undersøgelse Report* 89, 132pp.
- Rasmussen, E.S., 2004. Stratigraphy and depositional evolution of the uppermost Oligocene-Miocene succession in western Denmark. *Bulletin of the Geological Society of Denmark* 51, 89–109.
- Rasmussen, E.S., Dybkær, K., Piasecki, S., 2010. Lithostratigraphy of the Upper Oligocene-Miocene succession of Denmark. *Geological Survey of Denmark and Greenland Bulletin* 22. Geological Survey of Denmark and Greenland Ministry of Climate and Energy, Copenhagen Denmark, 92 pp.
- Rasser, M.W., Harzhauser, M., Anistratenko, O., Anistratenko, V.Y., Bassi, D., Belak, M., Berger, J.-P., Bianchini, G., Čičić, S., Čosović, V., Doláková, N., Drobne, K., Filipescu, S., Gürs, K., Hladilová, S., Hrvatovć, H., Jelen, B., Kasiński, J.R., Kováč, M., Kralj, P., Marjanac, T., Márton, E., Mietto, P., Moro, A., Nagymarosy, A., Nebelsick, J.H., Nehyba, S., Ogorelec, B., Oszczypko, N., Pavelić, D., Piwocki, M., Poljak, M., Pugliese, N., Redžepović, R., Rifelj, H., Roetzel, R., Skaberne, D., Silva, L., Standke, G., Tunis, G., Vass, D., Wagreeich, M., Wesselingh, F., 2008. Palaeogene and Neogene, in: McCann, T. (Ed.), *The Geology of Central Europe, Volume 2: Mesozoic and Cenozoic. Geological Society of London*, 1031–1140.
- Reicherter, K., 2008. Alpine Tectonics II - Central Europe north of the Alps, in: McCann, T. (Ed.), *The Geology of Central Europe, Volume 2: Mesozoic and Cenozoic. Geological Society of London*, 1233–1286.
- Reimnitz, E., Marshall, N.F., 1965. Effects of the Alaska earthquake and tsunami on recent deltaic sediments. *Journal of Geophysical Research* 70 (10), 2363–2376.
- Ribbert, K.-H., Wrede, V., 2005. Stratigraphische und tektonische Ergebnisse der Grundgebirgsbohrungen im Umfeld des Braunkohle-Tagebaus Hambach, in: *Geologischer Dienst Nordrhein-Westfalen (Ed.), Der tiefere Untergrund der Niederrheinischen Bucht - Ergebnisse eines Tiefbohrprogramms im Rheinischen Braunkohlenrevier. scriptum - Arbeitsergebnisse aus dem Geologischen Dienst Nordrhein-Westfalen* 13, 33–60.
- Rodrigues, N., Cobbold, P.R., Løseth, H., 2009. Physical modelling of sand injectites. *Tectonophysics* 474(3-4), 610–632.
- Rosenbaum, G., Lister, G.S., Duboz, C., 2002. Relative motions of Africa, Iberia and Europe during Alpine orogeny. *Tectonophysics* 359, 117–129.

9 References

- Ross, J.A., Peakall, J., Keevil, G.M., 2011. An integrated model of extrusive sand injectites in cohesionless sediments. *Sedimentology* 58 (7), 1693–1715.
- Schäfer, A., 1994. Die Niederrheinische Bucht im Tertiär - Ablagerungs- und Lebensraum, in: Koenigswald, W., Meyer, W. von (Eds.), *Erdgeschichte Im Rheinland. Fossilien und Gesteine aus 400 Millionen Jahren*, München, 155–164.
- Schäfer, A., Hilger, D., Gross, G., van der Hocht, F., 1996. Cyclic sedimentation in tertiary Lower-Rhine Basin (Germany) - the 'Liegendrücken' of the brown-coal open-cast Fortuna mine. *Sedimentary Geology* 103, 229–247.
- Schäfer, A., Utescher, T., Mörs, T., 2004. Stratigraphy of the Cenozoic Lower Rhine Basin, northwestern Germany. *Newsl. Stratigr.* 40(1), 73–110.
- Schäfer, A., Utescher, T., Klett, M., Valdivia-Manchego, M., 2005. The Cenozoic Lower Rhine Basin – rifting, sedimentation, and cyclic stratigraphy. *Int J Earth Sci (Geol Rundsch)* 94(4), 621–639.
- Schäfer, A., 2010. *Klastische Sedimente - Fazies und Sequenzstratigraphie*. Spektrum Akademischer Verlag, Heidelberg, 416 pp.
- Schäfer, A., Utescher, T., 2014. Origin, sediment fill, and sequence stratigraphy of the Cenozoic Lower Rhine Basin (Germany) interpreted from well logs. *Zeitschrift der Deutschen Gesellschaft für Geowissenschaften* 165(2), 287–314.
- Schneider, H., Thiele, S. *Geohydrologie des Erfgebietes*. Ministerium für Ernährung, Landwirtschaft und Forsten, Nordrhein-Westfalen, 185pp.
- Schumacher, M.E., 2002. Upper Rhine Graben: Role of preexisting structures during rift evolution. *Tectonics* 21(1), 6-1-6-17.
- Scott, A., Vigorito, M., Hurst, A., 2009. The process of sand injection: internal structures and relationships with host strata (Yellowbank Creek Injectite Complex, California, U.S.A.). *Journal of Sedimentary Research* 79, 568–583.
- Secor, D.T., 1965. Role of fluid pressure in jointing. *American Journal of Science* 263 (8), 633–646.
- Shanley, K.W., McCabe, P.J., Hettinger, R.D., 1992. Tidal influence in Cretaceous fluvial strata from Utah, USA: a key to sequence stratigraphic interpretation. *Journal of Sedimentary Research* 39, 905–930.
- Sissingh, W., 1997. Tectonostratigraphy of the North Alpine Foreland Basin: correlation of Tertiary depositional cycles and orogenic phases. *Tectonophysics* 282, 223–256.
- Sissingh, W., 1998. Comparative Tertiary stratigraphy of the Rhine Graben, Bresse Graben and Molasse Basin: correlation of Alpine foreland events. *Tectonophysics* 300, 249–284.
- Sissingh, W., 2001. Tectonostratigraphy of the West Alpine Foreland: correlation of Tertiary sedimentary sequences, changes in eustatic sea-level and stress regimes. *Tectonophysics* 333, 361–400.
- Sissingh, W., 2003. Tertiary paleogeographic and tectonostratigraphic evolution of the Rhenish Triple Junction. *Palaeogeography, Palaeoclimatology, Palaeoecology* 196(1-2), 229–263.
- Sissingh, W., 2006. Syn-kinematic palaeogeographic evolution of the West European Platform: correlation with Alpine plate collision and foreland deformation. *Netherlands Journal of Geosciences - Geologie en Mijnbouw* 85(2), 131–180.
- Smith, D.A., 1980. Sealing and nonsealing faults in Louisiana Gulf Coast Salt Basin. *AAPG Bulletin* 64 (2), 145–172.
- Somerton, W.H., Söylemezoglu, I.M., Dudley, R.C., 1975. Effect of stress on permeability of coal. *Int. J. Rock Mech. Min. Sci. & Geomech. Abstr.* 12, 129–145.
- Steffen, H., Kaufmann, G., Wu, P., 2006. Three-dimensional finite-element modeling of the glacial isostatic adjustment in Fennoscandia. *Earth and Planetary Science Letters* 250(1-2), 358–375.
- Stets, J., Schäfer, A., 2009. The Siegenian delta: land-sea transitions at the northern margin of the Rhenohercynian Basin. *Geological society, London, Special Publications* 314, 37-72.
- Stets, J.; Schäfer, A., 2011. The Lower Devonian Rhenohercynian Rift - 20 Ma of sedimentation and tectonics (Rhenish Massif, W-Germany). *ZDGG* 162(2), 93-115.
- Stock, A.T., Littke, R., Lücke, A., Zieger, L., Thielemann, T., 2016. Miocene depositional environment and climate in western Europe: The lignite deposits of the Lower Rhine Basin, Germany. *International Journal of Coal Geology* 157, 2–18.

- Svendssen, J.I., Alexanderson, H., Astakhov, V.I., Demidov, I., Dowdeswell, J.A., Funder, S., Gataullin, V., Henriksen, M., Hjort, C., Houmark-Nielsen, M., et al., 2004. Late Quaternary ice sheet history of northern Eurasia. *Quaternary Science Reviews* 23, 1229–1271.
- Sýkorová, I., Pickel, W., Christanis, K., Wolf, M., Taylor, G.H., Flores, D., 2005. Classification of huminite - ICCP System 1994. *International Journal of Coal Geology* 62(1-2), 85–106.
- Taşgın, C.K., 2011. Seismically-generated hydroplastic deformation structures in the Late Miocene lacustrine deposits of the Malatya Basin, eastern Turkey. *Sedimentary Geology* 235(3-4), 264–276.
- Taylor, G.H., Teichmüller, M., Davies, A., Diessel, C., Littke, R., Robert, P., 1998. *Organic Petrology: A new handbook incorporating some revised parts of Stach's Textbook of Coal Petrology*. Gebrüder Borntraeger, Berlin-Stuttgart, 704 pp.
- Teichmüller, M., 1958. Rekonstruktion verschiedener Moortypen des Hauptflöztes der niederrheinischen Braunkohle, in: Ahrens, W. (Ed.), *Die Niederrheinische Braunkohlenformation*. Fortschritte in der Geologie von Nordrhein und Westfalen 1 & 2, 559–612.
- Teichmüller, R., 1958. Die Niederrheinische Braunkohlenformation: Stand der Untersuchung und offene Fragen, in: Ahrens, W. (Ed.), *Die Niederrheinische Braunkohlenformation*. Fortschritte in der Geologie von Nordrhein und Westfalen 1 & 2, 721–750.
- Teichmüller, R., 1974. Die tektonische Entwicklung der Niederrheinischen Bucht, in: Illies, J.H., Fuchs, K. (Eds.), *Approaches to Taphogenesis*. Schweizerbart, Stuttgart, 269–285.
- Teichmüller, M., 1975. Origin of the petrographic constituents of coal, in: Stach, E., Mackowsky, M.-T., Teichmüller, M., Taylor, G.H., Chandra, D., Teichmüller, R. (Eds.), *Stach's Textbook of Coal Petrology*. Gebrüder Borntraeger, Berlin Stuttgart, 219–294.
- Teichmüller, M., 1989. The genesis of coal from the viewpoint of coal petrology. *International Journal of Coal Geology* 12(1-4), 1–87.
- Teichmüller, M., Thomson, P.W., 1958. Vergleichende mikroskopische und chemische Untersuchungen der wichtigsten Fazies-Typen im Hauptflöz der niederrheinischen Braunkohle, in: Ahrens, W. (Ed.), *Die Niederrheinische Braunkohlenformation*. Fortschritte in der Geologie von Nordrhein und Westfalen 1 & 2, 573–598.
- Thöle, H., Gaedicke, C., Kuhlmann, G., Reinhardt, L., 2014. Late Cenozoic sedimentary evolution of the German North Sea – A seismic stratigraphic approach. *Newsl. Stratigr.* 47(3), 299–329.
- Thome, K.N., 1959. Das Inlandeis am Niederrhein, in: Teichmüller, R., van der Brelie, G. (Eds.), *Pliozän und Pleistozän am Mittel- und Niederrhein*. Fortschritte in der Geologie von Nordrhein und Westfalen 4, 197–246.
- Thompson, B.J., Garrison, R.E., Moore, J.C., 2007. A reservoir-scale Miocene injectite near Santa Cruz, California, in: Hurst, A., Cartwright, J.A. (Eds.), *Sand injectites: implications for hydrocarbon exploration and production*. AAPG Memoir 87, 151–162.
- Ufer, K., Stanjek, H., Roth, G., Dohrmann, R., Kleeberg, R., Kaufhold, S., 2008. Quantitative phase analysis of bentonites by the Rietveld method. *Clays and Clay Minerals* 56(2), 272–282.
- Ufer, K., Kleeberg, R., Bergmann, J., Dohrmann, R., 2012. Rietveld refinement of disordered Illite-Smectite mixed-layer structures by a recursive algorithm. II: Powder-pattern refinement and quantitative phase analysis. *Clay and clay minerals* 60(5), 535–552.
- Ufer, K., Kleeberg, R., Monecke, T., 2015. Quantification of stacking disordered Si-Al layer silicates by the Rietveld method: application to exploration for high-sulphidation epithermal gold deposits. *Powder Diffraction* 30(S1), 111–118.
- Uncles, R.J., 2010. Physical properties and processes in the Bristol Channel and Severn Estuary. *Marine pollution bulletin* 61(1-3), 5–20.
- Utescher, T., Ashraf, A.R., Mosbrugger, V., 1992. Zur Faziesentwicklung im Neogen der Niederrheinischen Bucht, in: Kovar-Eder, J. (Ed.), *Palaeovegetational Development in Europe*, Vienna: Naturhistorisches Museum, 235–243.
- Utescher, T., Mosbrugger, V., Ashraf, A.R., 2000. Terrestrial climate evolution in Northwest Germany over the last 25 million years. *PALAIOS* 15, 430–449.
- Utescher, T., Mosbrugger, V., Ashraf, A.R., 2002. Facies and paleogeography of the Tertiary of the Lower Rhine Basin - sedimentary versus climatic control. *Netherlands Journal of Geosciences/ Geologie en Mijnbouw* 81(2), 185–191.
- Utescher, T., Mosbrugger, V., Ivanov, D., Dilcher, D.L., 2009. Present-day climatic equivalents of European Cenozoic climates. *Earth and Planetary Science Letters* 284(3-4), 544–552.

9 References

- Utescher, T., Ashraf, A.R., Dreist, A., Dybkjær, K., Mosbrugger, V., Pross, J., Wilde, V., 2012. Variability of Neogene continental climates in Northwest Europe - A detailed study based on microfloras. *Turkish Journal of Earth Sciences* 21, 289–314.
- Valdivia-Manchego, M., 1994. Rechnergestützte stereo-photogrammetrische Aufnahme und Auswertung fluvialer Sedimentstrukturen im tertiär der Niederrheinischen Bucht. *Zentralblatt für Geologie und Paläontologie* 1, 1011–1026.
- Van Balen, R., Busschers, F.S., Tucker, G.E., 2010. Modeling the response of the Rhine-Meuse fluvial system to Late Pleistocene climate change. *Geomorphology* 114, 440–452.
- Van der Burgh, J., 1973. Hölzer der niederrheinischen Braunkohlenformation, 2. Hölzer der Braunkohlengruben 'Maria Theresia' zu Herzogenrath, 'Zukunft West' zu Eschweiler und 'Victor' (Zülpich Mitte) zu Zülpich, Nebst einer systematisch-anatomischen Bearbeitung der Gattung Pinus L. *Review of Palaeobotany and Palynology* 15(2-3), 73-275.
- Van der Meer, J., Kjær, K.H., Krüger, J., Rabassa, J., Kilfeather, A.A., 2009. Under pressure: clastic dykes in glacial settings. *Quaternary Science Reviews* 28 (7-8), 708–720.
- Vanneste, K., Meghraoui, M., Camelbeeck, T., 1999. Late Quaternary earthquake-related soft-sediment deformation along the Belgian portion of the Feldbiss Fault, Lower Rhine Graben system. *Tectonophysics* 309(1-4), 57–79.
- Vigorito, M., Hurst, A., Cartwright, J., Scott, A., 2008. Regional-scale subsurface sand remobilization: geometry and architecture. *Journal of the Geological Society* 165, 609–612.
- Vigorito, M., Hurst, A., 2010. Regional sand injectite architecture as a record of pore-pressure evolution and sand redistribution in the shallow crust: Insights from the Panoche Giant Injection Complex, California. *Journal of the Geological Society* 167, 889–904.
- Vis, G.-J., Verweij, H., Koenen, M., 2016. The Rupel Clay Member in the Netherlands: towards a comprehensive understanding of its geometry and depositional environment. *Netherlands Journal of Geosciences*, 95(3), 221-251.
- Von der Brelie, G. & Wolf, M., 1981. 'Sequoia' und *Sciadopitys* in den Braunkohlenmooren der Niederrheinischen Bucht. In: Reiche, E. & Hilden, H.D. (Eds.): *Geologie und Lagerstättenerkundung im Rheinischen Braunkohlenrevier*. Fortschritte in der Geologie von Rheinland und Westfalen 29, 177–191.
- Ward, C.R., 1991. Mineral matter in low-rank coals and associated strata of the Mae Moh basin, northern Thailand. *International Journal of Coal Geology* 17(1), 69–93.
- Ward, C.R., 2002. Analysis and significance of mineral matter in coal seams. *International Journal of Coal Geology* 50(1-4), 135–168.
- Ward, C.R., 2016. Analysis, origin and significance of mineral matter in coal: An updated review. *International Journal of Coal Geology* 165, 1–27.
- Wedepohl, K.H., 1971. Environmental influences on the chemical composition of shales and clays. *Physics and Chemistry of the Earth* 8, 307–333.
- Werner, H., 1958. Der Nachweis mariner Beeinflussung von niederrheinischen Braunkohlen mit Hilfe des Ca/Mg-Verhältnisses, in: Ahrens, W. (Ed.), *Die Niederrheinische Braunkohlenformation*. Fortschritte in der Geologie von Nordrhein und Westfalen 1 & 2, pp. 95–99.
- Werner, H., 1963. Über das Calcium/Magnesium Verhältnis in Torf und Kohle, in: Hesemann, J., Dahn, H.-D. (Eds.), *Unterscheidungsmöglichkeiten mariner und nicht mariner Sedimente*. Fortschritte in der Geologie von Nordrhein und Westfalen. Geologisches Landesamt NRW, Krefeld, pp. 279–282.
- Westerhoff, W.E., Kemna, H.A., Boenigk, W., 2008. The confluence area of Rhine, Meuse, and Belgian rivers: Late Pliocene and Early Pleistocene fluvial history of the northern Lower Rhine Embayment. *Netherlands Journal of Geosciences - Geologie en Mijnbouw* 87 (1), 107–125.
- Whateley, M., Tuncali, E., 1995. Quality variations in the high-sulphur lignite of the Neogene Beypazari Basin, Central Anatolia, Turkey. *International Journal of Coal Geology* 27(2-4), 131–151.
- Williams, G.E., 2001. Neoproterozoic (Torridonian) alluvial fan succession, northwest Scotland, and its tectonic setting and provenance. *Geol. Mag.* 138(02).
- Wilson, M., Downes, H., 1992. Mafic alkaline magmatism in the European Cenozoic rift system, in: Ziegler, P.A. (Ed.), *Geodynamics of Rifting*. Volume 1. Case History Studies on Rift: Europe and Asia. *Tectonophysics* 208. Elsevier, 173–182.
- Wilson, M., Rosenbaum, J.M., Dunworth, E.A., 1995. Melilitites: partial melts of the thermal boundary layer? *Contrib. Mineral. Petrol.* 119, 181–196.

- WING, S. L. 1984. Relation of paleovegetation to geometry and cyclicity of some fluvial carbonaceous deposits. *Journal of Sedimentary Petrology* 54(1), 52–66.
- Winstanley, A.M., 1993. A review of the Triassic play in the Roer Valley Graben, SE onshore Netherlands. In: Parker, J.R. (Ed.), *Petroleum Geology of Northwest Europe*. Proceedings of the 4th Conference Geol. Soc., London, pp. 595–607.
- Woodroffe, C.D., 2000. Deltaic and estuarine environments and their Late Quaternary dynamics on the Sunda and Sahul shelves. *Journal of Asian Earth Sciences* 18(4), 393–413.
- Zachos, J., Pagani, M., Sloan, L., Thomas, E., Billups, K., 2001. Trends, rhythms, and aberrations in global climate 65 Ma to present. *Science* 292, 686–693.
- Zagwijn, W.H., 1975. Variations in climate as shown by pollen analysis, especially in the Lower Pleistocene of Europe, in: Wright, A.E., Moseley, F. (Eds.), *Ice ages: ancient and modern*. Liverpool, 137–152.
- Zagwijn, W.H., Hager, H., 1987. Correlations of continental and marine neogene deposits in the south-eastern Netherlands and the Lower Rhine District. *Meded. Werkgr. Tert. Kwart. Geol.* 24 (1-2), 59–78.
- Zagwijn, W.H., 1989. The Netherlands during the Tertiary and the Quaternary: a case history of coastal lowland evolution. *Geologie en Mijnbouw* 68, 107–120.
- Ziegler, P.A., 1990. Geological atlas of western and central Europe, 2nd ed. Shell Internationale Petroleum Mij., Geological Society, London, Publ. House, 238pp.
- Ziegler, P.A., 1992. European Cenozoic rift system, in: Ziegler, P.A. (Ed.), *Geodynamics of Rifting*. Volume 1. Case History Studies on Rift: Europe and Asia. *Tectonophysics* 208. Elsevier, 91–111.
- Ziegler, P.A., 1994. Cenozoic rift system of western and central Europe - an overview. *Geologie en Mijnbouw* 73 (2-4), 99–127.
- Ziegler, P.A., Cloetingh, S., van Wees, J.-D., 1995. Dynamics of intra-plate compressional deformation: the Alpine foreland and other examples. *Tectonophysics* 252, 7–59.
- Ziegler, P.A., Dèzes, P., 2005. Evolution of the lithosphere in the area of the Rhine Rift System. *Int J Earth Sci (Geol Rundsch)* 94, 594–614.
- Ziegler, P.A., Dèzes, P., 2006. Crustal evolution of Western and Central Europe, in: Gee, D.G., Stephenson, R.A. (Eds.), *European Lithosphere Dynamics*. Geol. Soc., London, Mem. 32, 43–56.
- Ziegler, P.A., Dèzes, P., 2007. Cenozoic uplift of Variscan Massifs in the Alpine foreland: Timing and controlling mechanisms. *Global and Planetary Change* 58(1-4), 237–269.
- Zijerveld, L., Stephenson, R., Cloetingh, S., Duin, E., van den Berg, M.W., 1992. Subsidence analysis and modelling of the Roer Valley Graben (SE Netherlands), in: Ziegler, P.A. (Ed.), *Geodynamics of Rifting*. Volume 1. Case History Studies on Rift: Europe and Asia. *Tectonophysics* 208. Elsevier, 159–171.
- Zimmermann, H., 2000. Tertiary seawater chemistry - implications from primary fluid inclusions in marine Halite. *American Journal of Science* 300, 723–767.
- <http://www.rwe.com/web/cms/de/59998/rwe-power-ag/energietraeger/braunkohle/standorte/tagebau-garzweiler/>
- <http://www.rwe.com/web/cms/de/60012/rwe-power-ag/energietraeger/braunkohle/standorte/tagebau-hambach/>
- <http://www.rwe.com/web/cms/de/60026/rwe-power-ag/energietraeger/braunkohle/standorte/tagebau-inden/>

Appendix

The following manuscript, which was already published in the Netherlands Journal of Geoscience, is not actually part of the PhD project, since it is based on a database from my preceding diploma thesis. However, as the publication developed during this PhD study, and comprises a completely reviewed interpretation, as well as a new discussion, it is attached to this thesis. Additionally, the facies analysis of the Neurath Sand (forming on of the parent sand units, see chapter 7), directly overlying the Frimmersdorf Seam, revealed some important information on the Serravallian-age, shallow-marine depositional environment, especially in terms of sea-level fluctuations and energy levels of waves and tidal currents.

A Facies analysis and depositional model of the Serravallian-age Neurath Sand, Lower Rhine Basin (W Germany)

Linda Prinz; Andreas Schäfer; Tom McCann; Torsten Utescher; Peter Lokay; Sven Asmus

Originally published in Netherlands Journal of Geosciences, 96(3), 211-231 (September 2017)

A.1 Abstract

The up to 60 m thick Neurath Sand (Serravallian, late middle Miocene) is one of several marine sands in the Lower Rhine Basin which were deposited as a result of North Sea transgressive activity in Cenozoic times. The shallow-marine Neurath Sand is well exposed in the Garzweiler open-cast mine, which is located in the centre of the Lower Rhine Basin. Detailed examination of three sediment profiles extending from the underlying Frimmersdorf Seam via the Neurath Sand and through to the overlying Garzweiler Seam, integrating both sedimentological and palaeontological data, has enabled the depositional setting of the area to be reconstructed.

Six subenvironments are recognised in the Neurath Sand, commencing with the upper shoreface (1) sediments characterised by glauconite-rich sands and an extensive biota (*Ophiomorpha* ichnosp.). These are associated with the silt-rich sands of a transitional

subenvironment (2), containing *Skolithos linearis*, *Planolites* ichnosp. and *Teichichnus* ichnosp. These silt-rich sands grade up to the upper shoreface subenvironment (1), which would be indicative of an initial regressive trend. The overlying intertidal deposits can be subdivided into a lower breaker zone (3), characterized by ridge and runnel systems, and the swash zone (4) where the surge and backwash of waves resulted in the deposition of high-energy laminites. The intertidal deposits were capped by aeolian backshore sediments (5). Extensive root traces present in this latter subenvironment reflect the development of the overlying peatland (i.e. Garzweiler Seam). Within the Garzweiler Seam, restricted sand lenses indicate a lagoonal or estuarine depositional environment (6). Regional correlation with adjacent wells establishes that shallow-marine conditions were widespread across the Lower Rhine Basin in middle Serravallian times. The shoreline profile, characterized by both tidal and wave activity, and influenced by fluvial input from the adjacent Rhenish Massif is indicative of the complexity of the coastal depositional setting within the Lower Rhine Basin.

A.2 Introduction

The Lower Rhine Basin extends from NW Germany through to SE Netherlands, and is an embayment (= Lower Rhine Embayment) which formed as a result of basin subsidence and related marine transgressions in Oligocene times (Teichmüller, R., 1958; Zagwijn & Hager, 1987; Hager, 1993; Schäfer et al., 1996; Klett et al., 2002; Becker & Asmus, 2005; Schäfer et al., 2005; Schäfer & Utescher, 2014), and within which sub- to supratidal (Longhitano et al., 2012) sediments were deposited (Schäfer et al., 1996). The basin is a rift, extending into the Rhenish Massif, and forming the NW part of the NW European Cenozoic Basin (Ziegler, 1992, 1994; Houtgast & van Balen, 2000; Klett et al., 2002; Sissingh, 2003; Ziegler & Dèzes, 2007; Fig 1). During the late early and middle Miocene, warm temperate climate conditions in a highstand systems tract (but at a point where eustatic sea level had already begun to fall and the highstand system sediment surface was exposed, but immediately prior to the erosion surface marking the falling-stage systems tract; Utescher et al., 2012, see also fig. 13 in Schäfer & Utescher, 2014) led to the formation of extensive coastal swamps and thick (up to 300 m) peat accumulations, that formed the present-day, up to 100 m thick Main Seam of the Ville Fm (Fig. 2). Peat formation was interrupted by the deposition of clastic sediments (Frimmersdorf and Neurath sands) as a result of repeated marine transgressions, which subdivided the Main Seam into three smaller seams (i.e. Morken, Frimmersdorf and Garzweiler lignite seams; Fig. 2). Active exploitation of these deposits within the Lower

Appendix

Rhine Basin provides an excellent opportunity to examine the sedimentary succession (e.g. Petzelberger 1994; Schäfer et al. 1996; Klett et al. 2002; Schäfer & Utescher 2014). The present study focusses on the Neurath Sand, a clastic unit which separates the Frimmersdorf and Garzweiler seams. The aim of the study is the three-dimensional reconstruction of the depositional setting of the Neurath Sand, integrating both detailed sedimentary profiles as well as mining industry well logs.

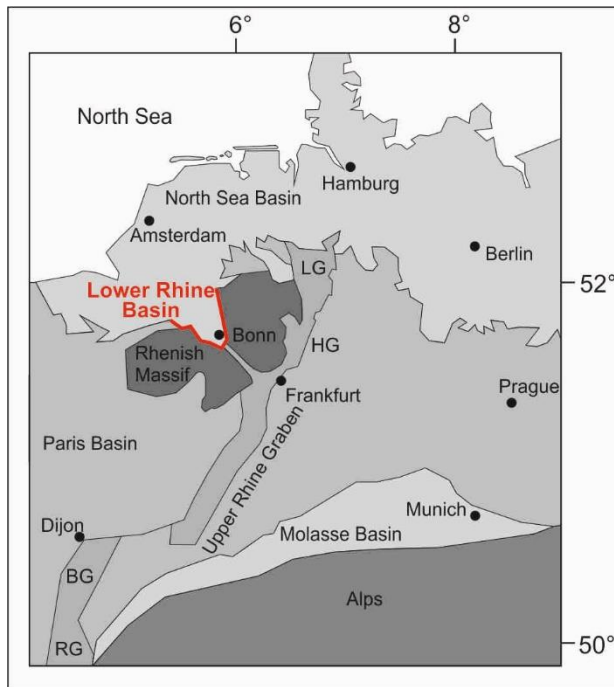


Fig. A-1: A structural map of the NW European Cenozoic Rift System. The Lower Rhine Basin is located at the northern end of the Upper Rhine Graben, NW of the Rhenish Triple Junction in the area of Frankfurt (Schumacher, 2002; Sissingh, 2003; Rasser et al. 2008). BG = Bresse Graben, HG = Hessen Graben, LG = Leine Graben, RG = Rhône Graben.

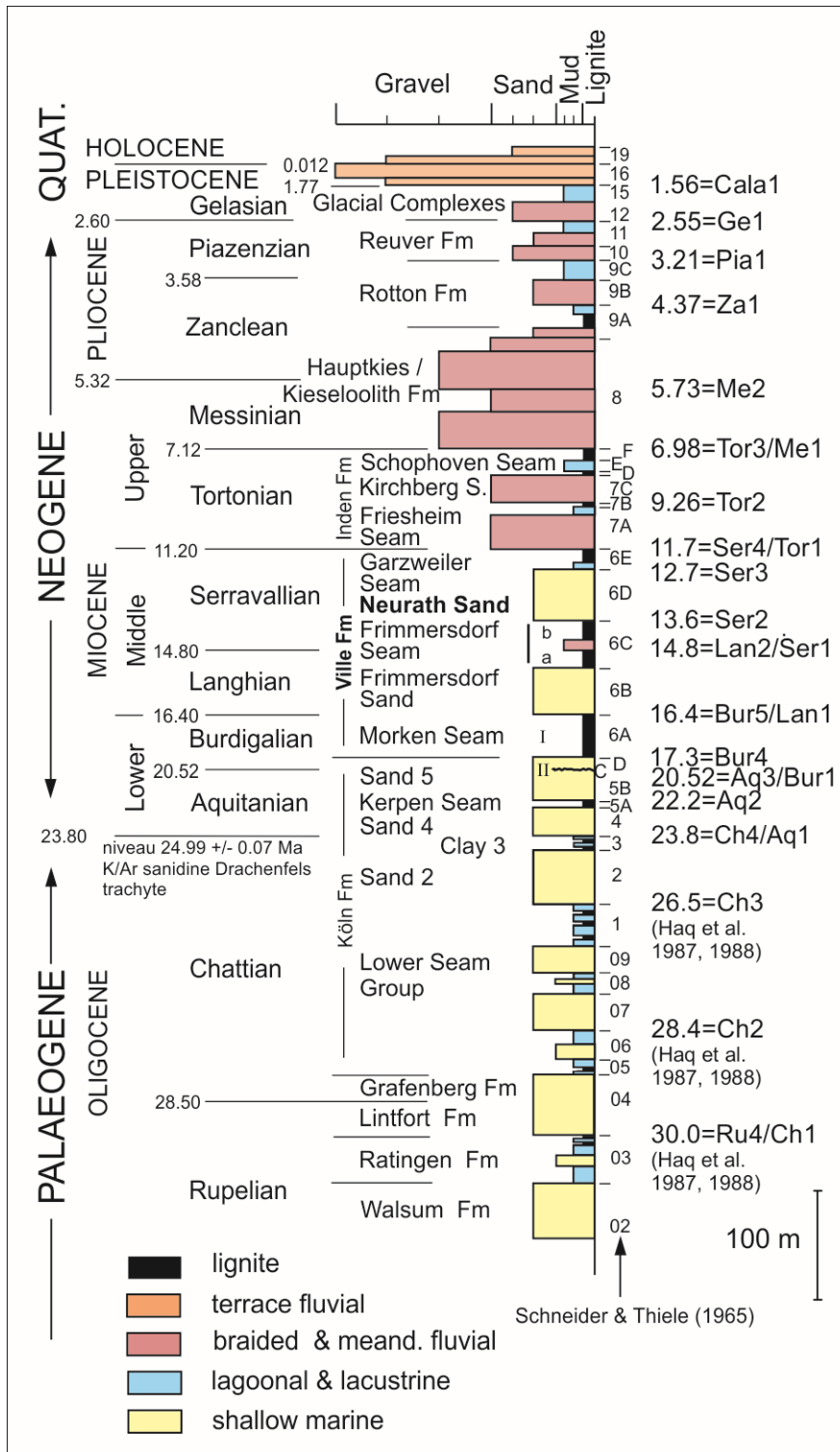


Fig. A-2: Stratigraphic log of the Lower Rhine Basin (modified after Klett et al., 2002; Schäfer et al., 2004, 2005; Schäfer & Utescher 2014). The lithostratigraphic log based on two well logs (SNQ 1, Erft Block, and Efferen, Köln Block; RWE Power AG) represents the stratigraphy at the centre of the Erft Block; lithostratigraphical code established by Schneider & Thiele (1965). Biostratigraphical ages (Ma) on the left after Berggren et al. (1995); cycle ages (Ma) on the right after Haq et al. (1987, 1988) and Hardenbol et al. (1998).

A.3 Geological Framework

The extensional Lower Rhine Basin formed in early Oligocene times (Ziegler 1994; Klett et al. 2002; van Balen et al. 2005) as the NW extension of the European Cenozoic Rift System (Ziegler 1992, 1994; Sissingh 2003, 2006; Ziegler & Dèzes 2007; Fig. 1), with subsidence ongoing throughout the Neogene (Schäfer et al. 2005). Extension was initiated along the NW margin of the Rhenish Massif, where several NW-SE-striking faults formed, which are still active today (Ziegler 1992; Hinzen 2003; Sissingh 2003, 2006; Reicherter et al. 2008; Schäfer & Utescher 2014; Grützner et al. 2016). These faults separate the basin into graben and horst structures (Fig. 3). Three tectonic units characterise the SE part of the Lower Rhine Basin. From E to W these are the Köln, Erft and Rur blocks, separated by the Erft and Rur faults, respectively. Towards the NW, three additional blocks occur, namely the Peel, Venlo (location of the Garzweiler open-cast mine) and Krefeld blocks. The Viersen Fault forms the contact between the latter two, while the Tegelen Fault separates the Venlo Block from the Peel Block (Fig. 3). The faults separating the individual blocks generally dip steeply (70-80°) to the SW (Schäfer et al. 2005). Subsidence across the region is variable, with up to 2000 m recorded for the Peel Block in the Roer Valley Graben, while the Erft Block subsidence has been measured at 1300 m (Klett et al. 2002).

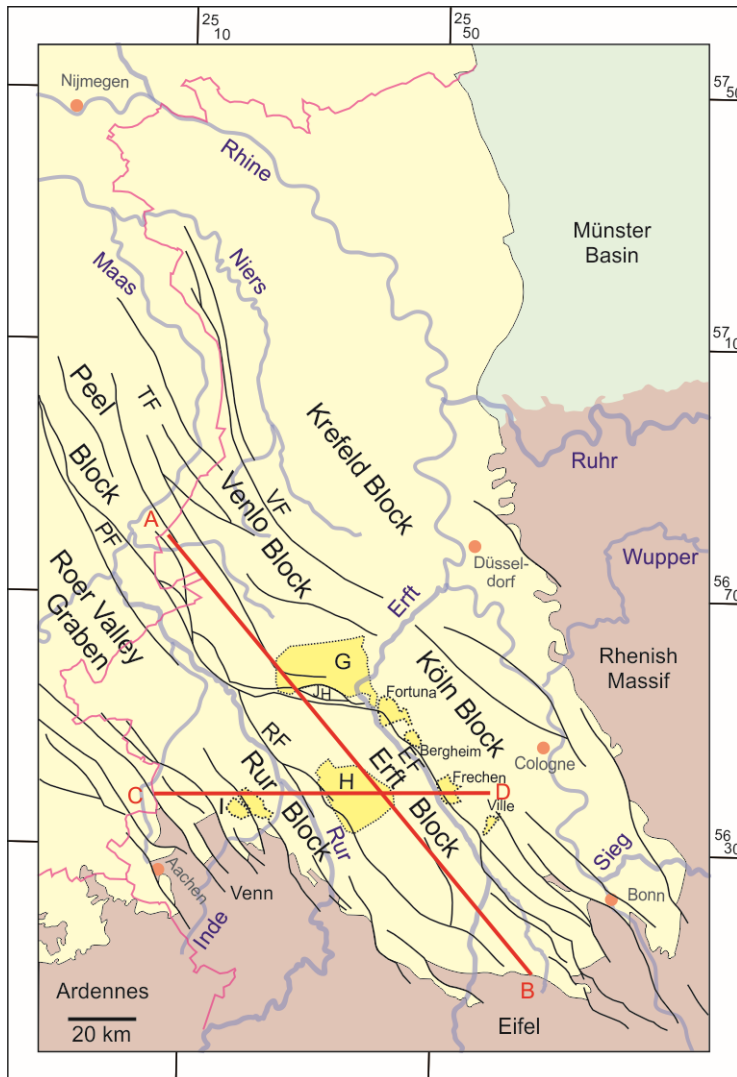


Fig. A-3: A structural map of the Lower Rhine Basin. The six main tectonic blocks (Rur, Ertf and Köln blocks in the SE; Peel, Venlo and Krefeld blocks in the NW) are bounded by the Rur (RF), Erft (EF), Peel Boundary (PF), Tegelen (TF) and Viersen faults (VF), as well as the fault system bounding the Jackerath Horst (JH). The Rur Block extends into the Roer Valley Graben in the NW. G = Garzweiler open-cast mine; H = Hambach open-cast mine; I = Inden open-cast mine; pink line: Germany-Netherlands-Belgium border. The two red lines mark the position of two cross sections (A-B and C-D), which are shown in Figure 4. Modified after Geluk et al. (1994), Schäfer et al. (1996), Klett et al. (2002) and Schäfer & Utescher (2014).

The Peel Block, as well as the Rur Block in the German part of the basin, are structurally part of the Roer Valley Graben (Fig. 3; Houtgast & van Balen 2000; Michon et al. 2003), an extended rift system in the Netherlands (Geluk et al. 1994; Grützner et al. 2016). Formerly, the terms Roer Valley Graben and Lower Rhine Basin have been used to refer to the same tectonic feature, and denoting either the German part (i.e. the Lower Rhine Basin), or its NW extension in the Netherlands (i.e. Roer or Rur Valley Graben; Ziegler 1992; Sissingh 2003). Alternatively, the Roer Valley Graben has been interpreted as the

central graben structure of the Lower Rhine Basin (e.g. Vanneste et al. 1999). However, in this study, the terms are used *sensu* Geluk et al. (1994), Houtgast & van Balen (2000), and Michon et al. (2003), and thus refer to two adjacent, and structurally interlinked tectonic grabens.

As noted above, subsidence within the Lower Rhine Basin allowed the Cenozoic-age North Sea to transgress across the region. In the resulting shallow-marine embayment (Schäfer et al. 1996), a clastic succession of sub- to supratidal sediments was deposited during Oligocene times (Fig 2). Sea-level highstand in the late early and middle Miocene coupled with warm temperate climatic conditions (Zagwijn & Hager 1987; Mosbrugger et al. 2005; Utescher et al. 2009) facilitated the development of extensive coastal swamps with associated peat bogs, marshes and bush forests (Mosbrugger et al. 1994). Ongoing basin subsidence combined with compaction of the peats resulted in the formation of thick (up to 100 m) lignite accumulations (i.e. Main Seam) in the SE Lower Rhine Basin (Hager 1986; Schäfer et al. 2005). To the NW, the Main Seam is separated into three subordinate seams, namely the Morken, Frimmersdorf and Garzweiler seams (=Ville Formation of Early to Mid-Miocene age). These are separated from one another by the marine sediments of the Frimmersdorf and Neurath sands, respectively. These sands were deposited as a result of short-lived marine transgressions during the Miocene which resulted in the deposition of thick (up to 100 m) marine beds along the NW rim of the Miocene-age coastal mires. Following regression of the North Sea in late Miocene to Pliocene times, meandering, and subsequently, braided river systems developed on top of the marine and paralic sediments (Klett et al. 2002; Schäfer & Utescher 2014).

A.3.1 Regional distribution of the Neurath Sand in the Lower Rhine Basin

The Neurath Sand is one of two shallow-marine sand bodies within the NW part of the Lower Rhine Basin (the other is the Frimmersdorf Sand), which separate the Main Seam into three subordinate seams (Fig. 4). Based on a sequence stratigraphical model, deposition of the Neurath Sand was continuous from 13.8 to 12.7 Ma, i.e. over a time span of 1.1 Ma (see Fig. 2; ages after Haq et al. 1987, 1988; Berggren et al. 1995 & Hardenbol et al. 1998).

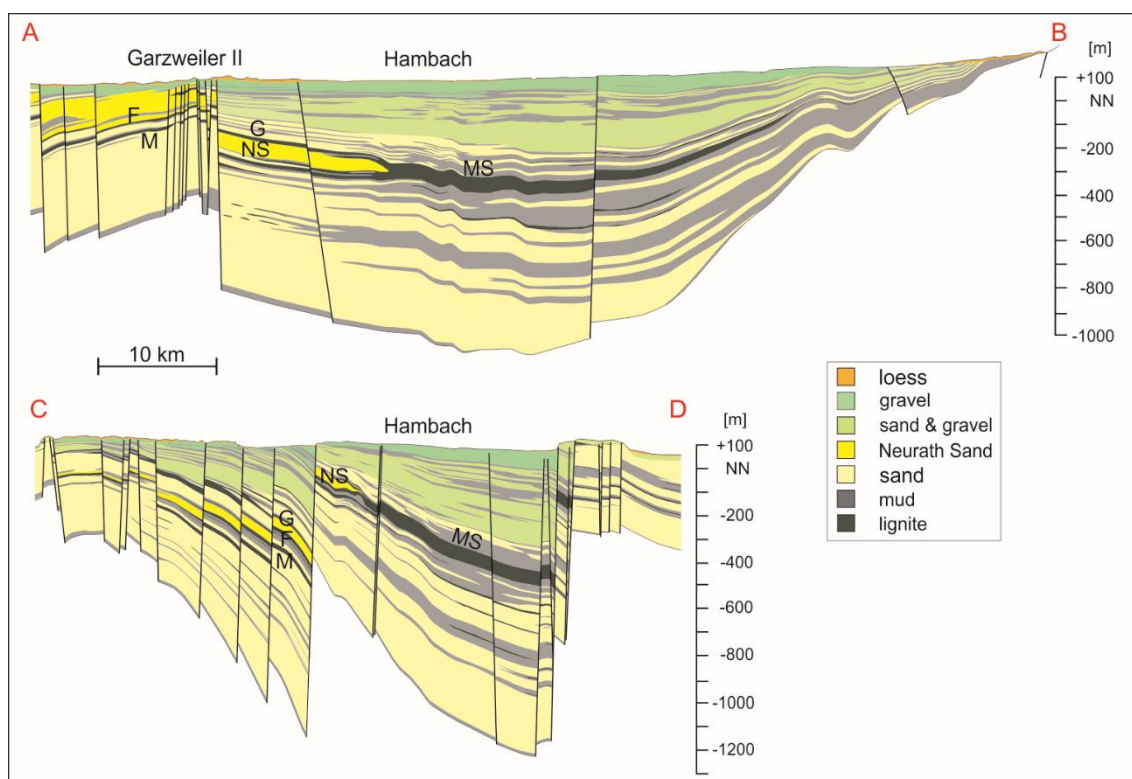


Fig. A-4: Cross sections A-B (NW-SE) and C-D (W-E; positions in the Lower Rhine Basin marked in Fig. 3), vertical exaggeration of 30. The Main Seam (MS) of the Middle Miocene-age Ville Formation is separated by transgressive sand units into three subordinate units: the Morken (M), Frimmersdorf (F) and Garzweiler seams (G). The Neurath Sand (NS) terminates to the SE and W, and increases in thickness to the NW. Modified after Becker & Asmus (2005).

Two cross sections (NW-SE- and W-E-oriented; Fig. 4) across the Lower Rhine Basin, and integrated with comprehensive well log data (Schäfer & Utescher 2014 for more details), allow the Neurath Sand to be traced laterally across the basin, while also allowing its thickness variability to be determined. It would appear that the morphology of the Neurath Sand is that of an oval lens oriented NW-SE. The maximum thickness of the Neurath Sand is up to 100 m on the Venlo and Erft blocks (Fig. 4). Landward (i.e. towards the SE, and the margin of the Rhenish Massif in the W, see Fig. 4), the Neurath Sand thins out. This thinning is accompanied by a change in lithology (from sand to muddy sand, and eventually mud; see Boersma 1991). The maximum SE extent of the sand-rich deposits is exposed in the Hambach open-cast mine (Fig. 5). Towards the region occupied by the coeval open sea (i.e. to the NW), the thickness of the Neurath Sand increases to c. 200 m, and it interdigitates with the shallow-marine Breda Formation (Burdigalian to Mid-Tortonian age), an up to 700 m thick unit covering most of the Netherlands (Wong et al. 2001; Verbeek et al. 2002; Munsterman & Brinkhuis 2004).



Fig. A-5: The maximum extent of the Neurath Sand as exposed in the Hambach open-cast mine (1998).

A.4 Methods

In the Garzweiler open-cast mine (located at the NW end of the mining region extending along the W margin of the Köln Block, i.e. the Ville Ridge, and including the older Ville, Frechen, Bergheim and Fortuna mines; Fig. 3), mining activity provided access to a vertical section prepared for this study by RWE Power AG. Three freshly-cut field sections along the western exploitation ramp were measured. Profile 1, with a total length of 67 m, covered the entire Neurath Sand, from the underlying Frimmersdorf Seam through to the overlying Garzweiler Seam. Parallel profiles were measured along the active exploitation ramp, each of which were located 200 m laterally and to the N from each other. Neither Profile 2 (35 m) nor Profile 3 (24 m) extended to the base of the Neurath Sand due to the working level of the lignite in this part of the open-cast mine. The three profiles allowed a three-dimensional facies analysis of the Neurath Sand to be carried out, as well as detailed examination of the sediments (e.g. grain size, sorting, sedimentary structures), and the integration of ichnological data. Lignite-derived humic acids have led to the dissolution of calcareous tests and shells within the sands, and thus, the only fossils present within the Neurath Sand are ichnofossils as well as wood/lignite fragments. Laboratory investigations (e.g. grain size analysis) were used to support the field observations as well as to provide additional information (e.g. petrological analysis). This latter analysis focussed on the examination of dark coloured sand clasts, which had been observed in all three measured profiles. These were sampled (Profile 2, 6.0 – 6.5 m, see below) and hardened with epoxy resin, with subsequent thin sections (n=10) being used to determine lithic fragment frequency and composition.

A.5 Sedimentary Facies and Facies Analysis

Six sediment facies have been recognised in the Neurath Sand and the overlying Garzweiler Seam, ranging from muddy and coarse- to fine-grained sands through to lignite (Table A-1). These will be described in detail below.

Table A-1: Sedimentary facies of the Neurath Sand and the overlying Garzweiler Seam, Garzweiler open-cast mine

Abbreviation		Sedimentary facies
Smu (muddy sands)		muddy sands with chert pebble lag
Sf (fine-grained sands)	Sf-u	non-stratified
	Sf-p	planar-laminated
	Sf-c	cross-/ trough cross-laminated
Sfm (fine- to medium-grained sands)	Sfm-u	non-stratified
	Sfm-p	planar-laminated
	Sfm-c	cross-/ trough cross-laminated
Sm (medium-grained sands)	Sm-p	planar-laminated
	Sm-c	cross-/ trough cross-laminated
Sc (coarse- to medium-grained sands)	Sc-c	cross-/ trough cross-laminated
L		Lignite

A.5.1 Muddy sands with chert-pebble lag (Smu)

Description – Dark grey-coloured, fine- to medium-grained sands with up to 15% mud which contain clasts of mud, wood and lignite (up to 2 cm), concentrated near the bed base. The base of the facies is characterized by a chert-pebble layer (ranging in thickness from a single pebble to 0.75 m; Fig. 6a) which lacks grading or structure. The matrix of the chert-pebble layer is white to light grey in colour, changing upsection into the more characteristic darker-coloured sands. Bed thicknesses range from 0.5 to 2 m. The beds are internally non-stratified and are not graded. The ichnofossils include simple vertical and unbranched burrows of *Skolithos linearis* (up to 20 cm long; Seilacher 1964; Alert 1974; Hiscott et al. 1984; Howard & Frey 1984; MacEachern et al. 2012) and subvertical unbranched burrows with spreiten (*Teichichnus* ichnosp.; Fig. 6b; Crimes 1977), as well as unbranched, (sub-) horizontal *Planolites* ichnosp (Curran & Frey 1977). The ichnofossils are distributed throughout the beds.

Interpretation – The relatively fine grain size and the presence of up to 15% of mud would suggest deposition within a relatively low- to moderate-energy environment. The chert

pebble bed at the base of this facies (Fig. 6a), however, indicates an initial high-energy transport regime, and represents a lag deposit. The lack of any internal structure within the muddy sands may result from a) rapid and turbulent flows, b) bioturbation, or, c) remobilization of sediments due to liquefaction. While the facies is bioturbated, the bioturbation is discrete and the facies does not have the mottled appearance associated with high degrees of bioturbation (e.g. Taylor & Goldring 1993; Bromley 1996; Tonkin et al. 2010). Additionally, there is no evidence of liquefaction (e.g. dish or pillar structures). Another possibility is that the lamination is present but not visible as a result of the preparation of the section by the bucket wheels of the front-wheel loaders cutting the access ramps.

Skolithos linearis is generally found in lower intertidal to shallow subtidal settings (above fairweather wave-base) with moderate to high energy conditions (MacEachern et al. 2012). However, *Skolithos* ichnosp. has also been observed in deeper environments, e.g. the transition zone on the shelf (Desjardins et al. 2010) or deep-sea sand fans (Crimes 1977; Uchman & Demircan 1999). The occurrence of *Teichichnus* ichnosp. (Fig. 6b) is restricted to muddy substrates in low-energy environments, which are permanently water-covered (i.e. below low tide line; Seilacher 1964; Pemberton & Frey 1984; Frey 1990; MacEachern et al. 2012). *Planolites* ichnosp. is a facies-crossing ichnospecies and so does not provide any information as to specific water depths or energy milieus.

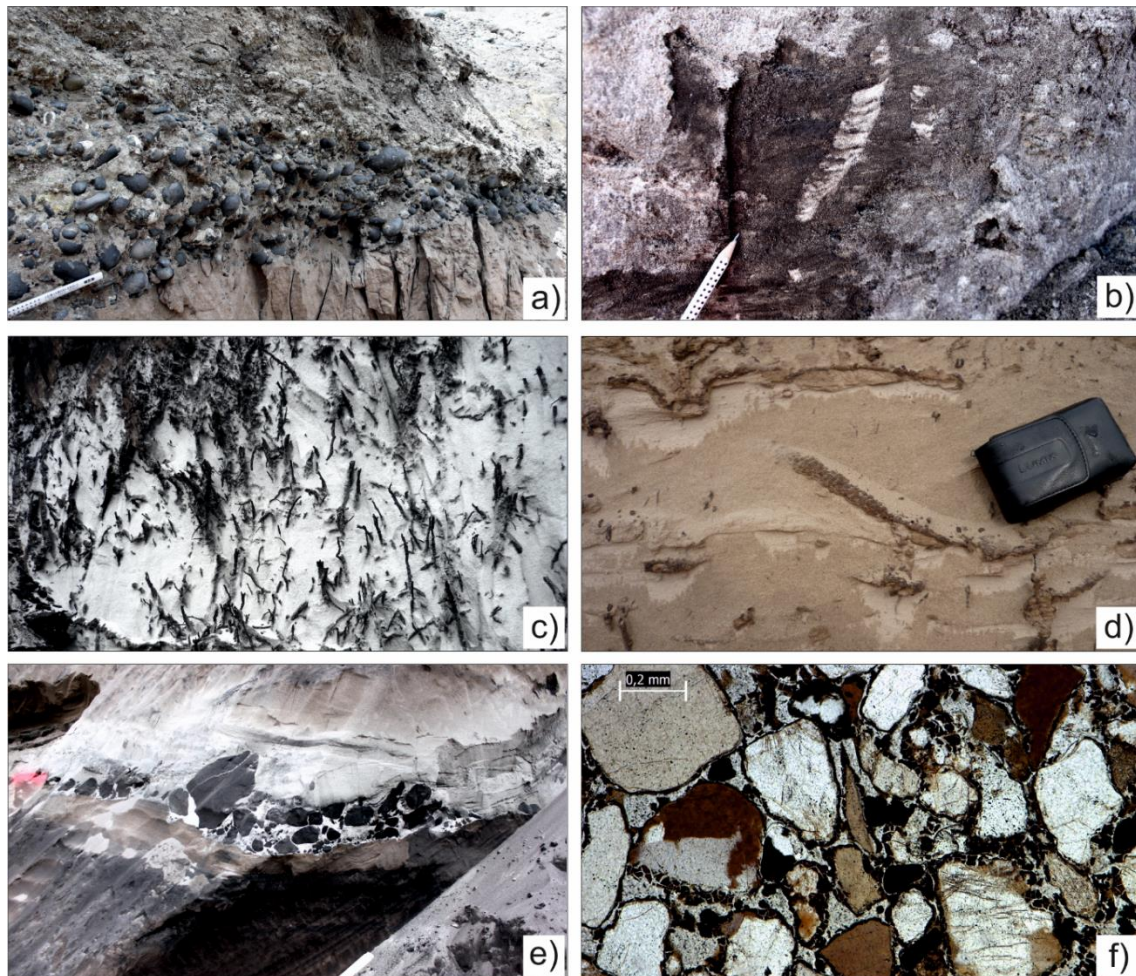


Fig. A-6: Facies characteristics of the Neurath Sand. (a) Chert-pebble bed at the base of the muddy sand (Smu) lithofacies; (b) *Teichichnus* ichnosp. in the muddy sand (Smu) lithofacies; (c) root horizons extending down into the Neurath Sand from the overlying Garzweiler Seam; (d) *Ophiomorpha* ichnosp. within fine-grained sands of the unstratified fine sand (Sf-u) lithofacies; € black sand-clast bed in profile 3 at c. 11 m; (f) microphotograph (crossed polars) of a black sand clast from profile 2 (c. 6 m in profile), showing mainly quartz grains, and dark, opaque humic substances occupying the interstitial pore volume.

A.5.2 Fine-grained sands (Sf)

Description – Fine-grained sands (< 10 % of mud, < 3 % of medium- and coarse-grained sand) which are non-stratified (Sf-u), planar (Sf-p), cross- or trough cross-laminated (Sf-c). Within the latter two, fine-grained sands comprising very thin (1-2 mm) sand-mud laminae were observed. Non-stratified sands may contain glauconite. Along the bases of some of the individual cross laminae thin lags (generally 1-2 grains thick, and medium- to coarse-grained sand) may occur. Bed thicknesses range from 0.2 to 4.0 m for Sf-p down to 0.2 to 3.5 m for Sf-c and 0.5 to 1.0 m for Sf-u. Root horizons, where present, are

restricted to the top of individual beds (Fig. 6c). Non-stratified and planar-laminated fine-grained sands are sporadically black coloured and frequently comprise wood fragments.

Frequently observed *Ophiomorpha* ichnosp. (restricted to Profile 1; Fig. 6d) are predominant within the non-stratified sands (Sf-u), but were also noted from one of the trough cross-laminated sand beds (Sf-c). The fine-grained sand beds can contain clasts of mud (up to 20 cm), lignite or wood (up to 30 cm, but generally smaller) that are either concentrated near the bed bases or distributed throughout the bed.

Within this facies (but also within other facies, see below) are beds, 20-50 cm thick, of black-coloured fine-grained sand and which are overlain by thin beds (20-30 cm) comprising fine-grained, black-coloured sand clasts. The sand clast beds (Fig. 6e) are covered by trough cross-laminated beds (up to 20 cm thick, containing wood fragments), topped by symmetrical ripples (2-7 cm high). The black sand clasts comprise mainly monocrystalline quartz (Qm, 47.51%; Fig. 6f; Table 2), showing undulose extinction and dust rims (indicative of phases of diagenetic crystal growth). Polycrystalline quartz (Qp, 16.69%) is also present. Both Qm and Qp may include mafic inclusions (often altered to kaolinite, 3.97%, or replaced by humic gel particles) either within the crystals or along their margins. K-feldspar (5.74%) is also present, usually as microcline or perthite, while rare plagioclase (1.96%) also occurs. Muscovites (on average 0.18%), where present, have an extinction colour suggesting they were originally biotite. Lithic fragments include quartz phyllites, phyllites, quartzites (8.91%), as well as rare mafic (0.83%, including volcanics, mostly weathered to kaolinite) and carbonate (0.1%) clasts. Possible glauconite was also noted (1.37%). The sand clasts can be classified as quartz-rich feldspathic litharenites (after Folk 1974; Fig. 7; Table 2), with little variation between the various profiles or within an individual profile. The interstitial pore volume of the sand grains is filled with dark-coloured, opaque humic substances (Fig. 6f).

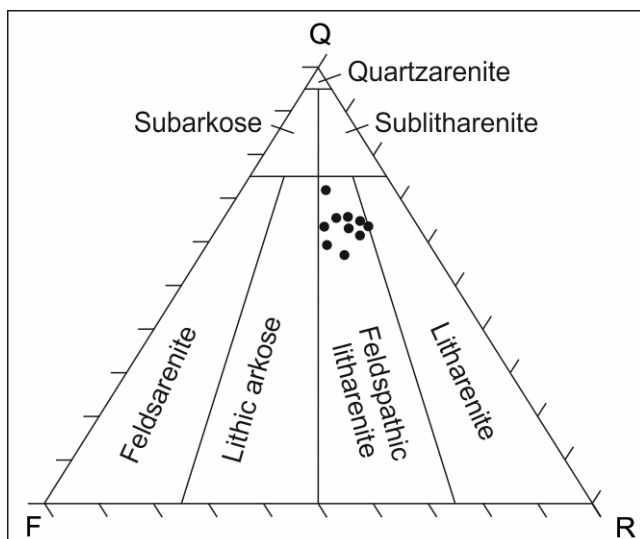


Fig. A-7: Modal analysis of thin sections ($n = 10$) of one black sand clast (profile 2) (after Folk, 1974; Graham & Midgley, 2000). These data are from the same clast bed as illustrated in Figure 6e. F = feldspar, Q = quartz, R = rock fragments.

Appendix

Table A-2: Modal analysis of the thin sections (n = 10) of one black sand clast (profile2).

thin sections		1	%	2	%	3	%	4	%	5	%
Q	qtz-mono	274	50,93	159	49,53	107	48,86	188	47,96	205	42,62
Q	qtz-poly	78	14,50	45	14,02	41	18,72	62	15,82	80	16,63
R	qtzite	43	7,99	22	6,85	33	15,07	32	8,16	47	9,77
R	chert	2	0,37	3	0,93	1	0,46	2	0,51	8	1,66
R	sedim.	46	8,55	7	2,18	8	3,65	45	11,48	16	3,33
F	fsp	8	1,49	11	3,43	6	2,74	3	0,77	22	4,57
F	K fsp	28	5,20	6	1,87	0	0,00	6	1,53	26	5,41
F	plag	4	0,74	4	1,25	4	1,83	5	1,28	14	2,91
F	qtz/fsp	36	6,69	34	10,59	1	0,46	22	5,61	29	6,03
R	musc.	0	0,00	0	0,00	1	0,46	1	0,26	1	0,21
R	biotite	1	0,19	2	0,62	0	0,00	0	0,00	3	0,62
R	heavy m.	0	0,00	0	0,00	0	0,00	0	0,00	0	0,00
R	glauconite	1	0,19	8	2,49	8	3,65	0	0,00	6	1,25
R	kaolinite	6	1,12	19	5,92	7	3,20	16	4,08	19	3,95
R	phyllite	10	1,86	0	0,00	1	0,46	2	0,51	4	0,83
R	mafite	1	0,19	0	0,00	1	0,46	0	0,00	1	0,21
R	volcanite	0	0,00	1	0,31	0	0,00	6	1,53	0	0,00
R	carbonate	0	0,00	0	0,00	0	0,00	2	0,51	0	0,00
sum		538	100,00	321	100,00	219	100,00	392	100,00	481	100,00
thin sections		6	%	7	%	8	%	9	%	10	%
Q	qtz-mono	224	49,67	185	52,11	115	45,45	185	48,68	140	39,33
Q	qtz-poly	61	13,53	45	12,68	51	20,16	88	23,16	63	17,70
R	qtzite	36	7,98	43	12,11	14	5,53	8	2,11	30	8,43
R	chert	9	2,00	1	0,28	4	1,58	0	0,00	4	1,12
R	sedim.	32	7,10	19	5,35	17	6,72	20	5,26	30	8,43
F	fsp	5	1,11	1	0,28	2	0,79	0	0,00	10	2,81
F	K fsp	17	3,77	15	4,23	5	1,98	17	4,47	17	4,78
F	plag	8	1,77	4	1,13	11	4,35	9	2,37	7	1,97
F	qtz/fsp	28	6,21	15	4,23	12	4,74	21	5,53	26	7,30
R	musc.	0	0,00	2	0,56	0	0,00	0	0,00	1	0,28
R	biotite	4	0,89	0	0,00	1	0,40	4	1,05	3	0,84
R	heavy m.	0	0,00	0	0,00	0	0,00	2	0,53	0	0,00
R	glauconite	2	0,44	11	3,10	1	0,40	2	0,53	6	1,69
R	kaolinite	18	3,99	10	2,82	15	5,93	15	3,95	17	4,78
R	phyllite	4	0,89	1	0,28	0	0,00	0	0,00	1	0,28
R	mafite	2	0,44	3	0,85	5	1,98	8	2,11	1	0,28
R	volcanite	0	0,00	0	0,00	0	0,00	0	0,00	0	0,00
R	carbonate	1	0,22	0	0,00	0	0,00	1	0,26	0	0,00
sum		451	100,00	355	100,00	253	100,00	380	100,00	356	100,00
Q	(mono- and poly-crystalline quartz)										
F	(K-feldspar, plagioclase, and feldspar/quartz aggregates)										
R	(total lithic rock fragments incl. heavy minerals, micas, and chert)										

Interpretation – The Sf facies contains three subfacies, as well as sand-mud laminae and black sands. The fine-grained nature of the facies would suggest deposition under low-energy conditions, although the sedimentary structures (e.g. Sf-p, Sf-c) would suggest periods of higher energy. The ichnofossil-rich beds tend to coincide with the occurrence of the structureless fine-grained sands (Sf-u), suggesting that the lack of structure is related to intense bioturbation (up to BI 4-6; see Tucker 2003) rather than an absence of sedimentary structures per se.

The cross-laminated sands (Sf-c) were deposited from migrating ripples or dunes indicative of higher wave energy, as well as tidal, wave or wind-induced currents (Dabrio 1982; Masselink & Anthony 2001; Reynaud & Dalrymple 2012; Hunt et al. 2015). The parallel-laminated sands (Sf-p) were also deposited under low-energy conditions, most probably aeolian (Otvos 2000; Collinson et al. 2006). However, the planar-laminated fine-grained sands can also include interbedded sand-mud laminae, which have been interpreted as tidal rhythmites (Tessier et al. 1995; Reesink & Bridge 2007; Bungenstock & Schäfer 2009). Such laminae record the passage of tidal currents alternating with periods of tidal slack water (Visser 1980; Reesink & Bridge 2007). The occurrence of two coupled mud laminae alternating with thin sand laminae could be interpreted as ebb and flood cycles, with such coupled mud laminae generally restricted to environments below low-tide level (Hovikoski et al. 2005).

The black-coloured clasts were indurated as a result of their infiltration by black humic gels most probably derived from exposed and reworked lignites as well as from nearby coastal mires. Alteration, and related induration, was initiated by the passage of low pH humic acids, which allowed the sands to be eroded from the underlying black-coloured sand, and redeposited as lags. The humic gels are preserved as dark brown films surrounding the sand grains, while organic substances are preserved as black angular fragments in the pore spaces (Fig. 6f).

Wood fragments indicate the input of organic material from nearby coastal mires, whereas black-coloured sands at the top of the Neurath Sand have been infiltrated by humic gels from the overlying Garzweiler lignite seam. Root horizons within the fine-grained sands, would appear to migrate downwards from the overlying lignite seams. Such concentrations of root horizons would suggest the former presence of a well-vegetated horizon, and one located in a continental/near-coastal setting (Darscheid 1981). This horizon would thus represent the period of initial colonisation by plants following the phase of marine regression. The black-coloured sand beds, frequently

covering the rooted horizons, suggest an infiltration of humic gels from the overlying lignite deposits.

Ophiomorpha ichnosp. (Fig. 6b) occurs in a range of energy settings, ranging from sand-rich, moderate to high-energy, as well as muddy, low-energy marine environments. It is generally found in marine environments ranging from lower intertidal through to shoreface, and above storm wave base (Seilacher 1964; Hiscott et al. 1984; Howard & Frey 1984; MacEachern et al. 2012).

A.5.3 Fine- to medium-grained sands (Sfm)

Description – The fine- to medium-grained sands (Sfm) comprise three subfacies, including non-stratified (Sfm-u, 0.6-1.0 m thick), planar (Sfm-p; 0.3-1.0 m) and cross laminated/bedded (Sfm-c; 0.3-2.0 m) sand beds. Lamination within the latter beds, in particular, results from the alternation of fine- with medium-grained sand laminae. Within individual beds, planar-bedded, fine- to medium-grained, sand alternations have been observed. These beds may show a fining upward. Within the trough cross-laminated sand beds (Sfm-c), mud-sand laminae may occur. Clasts of mud, wood and lignite, as well as roots are very common within both the non-stratified, as well as the planar laminated sands.

Interpretation – Fine- to medium-grained sands indicate deposition within a moderate energy setting, with the fine- and medium-grained sand alternations suggesting regularly changing energy levels. Within the planar bedded sands, the fining up would suggest waning energy levels. Clasts of lignite and wood within the non-stratified and planar laminated sand possibly indicate seaward transport of organic matter from the adjacent peat/swamp environment, as well as the reworking of laterally-exposed lignite deposits (e.g. peat/lignite accumulations of the present-day Frimmersdorf Seam). Rhizoturbated sediments, as described above, indicate the presence of a vegetation cover overlying the sand deposits.

Cross and trough cross lamination would suggest that these beds were deposited in a depositional setting controlled by wave or tidal currents. Such a setting would be supported by the presence of tidal bundles (sand-mud laminae) within the facies.

A.5.4 Medium-grained sands (Sm)

Description – This lithofacies comprises (trough or planar) cross laminated/bedded sand beds (Sm-c, ranging in thickness from 1.0 to 1.5 m), as well as planar-laminated sand beds (Sm-p; thicknesses range from 0.5 to 2.5 m). Planar-laminated, medium-grained sand beds (rarely black-coloured) may show evidence of upward fining within individual beds. In addition, lamina thickness also decreases within individual beds. The cross-laminated/cross-bedded sand beds may contain mud clasts (up to 2 cm), as well as rare coarse-grained laminae.

Medium-grained, cross-laminated/bedded sand units also contain beds with concentrations of black-coloured sand clasts. These sand clasts are surrounded by a matrix of grey-coloured medium-grained sand, which also contain concentrations of coarse-grained sand (concentrated at the base of the clast bed), small chert pebbles (up to 0.5 cm in diameter and concentrated within the interstices between the black sand clasts) and wood fragments (up to 1 cm, also concentrated within the interstices). These sand clast beds have a lateral extent of up to 4 m.

Interpretation – The medium-grained sands (Sm) were deposited in a setting characterised by moderate to high energy. Planar-laminated, medium-grained sands (Sm-p) are interpreted as high-energy laminites, which are characteristic of the swash zone. The presence of cross-laminated, medium-grained sands (Sm-c) would suggest deposition in an environment influenced by wave and tidal activity (Hori et al. 2001; Yang et al. 2005; de Raaf & Boersma 2007) as well as the migration of large-scale dunes (Reynaud & Dalrymple 2012), thus suggesting deposition within a ridge and runnel system (Dabrio 1982; Masselink & Anthony 2001). Such systems form as a result of the high wave energy within the breaker zone (dissipative shoreline, e.g. Stive et al. 2002; Aagaard & Hughes 2006). The ridges comprise trough cross-laminated dunes which are oriented parallel to the coastline. However, due to wave activity, tidal currents or the influence of an estuarine system, dunes may also be orientated perpendicular to the shoreline (Dalrymple et al. 2012). On top of these dunes, wave activity can lead to the deposition of high-energy parallel, or planar cross-lamination (Schäfer 2010). Horizontal surfaces between individual trough cross-laminated sections formed as a result of the erosion of the upper part of dunes, followed by the build-up of new sand dunes on top (i.e. compound dunes, see Reynaud & Dalrymple 2012). Mud clasts were probably eroded from adjacent muddy tidal flats (Fan 2012), and these were subsequently deposited on the lee-sides of the sand dunes/ridges/mega ripples. The coarser-grained

laminae within the Sm-c are probably indicative of periods of increased wave or tidal energy.

Sand dunes in such ridge and runnel systems are often cut by offshore-directed rip currents (Aagaard et al. 1997). The characteristic, laterally-restricted black sand clast beds with erosive lower boundaries may have been the result of these high-velocity currents, which erode small channels into the trough cross-laminated ridges and dunes (Dabrio 1982; Masselink & Anthony 2001; Hughes 2012). Within the sand clast beds, coarse-grained sands and chert pebbles embedded into the matrix of medium-grained sands are indicative of periods of higher-velocity currents. The sand clast beds are covered by small-scale ripple marks, indicating a decrease in current velocity.

Rip currents, such as those presumed responsible for the generation of the black sand clast beds, have been regarded as an important pathway for the exchange of water and sediment between the surf zone, and the inner shelf environments (Aagaard et al. 1997; Haller 2002; Castelle & Coco 2012). The velocities within rip currents increase during ebb tides (Aagaard et al. 1997) and, therefore, may have been responsible for the seaward-directed transport of wood fragments, peat or lignite clasts, as well as chert pebbles.

A.5.5 Coarse- to medium-grained sands (Sc)

Description – Coarse- to medium-grained sand beds, which range in thickness from 0.3-2 m are exclusively cross-laminated/bedded (Sc-c), and may be graded (fining up). They contain evidence of both planar cross- and trough cross-lamination/bedding, although the former is more common. Individual cross laminae within this section may contain fine-grained, organic material-rich and black coloured sands. The cross-laminated beds are internally bounded by horizontal surfaces, separating the individual sets of cross lamination and bedding. Wood fragments (branches and roots, up to 1 cm in diameter), where present, have been deposited parallel to these horizontal, erosive surfaces, as well as parallel to the trough cross laminae. Clasts also present within this facies include mud and lignite fragments. Up to 2 cm thick mud beds, covering the through cross-laminated, coarse- to medium- grained sand beds were also present.

Interpretation – This lithofacies was probably deposited in a higher energy environment in a shallow-marine setting, influenced by waves and tidal currents (Hori et al. 2001; Yang et al. 2005; de Raaf & Boersma 2007; Reynaud & Dalrymple 2012). The planar cross- and trough cross-laminated/bedded beds are indicative of large migrating

compound dunes (Collinson et al. 2006; Reynaud & Dalrymple 2012), and, therefore, may also be related to the development of a ridge and runnel system (see above). The lignite and wood fragments were most probably derived from the erosion of adjacent coastal mires.

A.5.6 Lignite (L)

Description – The lignite lithofacies comprises thick (up to 10 m) lignite beds. The beds may contain large wood fragments (branches, tree trunks, up to 4 m in length and 1 m in diameter), which were deposited parallel to the bedding direction (i.e. possibly not in situ), as well as (sub-) vertical-oriented wood remains (probably in situ). Root horizons, extending downward from the lignites into the underlying sands, are common.

Interpretation – the lignite deposits form part of the Garzweiler Seam, the uppermost of the three seams of the Ville Fm (Hager 1993; Schäfer et al. 2004; Schäfer & Utescher 2014). They were deposited within a coastal mire adjacent to the Serravallian-age North Sea. The mire comprised areas of different floral assemblages, based on their position and distance to the coastline, as well as water availability.

A.6 Facies Associations in sediment profiles

Three profiles, which range in thickness from 24 to 67 m, were measured from the Neurath Sand and overlying Garzweiler Seam in the Garzweiler open-cast mine and provide either a complete (Profile 1) or partial (Profiles 2 & 3) section through the sand body. The profiles can be subdivided, on the basis of the sedimentary facies present into six facies associations (FA; Fig. 8), and are described below.

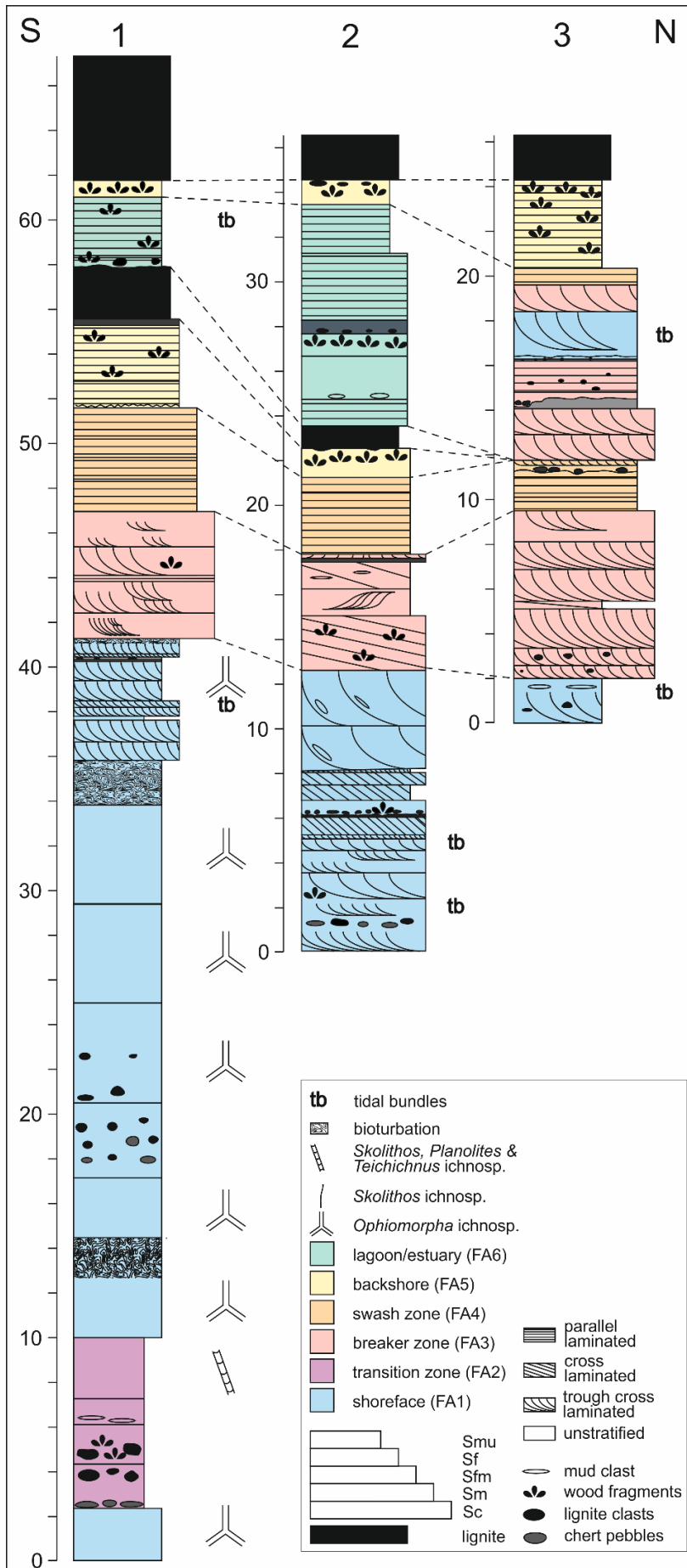


Fig. A-8: The measured profile through the Neurath Sand, Garzweiler open-cast mine. The three sections 1, 2 and 3 are laterally positioned 200 m from one other along a N-S axis. Six facies associations (Fa1-6) have been identified, composed of the various sedimentary facies (six in total), including lignite, medium- to coarse-grained sand, medium-grained sand, fine- to medium-grained sand, fine-grained sand and muddy sand.

A.6.1 Facies Association 1

Description – The lowermost facies (FA1) of the Neurath Sand is subdivided into three parts (FA1a, b, c) and comprises three facies (Sf-u, Sf-c, Sfm-c). The lowermost parts (FA1a, b) are only present in Profile 1, which commences with 2.4 m (FA1a) of heavily bioturbated sands (Sf-u) containing *Ophiomorpha ichnosp.* The horizontal *Ophiomorpha ichnosp.* burrows are mainly oval in shape, presumably as a result of subsequent compaction. Following an 8 m interval of FA2 (see below), the second part (FA1b) commences. This comprises mainly bioturbated sands (Sf-u), but also includes cross-laminated sand (Sf-c) (Fig. 8). Within the former, the percentage of bioturbation increases markedly from base to top within the individual beds. Bed tops are sharp (erosion); bioturbation recommences in the overlying bed.

The uppermost part of the facies association (FA1c) can be traced across all three of the sedimentary profiles (Fig. 8). This part comprises cross-laminated sands (Sf-c) and fine- to medium-grained sands (Sfm-c), both of which also include tidal bundles, with a black sand/sand clast layer also present in profiles 1 and 2.

Interpretation – As noted above, FA1 can be subdivided into three parts. The lowermost two parts (FA1a, b) are broadly similar (both comprising mainly Sf-u), while FA1c comprises mainly Sf-c and Sfm-c. FA1a, b would appear to have been deposited in a low-energy marine environment on the basis of grain size, and the presence of abundant *Ophiomorpha ichnosp.* (Seilacher 1964; Hiscott et al. 1984; Howard & Frey 1984; MacEachern et al. 2012).

The uppermost part (FA1c) comprises mainly fine- (occasionally medium-) grained sands with well-developed planar- and trough-cross lamination (Sf-c, Sfm-c), as well as tidal bundles and black sand/sand clast beds (see Fig. 6e). The former suggest deposition in a higher-energy setting than FA1a, b, thus evidencing a gradual increase in environmental energy within the lower part of the Neurath Sand. Deposition was most probably within the upper shoreface part of a subtidal environment, in contrast to the lower shoreface setting for FA1a, b. It is also possible that the transition from FA1a, b to FA1c marks a time gap between the two phases of this facies association. However, if that were the case, then it might be expected that a marked erosional horizon would be present at the boundary between FA1b and FA1c in Profile 1, or even possibly a lag deposit. In the marked absence of both, it would appear more feasible to conclude that the transition represents a phase of shallowing within the broader depositional setting. The presence of tidal bundles (occasionally including both flood and ebb couplets, see Hovikoski et al. 2005; Schäfer 2010) in FA1c would confirm the subtidal setting. Trough

cross-lamination may be indicative of wave activity; thus, FA1c was probably deposited within a ridge and runnel system below low tide line. Lignite and mud clasts are also present with the latter, most probably derived from the reworking of adjacent tidal flats (indicated by mud deposits bounding the Neurath Sands in the S; Schäfer & Utescher 2014), while the large wood fragments (e.g. up to 30 cm long branches) were probably transported by fluvial and tidal currents from the coastal mires. Similarly, the presence of organic fragments within the black sands/sand clast layers would suggest a proximity to abundant organic sources.

A.6.2 Facies Association 2

Description – Facies Association 2 (FA2), which is only present in Profile 1, comprises just one facies (Smu) in 5 different beds. It commences with a chert pebble lag where the matrix is light coloured. This passes upsection into a darker-coloured sand, with no evidence of any grading. The darker sands contain clasts of wood and lignite (mud clasts are present at the base of one bed at c. 6 m) concentrated into the lowermost beds of FA2 (Fig. 8). The overlying beds contain ichnofossil assemblages with initially a concentration of *Skolithos linearis* in the middle part of FA2, with *Planolites* ichnosp., *Teichichnus* ichnosp. and *Skolithos linearis* concentrated near the top of FA2 at c. 9 m (Fig. 8).

Interpretation – The chert pebble lag indicates an initial high-energy depositional environment which changed rapidly to a lower-energy one. Chert pebbles within the Ville Fm have been interpreted as marine deposits of the shoreface environment (Petzelberger 1994), possibly reflecting a transgressive surface (Utescher et al. 2012). The cherts are possibly derived from the Aachen-Limburg carbonate plateau (Albers & Felder 1981). Karstification of the Cretaceous-aged carbonates in the Aachen-Maastricht-Liège area (W margin of the Lower Rhine Basin; or possibly from the London-Brabant High?), was followed by transport of chert pebbles, commencing with the Oligocene-age transgression (Albers & Felder 1981). During Oligocene and Miocene times, the chert pebbles have been redistributed and deposited within marine sediments in the Lower Rhine Basin (Albers & Felder 1981; Petzelberger 1994).

The overlying non-stratified muddy sands (Smu) most probably represent a period of increasing water depth (following FA1), and decreasing environmental energy, which would be indicative of a transition zone. This is confirmed by the presence of *Skolithos*

linearis, *Planolites ichnosp.* and *Teichichnus ichnosp.*, which are indicative of the low- to moderate energy conditions below storm-wave base (MacEachern et al. 2012).

A.6.3 Facies Association 3

Description – FA3 can be observed within all three profiles, although its maximum thickness is only seen in the northernmost profile (Profile 3, 7.5 m at the base, and 6.4 m within the upper part of the profile, with up to 1.75 m of FA4 separating these two units); the thicknesses are reduced in Profiles 1 (5.4 m) and 2 (5.2 m). The facies association consists of two lithofacies, comprising cross-laminated and cross-bedded, medium-grained sands (Sm-c), as well as cross-laminated/cross-bedded, coarse- to medium-grained sands (Sc-c). The sands in Profiles 1 and 3 are mainly trough cross-laminated/bedded (Fig. 9a), while in Profile 2 they are predominantly planar cross-laminated/bedded. In contrast to FA1 no tidal bundles were observed in FA3.

Interpretation – The grain size and sedimentary structures as well as the absence of tidal bundles and ichnofossils, would suggest that the sand beds of FA3 were deposited in a lower intertidal (foreshore) environment. This setting is characterised by wave processes, as well as the regular exposure and covering during low and high tides, respectively (Le Hir et al. 2000; Fan 2012; Reynaud & Dalrymple 2012).

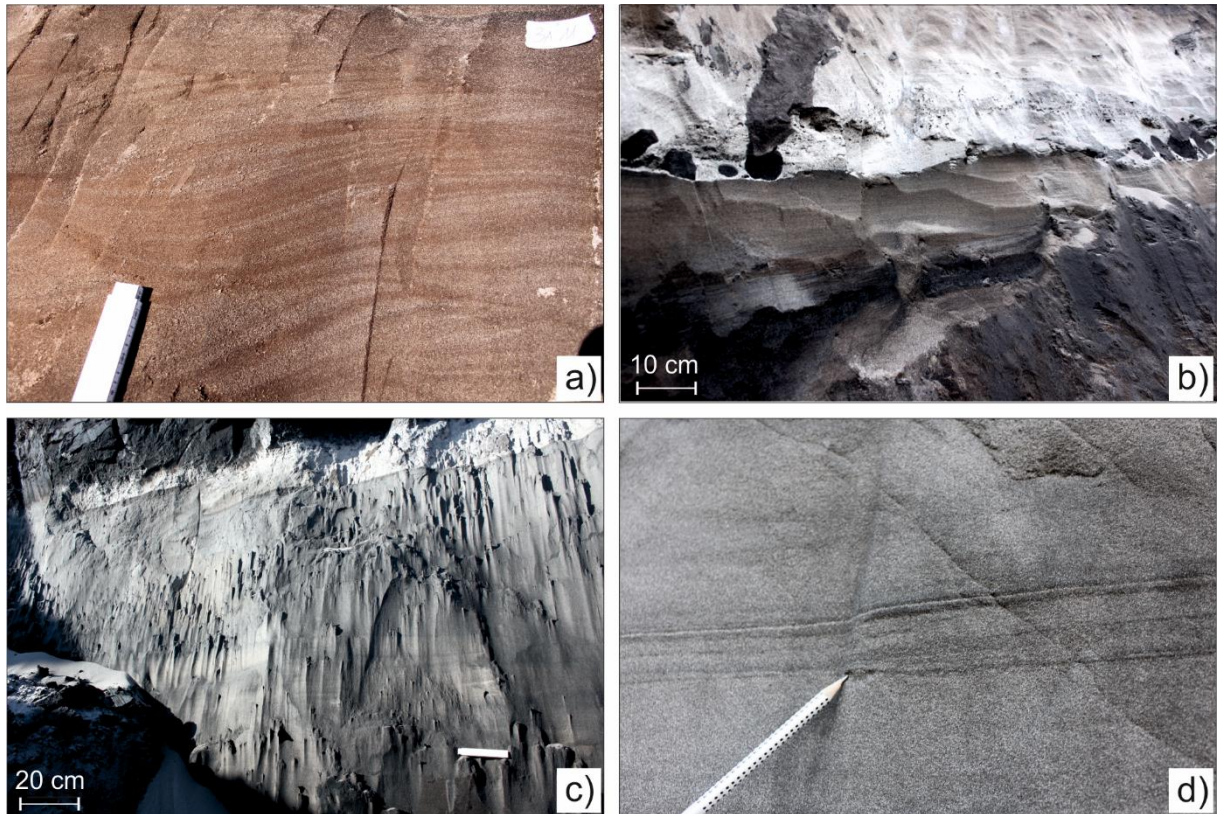


Fig. A-9: Selected facies associations from the Neurath Sand. (a) cross-laminated sands from FA3, profile 2; (b) planar-laminated, brown-coloured high-energy sands (FA4, swash zone), overlain by deposits of the breaker zone (FA3, light-grey sands). The overlying FA3 initiates with an erosionally bounded black sand-clast bed; (c) planar-laminated, fine- to medium-grained sands (comprising wood fragments) of the FA5 underlying the Garzweiler lignite seam (profile 1); (d) tidal rhythmite (sand-mud-sand-mud) in planar-laminated fine-grained sands of FA6 (profile 1).

A.6.4 Facies Association 4

Description – Facies Association 4 comprises three facies, dominated by parallel-laminated, medium-grained sand beds (Sm-p), and rare fine- to medium-grained beds (Sfm-p), sometimes alternating, or fining/thinning upwards. In Profile 1, the FA is topped by a 20 cm bed of cross-laminated sand with ripple lamination (Sm-c).

Interpretation – The medium-grained, planar-bedded sands indicate deposition within the upper foreshore (Clifton 1981). These beds formed under a high-energy flow regime, when breaking waves cause swash and backwash flows on the beach surface (Aagaard & Hughes 2006; Masselink & Puleo 2006). Alternations of fine- to medium-grained with medium-grained sand beds, as well as fining up beds, suggest variable energy conditions within the upper foreshore, possibly related to variations in wave height (e.g. seasonal, varying tidal current velocities). The thinning upward pattern observed within

the laminae of Profile 3 may be related to changes in water depth and a possible shift of the depositional setting from the swash to the breaker zone at the top of the FA (Fig. 9b). The small-scale ripples (Sm-c) most probably were deposited at the high-tide level, and mark the transition from the high-energy foreshore setting to the overlying backshore environment (FA5, see below).

A.6.5 Facies Association 5

Description – This FA (Fig. 9c), which can be traced across all three profiles, comprises three facies: fine-grained sand (which may be non-stratified, Sf-u, as well as planar laminated, Sf-p), fine- to medium-grained, planar laminated/bedded sand (Sfm-p) and thick (up to 10 m) lignite deposits (L). In addition, the FA5 overlies both FA4 and FA6 (Fig. 8). The sands are rich in both wood fragments and lignite clasts, with the concentrations increasing towards the lignite (i.e. near the top of the FA). The boundary between the lignites and sands is characterised by extensive root horizons (Fig. 6c), while the sands immediately underlying the lignites are generally black in colour. The boundaries between sand deposits and the overlying lignite are commonly gradational.

Interpretation – The sediment grain sizes, sedimentary structures (predominance of parallel lamination as a result of aeolian deposition) and the presence of lignite, would suggest that FA5 was deposited in a backshore environment with an adjacent coastal mire (Bartholdy 2012). The sand-rich lower part of the FA provides a link between the shallow-marine foreshore sediments and the coastal peat deposits, which formed subsequent to the marine regression (Bartholdy 2012). The black colour of the sands directly underlying the lignites resulted from infiltration of mobile dispersed organic matter (humic gels) derived from the lignites (see above).

A.6.6 Facies Association 6

Description – This FA comprises sand-rich lenses which show an irregular lateral distribution within the Garzweiler Seam, and is present in only two of the measured profiles (Fig. 8). The sand-rich lenses of FA6 comprise three lithofacies, including planar-laminated, fine-grained sands (Sf-p), and fine- to medium-grained sands, which are either non-stratified (Sfm-u), or planar-laminated (Sfm-p), with a clear erosive boundary (characterised by a concentration of wood fragments and angular to rounded lignite clasts) present in Profile 1. Tidal bundles may also be present (Fig. 9d). The upper part

of the FA is characterised by the presence of root horizons (extending from the overlying lignite) and rare lignite concentrations.

Interpretation – The sand lenses most probably have a marine origin, based on the presence of tidal bundles (Dalrymple et al. 1992; Archer 1996; Stupples 2002; Mazumder & Arima 2005; Kvale 2012), with deposition occurring in a moderate energy setting. Although these deposits combine characteristics of the subtidal, intertidal and supratidal environments, it is probable that they represent deposition in a bight, lagoon or estuarine setting due to the limited lateral extent of the sand bodies.

A.7 Discussion

A.7.1 Depositional model

On the basis of our detailed facies analysis from three measured sedimentary profiles, the sediments of the Neurath Sand from the Garzweiler open-cast mine are interpreted as a transgressive-regressive succession. The sequence of events, which occurred in the shallow-marine North Sea in Serravallian times, resulted in the deposition of a series of units as outlined below.

The base of the succession is represented by the lignites of the Frimmersdorf Seam, originally laid down in a near-coastal swamp environment which was slowly transgressed by the North Sea. The contact between the Neurath Sand and the underlying Frimmersdorf Seam was not exposed during the profile survey of this study, although former studies suggest it was erosional (Schäfer & Utescher 2014). The lowermost preserved glauconite-bearing sediments (containing *Ophiomorpha* ichnosp.) were deposited in a shoreface environment (subtidal), i.e. within the area between low tide level and the storm-wave base. *Ophiomorpha* ichnosp. are common within beach and shallow subtidal settings (Seilacher 1964; Hiscott et al. 1984; Howard & Frey 1984; MacEachern et al. 2012) and can be compared to the modern shrimps *Callinassa major* (Frey et al. 1978). *Ophiomorpha* ichnosp. is frequently found within marine sediments of the Lower Rhine Basin (e.g. *Ophiomorpha nodosa*; Suhr 1982, 1989; Petzelberger 1994).

The Ophiomorpha ichnosp.-rich bed is overlain by an extensive chert pebble bed which forms a significant marker horizon within the Garzweiler open-cast mine. Chert pebbles are widely distributed in the marine deposits of the Lower Rhine Basin (Petzelberger 1994) and have been traced back to the Aachen-Limburg carbonate plateau (Albers & Felder 1981). Following intense karstification of Cretaceous-aged carbonates, the residual cherts were redistributed throughout the Lower Rhine Basin by the repeated transgressions which occurred across the region (Albers & Felder 1981). In the Neurath Sand, it has been suggested that the chert pebble bed represents a transgressive surface (Utescher et al. 2012).

The overlying muddy sands (FA2) suggest a marked decrease in ambient energy levels within the depositional setting. This, together with a possible increase in water depth as suggested by the ichno-assemblage (*Skolithos linearis*, *Planolites ichnosp.*, *Teichichnus ichnosp.*) marks a change to a transitional environment, namely a nearshore setting linking the beach and shelf environments (MacEachern et al. 2012). These transitional deposits represent the maximum flooding stage of the Lower Rhine Basin in Serravallian times, and their deposition (heralded by the deposition of the chert pebble unit) was followed by the slow onset of regressive conditions (FA1 overlying FA2). The regressive period is represented by sands deposited within a subtidal environment. These contain *Ophiomorpha ichnosp.* in their lower parts, and are covered by (trough) cross-laminated sand units formed as dunes in a ridge and runnel system. The presence of sand-mud couplets have been interpreted as unequivocal evidence of tidal activity. These commonly occur as two paired couplets (i.e. sand-mud-sand-mud) and their presence would suggest that both ebb and flood currents were strong enough for sand transport to occur (Hori et al. 2001). These tidal bundles are indicative of subtidal conditions, as well as deposition within channels or estuaries (Dalrymple et al. 1992; Archer 1996; Stupples 2002; Mazumder & Arima 2005; Kvale 2012).

The regressive trend continued with the deposition of a series of sand beds within the foreshore environment (FA3, FA4). This intertidal succession commenced with the deposition of the sediments of the breaker zone, a high-energy setting dominated by wave and tidal processes. The ridge and runnel system within this sedimentary environment results from wave activity, tidal processes and longshore currents (Dabrio 1982; Kroon & Masselink 2002). These ridges comprise large to very large sand dunes (Reynaud & Dalrymple 2012) covered by smaller dunes and resulting in the formation of a complex pattern of compound cross-bedding (also observed in the Neurath Sand deposits). The overlying planar laminated/bedded, medium-grained sands are also interpreted as intertidal deposits, although these high-energy laminites were probably

deposited in the swash zone of the upper foreshore, as a result of the uprush and backwash of strong and unsteady wave flows on the beachface (Masselink & Puleo 2006).

The overlying supratidal sands (FA5) were deposited on the beach surface above high tide level. Small ripple structures between the supratidal and the underlying intertidal deposits indicate the high-tide line, or beach berm, thus marking the position of maximum tidal flooding (Schäfer 2010). There is no evidence of aeolian dune deposition within the Neurath Sand. Boersma (1991) suggested, low or non-existent dunes within the Lower Rhine Basin were the result of wet substrates at the backshore, associated with high water-levels in a back barrier lagoon. The backshore sands were, in turn, overlain by lignite, reflecting the accumulation of paralic peats in nearshore marshes and mires. The peat accumulations within the coastal mire can be up to 30 m thick (10 m thick present-day Garzweiler Seam) as a result of continuous subsidence of the basin. Roots from the plants growing in these paralic environments penetrated into the underlying sands (Fig. 6c) of the backshore environment. The degree of root penetration would suggest that the sands were flushed of marine interstitial pore waters and replaced with freshwater from rain and rivers. This flushing presumably occurred prior to the development of a continental flora (with the possible exception of saline-tolerant plants which represent the early pioneer plants on the recently drained surface; however, the remaining roots probably represent subsequent vegetation, based on the diameter and length of the roots; see Darscheid 1981). Various floral assemblages growing within the Miocene-aged mires have been analysed, depending on the distance to the sea as well as water availability (Teichmüller, R. 1958; Teichmüller, M. 1958).

Based on anatomical studies of wood and palynological data, the typical peat-forming vegetation of the coastal mires consisted of diverse open mixed forests and scrubs comprising conifers and angiosperms (van der Burgh 1973; von der Brelie & Wolf 1981; Mosbrugger et al. 1994; Figueiral et al. 1999). Analyses carried out on stump horizons indicate that, at times, relatively dense conifer forests existed. These were mainly composed of Taxodiaceae and Pinaceae (with *Sciadopitys* as the most common genus), and subordinate palms (Mosbrugger et al. 1994). A detailed palaeovegetation analysis (based on palynology) carried out on the Garzweiler Seam in the Hambach open-cast mine, provided the basis for a reconstruction of the vegetational succession of the seam (Huhn et al. 1997). A pine-ericalean pocosin type vegetation, representing well-drained soil conditions, developed at the base of the seam, and this was succeeded by scrub vegetation dominated by plant species of the *Myrica*, *Betula*, and *Cyrilla* genera. In the upper part of the seam, a gradual transition to a *Taxodium* - *Nyssa* association was

recorded, suggesting a change to a very high water table. Pollen analysis would suggest that angiosperm herbs did not play a significant role in the Garzweiler vegetation (Huhn et al. 1997). Organic petrological and organic geochemical analyses, carried out on samples from the Morken, Frimmersdorf and Garzweiler seams in the Garzweiler open-cast mine, suggested that the peat-forming vegetation of the coastal mires probably consisted of a combination of herbaceous-vegetated areas (Lücke et al. 1999; Stock et al. 2016).

The two lens-shaped sand intercalations within the Garzweiler Seam (FA5), separated by a thin lignite band, have been interpreted as a result of a regionally-restricted inundation of the swamp environment at its northern boundary. The sand beds contain tidal bundles, which are typical for the shoreface environment below the low-tide level. Planar lamination, on the other hand may indicate an intertidal depositional environment (i.e. high energy laminites, see above). The fine-grained nature of these deposits, however, would suggest a low- to moderate energy setting. As these sand deposits are of limited regional extent (10's of metres, Fig. 10) they are interpreted as representing a lagoonal or estuarine setting. To the north, the lens-shaped sand intercalations can be correlated with a cross-laminated, subaqueous (intertidal to subtidal) dune system (cross lamination and tidal bundles in the upper part of Profile 3). These represent either coast-parallel barrier sand bars (associated with barrier islands; i.e. wave breaker that protect the lagoonal milieu from the waves of the open sea; Fan 2012), or, possibly, tidal sand bars (stream-parallel), which are characteristic of estuarine mouth areas (Dalrymple et al. 2012).

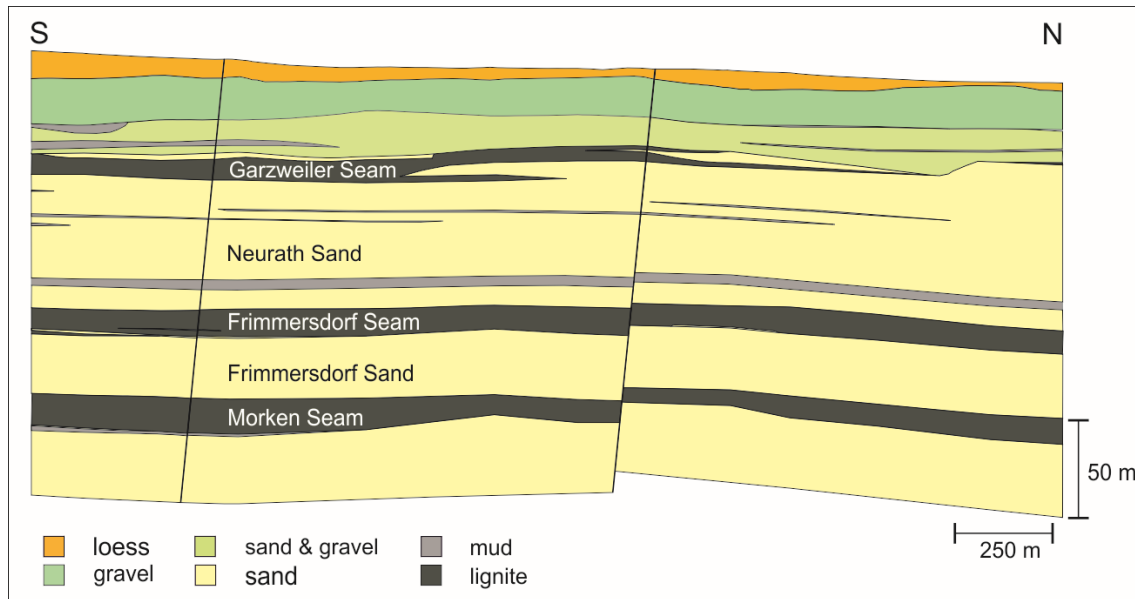


Fig. A-10: Cross section of the Ville Formation from the Garzweiler open-cast mine (W of the measured profiles), interpreted from exploration drillings and geophysical well logs (RWE Power AG). The cross section comprises the northernmost extent of the Garzweiler Seam, as well as laterally restricted sand bodies.

A.7.2 Channel deposits

Four characteristic beds containing black sand clasts were observed within the three measured profiles, and have been interpreted as channel deposits. The black sand clast-rich beds are interbedded with (trough-) cross-laminated sands, which were deposited within a ridge and runnel system (e.g. Dabrio 1982; Masselink & Anthony 2001). These beach-parallel sand ridges (i.e. longshore bars or dunes; Boersma 1991; Fan 2012; Reynaud & Dalrymple 2012) may be cut by rip channels (e.g. Aagaard et al. 1997; Haller 2002; Castelle & Coco 2012) or tidal channels (e.g. Weimer et al. 1982; Lanzoni 2002; Dalrymple & Choi 2007; Hughes 2012). Both rip as well as tidal channels are considered to be important pathways for water-sediment exchange between the coastal and shelf environments (Aagaard et al. 1997; Fan 2012; Hughes 2012).

The erosionally-bounded black-coloured sand beds and the associated intraformational (i.e. rip-up) clasts were deposited in tidal channels (Collinson et al. 2006). According to Hughes (2012), sand-dominated deposits in tidal channels represent the higher-energy periods of spring tides. Studies of tidal channels (mostly within intertidal environments; e.g. Lanzoni 2002; Hughes 2012), commonly note the presence of a coarse-sediment lag, including shells, wood fragments, mud clasts or pebbles, along the erosional bounding surface (Clifton 1982; Hughes 2012). These lag deposits also may include mud block breccias, which formed as a result of bank slumping or channel edge erosion

(Terwindt 1988; Hughes 2012). Neither shells nor mud blocks are found in association with the intraformational sands in the Neurath Sand, the former having been dissolved by the passage of humic acids through the sand body, and the latter most probably did not form due to the lack of adjacent mud banks.

Tidal channels are commonly characterized by features produced as a result of tidal activity (e.g. reactivation surfaces, mud drapes in cross sets, low angle dipping cross sets with alternating thicker and thinner packages of heterolithic sediments, flaser- and/or lenticular bedding or tidal bundles; de Raaf & Boersma 2007; Hughes 2012). None of these, however, have been observed in the Neurath Sand channel deposits. The absence of characteristic features indicative of changing flow directions (ebb and flood currents), suggests deposition under unidirectional flow conditions (i.e. either ebb or flood). Additionally, the presence of wood remains, as well as the black-coloured humic substances, forming coats around each individual grain within the channel deposits (see above) suggests an ebb-dominated environment, with strong ebb currents transporting the humic substances as well as wood remains from the coastal mires into the intertidal and subtidal environments. However, tidal bundles within the surrounding subtidal deposits would suggest that both ebb and flood currents were generally strong enough for sand transport. Tide-generated channels can also be interpreted in terms of estuarine systems (Dalrymple & Choi 2007; and see below). These tide-generated swatchways separate elongate tidal sand bars at the transition from the estuary mouth to the marine setting (Dalrymple et al. 2012).

Another possible explanation for the formation of channels within this depositional environment may be related to rip currents. These offshore-directed currents are the result of seaward return flows through narrow channels between sand bars, and are induced by the backwash of waves (Aagaard et al. 1997). The infill of channels may occur as a result of channel migration, or decreasing wave energy (Aagaard et al. 1997). However, rip currents are restricted to the intertidal environment (Masselink & Hegge 1995; Aagaard et al. 1997; Castelle & Coco 2012), and can thus only be regarded as responsible for the formation of the sand clast beds within the breaker zone.

The unidirectional flow conditions within the black sand clasts beds, the presence of humic substances, chert pebbles and wood fragments may all also be interpreted in terms of a single high-energy flow event. According to Hunt et al. (2015), erosion of sediments within the intertidal environment only occurs, when tidal currents are reinforced by increased wave or wind energy. Studies of recent rip channels have noted that their initial formation can occur as a result of storms (Aagaard et al. 1997).

Additionally, channel migration, and channel infill have been observed after storm events (e.g. Castelle & Coco 2012). During such events, increased wave energy can lead to extensive erosion of the coastal area (e.g. Russell 1993; Eisma 1998), followed by the distribution of backshore deposits into the marine setting through tidal channels and rip currents. However, the absence of hummocky cross stratification (generally characteristic of storm-induced sedimentation, and completely absent throughout the Lower Rhine Basin) might suggest an absence of storm activity. On the other hand, the presence of groden bedding (which forms as a result of storm surges inundating coastal marshes; Boersma 1991; Schäfer et al. 2004; Bungenstock & Schäfer 2009; Schäfer 2010) in the underlying Frimmersdorf Sand would suggest that storm deposition did indeed occur within the Lower Rhine Basin. Additionally, hummocky cross stratification may be deformed or destroyed due to tides or storm wave activity (Eyles & Clark 1986).

As noted above, flow velocities within rip currents generated by the backwash of waves can be increased/reinforced by tidal currents, in particular by seaward-directed ebb currents (Aagaard et al. 1997). The deposits of the Neurath Sand show both the distinct influence of wave activity, as well as the impact of tides. Therefore, both waves and tides (i.e. rip currents and tidal or estuarine currents) may have been responsible for the formation of the observed channel deposits.

A.7.3 Depositional environment: tidal delta vs. estuary

The broader depositional setting of the Neurath Sand is problematic. In general, the Lower Rhine Basin in Miocene times formed an embayment, bounded by the uplifting Rhenish Massif in the SE and SW, and extending into the North Sea Basin in the NW (e.g. Schäfer et al. 1996; Lücke et al. 1999; Klett et al. 2002).

Two sources of clastic sediment input have been identified from the Lower Rhine Basin (Hager 1993). The first, providing fine-grained quartz sands, was located in the SW North Sea, and the sediments were transported by coastal longshore currents (Breddin 1932; Hager 1993) following their deposition in the Lower Rhine Basin. The presence of large sand dunes and tidal bundles within the Neurath Sand provides unequivocal evidence for tidal and wave activity within the shallow-marine environment. The tidal range within the Miocene-age North Sea has been estimated at 2-4 m (mesotidal; Schäfer & Utescher 2014), although, both tidal range as well as wave height can increase as a result of funneling within embayments (e.g. estuaries or tidal inlets, Mazumder & Arima 2005; Dalrymple & Choi 2007; Longhitano et al. 2012).

The second sediment source was located to the SE (i.e. Rhenish Massif), with sediment transported by medium- to low-energy fluvial systems entering the Lower Rhine Basin (Hager 1993). It is probable that the Rhenish Massif in Miocene times was dewatered by several, small river streams (compared to the present-day fluvial system within the Lower Rhine Basin). Peat accumulation of the Main Seam (i.e. the combined Morken, Frimmersdorf and Garzweiler Seams in the SE) took place on the banks of one of these systems, extending through the centre of the basin (Zagwijn & Hager 1987). This river system, interpreted as a precursor of the present-day river Sieg (Hager 1993), subsequently shifted its location to the SW (Zagwijn & Hager 1987).

It has been suggested that a deltaic depositional environment formed at the entry point of the various fluvial systems (Boersma 1991; Hager 1993), based on the presence of a number of small to medium river systems, as well as the Rhenish Massif representing the provenance area. However, as described within this study, features that would represent characteristic deltaic deposits are not present within the Neurath Sand and, thus, such a model does not conform with the observations. Schäfer et al. (1996) have suggested that the sediments of the Neurath Sand were deposited in an estuarine system. Such a system develops in a transgressive setting (e.g. Dalrymple; Dalrymple et al. 1992; Dalrymple 2006; Dalrymple & Choi 2007), followed by the infill of the estuarine channels during progradation of the shoreline (Dalrymple et al. 2012). As noted above, the Serravallian-age North Sea transgressed onto the peat accumulation of the present-day Frimmersdorf Seam, and the lowermost part of the Neurath Sand (i.e. FA1a, FA2) was subsequently deposited in a deepening marine setting (i.e. transgressive). Subsequent regression of the North Sea (FA1b, c – FA5) resulted in the deposition of a progradational shoreline sequence. Studies on recent and ancient estuarine systems have shown that infilling estuaries form features which are transitional with deltas (Dalrymple et al. 2012). Within the Lower Rhine Basin, the deposits of the Garzweiler Seam, and particularly of the overlying Inden Fm mark the transition from a probable estuarine system (Neurath Sand), to a fluvial to deltaic system formed by the early Rhine river, which initially entered the Lower Rhine Basin in Tortonian times (Boenigk 2002; Sissingh 2006; Kemna 2008; Westerhoff et al. 2008). As such, the Neurath Sand could possibly be interpreted in terms of the estuarine model.

This model is confirmed by the presence of channel deposits (i.e. the black-coloured sand clasts), tidal bundles and sand dunes. The channel deposits, represented by the black sand clast beds, probably represent swatchways, separating elongate tidal sand bars (Dalrymple et al. 2012). The cross-laminated/-bedded dune deposits of the sub- to intertidal settings of the Neurath Sand are interpreted as subtidal and intertidal sand bars,

which are ubiquitous in the funnel-shaped mouth areas of estuaries (Dalrymple et al. 1992; Dalrymple et al. 2012). The orientation of the cross-laminated dunes, however, could not be measured (due to the outcrop situation), and, therefore, it is not possible to distinguish between coast-parallel orientated dunes (ridge and runnel systems, Dabrio 1982; Masselink & Anthony 2001), and tidal sand bars (estuary, Dalrymple et al. 1992), which are orientated mainly stream-parallel (and, therefore, broadly perpendicular to the coastline; Dalrymple et al. 2012). The lens-shaped sand intercalations within the Garzweiler Seam, as noted above, provide evidence of tide-dominated sand deposition within restricted areas of the mire, which may also be indicative of an estuarine origin (Dalrymple et al. 1992; Dalrymple et al. 2012). In contrast to modern and ancient estuaries (e.g. Bostock et al. 2007; Dalrymple & Choi 2007; Choi 2010; Uncles 2010; Dalrymple et al. 2012), however, there was no major fluvial system entering the Lower Rhine Basin in Miocene times, but several small river systems, dewatering the adjacent Rhenish Massif and the adjacent coastal mires (Zagwijn & Hager 1987; Hager 1993).

A.8 Conclusions

The Serravallian-age Neurath Sand is interpreted in terms of a characteristic shoreline succession within a tide- and wave-dominated embayment. The transgression of the North Sea resulted in the deposition of subtidal deposits covering the peat accumulations of the present-day Frimmersdorf Seam, followed by mud-rich sediments of the transition zone as a result of increasing water depth. Subsequently, regressive conditions resulted in the deposition of a sequence of subtidal, intertidal, and supratidal sediments, and, finally, the re-establishment of coastal mires (present-day Garzweiler Seam). Lens-shaped sand intercalations within the Garzweiler Seam, which comprise tidal bundles and are bounded by subaquatic sand dunes in the N, probably have been deposited in an estuarine or lagoonal milieu.

The interaction of wave and tidal currents with river systems, entering the Lower Rhine Basin from the adjacent Rhenish Massif, and also dewatering the peat accumulations of the present-day Main Seam in the S, are indicative of an estuarine system. The estuarine system was formed by several, comparably small rivers, flanked by coastal mires and marshes in the SE, which laterally passed into tidal mud flats, and, with increasing water depth to the NW, foreshore and shoreface environments in the centre of the Lower Rhine Basin.

Acknowledgements

We acknowledge the funding for this study from the RWE Power AG. Thanks to the staff members of the department GOC-L, especially the field crew of the Garzweiler open-cast mine, as well as Ulrich Krüger and Horst Hassel for editing datasets. The manuscript benefited greatly from the comments of Wim Westerhoff, Marinus Eric Donselaar and an anonymous reviewer.

A.9 References

- Aagaard, T. & Hughes, M.G., 2006. Sediment suspension and turbulence in the swash zone of dissipative beaches. *Marine Geology* 228: 117–135.
- Aagaard, T., Greenwood, B. & Nielsen, J., 1997. Mean currents and sediment transport in a rip channel. *Marine Geology* 140: 25–45.
- Albers, H.J. & Felder, W.M., 1981. Feuersteingerölle im Oligomiozän der Niederrheinischen Bucht als Ergebnis mariner Abrasion und Carbonatlösungsphasen auf der Kreide-Tafel von Aachen-Südlimburg. In: Reiche, E. & Hilden, H.D. (eds): *Geologie und Lagerstättenerkundung im Rheinischen Braunkohlenrevier*. Fortschritte in der Geologie von Rheinland und Westfalen 29: 469–482.
- Alert, S.P., 1974. Systematic review of the genus *Skolithos*. *Journal of Paleontology* 48(4): 661–669.
- Archer, A.W., 1996. Reliability of lunar orbital periods extracted from ancient cyclic tidal rhythmites. *Earth and Planetary Science Letters* 141: 1–10.
- Bartholdy, J., 2012. Salt Marsh Sedimentation. In: Davis, R.A., Jr. & Dalrymple, R.W. (eds): *Principles of Tidal Sedimentology*. Springer: 151–185.
- Becker, B. & Asmus, S., 2005. Beschreibung und Korrelation der känozoischen Lockergesteinsschichten der Grundgebirgsbohrungen im Umfeld des Tagebaus Hambach. In: *Der tiefere Untergrund der Niederrheinischen Bucht. Ergebnisse eines Tiefbohrprogramms im Rheinischen Braunkohlenrevier*. Scriptum 13: 61–74.
- Berggren, W.A., Kent, D.V., Swisher, C.C., III & Aubry, M.-P., 1995. A revised Cenozoic geochronology and chronostratigraphy. In: Berggren, W.A., Kent, D.V., Aubry, M.-P. & Hardenbol, J. (eds): *Geochronology, time scales and global stratigraphic correlation*. SEPM Special Publication 54: 129–212.
- Boenigk, W., 2002. The Pleistocene drainage pattern in the Lower Rhine Basin. *Netherlands Journal of Geosciences - Geologie en Mijnbouw* 81(2): 201–210.
- Boersma, J.R., 1991. A large flood-tidal delta and its successive spill-over apron: detailed proximal-distal facies relationships (Miocene Lignite Suite, Lower Rhine Embayment, Germany). In: Smith, D.G., Reinson, G.E., Zaitlin, B.A. & Rahmani, R.A. (eds): *Clastic Tidal Sedimentology*. Canadian Society of Petroleum Geologists Memoir 16 (Calgary): 227–252.
- Bostock, H.C., Brooke, B.P., Ryan, D.A., Hancock, G., Pietsch, T., Packett, R. & Harle, K., 2007. Holocene and modern sediment storage in the subtropical macrotidal Fitzroy River estuary, Southeast Queensland, Australia. *Sedimentary Geology* 201: 321–340.
- Bredden, H., 1932. Die Feuersteingerölle im Niederrheinischen Tertiär, ein Beweis für die paralische Natur der Braunkohlenflöze. *Centralblatt für Mineralogie, Geologie und Paläontologie B*: 395–404.
- Bromley, R.G., 1996. Trace fossils. Biology, taphonomy and applications. Taylor & Francis (Oxon & New York): 361 pp.
- Bungenstock, F. & Schäfer, A., 2009. The Holocene relative sea-level curve for the tidal basin of the barrier island Langeoog, German Bight, Southern North Sea. *Global and Planetary Change* 66: 34–51.
- Castelle, B. & Coco, G., 2012. The morphodynamics of rip channels on embayed beaches. *Continental Shelf Research* 43: 10–23.
- Choi, K., 2010. Rhythmic climbing-ripple cross-lamination in inclined heterolithic stratification (IHS) of a macrotidal estuarine channel, Gomsu Bay, West Coast of Korea. *Journal of Sedimentary Research* 80 (6): 550–561.
- Clifton, H.E., 1981. Progradational sequences in Miocene shoreline deposits, southeastern Caliente Range, California. *Journal of Sedimentary Petrology* 51 (1): 165–184.
- Clifton, H.E., 1982. Estuarine Deposits. In: Scholle, P.A. & Spearing, D. (eds): *Sandstone Depositional Environments*. AAPG Memoir 31: 179–189.
- Collinson, J., Mountney, N. & Thomson, D., 2006. *Sedimentary Structures*. Terra Publishing (Edinburgh): 292 pp.
- Crimes, T.P., 1977. Trace fossils of an Eocene deep-sea fan, northern Spain. In: Crimes, T.P. & Harper, J.C. (eds): *Trace fossils 2*. Seel House Press (Liverpool): 71–90.

- Curran, H.A. & Frey, R.W., 1977. Pleistocene trace fossils from North Carolina (USA.), and their Holocene analogues. In: Crimes, T.P. & Harper, J.C. (eds): Trace fossils 2. Seel House Press (Liverpool): 139–162.
- Dabrio, C.J., 1982. Sedimentary structures generated on the foreshore by migrating ridge and runnel systems on microtidal and mesotidal coasts of S. Spain. *Sedimentary Geology* 32: 141–151.
- Dalrymple, R.W., 2006. Incised valleys in time and space: an introduction to the volume and an examination of the controls on valley formation and filling. In: Dalrymple, R.W., Leckie, D.A. & Tillman, R.W. (eds): Incised valleys in time and space. SEPM Special Publication 85: 5–12.
- Dalrymple, R.W. & Choi, K., 2007. Morphologic and facies trends through the fluvial–marine transition in tide-dominated depositional systems: A schematic framework for environmental and sequence-stratigraphic interpretation. *Earth-Science Reviews* 81: 135–174.
- Dalrymple, R.W., Zaitlin, B.A. & Boyd, R., 1992. Estuarine facies models: conceptual basis and stratigraphic implications: perspective. *Journal of Sedimentary Petrology* 62 (6): 1130–1146.
- Dalrymple, R.W., Mackay, D.A., Ichaso, A.A. & Choi, K.S., 2012. Processes, morphodynamics, and facies of tide-dominated estuaries. In: Davis, R.A., Jr. & Dalrymple, R.W. (eds): Principles of Tidal Sedimentology. Springer: 79–107.
- Darscheid, E., 1981. Wurzelböden und Flözbasis in der rheinischen Braunkohle. In: Reiche, E. & Hilden, H.D. (eds): Geologie und Lagerstättenerkundung im Rheinischen Braunkohlenrevier. Fortschritte in der Geologie von Rheinland und Westfalen 29: 165–175.
- De Raaf, J. & Boersma, J.R., 2007. Tidal deposits and their sedimentary structures. *Geologie en Mijnbouw* 50 (3): 479–504.
- Desjardins, P.R., Mángano, M.G., Buatois, L.A. & Pratt, B.R., 2010. Skolithos pipe rock and associated ichnofabrics from the southern Rocky Mountains, Canada: Colonization trends and environmental controls in an early Cambrian sand-sheet complex. *Lethaia* 43: 507–528.
- Eisma, D., 1998. Intertidal Deposits. River mouths, tidal flats, and coastal lagoons. CRC Press LLC (Boca Raton): 527 pp.
- Eyles, N. & Clark, B.M., 1986. Significance of hummocky and swaley cross-stratification in late Pleistocene lacustrine sediments of the Ontario basin, Canada. *Geology* 14: 679–682.
- Fan, D., 2012. Open-coast tidal flats. In: Davis, R.A., Jr. & Dalrymple, R.W. (eds): Principles of Tidal Sedimentology. Springer: 187–229.
- Figueiral, I., Mosbrugger, V., Rowe, N.P., Ashraf, A.R., Utescher, T. & Jones, T.P., 1999. The Miocene peat-forming vegetation of northwestern Germany: an analysis of wood remains and comparison with previous palynological interpretations. *Review of Palaeobotany and Palynology* 104: 239–266.
- Folk, R.L., 1974. *Petrology of Sedimentary Rocks*. Hempill Publishing Company (Austin): 182 pp.
- Frey, R.W., 1990. Trace fossils and hummocky cross-stratification, Upper Cretaceous of Utah. *Palaios* 5 (3): 203–218.
- Frey, R.W., Howard, J.D. & Pryor, W.A., 1978. Ophiomorpha: its morphologic, taxonomic, and environmental significance. *Palaeogeography, Palaeoclimatology, Palaeoecology* 23: 199–229.
- Geluk, M.C., Duin, E.J.T., Duser, M., Rijkers, R.H.B., van den Berg, M.W. & van Rooijen, P., 1994. Stratigraphy and tectonics of the Roer Valley Graben. *Geologie en Mijnbouw* 73: 129–141.
- Graham, D.J. & Midgley, N.G., 2000. Technical Communication. Graphical representation of particle shape using triangular diagrams: an excel spreadsheet method. *Earth Surface Processes and Landforms* 25: 1473–1477.
- Grützner, C., Fischer, P. & Reicherter, K., 2016. Holocene surface ruptures of the Rurrand Fault, Germany—insights from palaeoseismology, remote sensing and shallow geophysics. *Geophysical Journal International* 204: 1662–1677.
- Hager, H., 1986. Peat accumulation and syngenetic clastic sedimentation in the Tertiary of the Lower Rhine Basin (F.R. Germany). *Mémoires de la Société Géologique de France* 149: 51–56.
- Hager, H., 1993. The origin of the Tertiary lignite deposits in the Lower Rhine region, Germany. *International Journal of Coal Geology* 23: 251–262.

- Haller, M.C., 2002. Experimental study of nearshore dynamics on a barred beach with rip channels. *Journal of Geophysical Research* 107: 14-1 – 14-21.
- Haq, B.U., Hardenbol, J., & Vail, P.R., 1987. Chronology of fluctuating sea levels since the Triassic. *Science* 235: 1156-1167.
- Haq, B.U., Hardenbol, J., & Vail, P.R., 1988. Mesozoic and Cenozoic chronostratigraphy and cycles of relative sea level change. In: Wilgus, C.K., Hastings, B.S., Kendall, G.C.St.C., Posamentier, H.W.; Ross, C.A. & van Wagoner, J.C. (eds): *Sea-level changes: an integrated approach*. SEPM Special Publication 42: 71-108.
- Hardenbol, J., Thierry, J., Farley, M.B., Jacquin, T., de Graciansky, C. & Vail, P.R., 1998. Mesozoic-Cenozoic Sequence Chronostratigraphy of European Basins. In: Graciansky, P.C. de, Hardenbol, J., Jacquin, T. & Vail, P.R. (eds): *Mesozoic and Cenozoic Sequence Stratigraphy of European Basins*. SEPM Special Publication No. 60: p. 84
- Hinzen, K.-G., 2003. Stress field in the Northern Rhine area, Central Europe, from earthquake fault plane solutions. *Tectonophysics* 377: 325–356.
- Hiscott, R.N., James, N.P. & Pemberton, S.G., 1984. Sedimentology and ichnology of the Lower Cambrian Bradore Formation, coastal Labrador: fluvial to shallow-marine transgressive sequence. *Bulletin of Canadian Petroleum Geology* 32 (1): 11–26.
- Hori, K., Saito, Y., Zhao, Q., Cheng, X., Wang, P., Sato, Y. & Li, C., 2001. Sedimentary facies of the tide-dominated paleo-Changjiang (Yangtze) estuary during the last transgression. *Marine Geology* 177: 331–351.
- Houtgast, R.F. & van Balen, R.T., 2000. Neotectonics of the Roer Valley Rift System, the Netherlands. *Global and Planetary Change* 27: 131–146.
- Hovikoski, J., Räsänen, M., Gingras, M., Roddaz, M., Brusset, S., Hermoza, W., Pittman, L.R. & Lertola, K., 2005. Miocene semidiurnal tidal rhythmites in Madre de Dios, Peru. *Geology* 33 (3): 177–180.
- Howard, J.D. & Frey, R.W., 1984. Characteristic trace fossils in nearshore to offshore sequences, Upper Cretaceous of east-central Utah. *Canadian Journal of Earth Sciences* 21 (2): 200–219.
- Hughes, Z.J., 2012. Tidal channels on tidal flats and marshes. In: Davis, R.A., Jr. & Dalrymple, R.W. (eds): *Principles of Tidal Sedimentology*. Springer: 269–300.
- Huhn, B.; Utescher, T.; Ashraf, A.R. & Mosbrugger, V., 1997. The peat-forming vegetation in the Middle Miocene Lower Rhine Embayment: an analysis based on palynological data. *Mededelingen Nederlands Instituut voor Toegepaste Geowetenschappen* 58: 211-218.
- Hunt, S., Bryan, K.R. & Mullarney, J.C., 2015. The influence of wind and waves on the existence of stable intertidal morphology in meso-tidal estuaries. *Geomorphology* 228: 158–174.
- Kemna, H.A., 2008. Pliocene and Lower Pleistocene fluvial history of the Lower Rhine Embayment, Germany: Examples of the tectonic forcing of river courses. *Quaternary International* 189: 106–114.
- Klett, M., Eichhorst, F. & Schäfer, A., 2002. Facies interpretation from well logs applied to the Tertiary Lower Rhine Basin fill. In: Schäfer, A. & Siehl, A. (eds): *Rift tectonics and syngenetic sedimentation - the Cenozoic Lower Rhine Graben and related structures*. Netherlands Journal of Geosciences 81 (2): 167–176.
- Kroon, A. & Masselink, G., 2002. Morphodynamics of intertidal bar morphology on a macrotidal beach under low-energy wave conditions, North Lincolnshire, England. *Marine Geology* 190: 591–608.
- Kvale, E.P., 2012. Tidal constituents of modern and ancient tidal rhythmites: criteria for recognition and analyses. In: Davis, R.A., Jr. & Dalrymple, R.W. (eds): *Principles of Tidal Sedimentology*. Springer: 1–17.
- Lanzoni, S., 2002. Long-term evolution and morphodynamic equilibrium of tidal channels. *Journal of Geophysical Research* 107: 1-1 – 1-13.
- Le Hir, P., Roberts, W., Cazaillet, O., Christie, M., Bassoullet, P. & Bacher, C., 2000. Characterization of intertidal flat hydrodynamics. *Continental Shelf Research* 20: 1433–1459.
- Longhitano, S.G., Mellere, D., Steel, R.J. & Ainsworth, R.B., 2012. Tidal depositional systems in the rock record: A review and new insights. *Sedimentary Geology* 279: 2–22.
- Lücke, A., Helle, G., Schleser, G.H., Figueiral, I., Mosbrugger, V., Jones, T.P. & Rowe, N.P., 1999. Environmental history of the German Lower Rhine Embayment during the Middle

- Miocene as reflected by carbon isotopes in brown coal. *Palaeogeography, Palaeoclimatology, Palaeoecology* 154: 339–352.
- MacEachern, J.A., Bann, K.L., Gingras, M.K., Zonneveld, J.-P., Dashtgard, S.E. & Pemberton, S.G., 2012. The Ichnofacies Paradigm. In: Knaust, D. & Bromley, R.G. (eds): *Trace fossils as indicators of sedimentary environments* 64. Elsevier (Amsterdam): 103–138.
- Masselink, G. & Anthony, E.J., 2001. Location and height of intertidal bars on macrotidal ridge and runnel beaches. *Earth Surface Processes and Landforms* 26: 759–774.
- Masselink, G. & Hegge, B., 1995. Morphodynamics of meso- and macrotidal beaches: examples from central Queensland, Australia. *Marine Geology* 129: 1–23.
- Masselink, G. & Puleo, J.A., 2006. Swash-zone morphodynamics. *Continental Shelf Research* 26: 661–680.
- Mazumder, R. & Arima, M., 2005. Tidal rhythmites and their implications. *Earth-Science Reviews* 69: 79–95.
- Michon, L., van Balen, R.T., Merle, O. & Pagnier, H., 2003. The Cenozoic evolution of the Roer Valley Rift System integrated at a European scale. *Tectonophysics* 367: 101–126.
- Mosbrugger, V., Gee, C.T., Belz, G. & Ashraf, A.R., 1994. Three-dimensional reconstruction of an in-situ Miocene peat forest from the Lower Rhine Embayment, northwestern Germany – new methods in palaeovegetation analysis. *Palaeogeography, Palaeoclimatology, Palaeoecology* 110: 295–317.
- Mosbrugger, V., Utescher, T. & Dilcher, D.L., 2005. Cenozoic continental climatic evolution of Central Europe. *Proceedings of the National Academy of Sciences of the United States of America* 102 (42): 14964–14969.
- Munsterman, D.K. & Brinkhuis, H., 2004. A southern North Sea Miocene dinoflagellate cyst zonation. *Netherlands Journal of Geosciences / Geologie en Mijnbouw* 83 (4): 267–285.
- Otvos, E.G., 2000. Beach ridges – definitions and significance. *Geomorphology* 32: 83–108.
- Pemberton, S.G. & Frey, R.W., 1984. Ichnology of storm-influenced shallow marine sequence: Cardium Formation (Upper Cretaceous) at Seebe, Alberta. In: Stott, D.F. & Glass, D.J. (eds): *The Mesozoic of Middle North America: A selection of papers from the symposium on the Mesozoic of Middle North America*, Calgary, Alberta, Canada. *Canadian Society of Petroleum Geologists Memoir* 9: 281–304.
- Petzelberger, B., 1994. Die marinen Sande im Tertiär der südlichen Niederrheinischen Bucht. *Sedimentologie, Fazies und stratigraphische Deutung unter Berücksichtigung der Sequenzstratigraphie*. *Bonner Geowissenschaftliche Schriften* 14: 1–112.
- Rasser, M.W., Harzhauser, M., Anistratenko, O.Y., Anistratenko, V.V., Bassi, D., Belak, M., Berger, J.-P., Bianchini, G., Čičić, S., Čosović, V., Doláková, N., Drobne, K., Filipescu, S., Gürs, K., Hladilová, Š., Hrvatović, H., Jelen, B., Kasiński, J.R., Kováč, M., Kralj, P., Marjanac, T., Márton, E., Mietto, P., Moro, A., Nagymarosy, A., Nebelsick, J.H., Nehyba, S., Ogorelec, B., Oszczypko, N., Pavelić, D., Pavlovec, R., Pavšič, J., Petrová, P., Piwocki, M., Poljak, M., Pugliese, N., Redžepović, Rifelj, H., Roetzel, R., Skaberne, D., Sliva, L., Standke, G., Tunis, G., Vass, D. & Wagreeich, M. & Wesselingh, F., 2008. Palaeogene and Neogene. In: McCann, T. (ed.): *The Geology of Central Europe. Mesozoic and Cenozoic*. The Geological Society (London): 1031–1139.
- Reesink, A.J.H. & Bridge, J.S., 2007. Influence of superimposed bedforms and flow unsteadiness on formation of cross strata in dunes and unit bars. *Sedimentary Geology* 202: 281–296.
- Reicherter, K., Froitzheim, N., Jarosiński, M., Badura, J., Franzke, H.-J., Hansen, M., Hübscher, C., Müller, R., Poprawa, P., Reinecker, J., Stackebrandt, W., Voigt, T., Eynatten, H. von & Zuchiewicz, W., 2008. Alpine tectonics north of the Alps. In: McCann, T. (ed.): *The Geology of Central Europe. Mesozoic and Cenozoic*. The Geological Society (London): 1233–1285.
- Reynaud, J.-Y. & Dalrymple, R.W., 2012. Shallow-marine tidal deposits. In: Davis, R.A., Jr. & Dalrymple, R.W. (eds): *Principles of Tidal Sedimentology*. Springer: 335–369.
- Russell, P.E., 1993. Mechanisms for beach erosion during storms. *Continental Shelf Research* 13 (11): 1243–1265.
- Schäfer, A., 2010. *Klastische Sedimente. Fazies und Sequenzstratigraphie*. Springer (Heidelberg): 416 pp.

- Schäfer, A. & Utescher, T., 2014. Origin, sediment fill, and sequence stratigraphy of the Cenozoic Lower Rhine Basin (Germany) interpreted from well logs. *Zeitschrift der Deutschen Gesellschaft für Geowissenschaften* 165 (2): 287–314.
- Schäfer, A., Hilger, D., Gross, G. & von der Hocht, F., 1996. Cyclic sedimentation in Tertiary Lower-Rhine Basin (Germany) - the 'Liegendrücken' of the brown-coal open-cast Fortuna mine. *Sedimentary Geology* 103: 229–247.
- Schäfer, A., Utescher, T. & Mörs, T., 2004. Stratigraphy of the Cenozoic Lower Rhine Basin, northwestern Germany. *Newsletters on Stratigraphy* 40 (1/2): 73–110.
- Schäfer, A., Utescher, T., Klett, M. & Valdivia-Manchego, M., 2005. The Cenozoic Lower Rhine Basin - rifting, sedimentation, and cyclic stratigraphy. *International Journal of Earth Sciences* 94: 621–639.
- Schneider, H. & Thiele, S., 1965. *Geohydrologie des Ertfgebiets*. Ministerium für Ernährung, Landwirtschaft und Forsten, Nordrhein-Westfalen (Düsseldorf): 185 pp.
- Schumacher, M.E., 2002. Upper Rhine Graben. Role of preexisting structures during rift evolution. *Tectonics* 21(1): 6-1 – 6-17.
- Seilacher, A., 1964. Sedimentological classification and nomenclature of trace fossils. *Sedimentology* 3: 253–256.
- Sissingh, W., 2003. Tertiary paleogeographic and tectonostratigraphic evolution of the Rhenish Triple Junction. *Palaeogeography, Palaeoclimatology, Palaeoecology* 196: 229–263.
- Sissingh, W., 2006. Syn-kinematic palaeogeographic evolution of the West European Platform: correlation with Alpine plate collision and foreland deformation. *Netherlands Journal of Geosciences / Geologie en Mijnbouw* 85 (2): 131–180.
- Stive, M.J.F., Aarninkhof, S.G.J., Hamm, L., Hanson, H., Larson, M., Wijnberg, K.M., Nicholls, R.J. & Capobianco, M., 2002. Variability of shore and shoreline evolution. *Coastal Engineering* 47: 211–235.
- Stock, A.T., Littke, R., Zieger, L. & Thielemann, T., 2016. Miocene depositional environment and climate in western Europe: The lignite deposits of the Lower Rhine Basin, Germany. *International Journal of Coal Geology* 175: 2–18.
- Stupples, P., 2002. Tidal cycles preserved in late Holocene tidal rhythmites, the Wainway Channel, Romney Marsh, southeast England. *Marine Geology* 182: 231–246.
- Suhr, P., 1982. *Ophiomorpha nodosa* LUNDGREN 1891 im Miozän der Lausitz. *Abhandlungen des Staatlichen Museums für Mineralogie und Geologie* 31: 173–176.
- Suhr, P., 1989. Beiträge zur Ichnologie des Niederlausitzer Miozäns. *Freiberger Forschungshefte C436*: 93–101.
- Taylor, A.M. & Goldring, R., 1993. Description and analysis of bioturbation and ichnofabric. *Journal of the Geological Society* 150 (1): 141–148.
- Teichmüller, M., 1958. Rekonstruktion verschiedener Moortypen des Hauptflözes der niederrheinischen Braunkohle. In: Ahrens, W. (ed.): *Die Niederrheinische Braunkohlenformation*. *Fortschritte in der Geologie von Rheinland und Westfalen* 2: 599–612.
- Teichmüller, R., 1958. Die Niederrheinische Braunkohlenformation. Stand der Untersuchungen und offene Fragen. In: Ahrens, W. (ed.): *Die Niederrheinische Braunkohlenformation*. *Fortschritte in der Geologie von Rheinland und Westfalen* 2: 721–750.
- Terwindt, J., 1988. Palaeo-tidal reconstructions of inshore tidal depositional environments. In: de Boer, P.L., van Gelder, A. & Nio, S.D. (eds): *Tide-influenced sedimentary environments and facies*. D. Reidel Publishing Company (Dordrecht): 233–263.
- Tessier, B., Archer, A.W., Lanier, W.P. & Feldman, H.R., 1995. Comparison of ancient tidal rhythmites (Carboniferous of Kansas and Indiana, USA) with modern analogues (the Bay of Mont-Saint-Michel, France). In: Flemming, B.W. & Bartholomä, A. (eds): *Tidal Signatures in Modern and Ancient Sediments*. Special Publication of the International Association of Sedimentologists 24: 259–271.
- Tonkin, N.S., McIlroy, D., Meyer, R. & Moore-Turpin, A., 2010. Bioturbation influence on reservoir quality. A case study from the Cretaceous Ben Nevis Formation, Jeanne d'Arc Basin, offshore Newfoundland, Canada. *AAPG Bulletin* 94(7): 1059–1078.
- Tucker, M.E., 2003. *Sedimentary Rocks in the Field*. John Wiley & Sons Ltd (West Sussex): 236pp.

- Uchman, A. & Demircan, H., 1999. Trace fossils of Miocene deep-sea fan fringe deposits from the Cingöz Formation, southern Turkey. *Annales Societatis Geologorum Poloniae* 69: 125–135.
- Uncles, R.J., 2010. Physical properties and processes in the Bristol Channel and Severn Estuary. *Marine Pollution Bulletin* 61: 5–20.
- Utescher, T., Mosbrugger, V., Ivanov, D. & Dilcher, D.L., 2009. Present-day climatic equivalents of European Cenozoic climates. *Earth and Planetary Science Letters* 284: 544–552.
- Utescher, T., Ashraf, A.R., Dreist, A., Dybkjaer, K., Mosbrugger, V., Pross, J. & Wilde, V., 2012. Variability of Neogene continental climates in Northwest Europe - a detailed study based on microfloras. *Turkish Journal of Earth Sciences* 21: 289–314.
- Van Balen, R.T., Houtgast, R.F. & Cloetingh, S.A.P.L., 2005. Neotectonics of the Netherlands: a review. *Quaternary Science Reviews* 24 (3-4): 439–454.
- Van der Burgh, J., 1973. Hölzer der niederrheinischen Braunkohlenformation, 2. Hölzer der Braunkohlengruben "Maria Theresia" zu Herzogenrath, "Zukunft West" zu Eschweiler und "Victor" (Zülpich Mitte) zu Zülpich. Nebst einer systematisch-anatomischen Bearbeitung der Gattung *Pinus* L. *Review of Palaeobotany and Palynology* 15: 73–275.
- Vanneste, K., Meghraoui, M. & Camelbeeck, T., 1999. Late Quaternary earthquake-related soft-sediment deformation along the Belgian portion of the Feldbiss Fault, Lower Rhine Graben system. *Tectonophysics* 309: 57–79.
- Verbeek, J.W., de Leeuw, C.S., Parker, N. & Wong, T.E., 2002. Characterisation and correlation of Tertiary seismostratigraphic units in the Roer Valley Graben. *Netherlands Journal of Geosciences / Geologie en Mijnbouw* 81(2): 159–166.
- Visser, M.J., 1980. Neap-spring cycles reflected in Holocene subtidal large-scale bedforms deposits: a preliminary note. *Geology* 8: 543–546.
- Von der Brelie, G. & Wolf, M., 1981. "Sequoia" und *Sciadopitys* in den Braunkohlenmooren der Niederrheinischen Bucht. In: Reiche, E. & Hilden, H.D. (eds): *Geologie und Lagerstättenerkundung im Rheinischen Braunkohlenrevier*. *Fortschritte in der Geologie von Rheinland und Westfalen* 29: 177–191.
- Weimer, R.J., Howard, J.D. & Lindsay, D.R., 1982. Tidal flats and associated tidal channels. In: Scholle, P.A. & Spearing, D. (eds): *Sandstone Depositional Environments*. The American Association of Petroleum Geologists (Tulsa): 191–245.
- Westerhoff, W.E., Kemna, H.A. & Boenigk, W., 2008. The confluence area of Rhine, Meuse, and Belgian rivers: Late Pliocene and Early Pleistocene fluvial history of the northern Lower Rhine Embayment. *Netherlands Journal of Geosciences / Geologie en Mijnbouw* 87 (1): 107–125.
- Wong, T.E., Parker, N. & Horst, P., 2001. Tertiary sedimentary development of the Broad Fourteens area, the Netherlands. *Netherlands Journal of Geosciences / Geologie en Mijnbouw* 80 (1): 85–94.
- Yang, B.C., Dalrymple, R.W. & Chun, S.S., 2005. Sedimentation on a wave-dominated, open-coast tidal flat, south-western Korea: summer tidal flat - winter shoreface. *Sedimentology* 52: 235–252.
- Zagwijn, W.H. & Hager, H., 1987. Correlations of continental and marine Neogene deposits in the south-eastern Netherlands and the Lower Rhine District. *Mededelingen van de Werkgroep voor Tertiaire en Kwartaire Geologie* 24 (1-2): 59–78.
- Ziegler, P.A., 1992. European Cenozoic rift system. In: Ziegler, P.A. (ed.): *Geodynamics of Rifting*, Volume 1. *Case History Studies on Rifts: Europe and Asia*. *Tectonophysics* 208: 91–111.
- Ziegler, P.A., 1994. Cenozoic rift system of Western and Central Europe: an overview. *Geologie en Mijnbouw* 73(2-4): 99–127.
- Ziegler, P.A. & Dèzes, P., 2007. Cenozoic uplift of Variscan Massifs in the Alpine foreland. Timing and controlling mechanisms. *Global and Planetary Change* 58: 237–269.

B Supplementary Material

B.1 Carbon, ash and sulphur contents of samples (Locations 1 to 6)

Location	Sample	material	TOC (wt%)	TIC (wt%)	TC (wt%)	ash (wt%)	sulphur (wt%)
1	14/416	sand	2,35	0,24	2,60	n.a.	n.a.
	14/417	lignite	58,77	1,63	60,41	4,67	0,64
	14/418	lignite	60,53	1,57	62,10	5,21	0,53
	14/419	lignite	61,33	1,20	62,53	5,21	0,88
	14/421	lignite	58,26	1,34	59,60	2,91	0,75
	14/422	lignite	60,40	0,99	61,39	5,44	0,65
	14/423	lignite	60,09	1,32	61,41	5,28	0,66
	14/424	lignite	62,23	1,71	63,94	5,19	0,57
	14/425	lignite	61,95	1,90	63,85	4,82	0,52
	14/426	sand	4,38	0,29	4,67	n.a.	0,15
	14/427	lignite	61,42	1,27	62,69	4,14	0,77
	14/428	lignite	62,42	1,23	63,65	4,03	0,81
	14/429	lignite	50,02	1,18	51,20	3,78	0,82
	14/430	lignite	62,62	1,61	64,23	4,94	0,79
	14/431	lignite	66,80	1,47	68,27	3,54	0,64
14/432	lignite	60,39	1,31	61,70	3,34	0,82	
2	14/433	lignite	62,02	2,38	64,40	5,14	1,27
	14/434	lignite	63,00	1,36	64,36	5,90	1,35
	14/435	lignite	59,49	1,16	60,64	4,44	1,36
	14/436	lignite	60,44	1,24	61,68	3,83	1,53
	14/437	lignite	61,03	1,20	62,23	3,69	1,34
	14/438	lignite	62,72	1,09	63,81	3,94	1,30
	14/439	lignite	60,63	1,18	61,81	3,63	1,25
	14/440	lignite	61,18	1,38	62,56	3,78	1,15
	14/441	lignite	62,59	1,29	63,88	4,59	1,27
	14/442	lignite	63,58	0,97	64,55	4,97	1,26
	14/443	lignite	61,25	1,00	62,25	3,47	0,76
	14/444	lignite	59,68	1,35	61,03	4,29	1,15
	14/445	lignite	59,55	1,20	60,75	4,88	1,80
	14/446	lignite	62,29	0,54	62,83	4,65	1,82
	14/447	lignite	62,48	1,08	63,56	5,77	1,04
	14/448	lignite	59,14	0,53	59,67	3,62	1,70
	14/449	lignite	57,20	0,98	58,17	4,58	1,16
	14/450	lignite	62,88	1,17	64,06	5,38	1,34
	14/451	lignite	62,99	1,20	64,18	5,62	1,24
	14/452	sand	3,56	0,18	3,74	n.a.	0,29
	14/453	sand	3,50	0,20	3,70	n.a.	0,15
14/454	sand	0,45	0,18	0,62	n.a.	n.a.	
14/455	sand	3,45	0,18	3,63	n.a.	0,30	
14/456	sand	4,39	0,18	4,57	n.a.	0,32	
14/457	sand	1,32	0,18	1,50	n.a.	n.a.	
14/458	clay	36,63	10,95	47,58	n.a.	n.a.	

Location	Sample	material	TOC (wt%)	TIC (wt%)	TC (wt%)	ash (wt%)	sulphur (wt%)
3	14/459	lignite	61,18	1,07	62,25	4,01	0,91
	14/460	sand	5,29	0,18	5,47	n.a.	0,97
	14/461	lignite	60,25	1,18	61,43	4,34	0,59
	14/462	sand	3,53	0,18	3,71	n.a.	0,55
	14/463	lignite	61,59	0,84	62,43	4,47	0,60
	14/464	lignite	58,39	1,73	60,12	4,16	0,70
	14/465	sand	4,08	0,31	4,40	n.a.	0,15
	14/466	lignite	59,92	0,97	60,89	3,05	0,79
	14/467	lignite	59,28	1,38	60,66	5,98	0,69
	14/468	sand	5,74	0,29	6,03	n.a.	3,29
	14/469	lignite	60,05	0,70	60,75	5,86	0,82
	14/470	lignite	58,36	1,37	59,73	5,88	0,83
	14/471	sand	3,32	0,31	3,63	n.a.	0,16
	14/472	lignite	60,67	1,34	62,02	3,29	0,60
14/473	lignite	62,30	1,24	63,54	3,63	0,67	
4	14/475	sand	1,61	0,21	1,83	n.a.	n.a.
	14/476	lignite	57,25	1,54	58,79	5,70	3,53
	14/477	lignite	46,14	1,37	47,51	3,44	2,83
	14/478	Sand	1,22	0,22	1,43	n.a.	3,48
	14/479	lignite	60,56	1,24	61,80	3,47	n.a.
5	14/480	sand	0,41	0,18	0,59	n.a.	n.a.
	14/481	sand	0,80	0,19	0,99	n.a.	n.a.
	14/482	sand	2,54	0,18	2,72	n.a.	n.a.
	14/483	wood	47,39	3,32	50,71	n.a.	6,53
	14/484	lignite	54,32	3,62	57,94	4,04	3,44
6	14/485	lignite	56,87	3,54	60,42	3,15	1,58
	14/486	lignite	59,34	1,24	60,58	3,55	1,14
	14/487	lignite	60,53	0,97	61,51	5,66	1,80
	14/488	clay	4,82	0,25	5,06	n.a.	n.a.
	14/489	sand	0,89	0,18	1,07	n.a.	n.a.
	14/490	lignite	62,39	1,20	63,59	5,77	1,16
	14/491	lignite	61,09	0,92	62,01	5,99	0,95
	14/492	lignite	60,79	1,11	61,90	5,73	1,89
	14/493	sand	2,45	0,18	2,63	n.a.	n.a.
	14/494	lignite	62,14	1,27	63,41	5,80	1,13

C Publications

- Prinz, L.; Schäfer, A.; McCann, T.; Lokay, P. & Asmus, S. (2017): Facies analysis and depositional model of the Serravallian-age Neurath Sand, Lower Rhine Basin (W Germany). *Netherlands Journal of Geosciences – Geologie en Mijnbouw*, 96(3), 211-231.
- Prinz, L.; Zieger, L.; Littke, R.; McCann, T.; Lokay, P. & Asmus, S. (2017): Syn- and post-depositional sand bodies in lignite – the role of coal analysis in their recognition. A study from the Frimmersdorf Seam, Garzweiler open-cast mine, western Germany. *International Journal of Coal Geology* 179, 173-186.
- Prinz, L.; McCann, T.; Schäfer, A.; Asmus, S. & Lokay, P. (2018): The geometry, distribution and development of sand bodies in the Miocene-age Frimmersdorf Seam (Garzweiler open-cast mine), Lower Rhine Basin, Germany: implications for seam exploitation. *Geological Magazine*, 155(3), 685-706.
- Prinz, L. & McCann, T. (submitted): Sand injectites – from source to emplacement: an example from the Miocene-age Frimmersdorf Seam, Garzweiler open-cast mine, Lower Rhine Embayment. *Geological Society of London Special Publication - Subsurface Sand Remobilisation and Injection*.